The Birimian event in the Baoulé Mossi domain (West African Craton) — regional and global context

Mikael Grenholm

Dissertations in Geology at Lund University,
Master's thesis, no 375
(45 hp/ECTS credits)

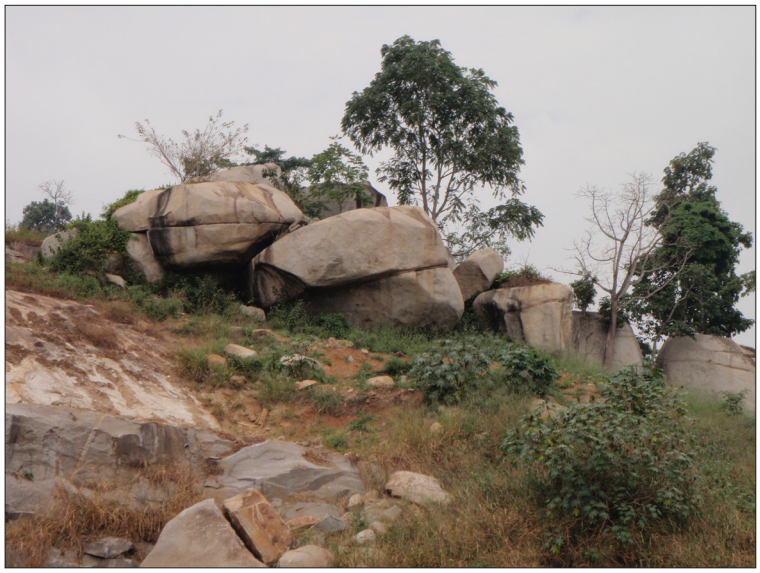

Department of Geology
Lund University
2014

The Birimian event in the Baoulé Mossi domain (West African Craton) — regional and global context

Master's thesis
Mikael Grenholm

Department of Geology
Lund University
2014

Contents

Cover Picture: Granitoid core-boulders in northern Kumasi basin. Photo by A. Scherstén.

The Birimian event in the Baoulé Mossi domain (West African Craton) — regional and global context

MIKAEL GRENHOLM

Grenholm, M., 2014: The Birimian event in the Baoulé Mossi domain (West African Craton) — regional and global context. *Dissertations in Geology at Lund University*, No. 375, 111 pp. 45 hp (45 ECTS credits).

Abstract: The crystalline basement of the West African Craton (WAC) was established during the Siderian to Orosirian (circa 2.35-1.95 Ga) Birimian event through accretion of extensive tracts of juvenile crust that was tectonically juxtaposed with Archean cratons. The Birimian crust is comprised of volcanic belts and sedimentary basins that have been intruded by multiple generations of intrusive rocks and experienced several tectonothermal events. The basement is mainly exposed in two shields in the northern and southern WAC, respectively, both of which are comprised of a western Archean and an eastern Birimian domain. The southern shield is called Man-Leo and includes the Archean Man and Birimian Baoulé Mossi domains.

The aim of this thesis has been to create a preliminary regional-global geodynamic model for the Birimian event in the Baoulé Mossi domain using mainly available literature data but also including some new data from Ghana in the SE Baoulé Mossi domain. Based on this compilation, the geodynamic evolution of the Baoulé Mossi domain is divided into four phases; the Eoeburnean (>2.13 Ga), Eburnean I (2.13-2.10 Ga), Eburnean II (2.10-2.07 Ga) and Eburnean III (<2.07 Ga).

The **Eoeburnean** phase likely began around 2.4-2.3 Ga and is characterized by the accretion of juvenile crust formed in island arcs. A rise in magmatic zircon ages after circa 2.25 Ga may be related to an increase in felsic magmatism as a result of crustal thickening and maturation but also increased preservation of accreted island arcs as a decrease in the number of active subduction zones may have reduced the rate of crustal recycling. Intrusive rocks emplaced during this phase were dominantly sodic granitoids but granites and monzogranites also occur. Tectonothermal and magmatic activity indicate that the Birimian crust in the Baoulé Mossi domain experienced both compression and extension during the Eoeburnean phase. By the end of this phase, an eastward dipping subduction zone had been established along the western margin of the Birimian crust in the Baoulé Mossi domain.

Several sedimentary basins in central and SE Baoulé Mossi were established during the **Eburnean I** phase. The opening of the sedimentary basins may have taken place during regional NE-SW dextral shearing leading to block rotation and development of N-S sinistral shear zones. This also coincided with the collision between the Archean crust of the Man domain and the Birimian crust in the SW Baoulé Mossi domain. The collision also affected the extension of the Baoulé Mossi domain in the Guyana shield of the Amazon Craton.

The **Eburnean II** phase is the most complex. Westward-directed slab rollback in NW Baoulé Mossi led to extension within the overriding Birimian crust. This led to the emplacement of high-K intrusive rocks and explosive extrusive magmatism in NW Baoulé Mossi, in what may constitute a *siliceous large igneous province*. Extension also led to the opening of younger sedimentary basins in central Baoulé Mossi, possibly along NE-SW oriented shear zones established during the Eburnean I phase. Ongoing collision between the Man domain and the Baoulé Mossi domain led to crustal thickening and associated high-P granulite facies metamorphism in the SE Man domain, possibly around 2.10-2.09 Ga. Granulite facies metamorphism is also recorded in the Archean Amapá block in the E Guyana shield at this time. The Amapá block is separated from the Man domain by a wide belt of low-grade Birimian crust. Simultaneous granulite facies metamorphism in both these areas may be explained by lower crustal detachment in hot Birimian crust. This may allow the upper crust to be displaced without significant thickening until it reaches cooler and more rigid crust were thrust belts are developed. Crustal thickening was followed by a switch to post-collisional sinistral transpression coupled with emplacement of extensive leucogranites between 2095-2080 Ma as the sedimentary basins in central Baoulé Mossi were closed. In contrast to other parts of the Baoulé Mossi domain, the NE part did not experience any significant magmatic activity during this phase, but may have been affected by tectonothermal activity.

The Baoulé Mossi domain experienced post-collisional extension during the **Eburnean III** phase that coincided with the formation of the Bakhuis UHT-granulite belt in the Guyana shield and decompression melting in the Archean crust of SE Man domain and the Amapá block. Limited intrusive and extrusive alkalic post-collisional magmatism was present within the Birmian crust, which cooled and stabilized between 2.0-1.9 Ga. Limited reactivation of the Birimian crust during this period may have taken place in response to far-field events.

On a global scale, the Birimian event led to the assembly of a continent — here referred to as Atlantica-Midgardia-Ur — that incorporated continental blocks now present in Africa, South America, India, East Antarctica, Western Australia and Eastern Europe, India, Antarctica and Western Australia. The assembly of Atlantica-

Midgardia-Ur coincided with rifting and breakup among crustal blocks now present in North America, northern Europe, North and south-central Australia, East Antarctica and northern Asia. These blocks were subsequently assembled along 2.0-1.7 Ga accretionary belts culminating with the formation of the supercontinent Columbia around 1.8-1.7 Ga, which also included Atlantica-Midgardia-Ur.

The assembly of Atlantica-Midgardia-Ur has many similarities with the assembly of Gondwana in the Neoproterozoic regarding the timing and duration as well as spatial distribution of tectonothermal and magmatic activity. In addition, many of the crustal blocks which formed part of Gondwana also formed part of Atlantica-Midgardia-Ur. Likewise, the behavior of the crustal blocks in North America, northern Europe, North and south-central Australia, East Antarctica and northern Asia during the assembly of Columbia is equivalent to the behavior of these blocks during the late Paleozoic (0.3 Ga) assembly of the supercontinent Pangea.

The assembly of both Atlantica-Midgardia-Ur and Gondwana coincided with distinct positive excursions in $^{87}Sr/^{86}Sr$ and $\delta^{13}C$ in marine carbonates. The peaks of $\delta^{13}C$ excursions coincide with accretionary orogenic activity during both the Birimian event and the assembly of Gondwana. Meanwhile, peaks in $^{87}Sr/^{86}Sr$ during both cycles coincide with collisional orogenic activity related to the assembly of Atlantica-Midgardia-Ur and Gondwana, respectively. The similarities between the assembly of Columbia and Pangea indicate that they represent two iterations of a particular type of supercontinent, here called Pangea-type.

The similarities between the tectonic events and the excursions in $^{87}Sr/^{86}Sr$ and $\delta^{13}C$ indicate that the global tectonic evolution during the Paleo- and Neoproterozoic was fundamentally the same. A supercontinent (Kenorland) equivalent to Rodinia should therefore have existed during the Neoarchean-Paleoproterozoic and broken up in a similar manner to Rodinia. For this reason, Kenorland and Rodinia, as well as the next supercontinent Amasia, can therefore be assumed to represent three iterations of another type of supercontinent, here called Rodinia-type.

Supercontinent cycles thus record the transition from either a Rodinia- to Pangea-type supercontinent, or vice versa. The Rodinia- to Pangea-type supercontinent cycles coincide with periods during which the oxygen concentration in the atmosphere was significantly increased. Rodinia- to Pangea-type supercontinent cycles therefore appear to be particularly important for the evolution of the atmosphere, biosphere and hydrosphere.

If Kenorland was the first supercontinent, then a "true" supercontinent cycle corresponds to the breakup of one Rodinia-type supercontinent and the subsequent assembly of the next Rodinia-type iteration. In this context, Pangea -type supercontinents are only transient stages when enough crust is aggregated to form a supercontinent. The breakup of Kenorland should have mirrored the "inside-out" breakup of Rodinia in the Neoproterozoic and the ongoing assembly of Amasia. This allows for a reverse schematic reconstruction of the continental blocks of Rodinia as they were positioned in Kenorland.

The consistent behavior of most continental blocks since the breakup of Kenorland suggests that they may be divided into three "continental cells". Each cell is characterized by a particular behavior during a Rodinia- to Rodinia-type supercontinent cycle. Transfer of continental blocks between cells may take place during the breakup of a Rodinia-type supercontinent. Transfer seemingly occur in a dynamic fashion in which a given cell "loses" a block to one cell but at the same time "gains" a block from the other cell. As such, the continental blocks are rotated between the cells even as the size of the cells remains unchanged.

Although there are differences between successive Rodinia- to Rodinia-type supercontinent cycles — as shown by the apparent absence of an Atlantic-type ocean during the Kenorland-Rodinia cycle — they are still controlled by the same fundamental cyclicity, which was established during the formation and subsequent breakup of Kenorland.

Keywords: Birimian event, Accretionary orogen, Atlantica, Lomagundi-Jatuli event, Supercontinent cycle

Supervisor: Anders Scherstén

Mikael Grenholm, Department of Geology, Lund University, Sölvegatan 12, SE-223 62 Lund, Sweden.
E-mail: mikael.grenholm@live.com

Det Birimiska eventet i Baoulé Mossi domänen (Västafrikanska kratonen) — regional och global kontext

MIKAEL GRENHOLM

Grenholm, M., 2014: Det Birimiska eventet i Baoulé Mossi domänen (Västafrikanska kratonen) — regional och global kontext. *Examensarbeten i geologi vid Lunds universitet*, Nr. 375, 111 sid. 45 hp.

Abstrakt: Det kristallina urberget i den Västafrikanska kratonen bildades under det Sideriska till Orosiriska (cirka 2,35-2,05 Ga) Birimiska eventet genom ackretion av stora volymer av juvenil skorpa, tektoniskt sammanslagen med Arkeiska kratoner. Den Birimiska skorpan utgörs av vulkaniska bälten och sedimentära bassänger vilka har intruderats av flera generationer av intrusiva bergarter och som påverkats av flera tektonotermala event. Det kristallina urberget är i huvudsak exponerat i två sköldar som återfinns i den norra respektive den södra delen av den Västafrikanska kratonen. Bägge sköldarna utgörs av en västlig Arkeisk och en östlig Birimisk domän. Den södra skölden kallas Man-Leo och utgörs av den Arkeiska Man domänen och den Birimiska Baoulé Mossi-domänen.

Syftet med den här uppsatsen har varit att skapa en preliminär regional-global geodynamisk model för det Birimiska eventet i Baoulé Mossi domänen genom att utnyttja dels tillgänglig litteraturdata men även ny data från Ghana i den SÖ delen av Baoulé Mossi. Baserat på den här sammanställningen har den geodynamiska utvecklingen av Baoulé Mossi domänen delats in i fyra faser; Eoeburnean (>2,13 Ga), Eburnean I (2,13-2,10 Ga), Eburnean II (2,10-2,07 Ga) samt Eburnean III (<2,07 Ga).

Den **Eoeburniska**-fasen inleddes troligen runt 2,4-2,3 Ga och karaktäriseras av ackretion av juvenil skorpa bildad i vulkaniska öbågar. En ökning av antalet åldrar från magmatiska zirkoner efter cirka 2,25 Ga kan vara relaterat till en ökning av felsisk magmatism som ett resultat av krustal förtjockning och mognad men även genom en ökad bevaring av ackreterade öbågar då en minskning av antalet aktiva subduktionszoner kan ha reducerat andelen återförd skorpa till manteln. Natriumrika granitoider dominerar denna fas men graniter och monzograniter förekommer också. Tektonotermal och magmatisk aktivitet indikerar att den Birimiska skorpan i Baoulé Mossi domänen uttsattes för både extension och kompression under den Eoeburniska fasen. Vid slutet av fasen hade en östligt stupande subduktionszon etablerats längs den västliga randen av den Birimiska skorpan.

Flera sedimäntära bassänger i centrala och SÖ Baoulé Mossi etablerades under **Eburnean I**-fasen. Öppnandet av dessa bassänger kan ha ägt rum under regional NÖ-SV dextral skjuvning som ledde till blockrotation och bildandet av N-S sinistrala skjuvzoner. Detta sammanföll med kollisionen mellan Arkeisk skorpa i Man domänen och Birimisk skorpa i SV Baoulé Mossi. Denna kollision påverkade även förlängningen av Baoulé Mossi-domänen som återfinns i Guyana skölden i Amazon kratonen.

Eburnean II-fasen är den mest komplexa. Västligt orienterad rörelse av den subducerande skorpan i NV Baoulé Mossi ledde till extension inom den överliggande Birimiska skorpan. Detta ledde till intrusion av kaliumrika granitoider samt explosiv eruptiv magmatism i NV Baoulé Mossi i vad som kan utgöra en *siliceous large igneous province*. Extension ledde också till att yngre sedimentära bassänger öppnades i centrala Baoulé Mossi, möjligen längs de NÖ-SV orienterade skjuvzoner som bildats tidigare under Eburnean I fasen. Fortsatt kollision mellan Man och Baoulé Mossi domänerna ledde till krustal förtjockning och högtrycks granulit-facies metamorfos i SÖ Man domänen, möjligen kring 2,10-2,09 Ga. Granulit-facies metamorfos har också påträffats vid den här tidpunkten i Amapá-blocket i östra delen Guyana skölden. Amapá-blocket är skiljt från Man domänen av ett brett bälte av metamorft låggradig Birimisk skorpa. Samtida granulit-facies metamorfos i bägge dessa områden kan förklaras med undre krustal avkoppling i varm Birimisk skorpa. Detta har möjliggjort för den övre krustala delen av skorpan att flyta ovanpå den undre. Den kan således förskjutas lateralt utan betydande förtjockning fram tills att den stöter på kallare och rigidare skorpa där överskjutning äger rum. Krustal förtjockning följdes av en övergång till sinistral post-kollisionsskjuvning kopplat med stora leucogranitintrusioner mellan 2095-2080 Ma när de sedimäntära bassängerna i centrala Baoulé Mossi stängdes. I kontrast mot övriga Baoulé Mossi-domänen påverkades inte den NÖ delen av någon betydande magmatisk aktivitet under Eburnean II fasen, även om tektonotermal påverkan kan ha förekommit.

Under **Eburnean III**-fasen genomgår Baoulé Mossi domänen post-kollisions extension som sammanfaller med bildanet av Bakhuis UTH-granulitbältet i Guyana skölden och dekopressionsmältning inom den Arkeiska skorpan i SÖ Man domänen och Amapá blocket. Begränsad intrusiv och extrusiv alkalisk post-kollisions magmatism förekommer också i den Birimiska skorpan som kyldes ner och stabiliserades mellan 2,0-1,9 Ga. Begränsad reaktivering kan ha ägt rum som en respons på tektonotermala event utanför den nuvarande Baoulé Mossi-domänen.

På en global nivå ledde the Birimiska eventet till bildandet av en kontinent — här kallad Atlantica-Midgardia-Ur — som inkluderade kontinentala block som nu återfinns i Afrika, Sydamerika, Västra Australien, Indien, Östra Antarktis och Östeuropa. Bildandet av Atlantica-Midgardia-Ur sammanföll med rifting och uppbrott bland krustala block som nu återfinns i Nordamerika, Nordeuropa, norra och sydcentrala Australien, Antarktis och norra Asien. Dessa block blev sedermera amalgamerade genom 2,0-1,7 Ga ackretions bälten vilket kulminerade i bildandet av superkontinenten Columbia runt 1,8-1,7 Ga, vilken också omfattade Alantica-Midgardia-Ur.

Bildandet av Atlantica-Midgardia-Ur har många likheter med bildandet av Gondwana under Neoproterozoisk tid både vad gäller timing och varaktighet såväl som rumslig fördelning av tektonotermal och magmatisk aktivitet. Utöver detta var också de krustala block som ingick i Gondwana i mångt och mycket desamma som de som ingick i Atlantica-Migardia-Ur. På samma sätt är beteendet hos de krustala blocken i Nordamerika, Nordeuropa, norra och sydcentrala Australien, Antarktis och norra Asien under bildandet av Columbia i stort detsamma som de senare hade under bildandet av den Senpaleozoiska (0,3 Ga) superkontinenten Pangea.

Bildandet av både Atlantica-Midgardia-Ur och Gondwana sammanföll med utpräglade positiva exkursioner av $^{87}Sr/^{86}Sr$ och $\delta^{13}C$ i marina karbonater. Topparna på exkursionerna av $\delta^{13}C$ sammanfaller med ackretionär orogen aktivitet under både det Birimiska eventet och bildandet av Gondwana medan topparna på $^{87}Sr/^{86}Sr$-exkursionerna sammanfaller med efterföljande kollisonsrelaterad orogen aktivitet under amalgameringen av Atlantica-Midgardia-Ur respektive Gondwana. Likheterna mellan bildandet av Columbia och Pangea indikerar att de representerar två iterationer av en särskild typ av superkontinent, här kallad Pangea-typ.

Likheterna mellan de storskaliga tektoniska förloppen samt exkursionerna i $^{87}Sr/^{86}Sr$ och $\delta^{13}C$ indikerar att den globala tektoniska utvecklingen under Paleo- och Neoproterozoisk tid var i grunden densamma. En superkontinent (Kenorland) motsvarande Rodinia bör således ha funnits under Neoarkeisk-Paleoproterozoisk tid och fragmenterats på ett sätt liknande Rodinia. Tillsammans kan därför Kenorland, Rodinia men även nästa superkontinent Amasia antas representera tre iterationer av en annan typ av superkontinent, här kallad Rodinia-typ.

Superkontinent-cykler skulle då alltså utgöra en övergång från en Rodinia- till Pangea-typ superkontinent, eller vice versa. Rodinia- till Pangea-typ superkontinent-cykler sammanfaller med perioder under vilken syre-koncentrationen i atmosfären höjdes väsentligt. De verkar däför vara särskilt viktiga för utvecklingen av atmosfären, biosfären och hydrosfären.

Om Kenorland var den första superkontinenten så utgörs en ”riktig” superkontinent-cykel av uppbrytandet av en Rodinia-typ superkontinent följt av bildandet av nästa Rodinia-typ iteration. Pangea-typ superkontinenter motsvarar då bara flyktiga perioder under vilka tillräckligt med kontinental skorpa är ansamlad för att utgöra en superkontinent. Uppbrytandet av Kenorland bör ha speglat ”inside-out” uppbrytandet av Rodinia i Neoproterozoisk och Paleozoisk tid samt det fortskridande bildandet av nästa superkontinent Amasia. Detta möjliggör en reversibel schematisk rekonstruktion av de kontinentala block som utgjorde Rodina såsom de var positionerade i Kenorland.

Det konsekventa beteendet bland olika kontinentala block sedan uppbrytandet av Kenorland indikerar att de kan delas in i tre ”kontinentala celler”. Vardera av dessa celler karaktäriseras av ett speciellt beteende under en Rodinia-till Rodinia-typ superkontinent-cykel. Överföring av block mellan celler kan äga rum under uppbrytandet av en Rodina-typ superkontinent. Överföringen sker i en till synes dynamisk process i vilken en cell ”förlorar” ett block till en cell medan den samtidigt ”erhåller” ett block från den andra cellen. På detta sättet kan kontinentala block rotera mellan cellerna utan att dessas storlek förändras.

Även om det finns skillnader mellan successiva Rodinia- till Rodinia-typ superkontinent-cykler — vilket illustreras av en till synes avsaknad av en motsvarighet till den Atlantisk Oceanen under Kenorland-Rodinia cykeln — så är de trots detta styrda av samma fundmentala cyklicitet, vilken etablerades under bildandet och det efterföljande uppbrytandet av Kenorland.

Nyckelord: Birimiska eventet, Ackretionär orogen, Atlantica, Lomagundi-Jatuli event, Superkontinent-cykel

Handledare: Anders Scherstén

Ämne: Berggrundsgeologi

Mikael Grenholm, Department of Geology, Lund University, Sölvegatan 12, SE-223 62 Lund, Sweden.
E-mail: mikael.grenholm@live.com

1 Introduction

Plate tectonics is characterized by two main types of orogens; accretionary and collisional (Cawood & Buchan 2007; Cawood et al. 2009). Accretionary orogens, such as Japan or the North American Cordilleras, form at long-lived convergent margins where cool and dense oceanic crust is subducted into the mantle beneath either oceanic or continental crust. Collisional orogens, e.g. the Himalayas, form when oceanic crust is consumed and two continental plates collide. Accretionary orogens are the primary site of crustal growth today (Cawood 2009), but are also sensitive to subduction erosion whereby crustal material is carried into the mantle along with the subducting oceanic crust (Scholl & Von Huene 2009; Stern 2011). Collisional orogens do not involve significant crustal growth but are instead important sites of crustal stabilization and preservation as subduction erosion is inhibited (Hawkesworth et al. 2009; Condie et al. 2011).

The question of when modern-style plate tectonics emerged is an intensely debated topic. The Earth may have been as much as 100-300°C warmer in the Archean owing to higher radiogenic heat production and residual heat from the formation of the Earth (van Hunen et al. 2008; Herzberg et al. 2010). This is thought to have had a profound effect on early Earth geodynamics. While many Archean rocks are compositionally similar to modern arc-related rocks there are nevertheless differing opinions regarding whether modern-style subduction of oceanic crust was viable on a hotter Earth (e.g. Hamilton 2007; Shirey et al. 2008). It has been proposed that subduction may have been more intermittent in the Archean because the oceanic crust and mantle may have been too weak to support the dense eclogitic portion of the subducting plate (van Hunen & Moyen 2012). Detachment of eclogitic crust may have temporarily stalled subduction as it would have decreased the effect of slab-pull, which is the main driver for subduction of oceanic crust in modern-style subduction. Alternatively, the Earth may have been dominated by a tectonic regime which did not involve subduction of oceanic crust. Such a pre-plate tectonic regime may have corresponded to "plume tectonics" in which rising mantle plumes erupted on "stagnant-lid" lithosphere to form thick successions of mafic lavas (e.g. Cawood et al. 2006; Bédard 2006; Hamilton 2007). Differentiation through lower crustal partial melting of thickened crust would have left an eclogitic residue that could subsequently founder into the mantle, providing a substitute for subducting oceanic plates. Regardless of what tectonic regime dominated the Archean, the transition to modern-style plate tectonics was likely gradual reflecting a progressively cooling Earth (Condie & Kröner 2008; Sizova et al. 2010).

Most workers have argued that plate tectonics began to operate during the Meso- to Neoarchean* (3.2-2.5 Ga, Williams et al. 1991; Dewey 2007; Brown 2008; Condie & Kröner 2008; Sizova et al. 2010; Shirey & Richardson 2011; Næraa et al. 2012). Nevertheless, there are those who instead argue that it may have begun as early as the Hadean-Eoarchean (Cawood et al. 2006; Shirey et al. 2008) or as late as the Neoproterozoic (Stern 2005; Hamilton 2007). What is clear is that many of the features associated with modern-style (Phanerozoic) plate tectonics, such as ophiolites and paired metamorphic belts, are either rare or absent in the Precambrian (Stern 2005; Brown 2008; Condie & Kröner 2008). The lack of these features has been attributed to the higher the Archean-Proterozoic geotherm (Brown 2008; Condie & Kröner 2008). A higher geotherm would have led to thicker and more buoyant oceanic crust as melting at spreading ridges must have been more extensive. A thicker crust would have been harder to obduct, potentially explaining the lack of Precambrian ophiolites. Meanwhile, a higher geotherm would also have meant that subducting oceanic crust would not be subjected to HP-LT conditions, accounting for the lack of paired metamorphic belts before the Neoproterozoic (Condie & Kröner 2008).

The transition from a pre-plate tectonic to plate tectonic regime which, once established, evolved into modern-style plate tectonics would also have had consequences for the location of the primary sites of magma generation and ultimately, its composition. The common occurrence of tonalite-trondhjemite-granodiorite (TTG)-suites and komatiites (highly magnesian lavas) in Archean crust is attributed to a higher geotherm which allowed widespread melting of mafic crust and large degrees of melting within the mantle (van Hunen et al. 2008; Moyen & Martin 2012). As subduction became widespread, and the geotherm was lowered, generation of felsic magma is considered to have gradually shifted from partial melting of mafic crust, either in the lower crust or from subducting oceanic crust (Bédard 2006; Martin & Moyen 2012), to partial melting of metasomatized peridotite in the mantle wedge (Arculus 1994; Tatsumi 2005) and/or more fertile crustal rocks, e.g. sediments. The long recognized change in composition of magmatic rocks across the Neoarchean-Paleoproterozoic transition has been attributed by many authors to the emergence of plate tectonics and the secular cooling of the Earth (e.g. Condie 1989; Kemp & Hawkesworth 2003; Condie 2008; Keller & Schoene 2012; Moyen & Martin 2012).

The cooling of the Earth and the emergence of plate tectonics is also considered to have led to significant changes in the tectonic style of orogens. The early Earth is thought by some to have been dominated by vertical tectonics characterized by gravitational readjustment between felsic low-density rocks such as TTGs and mafic-ultramafic supracrustals ("greenstones") with a high density (Van Kranendonk et al. 2004; Lin 2005; Hamilton 2007; Chardon et al. 2009). Diapiric rise of felsic crust and simultaneous sinking of dense supracrustals are considered to have given rise to the "dome-and-keel" structure seen in

* - The timescale of Gradstein et al. (2004) is used in this thesis

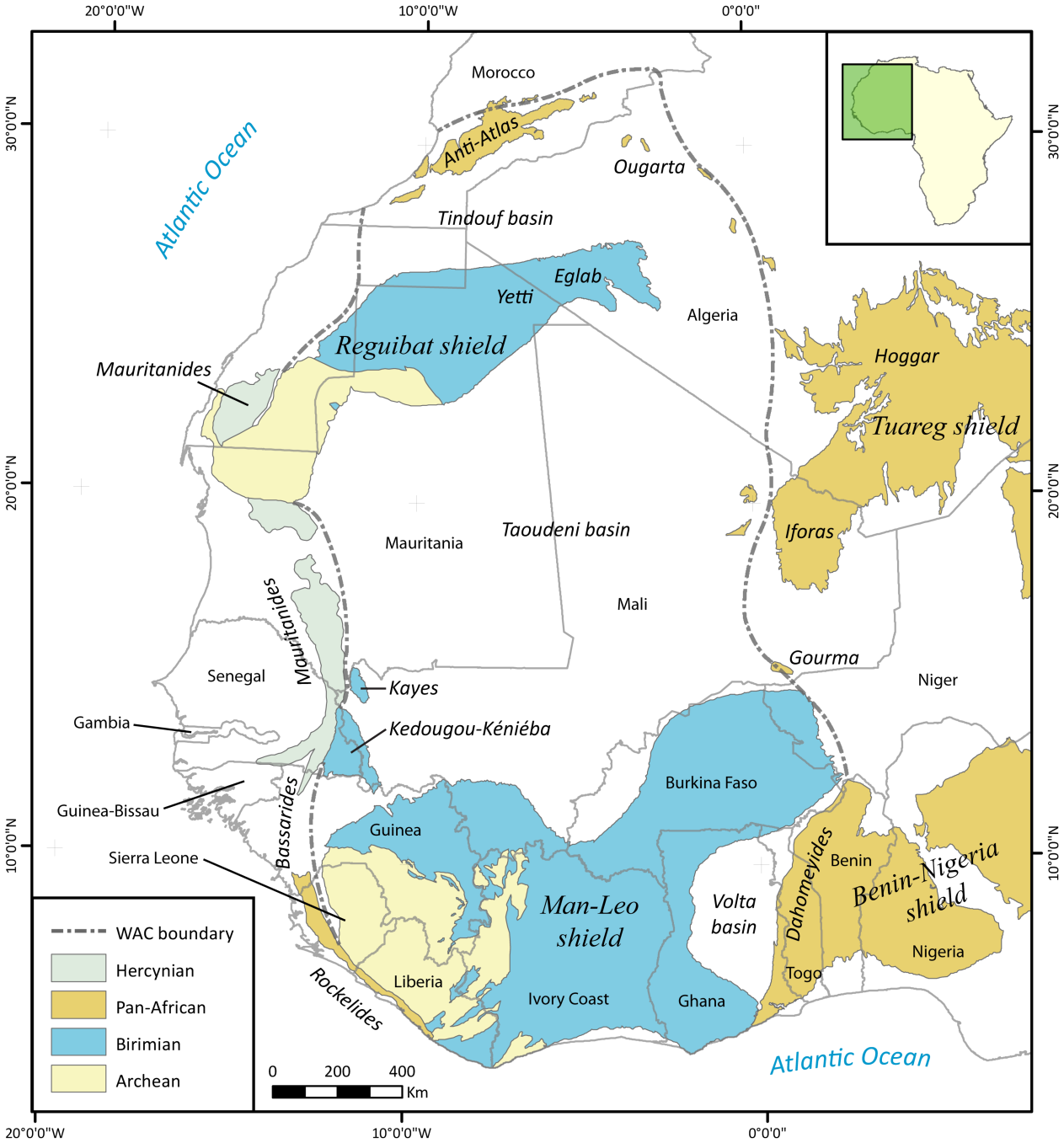

Fig. 1. Simplified tectonic map of the West African Craton and adjacent Pan-African-Hercynian fold and thrust belts. Mesoproterozoic to Recent sedimentary rocks are not depicted. The map has been compiled from the following sources; Man-Leo shield, Kedougou-Kéniéba, Kayes (Egal et al. 2002; Baratoux et al. 2011), Reguibat shield (Peucat et al. 2005; Schofield et al. 2012), Pan-African belts (Persits et al. 2002; Baratoux et al. 2011) and Hercynian belt (Abouchami et al. 1990; Schofield et al. 2012). WAC boundaries after Ennih & Liégeois (2008).

many Archean cratons, e.g. the Pilbara Craton in Western Australia (Van Kranendonk et al. 2004). Movement of rigid plates will instead give rise to horizontal tectonics characterized by lateral displacement through shearing or thrusting. Chardon et al. (2009) pointed out that the character of orogens is dependent on the strength of the lithosphere and thus the temperature at the Moho. These authors distinguished between two orogenic end-member types; ultra-hot (UHO) and cold orogens (CO). The former is characterized by a weak lithosphere which deforms through distributed strain and three-dimensional flow whereas in the latter, deformation is localized. While UHO are typical of Precambrian orogens and CO of modern, Himalayan-style orogens, they are not restricted to these time periods but simply reflect the prevailing geotherm.

Constraining when plate tectonics began to operate, and whether it differed from today, requires detailed studies on Archean and Proterozoic crustal domains incorporating petrological, geochemical, geochronological, metamorphic and structural data. One area were geodynamics and crust-forming processes during the early Paleoproterozoic can be studied is the West African Craton (WAC, fig. 1). The basement of the WAC is comprised of Archean cratons and juxtaposed early Paleoproterozoic (late Siderian to early Orosirian) crust, which formed during the Birimian event (e.g. Abouchami et al. 1990; Boher et al. 1992;

Ama-Salah et al. 1996; Vidal et al. 1996; Peucat et al. 2005). The basement is exposed primarily in two shields; the northern Reguibat and southern Man-Leo (Trompette 1994; Villeneuve & Cornée 1994). The Birimian crust consists of greenschist to amphibolite facies volcanic belts, sedimentary basins and granitoid-gneiss domains that has been affected by multiple tectonometamorphic events (e.g. Milési et al. 1989; Boher et al. 1992; Ama-Salah et al. 1996; Hirdes et al. 1996; Peucat et al. 2005; Feybesse et al. 2006; de Kock et al. 2009; Baratoux et al. 2011).

The origin and geodynamic evolution of the Birimian crust is a controversial subject; the debate surrounding it reflects the larger debate concerning whether plate tectonics were active during the early Paleoproterozoic. While some early workers proposed that the Birimian rocks had formed on rifted Archean continental crust (e.g. Leube et al. 1990) it was argued by Abouchami et al. (1990) and Boher et al. (1992) that they were — with some exceptions — juvenile. It must therefore have formed in an intra-oceanic setting, away from the influence of preexisting continental crust. From these studies it also became clear that the Birimian event constituted a major period of Siderian-Rhyacian crustal growth.

With the recognition that the Birimian crust is juvenile, two differing views have emerged regarding the geodynamic setting of the Birimian event. On one hand there are those workers who propose a setting involving plate tectonics. They favor models in which the Birimian crust formed in an accretionary orogen which developed into a collisional orogen as it collided with Archean continents (e.g. Mortimer 1992a; Sylvester & Attoh 1992; Feybesse & Milési 1994; Vidal & Alric 1994; Ama-Salah et al. 1996; Hirdes & Davies 2002; Pouclet et al. 2006; Baratoux et al. 2011; de Kock et al. 2012). On the other hand, there are those who argue against the involvement of plate tectonics during the Birimian event and instead propose a more "archaic" setting with plume-related mafic volcanism and vertical tectonics (Vidal et al. 1996; Doumbia et al. 1998; Lompo 2009, 2010; Vidal et al. 2009). The model proposed by Boher et al. (1992) — in which the Birimian crust formed from plume-related oceanic plateaus around which subduction zones subsequently developed — assumes an intermediate position between the two views.

Several studies have been made on Birimian rocks in recent years, which have yielded new geochronological, geochemical, structural and metamorphic data. However, these studies have focused on geographically restricted areas. The only studies with a regional scope were conducted in the early 90s (Milési et al. 1989, 1992; Feybesse & Milési 1994) but these also suffered from a lack of high-quality data such as robust radiometric ages or geochemical analyses. There is therefore a need for an updated regional synthesis which incorporates the relative wealth of data that has become available in the past two decades.

The purpose of this work is therefore to attempt to develop an internally consistent model for the geodynamic evolution during the Birimian event combining literature as well as recently collected and unpublished geochemical and geochronological data along with published structural and metamorphic data. The primary focus will lie on the Birimian crust exposed in the Man-Leo shield and Kedougou-Kéniéba and Kayes inliers in the southern WAC. However, crust equivalent to the Birimian is not limited to these areas, but is also present in the Reguibat shield in the northern WAC — as well as in other cratons and orogenic belts in Africa, South America, Europe and beyond. It thus becomes necessary to place the geodynamic evolution of the southern WAC within the context of the tectonothermal and magmatic activity seen in these areas. It follows that the plate tectonic movements of the WAC — and its participation in various paleocontinental configurations — must therefore also be considered.

2 Geological setting

2.1 The West African Craton

2.1.1 General outline

The Archean and Paleoproterozoic basement of the West African Craton (WAC) is exposed in the northern Reguibat shield, the southern Man-Leo shield and the west-central Kedougou-Kéniéba and Kayes inliers (fig. 1, Black 1980; Rocci et al. 1991; Trompette 1994; Villeneuve & Cornée 1994). It is overlain by Proterozoic to Phanerozoic sediment of the northern Tindouf, central Taoudeni and southeastern Volta basins. Both the Reguibat and Man-Leo shields can be divided into a western and an eastern domain comprised dominantly of Archean and Paleoproterozoic crust, respectively.

Although it has been proposed that the Archean domains of the Reguibat and Man-Leo shields may be connected the presence of the Kedougou-Kéniéba and Kayes inliers between them — which only contains juvenile Paleoproterozoic rocks — suggest that the Archean domains represent separate blocks (Abouchami et al. 1990). The Taoudeni basin, like the Volta and Tindouf basins, is therefore likely underlain by a largely Paleoproterozoic basement. Prior to the opening of the Atlantic Ocean the São Luís Craton in northeastern Brazil also formed part of the WAC (e.g. Trompette 1994; Feybesse et al. 2006). It has a basement of Paleoproterozoic rocks comparable to those found in the Man-Leo shield and paleogeographic reconstructions (Bullard et al. 1965; Onstott et al. 1984) position the São Luís Craton south of present day Ghana and southeastern Ivory Coast (fig. 2). The basement is exposed in a few scattered domains (fig. 2) but is otherwise overlain by younger sediment (e.g. Klein et al. 2001).

Apart from its southern border, which corresponds to the passive margin at the Atlantic coast, the

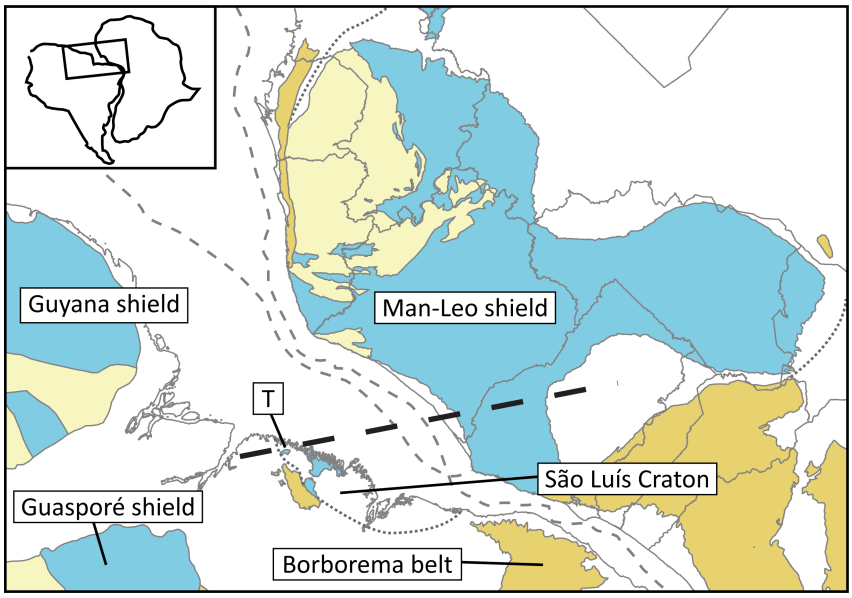

Fig. 2. Pre-Atlantic reconstruction of Africa and South America redrawn from Onstott et al. (1984), based on the fit of Bullard et al. (1965). Simplified tectonic maps after Klein & Moura (2001), Egal et al. (2002), Persits et al. (2002), Rosa Costa et al. 2006); Macambira et al. (2009) and Baratoux et al. (2011). See figure 1 for legend. The thick, dashed line shows the suggested projection between the Tracuateua (T) intrusive suite (Klein et al. 2008) in the São Luís Craton and the lithologically equivalent as well as coeval leucogranites in the Comoé-Sunyani basin (e.g. Hirdes et al. 1992; Zitzmann 1997; Vidal et al. 2009). See further discussion in section 4.3.3.2.

WAC is delineated by Neoproterozoic to Paleozoic fold and thrust belts that are partly covered by younger deposits (Trompette 1994; Villeneuve and Cornée 1994; Ennih & Liégeois 2008). Along the western border of the WAC these belts outcrop in the Rockelides, Bassarides and Mauritanides while the northern border is marked by the Anti-Atlas and Ougarta inliers. The Hoggar-Iforas belt together with the Gourma inlier and, in the southeast, the Dahomeyides, defines the eastern border. In Brazil, the São Luís Craton (fig. 2) is bordered by the Gurupie belt to the southwest and the Borborema belt to the east, while the Atlantic coast forms its northern border (Trompette 1994; Klein et al. 2001).

All fold and thrust belts originally formed during the Neoproterozoic to early Paleozoic Pan-African-Brasiliano orogenic cycle (Trompette 1994; Villeneuve & Cornée 1994; Villeneuve 2005). These belts consist of a mixture of Neoproterozoic supracrustals and granitoids together with Archean and Proterozoic terranes. Along the margin of the WAC, folding and thrusting remobilized the crystalline basement and overlying sedimentary sequences. In the internal parts of the WAC, the low-grade sedimentary strata of the Tindouf, Taoudeni and Volta basins is flat and unfolded but may be faulted and fractured. Proterozoic to Paleozoic sedimentation in the WAC was to a large degree controlled by the evolution of the fold and thurst belts along its margin. The Mauritanides were remobilized during the late Paleozoic Variscan-Hercynian orogeny.

2.1.2 Tectonic evolution

The WAC has been placed in two paleocontinental configurations; Atlantica (Rogers 1996; Zhao et al. 2004) and Midgardia (Johansson 2009), shown in figures 3 and 4, respectively. Both of these paleocontinents consist of a nucleus of Archean cratons juxtaposed with early Paleoproterozoic (Siderian to early Orosirian) crust. This core has subsequently grown by accretion of Proterozoic — as well as Archean — crust. They thus began to be assembled during a time interval corresponding to the Birimian event in the WAC. Although this period is known by other names outside of the WAC (e.g. the Transamazonian event in South America, see Brito Neves 2011) all Siderian to Orosirian tectonometamorphic activity and magmatism in the constituent cratons of Atlantica and Midgardia (see below) will be collectively referred to as the Birimian event in the following text, unless otherwise noted.

The Atlantica paleocontinental configuration (fig. 3) was first introduced by Rogers (1996) who proposed that it was comprised of the WAC, Congo Craton (CC) and West Nile Craton (a part of the Saharan Metacraton (SmC) as defined by Abdelsalam et al. 2002) in Africa and the São Luís Craton (SLC), Amazon Craton (AC), São Francisco Craton (SFC) and Rio de la Plata Craton (RPC) in South America. Rogers (1996) based this configuration on the recognition by a range of previous workers that cratons in Africa and South America shared many lithological, geochronological, structural and paleomagnetic similarities (e.g. Torquato & Cordani 1981; Onstott et al. 1984; Caen-Vachette 1988; Boher et al. 1992; Ledru et al. 1994).

Although the Kalahari Craton (KC) in southern Africa (fig. 3) contains Archean and Rhyacian-Orosirian crust (e.g. Hanson 2003) it has not been in-

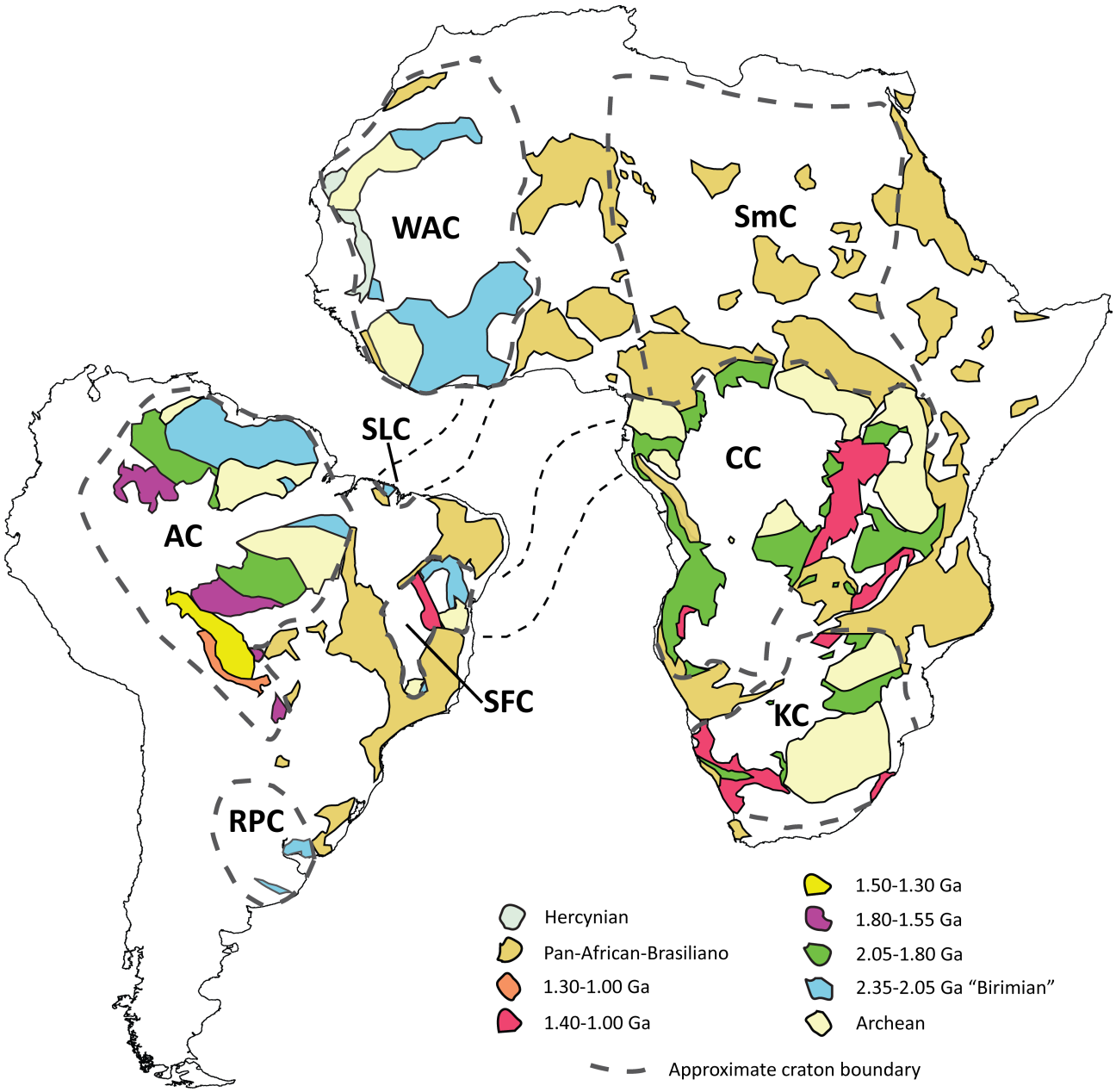

Fig. 3. Schematic map of cratons and thrust and fold belts in Africa and South America. Proterozoic to Recent sedimentary cover rocks are not shown. Abbreviations used in the figure: WAC - West African Craton; SmC - Saharan Metacraton; CC - Congo Craton; KC - Kalahari Craton; AC - Amazon Craton; SLC - São Luís Craton; SFC - São Francisco Craton; RPC - Rio de la Plata Craton. Compiled from Trompette (1994), Klein and Moura (2001), Abdelsalam et al. (2002), Persits et al. (2002), Hanson (2003), Milési et al. (2004), Feybesse et al. (2006), Ennih & Liégeois (2008), Macambira et al. (2009) and Rapela et al. (2011).

cluded into Atlantica. This appears to be largely due to paleomagnetic data obtained by Onstott et al. (1984), which showed that the KC has a distinctly different paleomagnetic pole at 2.0 Ga compared to the WAC and AC. This could mean that these cratons were connected during the Paleoproterozoic but have since been displaced relative to each other. Alternatively, it could indicate that they did not belong to a common continent at the time (Onstott et al. 1984; Zhao et al. 2004).

As can be seen in figure 3 the oldest Paleoproterozoic (2.20-2.05 Ga) domains are found in the WAC, AC, SLC, RPC and SFC while those in the CC and KC are younger with few ages older than 2.10 Ga, the majority being younger than 2.05 Ga (Hanson 2003). While only early Orosirian ages have been reported from the WAC rocks from this period are common in both the AC and the SFC (Cordani & Teixeira 2007; Brito Neves 2011). The onset of Paleoproterozoic activity in Atlantica thus appears to have been diachronous.

Atlantica is believed to have remained intact throughout the Paleo- and Mesoproterozoic (Zhao et al. 2004; Neves 2011) during which time it may have been incorporated into the supercontinents Columbia at 1.9-1.8 Ga (Zhao et al. 2004; Rogers & Santosh 2009) and Rodinia at 1.0 Ga (Li et al. 2008). Until recently no magmatic activity had been recognized in the WAC between 1.7-1.0 Ga which at this stage was

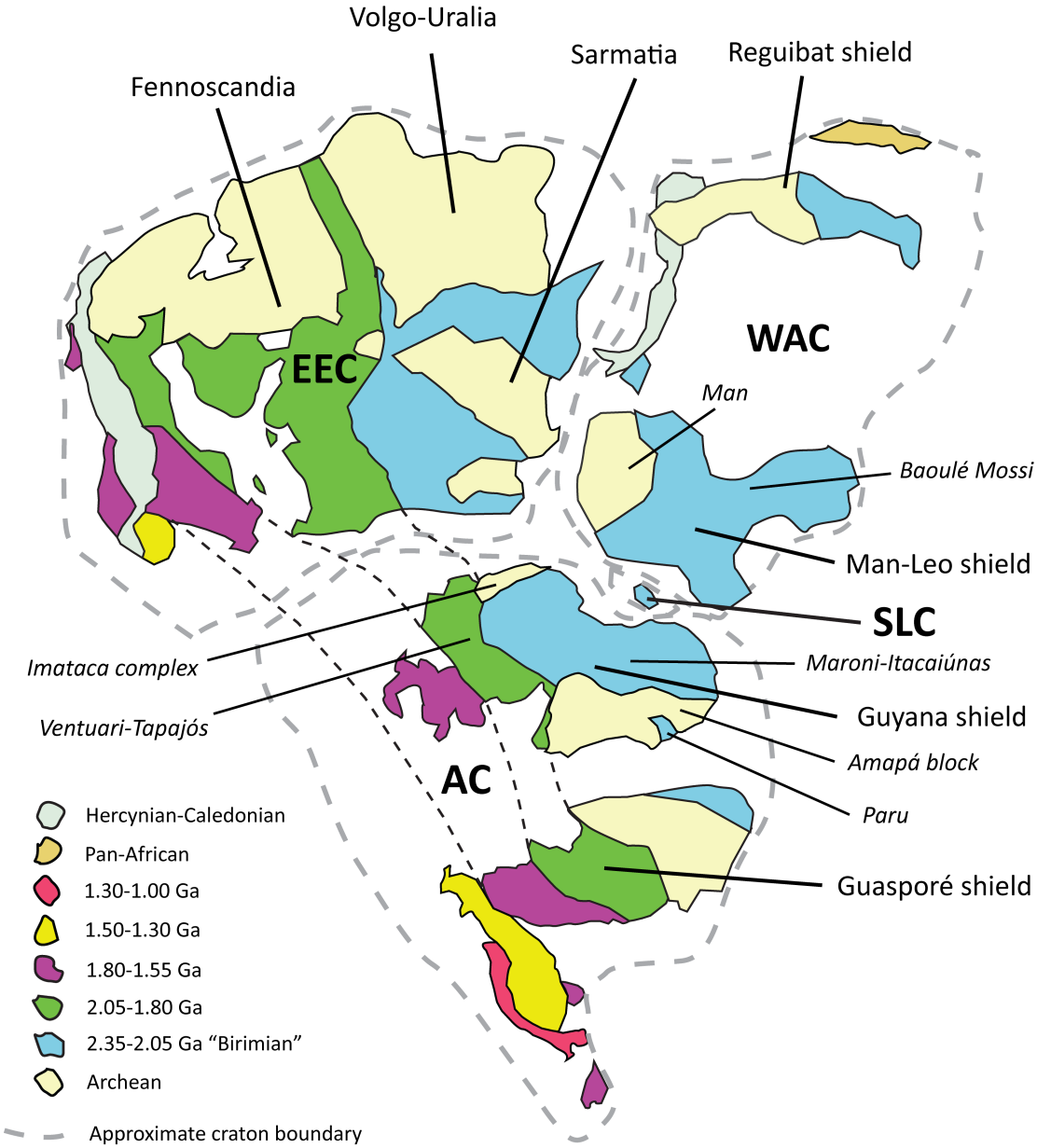

Fig. 4. The Midgardia configuration, redrawn after Johansson (2009) with minor modifications, of the West African Craton (WAC), São Luís Craton (SLC), East European Craton (EEC) and Amazon Craton (AC). The simplified tectonic maps are based on the following sources: WAC - Feybesse et al. (2006, in Johansson 2009); EEC - Bogdanova et al. (2008, in Johansson 2009); AC - Macambira et al. (2009), with modifications from Rosa Costa et al. (2006). Note that unlike the WAC and AC, the tectonic map of the EEC also show covered basement as it is otherwise only exposed in Fennoscandia and parts of Sarmatia (Bogdanova et al. 2008).

considered to have cooled off and cratonized (Ennih & Liégeois 2008). However, El Bahat et al. (2013) have reported 1.38 Ga ages from dolerite dykes in the Anti-Atlas showing that at least the northern portion of the WAC was affected by Mesoproterozoic activity, which these authors proposed may be associated with the breakup of Columbia.

During the Neoproterozoic Atlantica was fragmented into crustal blocks corresponding to the present day cratons as Rodinia began to disperse (Hoffman 1991; Zhao et al. 2004; Neves 2011). These blocks were subsequently reamalgamated along extensive mobile belts during the assembly of Gondwana in the late Neoproterozoic-Paleozoic. This cycle of breakup and reassembly is known as the Pan-African and Brasiliano orogenies in Africa and South America, respectively (e.g. Trompette 1994). In addition to juvenile Neoproterozoic crust the Pan-African-Brasiliano mobile belts also contain a significant amount of Archean and Paleoproterozoic rocks, either reworked or preserved as relatively intact terranes (Trompette 1994; Neves 2011). Large shear zones are common in the mobile belts along which hundreds of kilometers of displacement have occurred (Onstott et al. 1984; Trompette 1994; Liégeois et al. 2003)

During the Pan-African-Brasiliano orogeny, basins floored by oceanic crust developed on the western, northern, eastern and southeastern margins of the

WAC (e.g. Ennih & Liégeois 2008). However, the southwestern margin of the WAC, which bordered against the AC, does not appear to have developed into a oceanic basin but rather remained as an intracontinental rift (Trompette 1994; Neves 2011). Even so, Onstott et al. (1984) proposed that significant (1000 km) dextral strike-slip motion occurred between the WAC and AC during the Pan-African-Brasiliano orogeny. While the ocean bordering the eastern and southeastern margin of the WAC closed during the Pan-African-Brasiliano orogeny oceans remained to the west and north. These finally closed during the late-Paleozoic Variscan-Hercynian orogeny when Gondwana merged with Laurasia to form the supercontinent Pangea (Villeneuve and Cornée 1994).

Recently, Johansson (2009) proposed that the WAC had been connected with the AC (Cordani & Teixeira 2007) and East European Craton (EEC, Bogdanova et al. 2008) in a paleocontinental configuration he called Midgardia (fig. 4). In this configuration, the current southern margin of the WAC is connected with the current northeastern margin of the AC. This connects the Man and Baoulé Mossi domains in the WAC with the Imataca Complex and Maroni-Itacaiunas province in the AC, respectively. Meanwhile, the western margin of the WAC is placed next to the current southeastern margin of the EEC. In this position, the Archean domains in the Man and Reguibat shields are placed next to Archean Sarmatia and Volgo-Uralia blocks in the EEC. These two blocks are separated by an early Orosirian (2.05 Ga) collisional belt (Bogdanova et al. 2008), which connects with the Siderian-early Orosirian crust between the Archean domains of the Man-Leo and Reguibat shields. As for Atlantica, Johansson (2009) also argued that the Midgardia configuration remained intact throughout the Paleo- and Mesoproterozoic and was only fragmented during the Neoproterozoic when the EEC broke away from the WAC and AC.

Unlike the Atlantica configuration — which was drawn by Rogers (1996) using only a pre-Atlantic fit of Africa and South America, and which also included the Pan-African-Brasiliano mobile belts (his figure 5) — the Midgardia configuration is based on the position of the constituent cratons during the Paleoproterozoic. This does not mean that the Atlantica and Midgardia paleocontinental configurations are incompatible. However, the fit of the WAC and AC in the Midgardia configuration requires that the other cratons in the Atlantica configuration are repositioned from their present position as the former configuration is not compatible with a simple pre-Atlantic fit of Africa and South America. Given the likely considerable movement between the cratons during the Pan-African-Brasiliano orogeny (e.g. Onstott et al. 1984; Liégeois et al. 2003) it appears as if such reorganization is at the very least viable. Together, the Atlantica and Midgardia configurations could therefore have constituted a Proterozoic continent comprising the WAC, AC, SLC, EEC, SFC, RPC and CC, in addition to Archean and Proterozoic crust now present in neighboring Pan-African-Brasiliano mobile belts.

2.2 The Archean and Paleoproterozoic of the southern WAC

The Man-Leo shield lies within the West African countries Ghana, Niger, Togo, Burkina Faso, Mali, Ivory Coast, Guinea, Liberia and Sierra Leone (fig. 5). The Kedougou-Kéniéba Inlier (KKI) lies mostly in Senegal but also outcrops in western Mali and northern Guinea. The Kayes Inlier lies almost entirely within Mali were it straddles the border to Mauritania. The São Luís Craton (SLC) is located in northeastern Brazil (fig. 2).

The simplified geological map of the Man-Leo shield and KKI-KI shown in figure 5 — which will feature prominently in the latter parts of this text — is adapted from the simplified geological map of Baratoux et al. (2011, their figure 1). This map is in turn modified from the BRGM SIGAfrique geological map of Africa (Milési et al. 2004, in Baratoux et al. 2011). However, two important changes have been made to the geological map in figure 5 compared to the map of Baratoux et al. (2011). In Ghana, the map has been redrawn to fit with the recently compiled 1/1000000 national geological map (Agyei Duodu et al. 2009). Similarly, in eastern Guinea, the map has been redrawn according to the simplified geological map of Egal et al. (2002) which is based on fieldwork in that part of the country during the 90s. In this map eastern and northeastern Guinea is comprised entirely of Birimian rocks, an interpretation which is also supported by radiometric ages (Pb-Pb on zircon) obtained by Egal et al. (2002) from granitoids in this area.

However, this conflicts with the map of Baratoux et al. (2011) in which large parts of the same area is instead marked as Archean. Considering its recent date, finer scale and supporting geochronological data the map of Egal et al. (2002) is here given precedence over that of Baratoux et al. (2011). Since the map of Egal et al. (2002) only covers eastern Guinea this combination results in a distinct change of lithological units across the Guinean-Ivorian border. This combination of maps thus creates an apparent thin, north-south elongate embayment of Birimian rocks in eastern Guinea which is surrounded by Archean crust to the west, south and east (fig. 5).

It can be questioned whether the extent of Archean crust in northwestern Ivory Coast is as extensive as indicated on the map of Milési et al. (2004, in Baratoux et al. 2011). Radiometric ages (Pb-Pb and TIMS on zircon) obtained by Milési et al. (1989) on orthogneisses show that there are indeed Archean rocks present in northwestern Ivory Coast, near Ziemougoula (fig. 5). However, these are from a restricted area proximal to the Sassandra and Banifin shear zones. The reason why such a large area in northwestern Ivory Coast has been mapped as Archean remains unclear; through the course of this study no

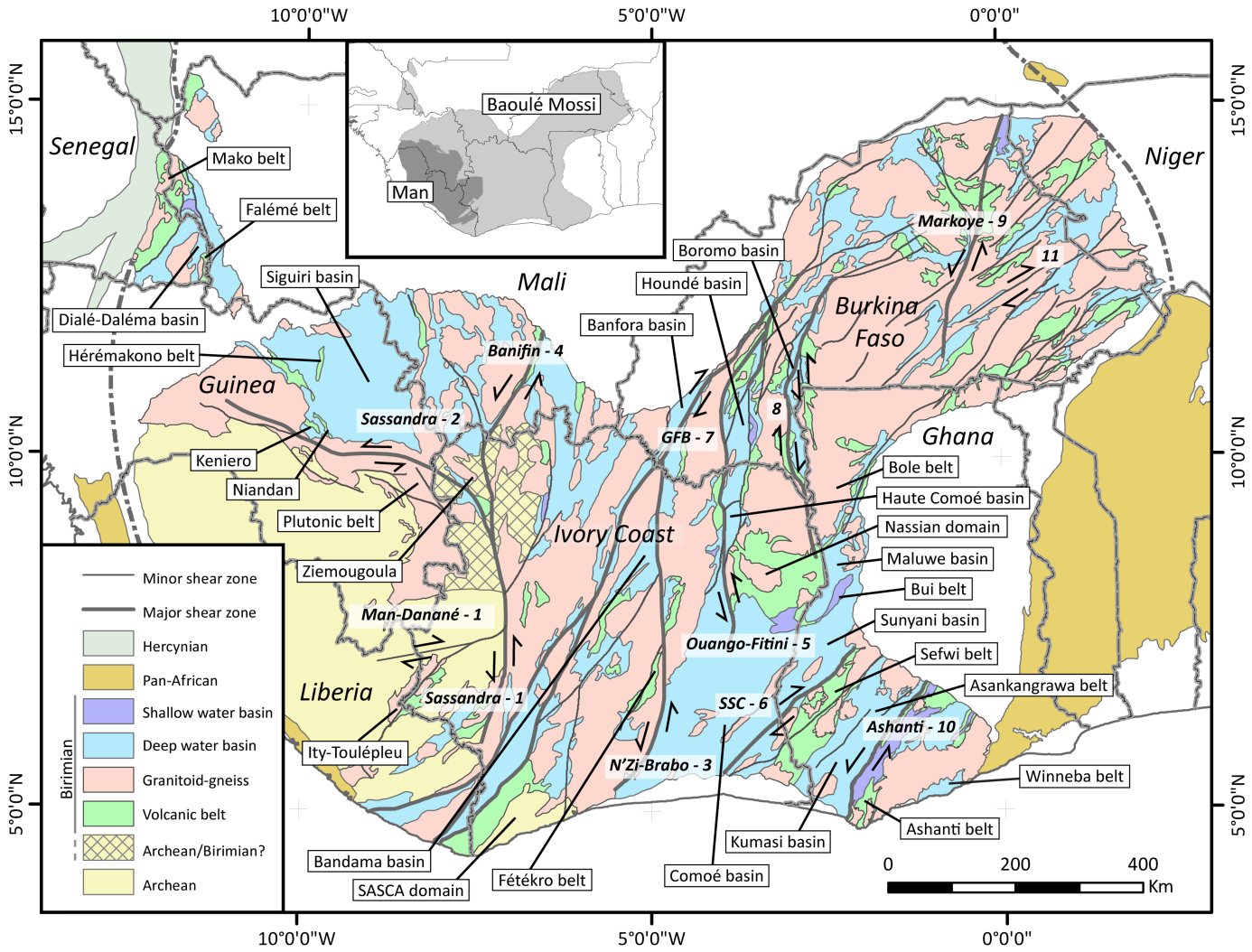

Fig. 5. Schematic geological map of Birimian rocks of the Man-Leo shield, Kedougou-Kéniéba (KKI) and Kayes (KI) inliers, together with Archean crust and adjacent Pan-African and Hercynian fold and thrust belts. Man-Leo shield, KKI and KI after Baratoux et al. (2011) with modifications by Egal et al. (2002) and Agyei Duodu et al. (2009). Pan-African and Hercynian fold and thrust belts after Abouchami et al. (1990), Persits et al. (2002) and Baratoux et al. (2011). Localities and shear zones discussed in the text are given in framed white and transparent white text boxes, respectively. GFB and SSC are abbreviations for the Greenville-Ferkéssédougou-Bobo-Dioulasso and Sefwi-Sunyani-Comoé shear zones, respectively. Numbers designates references for shear sense along these shear zones; **1** - Kouamelan et al. (1997); **2** - Egal et al. (2002); **3** - Mortimer (1992b), Doumbia et al. (1998); **4** - Liégeois et al. (1991); **5** - Vidal & Alric (1994), Vidal et al. (1996); **6** - Jessell et al. (2012); **7** - Milési et al. (1989), Baratoux et al. (2011); **8** - Baratoux et al. (2011); **9** - Tshibubudze et al. (2009); **10** - Perrouty et al. (2012); **11** - Naba et al. (2004). Small inset shows the extent of the Man and Baoulé Mossi domains as used in this text (see further discussion in section 2.2).

explanatory notes have been found for the BRGM SIGAfrique geological map. It should be noted that in an older regional map of the Man-Leo shield (Milési et al. 1989, 1992) a much smaller area in northwestern Ivory Coast was mapped as Archean — essentially covering only the area along the junction of the Sassandra and Banifin shear zones near from which Archean ages has been obtained. In this earlier regional map the Archean crust thus appear as a small domain surrounded by Birimian crust. Because of these uncertainties the Archean crust in northwestern Ivory Coast is shown with a cross-hatched pattern in figure 5 to highlight the fact that large parts of this crust may actually be Birimian. The southern limit of the hatched area is simply the eastwards extension of the Archean-Birimian contact as seen in Guinea (Egal et al. 2002).

As mentioned in section 2.1.1, the Man-Leo shield contains a western Archean and an eastern Birimian domain. These are called the Man and Baoulé Mossi domains, respectively. The boundary between these two domains is commonly held to be the Sassandra shear zone (e.g. Kouamelan et al. 1997; Baratoux et al. 2011). However, it should be noted that Archean and Birimian rocks are present on both of its sides. Archean rocks (from which Pb-Pb and TIMS zircon ages have been obtained) to the east of the Sassandra fault are present both in northwestern (Milési et al. 1989) and southwestern (the SASCA domain, Bard & Lemoine 1976; Kouamelan 1996) Ivory Coast (fig. 5). In addition, Sm-Nd isotope data from granitoids (*sensu lato*) indicate that Archean crust is present in southeastern Ghana (Leube et al. 1990) and in south-

ern Togo (Agbossoumondé et al. 2007). In addition, Birimian rocks occurring in fault-bounded basins are present in southeastern Liberia and west-central Ivory Coast (Feybesse et al. 1990; Kouamelan et al. 1997). There are also Birimian rocks to the west of the Sassandra fault in southeastern Guinea, southwestern Ivory Coast and eastern Liberia, which, apart from the Sassandra shear zone, appear to be connected with Birimian crust to the east.

As the Sassandra fault in many instances does not correspond to the actual contact between the Archean and Birimian crust in Man-Leo shield it seems unsuitable to use it as a border between the Man and Baoulé Mossi domains, if these are indeed meant to correspond to the Archean and Birimian crust in the Man-Leo shield, respectively. If the Sassandra fault were to remain as the boundary it is unclear exactly what geological meaning the two domains would have. For this reason the Man domain will, in the following text, be used for the coherent area of Archean crust in the western Man-Leo shield (inset in figure 5). It will include the small Birimian domains, such as Ity-Toulépleu, which are not connected with the larger mass of Birimian crust of the Baoulé Mossi domain. It will not include the Archean rocks in southwestern and northwestern Ivory Coast which instead belong to the Baoulé Mossi domain as defined here. In addition, the Baoulé Mossi domain will also include the KKI, Kayes Inlier and the São Luís Craton.

The remainder of this section has been divided into three parts. The first two parts will deal with the Archean and Birimian geodynamic evolution in the southern WAC and São Luís Craton, respectively. As such they do not deal specifically with the Man or Baoulé Mossi domains although they, by and large, are equivalent to Archean and Birimian crust, respectively. Finally, the last section will deal specifically with the contact and interaction between the Man and Baoulé Mossi domains, including the tectonometamorphic overprint on Archean crust during the Birimian event.

2.2.1 Archean

In the Man-Leo shield Archean crust is exposed in Sierra Leone, Guinea, Ivory Coast and Liberia. Archean rocks are largely restricted to the Man domain but there also some occurrences within the Baoulé Mossi domain (see above). Recent fieldwork and high-precision geochronology from the Man domain in Guinea led Thiéblemont et al. (2004) to revise the older lithostratigraphic division of the Archean crust. These authors divided the Archean evolution into four phases; the pre-Leonian phase (3.6-3.5 Ga), the Leonian phase (3.3-3.0 Ga), the Liberian phase (2.9-2.8 Ga) and a post-Liberian phase (<2.6 Ga).

The Pre-Leonian and Leonian phases are represented by grey gneisses and greenstone belts (Hurley et al. 1971; Beckinsale et al. 1980; Rollinson & Cliff 1982; Kouamelan et al. 1997; Thiéblemont et al. 2001, 2004). During the Liberian event the pre-Leonian and Leonian crust was subjected to medium-P granulite metamorphism, crustal anatexis and intruded by granites and charnockites. Although limited in its extent, Sm-Nd isotopic data from the west-central Ivory Coast indicate that magmatism during the pre-Leonian and Leonian phases was juvenile whereas Liberian magmatism was dominated by crustal reworking (Kouamelan et al. 1997).

Following the Liberian event there appears to have been little or no magmatic activity in the Man domain. Detrital zircon from minor supracrustal sequences (including banded iron formations) in Guinea indicate a maximum depositional age of circa 2.6 Ga (Billa et al. 1999; Thiéblemont et al. 2004) while their minimum age is bracketed by the Birimian event which affected the Man domain by circa 2.1 Ga at the latest, at which point the Archean crust had stabilized to form a craton (see section 2.2.3).

Milési et al. (1989) obtained an age of circa 2.49 Ga (Pb-Pb on zircon) from a granitoid boulder in Birimian sediment in the Ziemougoula area in northwestern Ivory Coast (fig. 5). While this age might possibly stem from mixing or Pb-loss there have been reports of 2.50-2.45 Ga granitoids from the Archean domain in the Reguibat shield (Schofield et al. 2012; Bea et al. 2013), which otherwise have a similar geological evolution to the Man domain (Potrel et al. 1996, 1998; Schofield et al. 2012). However, so far no such early Paleoproterozoic ages have been reported from the Man domain itself.

2.2.2 Birimian

2.2.2.1 Overview

Birimian crust is exposed primarily within the Baoulé Mossi domain (fig. 5), the exception being two small areas (e.g. Ity-Toulépleu) present in the southeastern Man domain. For this work, the Birimian crust is divided into three broad lithological groups: volcanic belts, sedimentary basins and granitoid-gneiss domains, which follows the classic lithostratigraphic divisions of Birimian rocks (e.g. Milési et al. 1989; Leube et al. 1990). The sedimentary basins can be further subdivided into deep and shallow water (including sub-aerial) basins depending on whether they contain sediment dominantly deposited in low or high-energy environments, respectively. The granitoid-gneiss domains are largely comprised of variably deformed intrusive rocks, which are equivalent in age and composition to those rocks that intrude the volcanic belts and sedimentary basins (Doumbia et al. 1998; Gasquet et al. 2003; Feybesse et al. 2006; Baratoux et al. 2011). Unfortunately, the manner in which the granitoid-gneiss domains are shown in figure 5 means that separate plutons within volcanic belts and sedimentary basins are lumped together with the larger continuous areas of intrusive rocks and gneisses, the latter of which correspond to the actual granitoid-gneiss domains.

The volcanic belts and deep water basins are equivalent to the volcanic and sedimentary greenstone

belts of Baratoux et al. (2011). The shallow water basins are equivalent to their Tarkwaian-type late basins. From a study on the geology of southern Ghana, Leube et al. (1990) interpreted the shallow water basin in the Ashanti belt to post-date Birimian deformation. Consequently, the authors placed them in a separate group called the Tarkwaian while the volcanic belts and other sedimentary basins were placed within the Birimian Supergroup. However, subsequent work on the Tarkwaian sediment in Ghana (Eisenlohr & Hirdes 1992) and other shallow water basins (Zitzmann 1997; Baratoux et al. 2011) have shown that they are affected by Birmian deformation. As such, the volcanic belts, deep water basins and shallow water basins may therefore be considered as part of an all inclusive Birimian Supergroup.

Granitoid-gneiss domains are the dominant lithological unit in the Baoulé Mossi domain and comprise approximately 50-60% of its total area (Milési et al. 1989). Volcanic belts and deepwater sedimentary basins together make up about 30% of the Baoulé Mossi domain; the remaining 10% is covered by shallow water basins. The São Luís Craton is comprised dominantly of granitoid-gneiss domains with subordinate volcanic and sedimentary supracrustals (Klein & Moura 2001).

The volcanic belts and sedimentary basins often have a linear — straight or arcuate — shape with a high aspect ratio. However, there are exceptions to this pattern as seen in the laterally extensive Comoé-Sunyani and Siguiri basins in Ivory Coast-Ghana and Guinea, respectively (fig. 5). As a whole, the Baoulé Mossi domain is characterized by a general north-northeast to south-southwest structural trend (e.g. Eisenlohr & Hirdes 1992; Hirdes et al. 1993; Pouclet et al. 2006; Baratoux et al. 2011; de Kock et al. 2012). Nevertheless, within this overall regional trend there may also be local variations between domains defined by different structural trends, e.g. northeast-southwest in southern Ghana and eastern Burkina Faso or north-south in western Burkina Faso and northeastern Ivory Coast.

The boundaries between the volcanic belts, sedimentary basins and granitoid-gneiss domains are usually tectonic and delineated by shear zones or faults (e.g. Milési et al. 1989; Liegéois et al. 1991; Gueye et al. 2007; Baratoux et al. 2011; de Kock et al. 2012). Gradual contacts between volcanic belts and sedimentary basins have been reported, e.g. between the Kumasi basin and Sefwi belt in southern Ghana (Leube et al. 1990; Hirdes et al. 1993). However, it has been shown that the rocks of Sefwi belt predate the opening of the Kumasi sedimentary basin (e.g. Feybesse et al. 2006). The apparent gradual contacts must therefore be due to other factors. This may include a thin sedimentary cover or post-depositional deformation which expose parts of the basement and may give the appearance of gradual contacts, in particular in areas with poorly exposed bedrock.

2.2.2.2 Volcanic belts

The volcanic rocks in the belts are dominantly tholeiitic basalts or basaltic-andesites but calc-alkaline dacites and rhyolites are also present, with either a bimodal or more gradual distribution (Attoh 1982; Mortimer 1992a, 1992b; Sylvester & Attoh 1992; Hirdes et al. 1993; Ama-Salah et al. 1996; Doumbia et al. 1998; Pawlig et al. 2006; Dampare et al. 2008; de Kock et al. 2009; Hein 2010; Baratoux et al. 2011). The felsic rocks may occur both as intercalated units with mafic volcanics (e.g. Milési et al. 1989; Mortimer 1992b) or as stratigraphically uppermost units grading from lower mafic volcanic rocks (e.g. Sylvester and Attoh 1992; Dampare et al. 2008; Baratoux et al. 2011). Pillow structures have been recognized across the Baoulé Mossi domain (Milési et al. 1989; Abouchami et al. 1990; Sylvester & Attoh 1992; Pawlig et al. 2006; Pouclet et al. 2006; Baratoux et al. 2011). Although high-Mg basalts occur in at least some belts (Mortimer 1992b; Sylvester & Attoh 1992) true komatiites do not appear to be present in the volcanic belts. However, such rocks are found in the Niandan volcanic range in the Siguiri basin (fig. 5, and see below). Baratoux et al. (2011) found plagioclase-porphyritic basalts in western Burkina Faso which in some cases were comprised of more than 90% plagioclase. The authors suggested that these rocks may be comparable to anorthosites.

Volcaniclastic rocks deposited in proximal to distal environments and which may be reworked into epiclastic successions appear to occur in all belts. Such rocks may be the predominant lithological unit in some belts, such as in Fétékro in central Ivory Coast (Mortimer 1992b) and Bole in northwestern Ghana (de Kock et al. 2009, 2012). The volcanic belts also contain subordinate sedimentary units similar to those found in the sedimentary basins (see below), e.g. shale, argillite, greywacke, sandstones, conglomerates as well as chemical sediment including manganese, carbonate and chert (Leube et al. 1990; Mortimer 1992b; Mucke et al. 1999; Pouclet et al. 2006; Vidal et al. 2009).

The presence of pillow lavas and hyaloclastites seen in volcanic sequences (e.g. Sylvester & Attoh 1992; Pouclet et al. 2006), in addition to sedimentary deposits such as shales and chemical sediments are consistent with deposition in an aquatic environment. Abouchami et al. (1990) suggested that the volcanic rocks formed in ocean basins based on the presence of pillow structures and sediment such as manganese deposits but also on the juvenile composition of mafic volcanic rocks. According to Mucke et al. (1999), the Nsuta manganese deposit in the southern Ashanti belt of Ghana was deposited in a shallow-marine environment.

Ages obtained from mafic and felsic rocks in the volcanic belts indicate that they formed early during the Birimian event. An amphibolitic lens in the Sefwi belts gave an age (K-Ar on amphibole) of 2222±32 Ma (Feybesse et al. 2006) while zircon ages

from rhyolites in Burkina Faso (Castaing et al. 2003, in Hein 2010) and Ghana (Hirdes & Davis 1998) have yielded ages of 2238±2 Ma (Pb-Pb) and 2189±1 Ma (TIMS), respectively. In the São Luís Craton, Klein et al. (2009) dated (Pb-Pb and SHRIMP on zircon) calc-alkaline dacites and rhyolites to 2160 Ma while Klein and Moura (2001) obtained an age of 2240±5 Ma (Pb-Pb on zircon) from a metapyroclastic rock.

2.2.2.3 Deep water sedimentary basins

The sedimentary basins are mainly siliciclastic, composed of turbiditic greywackes and mudstones, the latter may occasionally be carbonaceous (Milési et al. 1989, 1992; Hirdes et al. 1993; Vidal & Alric 1994; Doumbia et al. 1998; Pouclet et al. 2006; de Kock et al. 2009; Baratoux et al. 2011). However, some basins may also contain significant amounts of volcaniclastics as well as subordinate volcanic rocks and chemical sediment, which include manganese deposits and carbonates. Sediment within the deep water basins have been referred to as flysch-type sediment by several authors (e.g. Milési et al. 1989; Eishenlohr & Hirdes 1992; Feybesse et al. 2006). It was noted by Hirdes et al. (1993) that the transition between different types of sedimentary as well as volcaniclastic rocks in the Kumasi and Comoé-Sunyani basins in Ghana was gradual, reflecting that they represent different stages of reworking of the same source rocks.

Detrital zircon obtained from the deep water basins indicate maximum depositional ages of 2130-2120 Ma (Davis et al. 1994; Lüdtke et al. 1998, in Baratoux et al. 2011) for sedimentary basins in eastern Baoulé Mossi (fig. 5). However, basins to the west, including the Bandama-Banfora (Doumbia et al. 1998), Siguiri (Milési et al. 1989) and Dialé-Daléma (Milési et al. 1989; Hirdes & Davis 2002) include younger zircons indicating a maximum depositional age around 2100 Ma. The maximum and minimum ages of intrusive rocks also varies between different deep water basins. For example, in the Maluwe basin the peak of magmatism occurred between 2135-2118 Ma (de Kock et al. 2011), for the Kumasi and Haute-Comoé basins between 2116-2090 Ma (Hirdes et al. 1992; Hirdes et al. 1996; Oberthür et al. 1998) while activity in the Comoé-Sunyani (Hirdes et al. 1992; Zitzmann 1997), Bandama-Banfora (Doumbia et al. 1998), Siguiri (Milési et al. 1989; Lièbgeois et al. 1991; McFarlane et al. 2011) and Dialé-Daléma (Milési et al. 1989; Hirdes & Davis 2002) basins took place between 2100-2070 Ma.

Mafic to felsic volcanic and volcaniclastic rocks intercalated with the sediment have been reported from some basins, e.g. Siguiri (Tegyey & Johan 1989; Lahondère et al. 2002), Bandama (Doumbia et al. 1998; Pouclet et al. 2006), Maluwe (de Kock et al. 2009, 2012) and Kumasi (Adadey et al. 2009). Mafic and felsic dykes have also been reported from different basins such as Comoé-Sunyani (Feybesse et al. 2006) and Kumasi (Yao & Robb 2000; Feybesse et al. 2006). Yao & Robb (2000) reported dolerite dykes near Obuasi in the east-central Kumasi basin which were cut by granitoids dated to circa 2.10 Ga by Oberthür et al. (1998).

Notable areas of volcanic rocks within deep water basins are the Hérémakono, Niandan and Keniero volcanic ranges in the Siguiri basin in central Guinea, the Falémé belt in eastern Senegal and the Asankangrawa belt in the Kumasi basin in southern Ghana (fig. 5). The Niandan and Keniero volcanic ranges were deposited in the Siguiri basin around 2.09 Ga and are coeval with the other widespread intrusive and extrusive magmatism in that part of Baoulé Mossi (e.g. Milési et al. 1989; Liégeois et al. 1991; Egal et al. 2002). The Niandan range is composed of a komatiitic to basaltic volcanic suite (Tegyey & Johan 1989). Such rocks appear to be absent elsewhere within the Baoulé Mossi domain with the possible exception of scattered outcrops in the northern Ivory Coast (Milési et al. 1989). The Keniero range is instead composed of bimodal volcanics where basaltic rocks show an affinity with rift-related mafic rocks (Lahondère et al. 2002, and references therein). The Falémé (Hirdes & Davis 2002) and Hérémakono (Lahondère et al. 2002) belts contain intermediate to felsic volcanic rocks along with abundant volcaniclastic rocks. The Dialé-Daléma and Siguiri deep water basins — which the aforementioned belts occur within (fig. 5) — in places also contain significant volcaniclastic deposits (Hirdes & Davis 2002; Lahondère et al. 2002). This is also the case for the Asankangrawa belt and the Kumasi basin (Hirdes et al. 1993; Agyei Duodu et al. 2009).

Many lines of evidence indicate that the sedimentary rocks of the deep water basins are derived from the volcanic belts. This includes the presence of clasts of intrusive rocks found in neighboring volcanic belts (Feybesse et al. 2006), the distribution of detrital zircon data equivalent to the magmatic ages of intrusive and volcanic rocks of the belts (Davis et al. 1994; Doumbia et al. 1998; Lüdtke et al. 1998, in Baratoux et al. 2011) and the chemical composition of the sediment, which indicates derivation from both mafic and felsic rocks (Asiedu et al. 2009). The sedimentary basins were likely deposited in marine basins (e.g. Leube et al. 1990; Egal et al. 2002; Vidal et al. 2009) although there does not appear to be any studies investigating temporal changes in the depositional environment with possible transitions between marine and lacustrine settings.

2.2.2.4 Shallow water sedimentary basins

The shallow water basins are filled with siliciclastic sediment dominantly made up of sandstones and conglomerates with subordinate mudstones (e.g. Milési et al. 1989; Leube et al. 1990; Bossière et al. 1996; Zitzmann 1997; Pigois et al. 2003; Perrouty et al. 2012). The basins are interpreted to have been deposited in a subaerial, fluviodeltaic, possibly lacustrine environment (Zitzmann 1997; Pigois et al. 2003) and are often referred to as molasse-type sediment (e.g. Milési et al. 1989; Turner et al. 1993; Eisenlohr & Hirdes 1992;

Feybesse et al. 2006). Detrital zircon studies from deposits in western Burkina Faso (Bossière et al. 1996) and the Tarkwaian basin in the Ashanti belt in southern Ghana (Davis et al. 1994; Pigois et al. 2003) indicate maximum depositional ages between 2.13-2.12 Ga.

The shallow water deposits in the Tarkwaian basin located in the Ashanti belt of southern Ghana (fig. 5) are intruded by a post-collisional K-feldspar porhyritic granite (Oberthür et al. 1998) and dolerite-gabbro sills (Pigois et al. 2003; Adadey et al. 2009), both of which have been dated to circa 2.10 Ga. Unlike the Tarkwaian basin, other shallow water basins have not been intruded by igneous rocks e.g. the sediment located in the Bui belt in west-central Ghana (Zitzmann 1997).

The basins are mostly found in association with volcanic belts which they unconformably overlie (e.g. Leube et al. 1990; Pigois et al. 2003; Baratoux et al. 2011) However, exceptions to this relationship also exist, as exemplified by the deposits in the Bui belt that overlie the sediment found within the Maluwe deep water basin to the north (fig. 5), with which they have a gradual or weakly unconformable contact (Zitzmann 1997). Nevertheless, the Bui belt is also spatially associated with elongate bands of mafic volcanics which are parallel with the shallow water deposits.

The shallow water basins are reported to contain clasts of intrusive, felsic volcanic and sedimentary rocks as well as rare mafic volcanics, some of which are deformed (Milési et al. 1989; Eishenlohr & Hirdes 1992; Turner et al. 1993; Pigois et al. 2003). These clasts are interpreted to have been derived from older Birimian rocks. This is also supported by ages obtained from detrital zircon, which fall between 2240-2120 Ma (Davis et al. 1994; Bossière et al. 1996; Pigois et al. 2003).

2.2.2.5 Intrusive rocks

Intrusive rocks within the Baoulé Mossi domain exhibit a wide range of compositions. In general, the older intrusive rocks (older than about 2.15 Ga) are described as belonging to the tonalite-trondhjemite-tonalite suite (TTGs), commonly containing mafic enclaves. Younger rocks are usually more K-rich with more abundant sedimentary xenoliths (e.g. Boher et al. 1992; Hirdes et al. 1992; Doumbia et al. 1998; Gasquet et al. 2003; Dioh et al. 2006; Pouclet et al. 2006; Lompo et al. 2009; Baratoux et al. 2011). In addition to quartz and feldspar, biotite, muscovite, amphibole and clinopyroxene are common minerals found in Birimian intrusive rocks. Cordierite appears to be absent. Similarities in composition and age suggest that the granitoid-gneiss domains may be middle crustal equivalents to the volcanic belts. Intrusive magmatism was ongoing throughout the Birimian event and magmatic ages overlap magmatic activity seen among volcanic rocks within the volcanic belts and the sedimentary basins. However, the available ages may not have been obtained from spatially associated rocks.

There has been a range of classification schemes proposed for Birimian intrusive rocks, e.g. the classic belt and basin classification used primarily in Ghana (e.g. Leube et al. 1990). However, these classification schemes are only appropriate for certain areas and fail to incorporate the compositional and structural diversity of intrusive rocks from the entire Baoulé Mossi domain. For example, it was recently argued by de Kock et al. (2009) that the belt and basin classification should be discarded because the criteria it used (based on rocks in southern Ghana) could not be applied in any meaningful way to intrusive rocks in northwestern Ghana.

Although generally referred to as TTGs, granites and monzogranites are also are also present among older intrusive rocks, although they appear to be restricted to around 2200-2190 and 2160-2150 Ma, respectively, at least in eastern Baoulé Mossi (Feybesse et al. 2006; Klein et al. 2008; de Kock et al. 2009, 2011). As such, the magmatism during the early part of the Birimian event broadly defines a gabbro-diorite-tonalite-granodiorite-granite suite, although dominated by more sodic compositions. The monzogranites represent a late pulse of more syenitic magmatism. Ultramafic rocks have also been reported from volcanic belts, at least in Ghana (Loh & Hirdes 1999; Attoh et al. 2008), the Ivory Coast (Pouclet et al. 2006) and Burkina Faso (Béziat et al. 2000).

Intrusive rocks from the latter part of the Birimian event (younger than about 2.15 Ga) are found in both volcanic belts, granitoid-gneiss domains as well as in the sedimentary basins that were opened at this time. Although K-rich intrusive rocks become more common during the later part of the Birmian event, it would be wrong to say that this corresponds to a trend. Indeed, a more apt description might be that the compositional spectrum of Birimian intrusive rocks widens, reflecting the appearance of large sedimentary basins and more extensive crustal reworking which provides new and more enriched source rocks (Hirdes et al. 1992; Doumbia et al. 1998; Gasquet et al. 2003; Dioh et al. 2006; de Kock et al. 2009; Baratoux et al. 2011).

The appearance of extensive sedimentary sequences in the source region of magmatic rocks is reflected by the intrusion of leucogranites and granites in sedimentary basins, with gradual transition into migmatites in the surrounding sediment (e.g. Hirdes et al. 1993; Doumbia et al. 1998; Klein et al. 2008; Vidal et al. 2009). Monzogranite and K-rich granites are also common (Agyei Duodu et al. 2009; Baratoux et al. 2011), e.g. the Tenkodogo-Yamba (Naba et al. 2004) and the Tonton (Adadey et al. 2009) plutons. Tonalites, trondhjemites and granodiorites are also present in the latter part of the Birimian event, e.g. in the Kumasi basin (Hirdes et al. 1996; Doumbia et al. 1998; Oberthür et al. 1998).

The high-Mg Bomburi pluton and late gabbro

and alkaline intrusion in the Maluwe basin (de Kock et al. 2009), along with the sanukitoid-like Palimé-Amlamé pluton in Togo (Agbossoumondé et al. 2007) show that some intrusive rocks were derived from mantle sources also during the later stages (2130-2120 Ma) of the Birimian event. In southern Mali, Liégeois et al. (1991) identified a magmatic suite dated between 2100-2070 Ma which characterized a high-K calc-alkaline trend including syeno-, monzo- as well as alkali-granites. Granites from this suite display mixing relationships with a mafic component.

Late K-rich and alkaline intrusions have been reported by some workers. Examples include the Ninakri syenites (including both quartz saturated and undersaturated variants) in central Ivory Coast (Doumbia et al. 1998) and a 2097±3 Ma (TIMS on zircon) K-feldspar phyric intrusion in the northern Ashanti belt (Leube et al. 1990; Oberthür et al. 1998, Agyei Duodu et al. 2009). Late alkaline intrusions dated at circa 1.9-1.8 Ga have also been reported from Burkina Faso (Castaing et al. 2003, in Vegas et al. 2008). Multiple generations of pegmatites, leuco- and microgranitic dykes and quartz veins are also common in many areas (e.g. de Kock et al. 2012)

There is no direct correlation between the age and degree of deformation among different generations of intrusive rocks. Older intrusive rocks in Ghana are commonly more or less undeformed (Leube et al. 1990) while coeval rocks in northwestern Ghana (de Kock et al. 2012) or western Burkina Faso (Baratoux et al. 2011) might record multiple periods of deformation. P-T data obtained by Doumbia et al. (1998) and Lompo (2010) from intrusive rocks in the Ivory Coast and Burkina Faso indicate that they crystallized at pressures between 2-6 Kbar. In Burkina Faso, Béziat et al. (2000) estimated that ultramafic-gabbroic cumulate rocks had crystallized in a magma chamber where pressure exceeded 8 Kbar.

2.2.2.6 Lithostrathigraphy and geochronology

The lithostrathigraphy of the Baoulé Mossi domain, and in particular the relative position (upper or lower) of the volcanic belts and sedimentary basins, has been a controversial subject (e.g. Milési et al. 1989, 1992; Mortimer 1992b; Hirdes et al. 1996). However, since precise radiometric ages have become more widely available it has been shown that the volcanic belts predate the sedimentary basins in their respective area (e.g. Hirdes et al. 1992, 1996; Doumbia et al. 1998; Gasquet et al. 2003; Feybesse et al. 2006; Gueye et al. 2007; Klein et al. 2008, 2009; de Kock et al. 2011; Tapsoba et al. 2013). Volcanics and syn-volcanic granitoids in the volcanic belts have been dated between ca 2240-2070 Ma whereas the sedimentary basins host younger volcanics and granitoids between 2130-2070 Ma. The granitoid-gneiss domains exhibit the same range of ages as the volcanic belts. Limited detrital zircon studies from the Kumasi (Davis et al. 1994; Oberthür et al. 1998), Boromo (Lüdtke et al. 1998, in Baratoux et al. 2011), Bandama (Doumbia et al. 1998) and Dialé-Daléma (Milési et al. 1989) basins show maximum depositional ages between 2135-2100 Ma.

There are only a handful of magmatic ages younger than 2070 Ma in the Baoulé Mossi domain showing the lack of magmatic activity after this period (e.g. Gueye et al. 2007; de Kock et al. 2011). Hydrothermal xenotime associated with the large lode-gold deposits in the Ashanti belt has been dated to 2063±9 Ma (SHRIMP on xenotime, Pigois et al. 2003) while diamond-bearing volcaniclastic dykes intruded the Cape Coast basin at 2029±22 Ma (TIMS on titanite, Delor et al. 2004). K-Ar and $^{40}Ar/^{39}Ar$ cooling ages from amphibole, biotite and muscovite from the KKI (Gueye et al. 2007) and southeastern Ghana (Chalokwu et al. 1997; Feybesse et al. 2006) cluster around 2050-1900 Ma which records the fading thermal effect of the Birimian event.

Although early geochronological data indicated a trend of progressively younger ages from the southeast towards the northwest within the Baoulé Mossi domain (Hirdes et al. 1992, 1996; Hirdes & Davis 2002) an increasing amount of geochronological data have shown a more complex distribution of ages (de Kock et al. 2011). Hirdes et al. (1996) divided the Man-Leo shield and KKI into two subprovinces based on the — at the time — available geochronology. These subprovinces were the eastern "Birimian" province which contained older ages (2185-2150 Ma) compared to the younger western "Bandamian" (<2105 Ma) province. Hirdes et al. (1996) proposed that they were separated by a roughly north-south boundary running through western Burkina Faso and central Ivory Coast. However, since then ages between 2210-2150 Ma have been reported from the Mako belt of the KKI (Dia et al. 1997; Gueye et al. 2007) and northern Guinea (Lahondère et al. 2002), all of which fall within the "Bandamian" subprovince as envisaged by Hirdes et al. (1996). Although this shows that the Man-Leo shield and KKI cannot be divided into two age provinces as originally proposed by Hirdes et al. (1996) their division highlights that there are differences between the western and eastern parts of this area in that the former — including Guinea (Milési et al. 1989; Liégeois et al. 1991; Egal. et al. 2002), northwestern Ivory Coast (Milési et al. 1989) and eastern KKI (Milési et al. 1989; Hirdes & Davis 2002) — is generally younger (<2100 Ma) than the eastern part of the Baoulé Mossi domain. Also, as pointed out by Hirdes and Davis (2002), there appears to be a difference in the maximum depositional ages obtained from detrital zircon in different sedimentary basins with apparent older ages in southeastern Baoulé Mossi (2130 Ma in the Kumasi basin) and younger (2110 to 2100 Ma) ages towards the northwest.

The classic lithostratigraphic division of Birimian supracrustals, in which they are grouped in a volcanic or a (volcano-) sedimentary unit, is a simplification that masks the fact that there may also be significant variations within these two broad units, both

in terms of their rock makeup as well as their age (e.g. Mortimer 1992b; de Kock et al. 2012). In other words, the two units may contain volcanic belts or sedimentary basins that do not share a common geological history as they experienced different types of magmatic and tectonothermal activity at different times during the course of the Birimian event (e.g. Mortimer 1992b; Turner et al. 1993; de Kock et al. 2012). For example, the Maluwe, Comoé-Sunyani and Kumasi basins in Ghana and the Ivory Coast may all be characterized as deep water sedimentary basins but their main intrusive magmatic phases are recorded between 2135-2118 Ma (de Kock et al. 2011), 2095-2080 Ma (e.g. Hirdes et al. 1992, 2007; Zitzmann 1997) and 2116-2090 Ma (e.g. Hirdes et al. 1992; Oberthür et al. 1998; Adadey et al. 2009), respectively.

A source of some confusion, at least historically, is the presence of volcanic "belts" within the sedimentary basins. These include the Hérémakono, Niandan and Keniero volcanic ranges in western Guinea (Lahondère et al. 2002), the Falémé belt in eastern Senegal (Hirdes & Davis 2002) and the Asankangrawa belt in the Kumasi basin (Leube et al. 1990). While these "belts" are coeval with the basins in which they occur, early workers (e.g. Milési et al. 1989; Leube et al. 1990) considered them as belonging to the volcanic belts (*sensu stricto*). Their intrusive relationship with the sedimentary basins was thus an important reason for considering the sedimentary basins as the oldest unit. Although this has proved to be wrong, as the volcanic belts (*sensu stricto*) have been shown to be the oldest, the presence of volcanic rocks within the sedimentary basins nevertheless highlight that volcanic activity was active throughout the Birimian event. As the volcanic rocks within the sedimentary basins have been linked to crustal extension (Milési et al. 1989; Leube et al. 1990; Lahondère et al. 2002), it also shows that this process was important for some volcanic activity during the Birimian event.

In a similar manner, it is also generally recognized that different shallow water basins may not be coeval, although they generally assume an uppermost stratigraphic position within their respective area (Milési et al. 1989; Eishenlohr & Hirdes 1992; Turner et al. 1993; Bossière et al. 1996; Baratoux et al. 2011; Perrouty et al. 2012). In western Burkina Faso, Baratoux et al. (2011) proposed that this type of sediment (which they called Tarkwaian-type) may be lateral facies equivalents to the deepwater sediments deposited in a more proximal setting.

2.2.2.7 Timing of crustal growth

The Baoulé Mossi domain has been shown to be largely juvenile (Abouchami et al. 1990; Boher et al. 1992; Ama-Salah et al. 1996; Doumbia et al. 1998; Gasquet et al. 2003; Pawlig et al. 2006; Klein et al. 2008; Tapsoba et al. 2013). Sm-Nd model ages tend to be no more than 100-300 Ma older than the magmatic age of the sampled rocks. The exception are Birimian granitoids from southeastern Ghana (Leube et al. 1990) and southern Togo (Agbossoumondé et al. 2007) which have been shown, on the basis of Sm-Nd isotopic data, to have been derived from an older, Archean source.

Because of their higher metamorphic grade and migmatitic nature it was proposed by some early workers (Milési et al. 1989, and references therein) that gneisses in the granitoid-gneiss complexes corresponded to the basement of the Birimian supracrustals in the volcanic belts and sedimentary basins. These gneisses, called "Dabakalan" after their type-locality in central Ivory Coast, were proposed to have formed during a pre-Birimian event called the "Burkinian" (Hirdes et al. 1996, and references therein). These gneisses have subsequently been shown to be coeval with the volcanic belts and are thus high-grade equivalents of other Birimian rocks (Boher et al. 1992; Mortimer 1992b; Hirdes et al. 1996). Nevertheless, Gasquet et al. (2003) obtained an age of 2312±17 Ma (SIMS) from a zircon core in a granitoid from the Dabakala area. Since the age of this core coincides with a peak in model ages of Birimian rocks it was proposed by Gasquet et al. (2003) that it recorded an early (circa 2.3 Ga) phase of crustal growth in the Baoulé Mossi domain.

2.2.2.8 Metamorphism

The Birimian crust of the Baoulé Mossi domain has been regionally metamorphosed in greenschist-amphibolite facies conditions (Milési et al. 1992; Hirdes et al. 1993; John et al. 1999; Klemd et al. 2002; Feybesse et al. 2006; Kříbek et al. 2008; Vidal et al. 2009; Lompo 2010; Baratoux et al. 2011). The metamorphic conditions are relatively evenly distributed and there appear to be no major inverse metamorphic gradients (Vidal et al. 2009; Lompo 2010; Baratoux et al. 2011). The volcanic belts tend to have a higher metamorphic grade at greenschist-amphibolite facies conditions compared to the sedimentary basins which commonly are metamorphosed in greenschist facies or even at lower grade conditions (Liegéois et al. 1991; Doumbia et al. 1998; Feybesse et al. 2006; de Kock et al. 2009). However, amphibolite facies metamorphism has also been reported from the contacts of granitoid intrusions in the sedimentary basins (Hirdes et al. 1993; Doumbia et al. 1998; Vidal et al. 2009).

Quantitative and inferred P-T data obtained from regional and contact metamorphic rocks in southern Ghana (Opare-Addo et al. 1993; John et al. 1999; Klemd et al. 2002; Galipp et al. 2003), northwestern Ivory Coast (Caby et al. 2000) and northeastern Burkina Faso (Debat et al. 2003) generally record conditions between 4-6 kbar and 500-650°C. However, temperatures around 700-800°C were recorded by Opare-Addo et al. (1993) in the Suhum basin of southeastern Ghana and by Caby et al. (2000) in northwestern Ivory Coast. Both areas were reported by the authors to be migmatitic. Additionally, pressure estimates obtained by Opare-Addo et al. (1993) from the Suhum basin ranged between 5-8 kbar and thus reach higher pres-

sures compared to the other studies within the Baoulé Mossi domain. In southern Ghana, both John et al. (1999) and Galipp et al. (2003) interpreted the amphibolite grade rocks they investigated (in the Ashanti and Sefwi belts, respectively) to have followed a clockwise P-T-t path and retrograde movement characterized by simultaneous cooling and decompression.

There appears to be a tendency for high-grade domains to occur in association with Archean crust. In southern Ghana, Opare-Addo et al. (1993) noted that migmatites in the Suhum basin recorded high P and T compared with intrusive rocks in the Ashanti belt. Vidal et al. (2009) distinguished a sillimanite isograd around the SASCA domain of southwestern Ivory Coast implying that higher grade conditions prevailed in this domain. As will be further discussed in section 2.2.3 high grade conditions were also obtained in the southeastern Man domain along the contact with the Baoulé Mossi domain. These high grade conditions contrast with the generally lower grade conditions of Birmian crust elsewhere in the Baoulé Mossi domain although this may also be due to lack of data.

No primary high pressure-low temperature assemblages have so far been reported from the Baoulé Mossi domain. However, a relict blueschist facies mineral assemblage (formed at 10-12 kbar and 400-450°C) in greenschist facies volcaniclastic sediment from south-central Burkina Faso have been reported by Ganne et al. (2012). The authors suggested that such assemblages may have been more widespread but have been overprinted by later thermal events.

Because of the lack of apparent metamorphic gradients, the prevalence of greenschist-amphibolite facies metamorphic conditions, extensive transcurrent shearing and long-lived magmatism it has been argued that the crust of the Baoulé Mossi domain must have been thin and warm during the Birimian event (Vidal et al. 2009; Baratoux et al. 2011). The inferred presence of vertical tectonics also requires a weak crust in order to facilitate gravity-induced movements which were recognized by Vidal et al. (2009) in the Nassian domain of northeastern Ivory Coast.

Using thermal modelling, Harcoüet et al. (2007) estimated a mantle heat flow value of circa 30 mW/m2, corresponding to a temperature of 800-900°C at a crustal depth of about 30 km, for southern Ghana at 2.1 Ga. These authors noted that such a value is 2-3 times higher compared to stable cratons with a thick lithosphere. Chardon et al. (2009) considered the Birimian crust to be an example of an ultra-hot orogen, implying a thin lithosphere with Moho temperatures greater than 900°C.

2.2.2.9 Shear zones and faults

The Baoulé Mossi domain is crosscut by abundant shear zones and faults (fig. 5). There has been a debate concerning whether shallow thrusting or subvertical shear zones dominate the structural makeup of the Baoulé Mossi domain. Milési et al. (1989) and Feybesse and Milési (1994) described a generalized structural evolution for the Baoulé Mossi domain in which an early deformational phase (D1) led to crustal thickening through thrusting while two subsequent deformational phases (D2-3) were instead characterized by the development of extensive shear zones. According to these authors, the intensity of the different deformational phases varied in time and place within in the Baoulé Mossi domain, with some areas recording mainly one of the deformational phases.

The model by Milési et al. (1989) and Feybesse and Milési (1994) have been challenged by later workers who point to the lack of field evidence for extensive shallow thrusts (e.g. Vidal & Alric 1994; Kouamelan et al. 1997; Baratoux et al. 2011) as well as coupled structural and geochronological data that shows complex deformational histories in regions which involve multiple generations of shearing (Gasquet et al. 2003; de Kock et al. 2012). In addition, new structural data also indicate that deformation has been active throughout the Birimian event, extending back to at least 2.20 Ga (Gueye et al. 2008; de Kock et al. 2012; Perrouty et al. 2012). Based on structural data from synkinematic intrusive rocks in central Ivory Coast, Gasquet et al. (2003) suggested that their study area had been subjected to the same strain pattern for close to 120 Ma. This broadly corresponded to northwest-southeast to north-northwest-south-southeast compression and is recorded as discrete deformational events related to magmatic activity or formation of sedimentary basins.

While thrusting may not have occurred on a regional scale along shallow faults, reverse movements and thrusting have nevertheless been reported in association with transpressive shear zones (Vidal & Alric 1994; Egal et al. 2002; Perrouty et al. 2012). In southern Ghana, Feybesse et al. (2006) reported that thrusting had led to the emplacement of high grade rocks on underlying lower grade rocks, suggesting that significant displacement have occurred. Thrusting followed by sinistral shearing has also been reported from the Ashanti fault which marks the contact between the Kumasi basin and Ashanti belt in Ghana (Perrouty et al. 2012).

Faults and shear zones within the Baoulé Mossi domain may form anastamosing networks, such as the Sassandra shear zone in Guinea (Egal et al. 2002) or shear zones in Burkina Faso (Chardon et al. 2009; Baratoux et al. 2011). However, they might also be more localized, such as the Ashanti fault in Ghana (e.g. Perouty et al. 2012). Faults and shear zones sometimes show signs of reactivation. Perrouty et al. (2012) proposed that the Ashanti fault could have utilized a detachment fault formed during the opening of the Kumasi basin while different generations of shearing with opposing sense of displacement have been reported from the Banifin (Liégeois et al. 1991) and Markoye (Tshibubudze et al. 2009) shear zones.

Most north-south trending shear zones within the Baoulé Mossi domain, such as the N'Zi-Brabo (Mortimer 1992b; Doumbia et al. 1998), Ouango-

Fitini (Vidal and Alric 1994; Gasquet et al. 2003), Banifin (Liégeois et al. 1991) and Markoye (Tshibubudze et al. 2009) record sinistral lateral displacement (fig. 5). However, the Markoye shear zone was also subject to earlier dextral movement (Tshibubudze et al. 2009) while the Banifin shear zone was reactivated through dextral displacement following the main Birimian event (Liégeois et al. 1991). In the Baoulé Mossi domain, northeast-southwest trending shear zones can be both sinistral and dextral. The extension of the Sassandra shear zone in Guinea stands out by having a northwest-southeast orientation (Egal et al. 2002), although it is sinistral as its extension into the Ivory Coast where it also bends into a north-south orientation (Kouamelan et al. 1997).

Late (<2150 Ma) deformation within the Baoulé Mossi domain is attributed by many authors to west-east or northwest-southeast compression (e.g. Eishenlohr and Hirdes 1992; Feybesse & Milési 1994; Feybesse et al .2006; Baratoux et al. 2006; de Kock et al. 2012). However, Egal et al. (2002) noted that the sinistral displacement along the northwest-southeast trending Sassandra fault in Guinea required northeast-southwest compression. The orientation of the stress field during the later of the Birmian event was thus clearly not equal across the Baoulé Mossi domain. Early (>2150 Ma) deformational phases recognized within the Baoulé Mossi domain instead record north-south or northeast-southwest compression which further highlights the complex deformational history of the Baoulé Mossi domain (Tshibubudze et al. 2009; Perrouty et al. 2012).

There are few estimates of relative displacement along the shear zones developed during the Eburnean orogeny. Mortimer (1992b) estimated that 40 km of sinistral displacement had taken place along the north-south N'Zi-Brabo shear zone in central Ivory Coast (fig. 5). He based this estimate on the apparent relative displacement between two sections of the Fétékro belt. Recently, Jessell et al. (2012) proposed that extensive shearing (up to 400 km) has occurred along a northeast-southwest oriented shear zone located at the contact between the Sefwi belt and Sunyani-Comoé basin which they called the Sefwi-Sunyani-Comoé (SSC) shear zone (fig. 5). They argued that this took place after the emplacement and crystallization of the abundant two-mica leucogranites in the Sunyani-Comoé basin which have been dated between 2095-2080 Ma (e.g. Hirdes et al. 1992; Yao et al. 1995, in Vidal et al. 2009). As to the sense of displacement, Jessell et al. (2012) proposed that it was dextral but also acknowledged the lack of reliable kinematic indicators to support that conclusion.

2.2.2.10 Geodynamic evolution

The Baoulé Mossi domain has been subjected to multiple tectonometamorphic events and records a complex deformational history. The main phase of tectonometamorphic activity occurred between circa 2130-2070 Ma and is commonly referred to as the Eburnean orogeny (e.g. Feybesse et al. 2006; Gueye et al. 2008; Baratoux et al. 2011; de Kock et al. 2012). Older tectonometamorphic events (>2150 Ma) have also been recognized in Ghana (de Kock et al. 2009, 2012; Perrouty et al. 2012), Burkina Faso (Boher et al. 1992; Tshibubudze et al. 2009; Hein 2010) and the Mako belt of the KKI (Gueye et al. 2008). However, the understanding of these early events is relatively poor due to scarce outcrops and overprinting by later events.

The Eburnean orogeny is comprised of polyphase deformation and metamorphism which led to folding and the development of multiple generations of shear zones and faults (e.g. Gasquet et al. 2003; Feybesse et al. 2006; Hein 2010; Baratoux et al. 2011; Perrouty et al. 2012). Deformation during the Eburnean orogeny was also accompanied by intrusion of multiple generations of granitoids (e.g. Gasquet et al. 2003; Baratoux et al. 2011; de Kock et al. 2012). It affected all lithological units within the Baoulé Mossi domain (including the late shallow water deposits). However, its intensity varies and some areas are largely unaffected, such as the Nassian domain in northeastern Ivory Coast (Vidal et al. 2009).

Geodynamic models for the Baoulé Mossi domain can be broadly divided into two phases, regardless of which tectonic setting (plate tectonic or "archaic") they favor (e.g. Vidal et al. 1996, 2009; Feybesse et al. 2006; Pouclet et al. 2006; de Kock et al. 2009, 2012; Lompo 2009, 2010; Baratoux et al. 2011; Perrouty et al. 2012).

The first phase, called the Pre-Eburnean by Feybesse et al. (2006) or Eoeburnean by de Kock et al. (2009, and used here), involves the formation of volcanic belts and coeval granitoids in an intra-oceanic environment which may have begun as early as circa 2.35 Ga (Gasquet et al. 2003; Feybesse et al. 2006) and lasted until around 2.15-2.13 Ga. This phase involved multiple periods of both compressional and extensional deformation (de Kock et al. 2009, Perrouty et al. 2012; Hein 2010). According to Feybesse et al. (2006), the Eoeburnean phase in southern Ghana ended with the intrusion of abundant monzogranites between 2.16-2.15 Ga, which they considered as the establishment of continental crust. Klein et al. (2008, 2009) noted a progressive maturation of magmatic rocks in the São Luís Craton during the Eoeburnean, which they interpreted to reflect the growth of a volcanic arc.

The second phase comprises the formation of sedimentary basins followed by regional deformation during the Eburnean orogeny, starting at circa 2130 Ma. The sedimentary basins are commonly interpreted to have formed during extension or transtension of the Eoeburnean crust (Vidal & Alric 1994; Feybesse et al. 2006; de Kock et al. 2012; Perrouty et al. 2012). In these cases, the formation of the basins is often considered as a transitional period between the Eoeburnean phase and the subsequent Eburnean orogeny. Closure of the basins may also have been partly simultaneous with sedimentation (Feybesse et al. 2006). However,

in western Burkina Faso, Baratoux et al. (2011) proposed that the Boromo, Houndé and Banfora basins could have formed in synclines developed during sustained regional compression. In that case, the establishment of the basins does not represent a distinct stage during the geodynamic evolution of the Baoulé Mossi domain but rather the result of continuous convergence.

2.2.3 Man and Baoulé Mossi contact

Milési et al. (1989) and Feybesse and Milési (1994) argued that the Man and Baoulé Mossi contact corresponded to a modern-style fold and thrust belt in which nappes of Birimian rocks had been thrust onto the Archean crust of the Man domain. However, this view has been challenged by subsequent workers in the region (Kouamelan et al. 1997; Egal et al. 2002; Pitra et al. 2010) who have not found field evidence for thrusting as required by the model of Milési et al. (1989) and Feybesse and Milési (1994). They have instead pointed to structures which indicate lateral sinistral displacement between the Man and Baoulé Mossi domains along subvertical shear zones in which thrusts are absent or only assume a subordinate role.

On the basis of the recent work carried out along the Man and Baoulé Mossi contact it seems as if it can be divided into two parts; one located in the southeast and another in the north. These will be discussed separately below. However, it should be kept in mind that data from the contact is scarce and the understanding of its structure and evolution thus remains poor.

2.2.3.1 Southeastern contact

Working in the Ivorian part of the Man domain, Kouamelan et al. (1997) recognized that it could be divided into two parts, separated by the Man-Danané shear zone (fig. 5). The southern part has a strong Birimian tectonometamorphic overprint while the northern one is less affected, preserving older Archean structures and metamorphic conditions. The southern part also includes the Ity-Toulépleu domain (fig. 5) which is a fault bounded volcano-sedimentary basin intruded by a juvenile ($\varepsilon Nd_{2.1}$ Ga 3.0-2.7) tonalite (the Ity-Toulépleu massif) dated by Kouamelan et al. (1997) to 2104±3 Ma (Pb-Pb on zircon). Prior to dating of the Ity-Toulépleu massif it was considered to be Archean by Feybesse et al. (1990) who proposed that the Birimian supracrustals were allochthonous, forming a klippe (i.e. the remnants of a nappe) of Birimian crust.

Thermobarometric studies from the southeastern Man domain show that it was subjected to HP-HT (750-1000°C and 13-14 kbar) metamorphism during the Birimian event (Triboulet & Feybesse 1998; Pitra et al. 2010). In addition, Triboulet and Feybesse (1998) reported a counter-clockwise P-T-t path based on two metabasitic samples with lower peak P-T conditions at 6.5-8 kbar and 630-670°C. Pitra et al. (2010) also reported a cooling path from peak conditions at 13 kbar and 750°C to <7 kbar and 700-800°C.

Temporal constraints on the Birimian tectonometamorphic overprint in the southeastern Man domain is provided by Kouamelan et al. (1997) and Cocherie et al. (1998). Kouamelan et al. (1997) dated high-grade rocks (granulite, kinzigite, migmatite) using Sm-Nd isochrons (whole rock, garnet, feldspar) and obtained ages between 2250-2200 Ma and 2050-2030 Ma. Cocherie et al. (1998) also obtained ages between 2050-2030 Ma on monazites (electron microprobe (EMP)) from migmatitic gneisses. The 2250-2200 Ma regressions from Kouamelan et al. (1997) have high MSWD (17-25) and could be rotated due to mixing between Archean and Birimian components. This interpretation is supported by an age of 2048±44 Ma (EMP on monazite) which Cocherie et al. (1998) obtained from a sample that Kouamelan et al. (1997) dated to 2203±21 Ma using a Sm-Nd isochron (garnet, whole rock, plagioclase). Ages between 2050-2020 Ma have also been obtained from granitoids (SHRIMP on zircon) and gneisses (SHRIMP on zircon rims) in southeastern Guinea (Thiéblemont et al. 2004).

The monazite ages obtained by Cocherie et al. (1998) were interpreted to record migmatization, which is further supported by the presence of coeval granitoids from southeastern Guinea dated to 2050-2020 Ma (Thiéblemont et al. 2004). Pitra et al. (2010) proposed that this migmatization was contemporaneous with the peak P-T conditions they had estimated at 13 kbar and 750°C. The metabasitic sample Pitra et al. (2010) studied had previously been dated to 2031±13 Ma by Kouamelan et al. (1997) using a Sm-Nd isochron (garnet, whole rock, plagioclase). According to Pitra et al. (2010) this age could either record the peak or retrograde conditions they had obtained from their thermobarometric study since the closure temperature of Sm-Nd in garnet (700-800°C) straddles the metamorphic temperatures they had estimated.

Pitra et al. (2010) also discussed the possibility that the HP-HT granulite facies conditions they obtained could instead be Archean while the retrograde conditions corresponded to a Birimian overprint. However, they considered this unlikely because of the lower pressure conditions previously reported from Archean rocks (e.g. Kouamelan et al. 1997) and the striking clustering of ages from high-grade metamorphic rocks at 2.05-2.03 Ga while Archean ages are absent. Also, the rocks investigated by Pitra et al. (2010) are associated with granulitic supracrustal sequences similar to those in Guinea which, based on detrital zircon ages, are interpreted to have been deposited after 2.6 Ga (Billa et al. 1999; Thiéblemont et al. 2004). If the supracrustals in the Ivory Coast are indeed coeval with those in Guinea then they postdate the 2.9-2.8 Ga Liberian phase. Excluding the Liberian phase, then the Birimian event is left as the only period during which the rocks could have been subject to granulite facies metamorphism.

Pitra et al. (2010) proposed a model for the southeastern Man domain were they argued that it had

been metacratonized (i.e. remobilized without losing its preexisting structure, see Adelsalam et al. 2002) during collision with Birimian crust of the Baoulé Mossi domain. As a consequence of metacratonization steep shear zones developed within the Man domain which subsequently acted as conduits for juvenile magma, which formed the Ity-Toulépleu massif. The development of steep shear zones along the Man and Baoulé Mossi contact (i.e. the Sassandra shear zone) was attributed to the weakness of the young and hot Birimian crust which Pitra et al. (2010) argued would be too weak to be thrust upon the Man domain. It would instead have flowed around the cooler and more rigid Archean crust.

While the high pressure conditions obtained from thermobarometric studies were interpreted by Triboulet and Feybesse (1998) in support of a model of nappe-stacking it was instead argued by Pitra et al. (2010) that such conditions could also be achieved through homogenous thickening during convergence. Heat from early intrusions (such as the Ity-Toulépleu massif) and the Birimian crust would have softened the Archean crust allowing for fold-assisted thickening.

It is worth noting the position assumed by the Ity-Toulépleu massif in the two models mentioned above regarding the timing of collision. In the model of Pitra et al. (2010) the intrusion of the Ity-Toulépleu massif corresponds to a minimum age for collision between the Archean crust of the Man domain and the Baoulé Mossi domain, assuming of course that it did not form in separate, unrelated event. If the Ity-Toulépleu domain (including the massif) instead corresponds to a klippe originally emplaced as part of an allochthonous thrust sheet, as proposed by Feybesse et al. (1990) and Feybesse and Milési (1994), then it provides a maximum age for thrusting and the main collision phase.

2.2.3.2 Northern contact

In contrast to the model of Pitra et al. (2010), it was proposed by Egal et al. (2002) that the Man and Baoulé Mossi contact in Guinea corresponds to a short-lived continental arc active between circa 2090-2070 Ma. This continental arc is now preserved as the plutonic belt (fig. 5) which is comprised of synkinematic biotite and biotite-amphibole ±clinopyroxene granodiorites cut by late, undeformed syenogranites. The enriched composition of these intrusive rocks led Egal et al. (2002) to propose that they formed in a continental arc setting analogous to the Andes. Boher et al. (1992) have shown using Sm-Nd isotopes that granitoids from this region contain an older — possibly Archean — component, which is in line with the model proposed by Egal et al. (2002).

Convergence and deformation along the contact was accommodated by lateral displacement along sinistral subvertical shear zones (Egal et al. 2002). Sediment in the southern part of the Siguiri basin that is in contact with the plutonic belt have been metamorphosed and deformed to mica schists with a staurolite-garnet-sillimanite assemblage indicative of amphibolite facies conditions (Egal et al. 2002; Lahondère et al. 2002; Lerouge et al. 2004). Based on petrographic studies and classic thermobarometry, Lerouge et al. (2004) estimated that supracrustal rocks at the Archean-Birimian contact along the southern margin of the Siguiri basin (fig. 5) experienced a clockwise P-T-t path were peak metamorphic conditions reached 800°C and 4-6 Kbar.

3 Methods and data

This thesis grew from the work on a number of granitoid (*sensu lato*) samples collected by A. Scherstén (Department of Geology, Lund University) and P. Kalvig (GEUS) in Ghana during fieldwork in 2009 and 2011 as part of an ongoing project aimed at improving the understanding of Birimian crust in the West African Craton. During the course of this study these samples have been examined petrographically and geochemically (see data in Appendix A). A few selected samples have previously been dated (A. Scherstén, unpublished data).

On their own, petrographic, geochemical and geochronological studies of these samples can provide valuable information regarding their petrogenesis and by extension the processes which formed and shaped the Birimian crust. Nevertheless, in order to fully utilize such data it needs to be related to other aspects of the Birimian crust, such as its tectonothermal evolution. In addition, because of the vast extent of the Birimian crust it is necessary to have a regional perspective and to incorporate data from across the West African Craton but also from other areas were equivalent crust can be found.

The rationale behind this thesis has therefore been to create a geodynamic model for the Birmian event in the Man-Leo shield that incorporates structural, metamorphic, magmatic and sedimentological data and which can provide a context for the individual samples. This approach is "mutually beneficial" as the samples can then be revisited in future studies to extract more data that can be used to test and improve the geodynamic model. The geodynamic model is presented in this thesis as a discussion on various important aspects of the Birimian event, all presented in a chronological order. The primary focus is on the Man-Leo shield but by necessity the model also incorporates data from the Reguibat shield and the Amazon Craton.

In order to develop a geodynamic model for the Birimian event in the WAC it has been necessary to compile data from the literature, in addition to the new samples obtained by A. Scherstén and P. Kalvig. To this end, published and unpublished geochronological and geochemical data has been compiled in GIS-(Geographical Information System) and Microsoft Excel-based datasets. In addition, GIS-based lithological and structural maps have also been compiled from

various sources. All GIS data has been handled using the software ArcGIS 10.0 by ESRI. Compilation of data has been done intermittently since mid-2011.

The geodynamic model should be seen as a preliminary attempt to explain the complex history of the Birimian crust, other explanations for various aspects of its geodynamic evolution may be just as viable. In many situations the available data — in particular regarding P-T-t-D — is limited, a situation which can be considered as both a blessing and a curse. While it provides a lot wiggling room for various "preferred" interpretations it also means that many parts of the model remains poorly constrained. In the very least, it is hoped that the model may serve to highlight various aspects of the Birimian crust which needs to be considered in any geodynamic model, regardless of how they are ultimately interpreted to have formed.

3.1 GIS-based data

The advantage of using GIS-based datasets is that it makes it possible to handle large amounts of data within a spatial context. Data within a GIS is either raster or vector based; the former represent continuous surfaces (e.g. elevation) while the latter corresponds to discrete objects which can be polygons (e.g. granite), lines (e.g. a fault or dyke) or points (e.g. a sample site). Raster and vector data (either as polygons, lines or points) correspond to layers which can be viewed as being placed on top of each other like a stack of papers. This makes it possible to show e.g. sample sites (points) on top of a geological map showing structures (lines) and lithologies (polygons) or a raster showing elevation. Methods for compiling the data used in this work are discussed briefly in the following sections.

3.1.1 Geological maps

The geological maps, including both polygon and line layers, have been compiled from various sources ranging from national geological maps to schematic maps from scientific articles. References used for maps in this work are given in the associated figure captions. All national borders and coastlines used in figures within this work have been obtained from the Digital Chart of the World (downloaded from GIS-LAB, http://gis-lab.info/qa/vmap0-eng.html. Last accessed 25-11-2013). Unless stated otherwise, the maps are projected with an Albert equal-area conic projection using two standard parallels and the WGS 1984 datum.

The process of drawing maps in GIS is referred to as digitization. In order to digitize a GIS-based map the source map must be GIS-based itself. Unless previously available in raster or vector format this requires that the map (an image in raster form) is georeferenced, essentially assigning it a fixed position within a geographical or projected coordinate system. Once a source map has been georeferenced it can act as a base layer on which new geological maps can be digitized.

The accuracy of the digitized data is dependent not only the quality of the original map, but also on how well it was georeferenced and finally depicted during digitization. As such, there are multiple factors which can serve to lower the accuracy and precision of the final digitized map. This makes it hard to make a quantitative estimate of the combined error associated with these factors. Nevertheless, it is considered here that the maps are sufficiently accurate depictions of the source maps. The schematic nature of both the source maps and the digitized maps also negate the need for highly accurate depictions during digitization.

3.1.2 Geochronological dataset

A GIS-based dataset of Birimian radiometric ages has been compiled using the same approach as for the geological maps described above. They are comprised mainly by published ages obtained from the literature but also include unpublished data by A. Scherstén. The radiometric ages are collected as point data and include magmatic, metamorphic, inherited and maximum depositional ages were available, in addition to a brief petrographic description of the dated sample.

The uncertainty regarding the exact location of the dated samples varies. Occasionally, geographical coordinates are provided by the authors (although never together with a datum), which enables accurate location of the dated sample in the dataset. Usually however, the sample location is only given in a figure depicting the study area, requiring that the figure is first georeferenced in order to act as a sketch for digitization in GIS software. In some instances, the location is not marked on any figures but only specified in text (e.g. as a particular pluton in turn shown on a geological sketch map). While the latter cases lead to an increased uncertainty regarding the exact position of the dated samples, the error is usually on the scale of kilometers. When the location of dated samples are plotted in figures in this work the symbols representing them in almost all cases covers the error regarding their location.

As for the geochemical dataset, an inclusive approach has also been adopted when collecting geochronological data. As such, all ages obtained by dating zircon (regardless of method, number of grains, MSWD etc.) have been included. Several magmatic and metamorphic $^{40}Ar/^{39}Ar$, K-Ar and Sm-Nd isochron ages have also been included although many have also been excluded because of associated large errors. For the same reason, Rb-Sr ages are also excluded. While the geochronological dataset is not a complete collection of the available geochronological data it nevertheless provides a comprehensive overview of the distribution of radiometric ages in the Baoulé Mossi and Man domains.

3.2 Geochemical dataset

A dataset of geochemical data from Birimian rocks in the WAC (including remobilized crust within the Dahomeyides) and the São Luís Craton have been com-

piled in a Microsoft Excel spreadsheet. This dataset includes analyses of igneous, sedimentary and high grade rocks from a wide range of literature sources. In addition, new data for samples collected by A. Scherstén and P. Kalvig in Ghana are also presented in this thesis.

The geochemical data include whole rock (major and trace element) geochemistry and, where available, Sm-Nd and Rb-Sr isotopes. Each sample is also associated with petrographical and geographical information (craton, shield, domains etc.) which allows it to be placed within a spatial context. When available, measured or inferred radiometric ages (magmatic, metamorphic and inherited) are also included. Radiometric ages included in the dataset are primarily obtained from zircon but also include a few Rb-Sr and Sm-Nd isochron ages.

For this work no screening of data has been performed based on the availability of analyzed elements or analytical method. While this inclusive approach means that the dataset contains data of variable quality it also increases the quantity and coverage (both spatial and temporal) of data. The use of a large dataset also means that in cases where trace elements of low concentrations (e.g. Nb, Y, Rb, Zr) are analyzed using relatively imprecise methods (e.g. XRF) the sheer amount of analyzed samples may nevertheless compensate for the poor quality of the data for the purpose of identifying general trends.

4 The Birimian event in the Baoulé Mossi domain

The aim of this section is to present a geodynamic model for the Birimian event in the Baoulé Mossi and Man domains. Such a model must account for the relationship between the various volcanic belts, sedimentary basins and granitoid-gneiss domains in the Baoulé Mossi domain as well as the interaction and juxtaposition of the Birimian crust with the Archean crust of the Man domain. The geodynamic model for these domains also needs to be compared with that of the Reguibat shield (fig. 1) given that it by all likelihood forms a continuation of the Archean and Birimian crust exposed in the southern WAC. In addition, it also needs to be compared with the Birimian crust of the Amazon and East European cratons which were positioned south and west, respectively, of the present day WAC during the Birimian event (see figure 4 and section 2.1).

As a first step towards the geodynamic model it is fundamental to attempt to establish in what tectonic setting the Birimian event took place. In essence, this boils down to whether the Birimian event formed in a setting governed by plate tectonics or whether more "archaic" process (e.g. plume and vertical tectonics) was at work. This will be done in the next section. This will be followed by a brief overview and outline of the geodynamic model covering the general characteristics that define the different phases, as proposed here, of the Birimian event in the Baoulé Mossi and Man domains. After this the respective phases will be discussed in more detail in separate sections. Finally, the geodynamic model will be summarized and placed within a plate tectonic context involving other cratons with crust equivalent to the Birimian crust of the WAC, such as the Amazon and East European cratons.

4.1 An accretionary to collisional orogenic setting

As discussed in the introduction, the presence or absence of modern-style plate tectonics in the Archean-Proterozoic is a controversial issue (cf. e.g. Stern 2005 and Shirey & Richardson 2011). However, for the geodynamic model presented here it is inferred that plate tectonics were operating and that subduction of oceanic crust was ultimately responsible, directly or indirectly, for most of the magmatic and tectonothermal activity during the Birimian event. Data in support for this assumption is presented below. This assumption is also in line with the accretionary to collisional orogenic setting envisioned by a range of authors throughout the Baoulé Mossi domain on the basis of lithological, geochemical and structural data (e.g. Mortimer 1992a; Sylvester & Attoh 1992; Feybesse & Milési 1994; Ama-Salah et al. 1996; Pouclet et al. 2006; Baratoux et al. 2011; de Kock et al. 2012). While oceanic plateaus may certainly have been present within this setting (as proposed by e.g. Abouchami et al. 1990 and Béziat et al. 2000) it would still ultimately be governed by plate tectonic processes, like oceanic plateaus are in recent accretionary orogens (e.g. Kerr 2003).

4.1.1 A subduction signature

Discrimination diagrams in themselves are not sufficient to "prove" the tectonic setting of a given rock, but they may nevertheless be used as an indicator of the setting in which the rock may have formed. In figure 6, volcanic and intrusive rocks from the geochemical dataset (see section 3.2, using analyses of Birimian rocks in the WAC and São Luís Craton) have been plotted on the Nb/Yb-Th/Yb diagram of Pearce (2008) and the Rb-Y-Nb diagrams of Pearce et al. (1984). In all these diagrams, the volcanic and intrusive rocks display a behavior consistent with rocks formed in an arc environment.

The Nb-Yb/Th/Yb diagram is designed for basaltic rocks and constructed in such a way that subduction processes would act to shift the magma composition away from the MORB-OIB array towards higher Th/Yb. In figure 6a, it can be clearly seen that volcanic rocks (ranging from tholeiitic basalts to calc-alkaline rhyolites) diverge from the MORB-OIB array. Indeed, there is no trend towards the average OIB composition (from Sun & McDonough 1989). Importantly, the composition of the mafic volcanic rocks plot around MORB to E-MORB compositions while more evolved rocks (andesites and rhyolites) have progressively higher Th/Yb, as do most intrusive rocks. The compo-

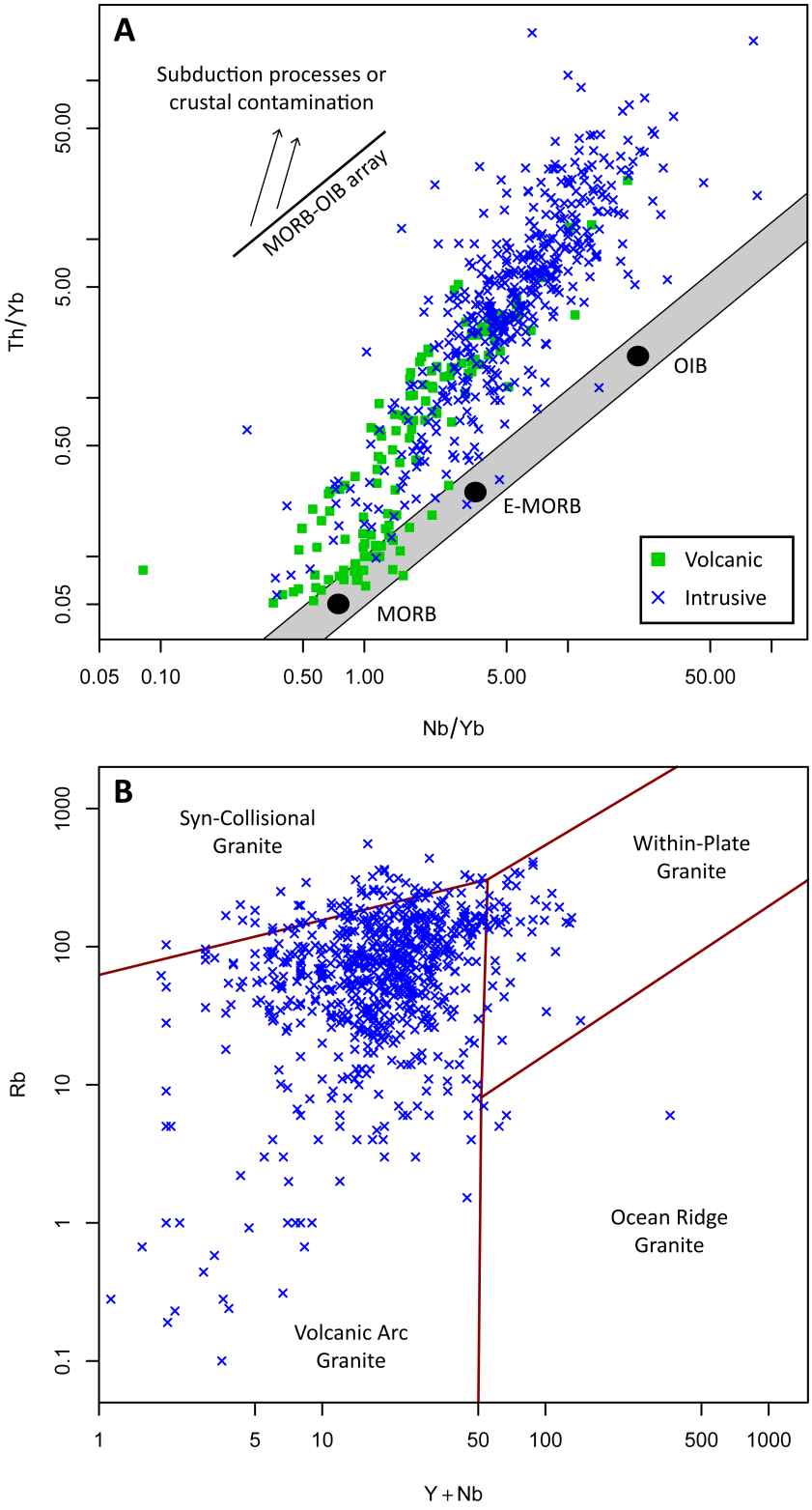

Fig. 6. Tectonic discrimination diagrams for Birimian intrusive and volcanic rocks. **A)** Th/Yb vs. Nb/Yb diagram after Pearce (2008). MORB, E-MORB and OIB from Sun and McDonough (1989). **B)** Rb vs. Y+Nb diagram after Pearce et al. (1984). Data from A. Scherstén (unpublished data), Toure et al. (1987), Tegyey & Johan (1989), Abouchami et al. (1990), Liégeois et al. (1991), Boher et al. (1992), Mortimer (1992a, 1992b), Sylvester & Attoh (1992), Hirdes et al. (1993), Vidal & Alric (1994), Ama-Salah et al (1996), Pouclet et al. (1996), Kouamelan et al. (1997), Ndiaye et al. (1997), Doumbia et al. (1998), Koeberl et al. (1998), John et al. (1999), Loh and Hirdes (1999), Béziat et al. (2000), Yao & Robb (2000), Egal et al. (2002), Lahondére et al. (2002), Galipp et al. (2003), Gasquet et al. (2003), Kahoui & Mahdjoub (2004), Naba et al. (2004), Dampare et al. (2005, 2008), Peucat et al. (2005), Attoh et al. (2006), Dioh et al. (2006), Pawlig et al. (2006), Agbossoumondé et al. (2007), Karikari et al. (2007), Klein et al. (2008, 2009), Vegas et al. (2008), Adadey et al. (2009), de Kock et al. (2009), Siegfried et al. (2009), Thomas et al. (2009), Ngom et al. (2010), Baratoux et al. (2011), McFarlane et al. (2011) and Tapsoba et al. (2013).

sitions exhibited by the intrusive and volcanic rocks are compatible with arc-backarc settings (Pearce 2008).

The lack of samples with an OIB-like composition is significant, since it points to the absence of oceanic plateaus (assuming they would have had a composition equivalent to that of the average OIB) in the WAC and São Luís Craton during the Birimian event, contrary to what was proposed by Abouchami et al. (1990). With that said, it should be noted that the samples of Abouchami et al. (1990) were never analyzed for Th and are thus not plotted in figure 6a. However, when considering other elements, the samples of Abouchami et al. (1990) do not show a deviating behavior from samples that have been analyzed for Th-Nb-Yb and which diverge from the MORB-OIB array in figure 6a. It also seems unlikely that Abouchami et al. (1990) would only sample OIB-basalts whereas subsequent workers only collected basalts with an arc-signature, despite the fact they in many cases worked in the same areas.

Crustal contamination would have the same effect as subduction processes in shifting the magma composition away from the MORB-OIB array (Pearce 2008). However, it seems unlikely that it would be responsible for the trend seen in figure 6a given the juvenile nature of Birimian volcanics (as well as granitoids) and the fact that the volcanics are among the oldest rocks within the Baoulé Mossi domain. When considering the intrusive rocks together with the volcanic rocks the trend may instead be interpreted as reflecting the progressive differentiation and maturation of the Birimian crust.

The Rb-Y-Nb diagram of Pearce et al. (1984) is designed for granitoids (*sensu lato*) and to distinguish between those formed in volcanic arc, collisional orogen, within-plate or oceanic ridge settings. As for the Nb/Yb-Th/Yb diagram both the volcanics and the intrusive rocks consistently plot within the field of arc-related granitoids defined by Pearce et al. (1984) with only minor overlap with the fields for collisional orogens and within-plate settings (fig. 6b). While Rb may be sensitive to alteration

It has been pointed out that discrimination diagrams may be misleading as the signature composition taken to indicate a particular tectonic setting may be inherited (Arculus 1987; Robert & Clemens 1993) or caused by factors unrelated to a particular tectonic setting (Bédard 2006). An example of the latter is the fractionation of Nb-Ta and Ti which is considered typical of subduction-related rocks (e.g. Pearce et al. 1984). However, it can also be obtained through high-pressure melting with residual rutile in settings that does not involve plate tectonics (e.g. Bédard 2006). The consequence of an inherited signature is that a rock, which plot within a field indicating formation in e.g. a volcanic arc may not be spatially or temporally associated with active subduction and arc magmatism at the time of its formation. However, it requires that it was derived from a source rock which formed in such a setting.

Despite the uncertainties surrounding the use of discrimination diagrams, the consistent behaviour of Birimian igneous rocks, spanning a compositional range for mafic volcanics to evolved granites, nevertheless indicates that they formed in a tectonic setting that was ultimately dominated by subduction processes. However, the effect of inheritance means that many of the younger Birimian intrusive and volcanic rocks may not be directly associated with active subduction, even though they plot in fields indicating such an environment.

As will be detailed in the geodynamic model presented below — incorporating lithological, geochemical, geochronological, structural and metamorphic data — the evolution of the Birimian crust can be explained in the context of plate tectonics. Even though there are Birimian rocks that are not usually associated with subduction processes — such as the komatiites (Tegyey & Johan 1989) and continental basalts (Lahondère et al. 2002, and references therein) of the Niandan and Keniero volcanic ranges in Guinea — their presence may nevertheless be ultimately controlled by plate tectonic processes in a within-plate setting, as will be further discussed below.

4.1.2 Birimian ophiolites?

Ophiolites are considered remnants of oceanic crust which have been preserved from subduction along convergent margins by being incorporated into continental crust (Dilek & Furnes 2011; Furnes et al. 2013). The classic Penrose-type ophiolite consists of a basal layer of peridotite, overlain by isotropic gabbro, a sheeted dyke complex, finally massive or pillowed basalt and a thin layer of pelagic sediment. The sheeted dyke complex is a strong indicator of lateral extension and thus modern-type plate tectonics. The absence of unequivocal Penrose-type ophiolites from the geological record prior to the Neoproterozoic have been interpreted by some authors as indicating that modern-type plate tectonics was not active during these times (e.g. Stern 2005).

However, not all ophiolites contain sheeted dike complexes whose formation is dependent on both spreading rate and magma supply (Robinson et al. 2008) and will consequently not conform to the Penrose-type structure. Dilek and Furnes (2011) presented a broader definition for ophiolites in which they correspond to “suites of temporally and spatially associated ultramafic to felsic rocks related to separate melting episodes and processes of magmatic differentiation in particular (oceanic) tectonic environments”. They further introduced different groups of ophiolites which they separated into those that were related to subduction zones (supra-subduction zone and volcanic arc) and those which were not (e.g. MORB or oceanic plateaus).

So far, no unequivocal Penrose-type ophiolitic sequence has been reported from the Birimian crust in the WAC. The best current candidate is represented by

Fig. 7. Overview of the crustal domains associated with phases of the geodynamic model shown on the schematic geological map of figure 5. Framed rectangular boxes refer to localities discussed in the text. Round framed boxes refer to specific plutons, also discussed in the text, using the following abbreviations; T-Y - Tenkodogo-Yamba, Ko - Kowara, Fe - Ferkéssédougou. Transparent text boxes refer to shear zones discussed in the text, see figure 5 for references and abbreviations. The geochronological data has been compiled from the following references (also includes references for figures 8, 11, 14 and 18), given in numerical order: **1** - Barth et al. (2002); **2** - Goujou et al. (1999), in Thiéblemont et al. (2004); **3** - Thiéblemont et al. (2001); **4** - Milési et al. (1989); **5** - Kouamelan et al. (1997); **6** - Kouamelan (1996); **7** - Lahondére et al. (2002); **8** - Gueye et al. (2007); **9** - Dia et al. (1997); **10** - Dia (1988), in Gueye et al. (2007); **11** - Boher et al. (1992), in Vidal et al. (2009); **12** - Gasquet et al. (2003); **13** - Lemoine (1988), in Vidal et al. (2009); **14** - Lüdtke et al. (1992, 1998a), in Vidal et al. (2009); **15** - Hirdes et al. (1996); **16** - Castaing et al. (2003), in Baratoux et al. (2011); **17** - Lompo (1991), in Baratoux et al. (2011); **18** - Schwartz & Melcher (2003), in Baratoux et al. (2011); **19** - Tapsoba et al. (2013); **20** - Castaing et al. (2003), in Hein (2010); **21** - Boher et al. (1992); **22** - Castaing et al. (2003), in Vegas et al. (2008); **23** - Klockner (1991), in Soumaila et al. (2008)**; 24** - Cheilletz et al. (1994), in Soumaila et al. (2008); **25** - Soumaila et al. (2008); **26** - Abdou et al. (1998), in Soumaila et al. (2008); **27** - Ama-Salah et al. (1996); **28** - Agyei Duodu et al. (2009); **29** - Thomas et al. (2009); **30** - Siegfried et al. (2009); **31** - de Kock et al. (2009); **32** - Zitzmann (1997); **33** - Delor et al. (1995), in Vidal et al. (2009); **34-** - Siméon et al. (1995), in Vidal et al. (2009); **35** - Feybesse et al. (2006); **36** - Hirdes & Davis (1998); **37** - Hirdes et al. (1992); **38** - A. Scherstén, personal communication; **39** - Adadey et al. (2009); **40** - Opare-Addo (1992), in Agyei Duodu et al. (2009); **41** - Loh et al. (1999)**, in Agyei Duodu et al. (2009); **42** - Oberthür et al. (1998); **43** - Attoh et al. (2006); **44** - Hirdes et al. (2007), in Agyei Duodu et al. (2009); **45** - Doumbia et al. (1998); **46** - Leake (1992), in Vidal et al. (2009); **47** - Loh & Hirdes 1999; **48** - Agbossoumondé et al. (2007); **49** - Lüdtke et al. (1998b), in Baratoux et al. (2011); **50** - Abdou et al. (1992), in Soumaila et al. (2008); **51** - Melcher et al. (2008) **, in Agyei Dudou et al. (2009); **52** - Davis et al. (1994); **53** - Hirdes et al. (2007), in Assie (2008); **54** - Yao et al. (1995), in Vidal et al. (2009); **55** - C. Delor & A. Cocherie, unpub., in Kouamelan (1996); **56** - Liégeois et al. 1991; **57** - Thiéblemont et al. (2004); **58** - Egal et al. (2002); **59** - Feybesse et al. (1999), in Lahondére et al. (2002); **60** - McFarlane et al. (2011); **61** - Hirdes & Davis (2002); **62** - Kalsbeek et al. (2012); **63** - Delor et al. (2004); **64** - Chalokwu et al. (1997); **65** - Pigois et al. (2003); **66** - Cocherie et al. (1998); **67** - Bossière et al. (1996); **68** - Onstott et al. (1984). ** - Note that full references for these sources have not been found during the course of this work.

the volcanic and intrusive ultramafic rocks found in the southern Ashanti belt in southern Ghana, as proposed by Attoh et al. (2006), although this sequence lacks a clearly identifiable sheeted dyke complex. However, using the definition by Dilek and Furnes (2011), the subduction-affinity of temporally and spatially related Birimian volcanic and intrusive rocks (fig. 6) mean that most volcanic belts might be classified as subduction-related ophiolites. Exceptions may include the volcanic suites of the Keniero and Niandan ranges in Guinea.

The association of ultramafic-gabbroic rocks interpreted as lower crustal cumulates (Béziat et al. 2000) with anorthosite-like plagioclase-megacrystic basaltic rocks (Baratoux et al. 2011) in volcanic belts in Burkina Faso may also indicate that they formed in a subduction zone setting. In the Meso- to Neoarchean North Atlantic Craton in southern Greenland, Windley and Garde (2009) compared similar rock associations found there (i.e. ultramafic rocks, cumulatic gabbros, anorthosites) with analogous assemblages found in Phanerozoic ophiolites in e.g. the North American Cordilleras, Fiordland in New Zealand and Kohistan in northern Pakistan. Windley and Garde (2009) suggested that the similarities between the Phanerozoic ophiolites and the Archean rocks in Greenland indicated that the latter had formed in a subduction zone setting, with the implication that modern-style subduction had been active since at least that time.

4.1.3 Thermal structure of accretionary orogens

It was shown by Hyndman et al. (2005) and Currie and Hyndman (2006) that circum-Pacific oceanic and continental backarcs (e.g. Sundaland in SE Asia and the Cordilleras of North America) are defined by a high heat flow and a thin lithosphere; conditions that extend from 250 to more than 900 km behind the main arc, regardless of whether the backarc had experienced recent extension or not. These authors explained the elevated heat flow in the backarcs by vigorous small-scale thermal convection in the upper mantle. The introduction of fluids derived from the subducting oceanic crust has the effect of lowering the viscosity of mantle rocks, enhancing this type of convective flow in the backarc region. Temperatures at the Moho in continental backarcs (circa 35 km depth) were estimated by Currie and Hyndman (2006) to be between 800-1000°C. This contrasts with the lowered geotherm at the trench which is caused by subduction of cool oceanic crust.

Assuming that plate tectonics was operating during the Birimian event - and that the juvenile Birimian crust formed in an accretionary orogen - then large portions of the Birimian crust would reasonably have been thin and defined by a high heat flow, the only exceptions being forearc regions. As discussed in section 2.2.2.7 the Birimian crust is interpreted to have been thin and hot (Vidal et al. 2009; Baratoux et al. 2011); conditions equivalent to those of modern backarcs. Indeed, the thermal conditions obtained through thermal modeling by Harcoüet et al. (2007) for southern Ghana (800-900°C at a Moho of 30 km depth) is within the range of temperatures seen in recent backarcs (Hyndman et al. 2005; Currie & Hyndman 2006).

Hyndman et al. (2005) pointed out that the presence of a hot backarc would also have important implications for collisional orogens — the ultimate fate of the accretionary orogens — as it would constitute a source of orogenic heat that was in place before the collision. Hot backarcs therefore have important implications for deformation during collision in addi-

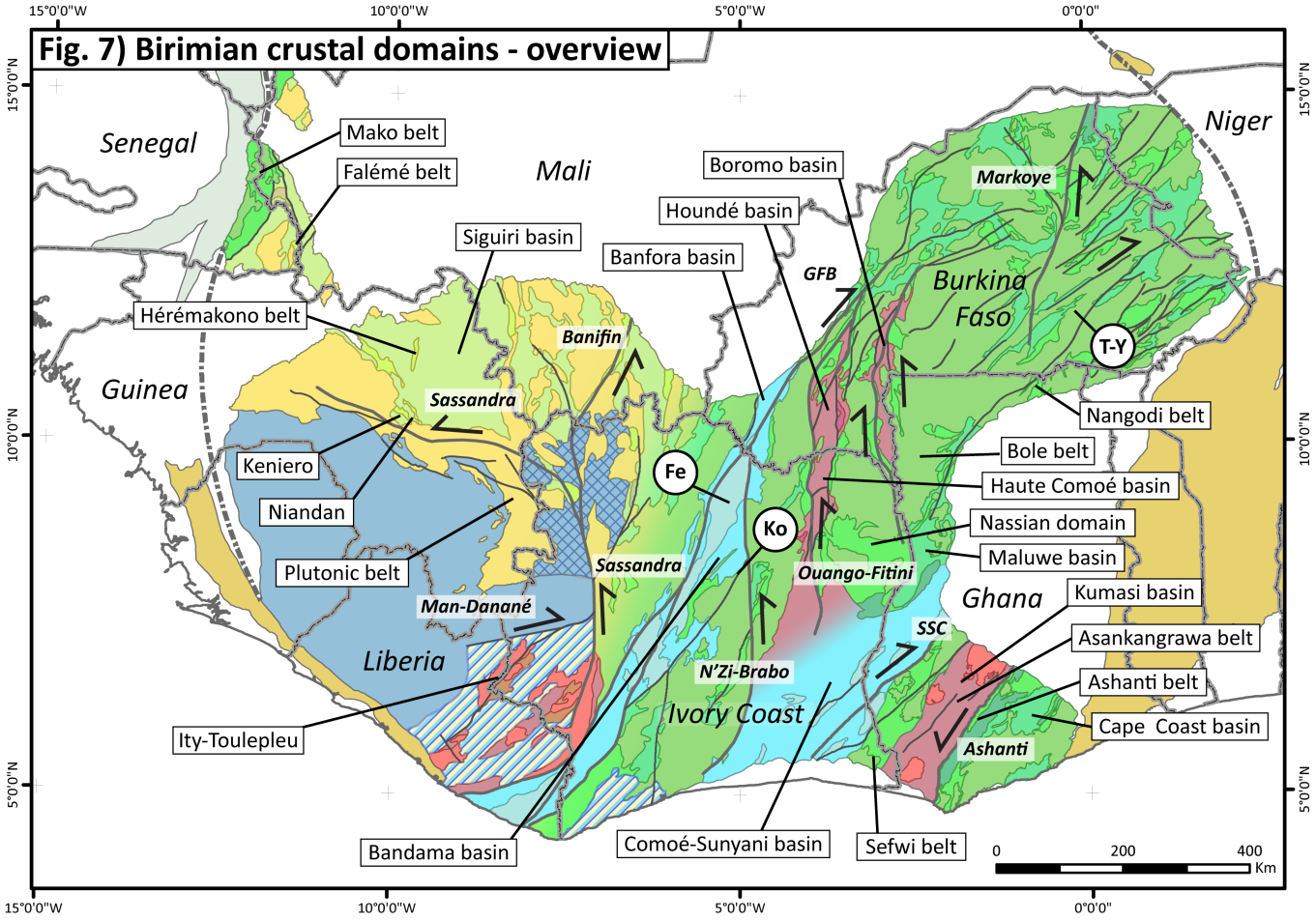

Age	Phase	Domain	Geochronology
<2.07	Eburnean III		
2.10-2.07	Eburnean II	IIA IIB	
2.13-2.10	EI overprint / Eburnean I		
>2.13	Eoeburnean		
>2.50	Archean		

Magmatic
Metamorphic
Detrital

Age, Ma — Method — Mineral — Reference

2174±2 *T-z,t* **(42)**

Method

T - TIMS; *P* - Pb-Pb; *S* - SHRIMP; *L* - LA-ICPMS; *E*- EMP; *A* - Ar-Ar; *K* - K-Ar; *U* - U-Th-Pb; *Si* - SIMS; *SN* - Sm-Nd

Mineral

z-zircon; *m*-monazite; *r*-rutile; *t*-titanite; *a*-amphibole; *ms*-muscovite; *b*-biotite; g-garnet; *wr*-whole rock; *p*-plagioclase; *f*-feldspar; *x*-xenotime

tion to providing a heat source for associated magmatism. Chardon et al. (2009) also emphasized the importance of the temperature and thickness of the lithosphere in determining orogenic styles. These authors proposed that the Birimian crust corresponded to an ultra-hot orogen which are characterized by a thin lithospheric mantle and Moho temperatures >900°C. For the model presented below, it is assumed that the Birimian crust of the Baoulé Mossi domain was thin and hot, and consequently weak, during the Birimian event.

4.2 Overview of the geodynamic model

In the geodynamic model presented in this section the Birimian event in the Man and Baoulé Mossi domains has been divided into four phases; the Eoeburnean (EE, >2.13 Ga), Eburnean I (EI, 2.13-2.10 Ga), Eburnean II (EII, 2.10-2.07 Ga) and the Eburnean III (EIII, <2.07 Ga). Although the terms Eoeburnean and Eburnean are taken from de Kock et al. (2009, 2011) it should be noted that the phases used in this model are not equivalent to those of these authors. The timing of the phases should only be considered approximate; the phases, especially the Eburnean ones, are in this model considered to form part of a continuum. The Archean crust in the Man and Baoulé Mossi domains are bundled together into a separate Archean phase that is not considered in the geodynamic model presented here.

The Baoulé Mossi and Man domains can be divided into crustal domains — essentially corresponding to combinations of volcanic belts, sedimentary basins and granitoid-gneiss domains — which can be constrained to have formed during a specific phase of the Birimian event. An overview of these crustal domains is shown in figure 7 together with the same geological map as shown in figure 5. In figure 7 it can be seen that the crustal domain associated with a particular phase do not necessarily form a coherent unit. Also, as will be seen below, tectonothermal and magmatic activity during a particular phase is not limited

to the crustal domains it is associated with but may also occur within crustal domains formed during earlier phases.

In the case of EI and EII phases the crustal domains have been divided into two parts to reflect the different geodynamic evolution of these areas; this is discussed further in the sections covering these phases. There is no domain associated with the EIII phase as it represents a period of the Birimian event which was characterized by limited magmatism and tectonothermal activity affecting crust within the Baoulé Mossi and Man domains formed during previous phases.

The division of the Man and Baoulé Mossi domains is based primarily on the distribution of radiometric ages (magmatic, metamorphic and detrital) to constrain when each respective domain formed. Since the radiometric ages only represent point data the schematic geological map shown in figure 5 has been used to constrain the lateral extent of these crustal domains. Given the schematic nature of this map the boundaries and extent of the domains shown in figure 7 should only be considered provisional. The approach used for the crustal domains is particularly problematic in areas where there is both a lack of radiometric ages and where the understanding of the local geology is less well constrained, such as southwestern Ivory Coast and Liberia.

The division of the crustal domains relies heavily upon the use of magmatic ages. This means that what is traced among the domains is mostly the timing of magmatic activity. As such, they can only provide a minimum age for the timing of formation of a particular domain. However, by using the limited amount of available detrital zircon data, as well as relationships between different crustal domains (e.g. the presence of a younger domain between two older ones) it is also possible to establish reasonably good maximum ages for the domains. Nevertheless, it should be emphasized that the timing of the formation of various crustal domains — and by extension the timing of the phases of the Birimian event used in this model — only forms a first approximation.

Finally, while the São Luís Craton is not included in figure 7 (or the subsequent figures 8, 11, 14 and 18 depicting the geodynamic model, see further below) the minor area that it constitutes means that its omission does not impact the presentation of the geodynamic model. Petrological and geochemical data from the São Luís Craton is nevertheless included in the following discussion.

4.3 Phases of the Birimian event

The phases of the geodynamic model outlined above will here be presented in separate sections. For each of these sections there is an accompanying figure (figures 8, 11, 14 and 18) which shows the distribution of radiometric ages and crustal domains during the particular phase the section covers. Each figure also includes the crustal domains and symbols for radiometric ages of any previous phases. A legend showing which phase the crustal domains and symbols (for radiometric ages) are associated with are given together with figure 7. There is also a legend together with figure 7 that explains the abbreviations used for radiometric ages given in figures 8, 11, 14 and 18. To preserve the clarity of these figures all names of e.g. localities, shear zones or volcanic belts discussed in the following text are presented in figure 7, which is based on the same map as figures 8, 11, 14 and 18.

In each of figures 8, 11, 14 and 18 there is also an inset showing a schematic depiction of the geodynamic evolution during each phase with matching colors for the crustal domains given in the main figure. These schematic models are meant to place the crustal domains and radiometric ages given in the main figure in a geodynamic context. While they may show a possible geodynamic evolution, it may not necessarily be the only option. The geodynamic evolution during each phase is further discussed in the relevant sections below.

Geochemical data of igneous rocks from the geochemical dataset (see section 3) has — when possible — been assigned to one of the phases of the geodynamic model using either relative or absolute ages. This data has subsequently been used to investigate geochemical trends within and between the different phases of the geodynamic model. When assigning samples to a phase some will inevitably be classified incorrectly. However, this mostly regards samples which straddle the boundary between two phases; the "misclassification" being more an artefact of the temporal limits set for the phases in the geodynamic model (which really form part of a continuum). Regardless, any misclassified samples are not considered to have any significant impact on the geochemical trends shown by igneous rocks from the different phases.

4.3.1 Eoeburnean (>2.13 Ga) — figure 8

The Eoeburnean phase corresponds to a long-lasting period in which island arcs (and possibly oceanic pla-

Fig. 8. The spatial extent of Archean and Eoeburnean crustal domains together with a compilation of geochronological data from the Archean and Eoeburnean phases. See figure 7 for legend and references. Inset shows a schematic depiction of the geodynamic setting during the Eoeburnean phase (>2.13 Ga). This phase was characterized by the amalgamation of juvenile crust in an accretionary orogenic setting, likely involving amalgamation of multiple island arcs. Structural, metamorphic and magmatic data indicate that the Eoeburnean crust was subjected to both compression (1) and extension (2) during this phase. At this time the Archean crust in the Man domain was not in contact with the Eoeburnean crust but instead constituted a separate continent fringed by passive margins. To the present-day east, the Eoeburnean crust may have docked with an Archean continent represented by Archean crust now present in the Amapá block (fig. 4) and southeastern Ghana-Togo. By the end of the Eoeburnean phase, an eastward dipping (present-day orientation) had been established on the western margin of the Eoeburnean crust.

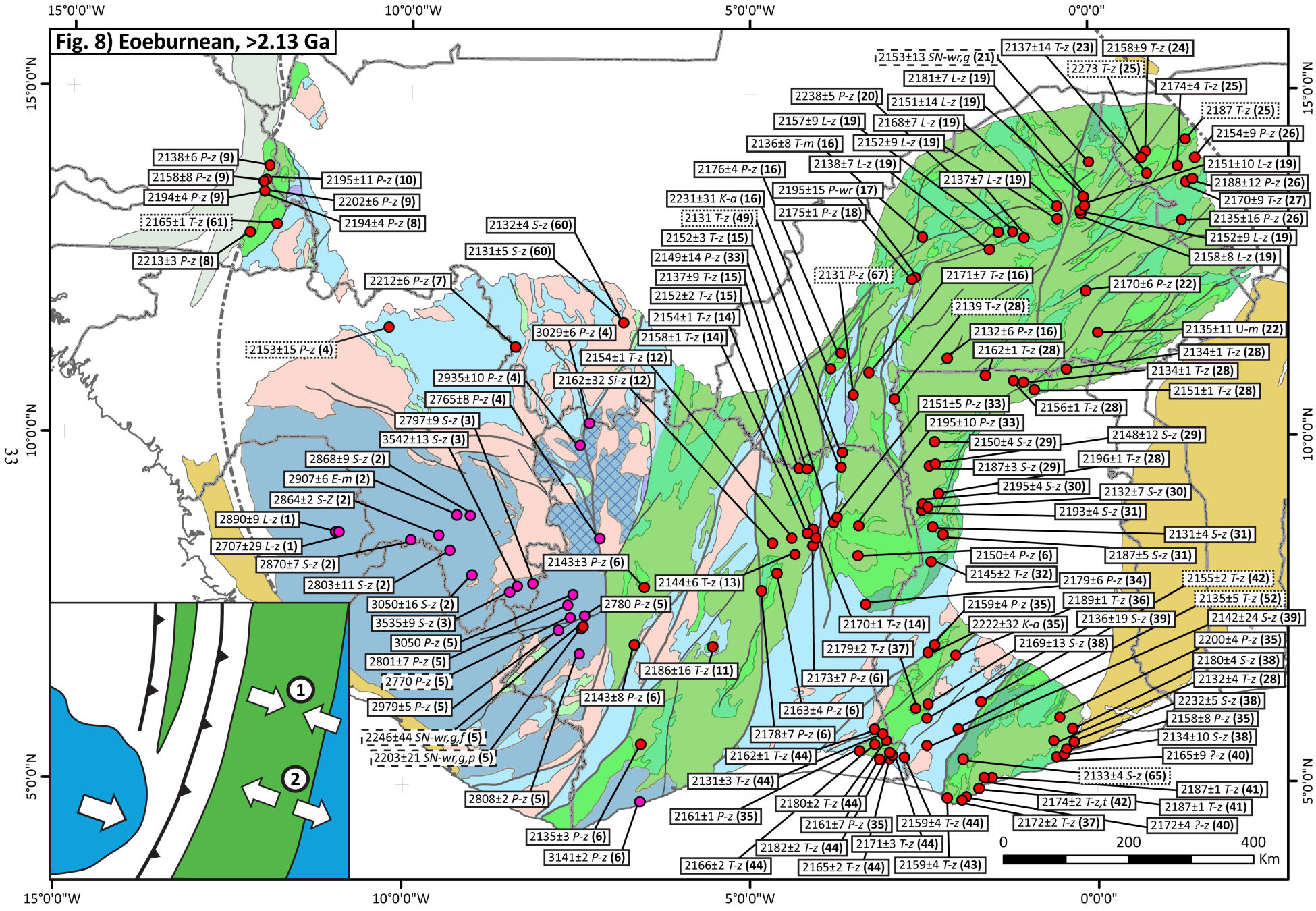
Fig. 8) Eoeburnean, >2.13 Ga
15°0'0"W
10°0'0"W
5°0'0"W
0°0'0"
15°0'0"N
10°0'0"N
5°0'0"N
2138±6 P-z (9)
2158±8 P-z (9)
2194±4 P-z (9)
2165±1 T-z (61)
2213±3 P-z (8)
2195±11 P-z (10)
2202±6 P-z (9)
2194±4 P-z (8)
2132±4 S-z (60)
2131±5 S-z (60)
2212±6 P-z (7)
2153±15 P-z (4)
3029±6 P-z (4)
2935±10 P-z (4)
2765±8 P-z (4)
2797±9 S-z (3)
3542±13 S-z (3)
2868±9 S-z (2)
2907±6 E-m (2)
2864±2 S-Z (2)
2890±9 L-z (1)
2707±29 L-z (1)
2870±7 S-z (2)
2803±11 S-z (2)
3050±16 S-z (2)
3535±9 S-z (3)
3050 P-z (5)
2801±7 P-z (5)
2770 P-z (5)
2979±5 P-z (5)
2246±44 SN-wr,g,f (5)
2203±21 SN-wr,g,p (5)
2808±2 P-z (5)
2135±3 P-z (6)
3141±2 P-z (6)
2143±3 P-z (6)
2144±6 T-z (13)
2780 P-z (5)
2186±16 T-z (11)
2143±8 P-z (6)
2158±1 T-z (14)
2154±1 T-z (12)
2162±32 Si-z (12)
2153±13 SN-wr,g (21)
2181±7 L-z (19)
2238±5 P-z (20)
2151±14 L-z (19)
2157±9 L-z (19)
2168±7 L-z (19)
2136±8 T-m (16)
2152±9 L-z (19)
2138±7 L-z (19)
2176±4 P-z (16)
2195±15 P-wr (17)
2231±31 K-a (16)
2175±1 P-z (18)
2131 T-z (49)
2152±3 T-z (15)
2149±14 P-z (33)
2137±9 T-z (15)
2152±2 T-z (15)
2154±1 T-z (14)
2131 P-z (67)
2137±14 T-z (23)
2158±9 T-z (24)
2273 T-z (25)
2174±4 T-z (25)
2187 T-z (25)
2154±9 P-z (26)
2151±10 L-z (19)
2137±7 L-z (19)
2188±12 P-z (26)
2170±9 T-z (27)
2135±16 P-z (26)
2152±9 L-z (19)
2158±8 L-z (19)
2171±7 T-z (16)
2170±6 P-z (22)
2139 T-z (28)
2132±6 P-z (16)
2135±11 U-m (22)
2162±1 T-z (28)
2134±1 T-z (28)
2134±1 T-z (28)
2151±1 T-z (28)
2156±1 T-z (28)
2151±5 P-z (33)
2195±10 P-z (33)
2150±4 S-z (29)
2148±12 S-z (29)
2187±3 S-z (29)
2196±1 T-z (28)
2195±4 S-z (30)
2132±7 S-z (30)
2193±4 S-z (31)
2131±4 S-z (31)
2187±5 S-z (31)
2150±4 P-z (6)
2145±2 T-z (32)
2179±6 P-z (34)
2155±2 T-z (42)
2135±5 T-z (52)
2159±4 P-z (35)
2189±1 T-z (36)
2222±32 K-a (35)
2136±19 S-z (39)
2142±24 S-z (39)
2170±1 T-z (14)
2169±13 S-z (38)
2200±4 P-z (35)
2179±2 T-z (37)
2180±4 S-z (38)
2173±7 P-z (6)
2132±4 T-z (28)
2163±4 P-z (6)
2232±5 S-z (38)
2178±7 P-z (6)
2158±8 P-z (35)
2162±1 T-z (44)
2134±10 S-z (38)
2131±3 T-z (44)
2165±9 ?-z (40)
2161±1 P-z (35)
2180±2 T-z (44)
2133±4 S-z (65)
2161±7 P-z (35)
2159±4 T-z (44)
2187±1 T-z (41)
2174±2 T-z,t (42)
2172±2 T-z (37)
2187±1 T-z (41)
2182±2 T-z (44)
2171±3 T-z (44)
2172±4 ?-z (40)
2166±2 T-z (44)
2165±2 T-z (44)
2159±4 T-z (43)
0
200
400
Km
1
2

teaus) were accreted to form a large crustal domain by 2.15-2.13 Ga comprised of dominantly juvenile crust. Eoeburnean crustal domains occur as a largely continuous area extending from southwestern Ivory Coast and Liberia to Burkina Faso and Ghana. In addition, the Mako belt in the KKI and KI is also comprised of Eoeburnean crust. Although data concerning the nature of the basement of the basins which constitute the Eburnean I and IIB domains (figs. 7, 8, 11, 14 and 18) is limited it is likely composed of rocks equivalent to those of the Eoeburnean domains (e.g. Vidal & Alric 1994; Feybesse et al. 2006; Adadey et al. 2009; Vidal et al. 2009; Baratoux et al. 2011). Finally, limited occurrences of Eoeburnean rocks have also been reported from eastern Guinea (Lahondère et al. 2002) and southern Mali (McFarlane et al. 2011) where Eoeburnean rocks are otherwise absent.

4.3.1.1 Onset of the Eoeburnean phase

Determining the onset of magmatic and tectonothermal activity of the EE phase is a problematic issue. Available magmatic ages (primarily U-Pb and Pb-Pb on zircon) from the Baoulé Mossi domain dominantly fall within the time span 2.24-2.07 Ga (fig. 9b). Although sensitive to the model mantle against which they are calculated, Sm-Nd model ages from Birimian volcanic, intrusive and sedimentary rocks are on average some 100-300 Ma older (fig. 9a). However, inherited zircons ages older than 2.24 Ga have been encountered in some intrusive rocks within the Baoulé Mossi domain (e.g. Gasquet et al. 2003; de Kock et al. 2011; Tapsoba et al. 2013). In addition, magmatic ages from intrusive rocks with an arc-affinity in the northeastern Guasporé shield (fig. 4) in the Amazon Craton (Vasquez et al. 2008; Macambira et al. 2009), the southern São Francisco Craton (fig. 3, Rosa Sexias et al. 2012) and northwestern Borborema belt (fig. 2, Santos et al. 2009) have yielded ages between 2.40-2.30 Ga. They are also spatially associated with younger rocks which are coeval with those in the Baoulé Mossi domain.

Gasquet et al. (2003) dated (SIMS) a zircon core to 2312±17 Ma which, as they noted, coincided with a peak of Sm-Nd model ages obtained by Boher et al. (1992) and Doumbia et al. (1998) on different Birimian rocks. On the basis of this age, they proposed that the Sm-Nd model ages could have corresponded to an important early period of crustal growth within

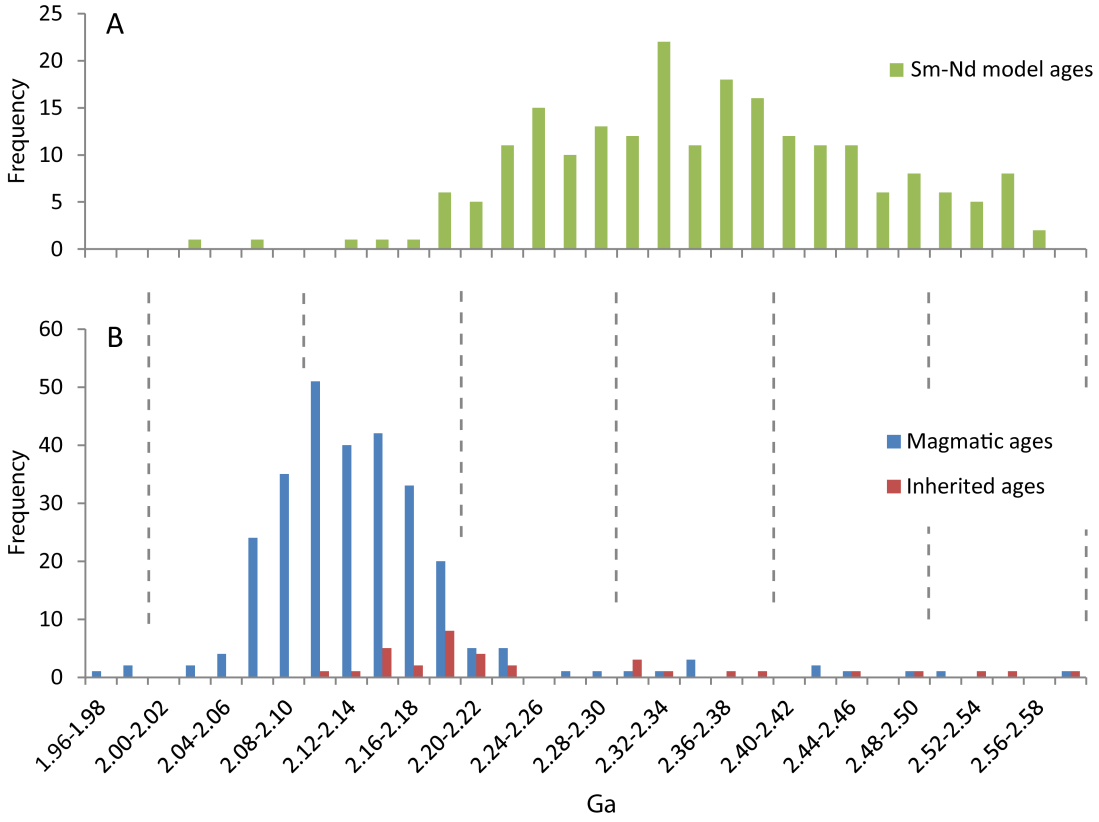

Fig. 9. **A)** Sm-Nd model ages for rocks in the WAC and AC. Compiled from A. Scherstén (unpublished data), Abouchami et al. (1990), Boher et al. (1992), Ama-Salah et al (1996), Kouamelan et al. (1997), Doumbia et al. (1998), Gasquet et al. (2003), Pawlig et al. (2006), Soumaila et al. (2008), Klein et al. (2009), Dampare et al. (2009) and Tapsoba et al. (2013). Model ages have been calculated against a depleted mantle (DM) using the following formula from Rollinson (1993); $T_{DM} = (1/\lambda) * \ln [(^{143}Nd/^{144}Nd_{sample\ today} - {}^{143}Nd/^{144}Nd_{DM\ today})/(^{147}Sm/^{144}Nd_{sample\ today} - {}^{147}Sm/^{144}Nd_{DM\ today})]$, where λ is $6.54*10^{-12}$ yr^{-1}. Depleted mantle values for $^{143}Nd/^{144}Nd$ and $^{147}Sm/^{144}Nd$ are 0.51315 and 0.2139, respectively. **B)** Magmatic and inherited ages from Birimian rocks in the WAC, AC and the Borborema belt in NE Brazil. Compiled from Klein et al. (2001, 2005a, 2005b, 2008, 2009), Vasquez et al. (2008), Macambira et al. (2009), Palheta et al. (2009) and Santos et al. (2009) in addition to references given in figure 7.

the Baoulé Mossi domain which is now preserved only as inherited zircon ages and through the isotopic composition of Birimian rocks. Feybesse et al. (2006) also argued for an early beginning for the Birimian event around 2.35 Ga which they based on the presence of rocks of this age in the Borborema belt (e.g. Santos et al. 2009).

A further complicating issue regarding the onset of the EE phase in the Baoulé Mossi domain is that the older ages encountered in South America (Amazon Craton, São Francisco Craton, Borborema belt, see figures 2 and 3) appear to be separated from the Baoulé Mossi domain and its extension into the Amazon Craton by the Amapá block (e.g. Rosa-Costa et al. 2006) in the Guyana shield (fig. 4). This is an elongate sliver of Archean crust whose orientation in the SAMBA-configuration (fig. 4) suggests that it may have been connected with the Archean crust indicated to be present in the southeastern Baoulé Mossi domain (Leube et al. 1990; Agbossoumondé et al. 2007, see section 2.2). Although this may be impossible to verify — and would in any case require more geometrically accurate reconstructions than in figure 4 — it nevertheless raises the possibility that the older rocks found in the Guasporé shield, São Francisco Craton and Borborema belt may have formed in a separate ocean basin that began to close earlier compared with the rocks in the Baoulé Mossi domain, and its extension into the Guyana shield.

Even if the older ages in the Guasporé shield, São Francisco Craton and Borborema belt are not related to the magmatic activity in the Baoulé Mossi domain there is still a need to explain the origin of the inherited zircon ages and how they relate to the peak in Sm-Nd model ages. One possibility may be that the Sm-Nd model ages record the formation of oceanic crust as the ocean in which the Baoule Mossi domain formed began to open and/or early primitive island arcs. Rare felsic magma may have crystallized zircon such as the one dated by Gasquet et al. (2003), but the setting would otherwise have been dominated by mafic magmatism. Subduction erosion (e.g. Stern 2011) may have recycled much of the early primitive island arc crust (including any felsic rocks) to the mantle, although their isotopic composition might have been preserved through the transfer of fluids and melts from eroded and subducted material.

The rise in magmatic ages may be linked to a period in which closure of the oceanic basin reached a point when island arcs began to accrete into larger masses of juvenile crust (see also next section). This may have shielded the crust more efficiently from subduction erosion as the number of active subduction zones decreased. However, thickening and maturation of islands arcs would also have led an increase in felsic magmatism through infracrustal melting, contamination and increased fractionation. As most ages in figure 9 are derived from zircons (a siliceous mineral) such a development may account for the rise in magmatic ages at this point.

Altogether, this suggests that the magmatic activity was ongoing for a considerable period of time (100-300 Myr) prior to the start of EI phase at circa 2.13 Ga. The possibility that widespread magmatic activity extended as far back as 2.40 Ga during the Birimian event is at odds with the proposal by Condie et al. (2009) that the period 2.45-2.20 Ga might have corresponded to a period of global magmatic shutdown. This proposal arose from the fact that there have so far been few zircon ages obtained from this time interval, indicating a global lack of magmatic activity. However, younger Mesoproterozoic to Phanerozoic time intervals that are also characterized by apparent low degrees of magmatic activity —although not as pronounced as during the Paleoproterozoic — have instead been attributed to a low potential of preservation of magmatic rocks due to subduction erosion, rather than the absence of magmatic activity altogether (Hawkesworth et al. 2009; Condie et al. 2009). The Sm-Nd model ages of Birimian rocks as well as both inherited and magmatic zircon ages indicates that this explanation may also be valid for the early Paleoproterozoic. The apparent absence of magmatic activity may thus be a combination of subduction erosion and predominantly mafic magmatism, but also reflect sampling bias as much of the crust from this period is found in undersampled areas of Africa and South America.

4.3.1.2 Amalgamation of Birimian crust

4.3.1.2.1 Accretion of island arcs and Archean crust

As discussed in section 4.1, the Birimian crust is here considered to have formed in an accretionary orogenic setting. Volcanic rocks are dominated by tholeiitic basalts and basaltic-andesites but also include more felsic calc-alkaline rocks (fig. 10). Intrusive magmatism at this time is mainly sodic and comprised of gabbro-diorite-tonalite-granodiorite compositions, although more K-rich granites also occur. The range of compositions is equivalent to those found among Phanerozoic island and continental arcs (e.g. Patiño Douce 1999; Frost et al. 2001). The predominantly sodic composition of the intrusive rocks suggest that they were derived from fractionation of magma derived from melting of metasomatized mantle (Arculus 1994; Tatsumi 2005), amphibolites (Moyen & Martin 2012) or immature sediment such as greywackes (Patiño Douce 1999).

Because of its large areal extent it seems reasonable to assume that the Baoulé Mossi domain is comprised of multiple accreted island arcs, now occurring as terranes. However, a lack of geochronological, structural, metamorphic and isotopic data makes it hard to distinguish any such arc terranes at this stage. A possible proxy for arc-arc accretion may be deformation events involving compression which occurred during the EE phase. For example, de Kock et al. (2009, 2012) recognized deformation sometime prior

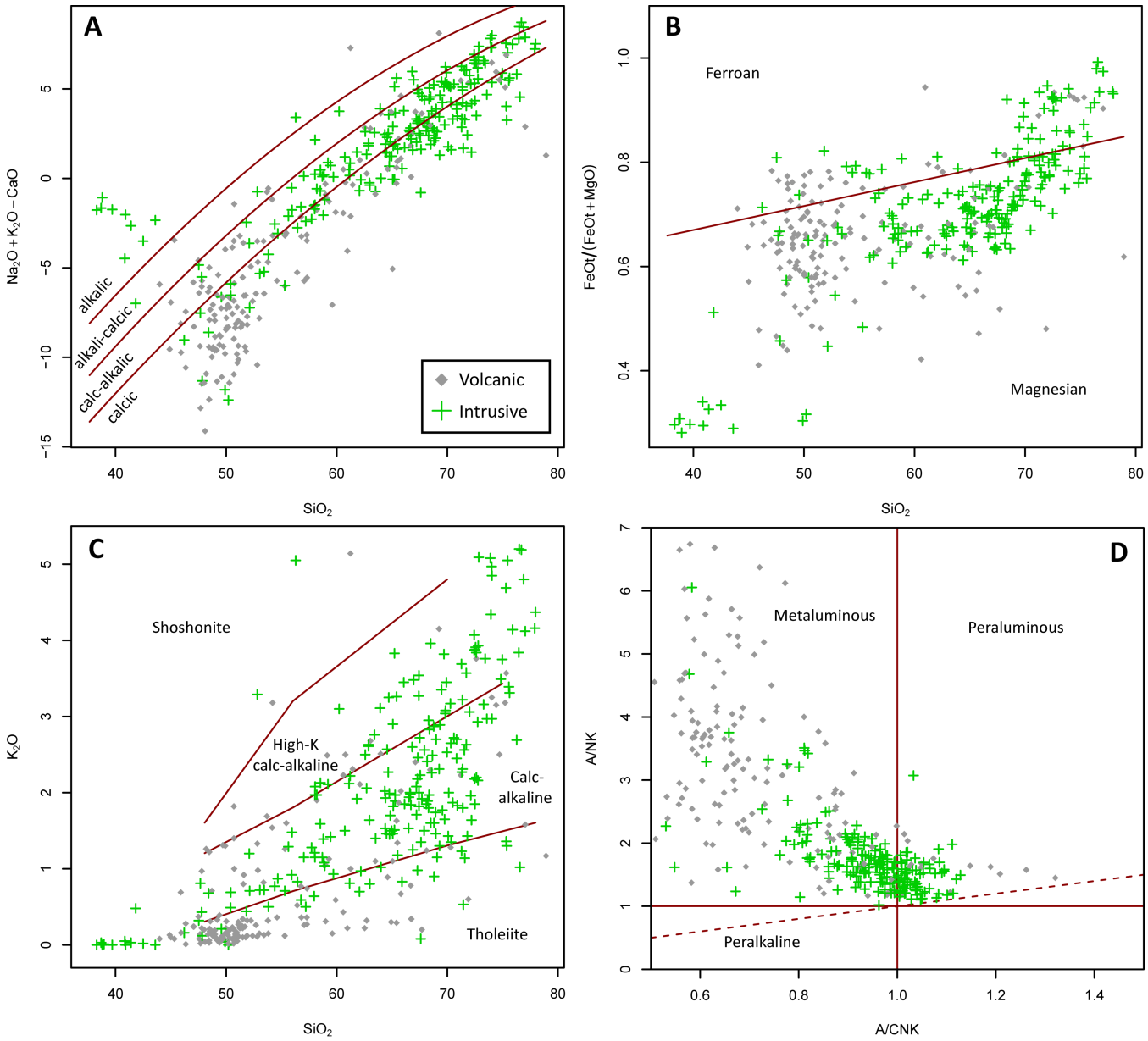

Fig. 10. Geochemical data for volcanic and intrusive rocks formed during the Eoeburnean phase (>2.13 Ga). **A)** Na_2O+K_2O-CaO vs. SiO_2 after Frost et al. (2001). **B)** $FeO_t/(FeO_t+MgO)$ after Frost et al. (2001). **C)** K_2O vs. SiO_2 diagram after Peccerillo and Taylor (1976). **D)** A/NK vs. A/CNK after Shand (1943). Data from A. Scherstén (unpublished data), Toure et al. (1987), Abouchami et al. (1990), Boher et al. (1992), Sylvester and Attoh (1992), Ama-Salah et al (1996), Pouclet et al. (1996), John et al. (1999), Loh and Hirdes (1999), Lahondére et al. (2002), Gasquet et al. (2003), Naba et al. (2004), Dampare et al. (2005, 2008), Dioh et al. (2006), Pawlig et al. (2006), Adadey et al. (2009), Attoh et al. (2006), Klein et al. (2008, 2009), de Kock et al. (2009), Siegfried et al. (2009), Thomas et al. (2009), Ngom et al. (2010), Baratoux et al. (2011) and Tapsoba et al. (2013).

to the intrusion of circa 2195±4 Ma (SHRIMP on zircon) granites in the Bole belt. This was followed by formation of enriched basalts and emplacement of granodiorites and tonalites at 2187±5 Ma (SHRIMP on zircon). Although these authors favored a model of intra-arc rifting - leading to formation of oceanic crust in a backarc basins and its subsequent closure - to account for the magmatism, it seems as if it could also be accounted for by post-collisional extension following accretion of two island arcs, perhaps accompanied by extension following resumption of subduction outboard the recently amalgamated crust. However, as mentioned above, recognizing events that record docking of different arcs requires more data from across the Baoulé Mossi domain. It is also hampered by overprinting of later events.

It is also of interest to understand when and to what extent the Birimian crust interacted with Archean crust during the EE phase. The Winneba (Leube et al. 1990) pluton in southeastern Ghana has been dated to 2113±1 Ma (TIMS on zircon) by Agyei Dudodu et al. (2009) while the Palimé-Amlamé pluton in Togo was dated to 2127±2 (TIMS on zircon) by Agbossoumondé et al. (2007). Both of these plutons have negative εNdt indicative of an Archean crustal component. The above ages are coeval with magmatic activity elsewhere within the Baoulé Mossi domain and thus indicate that the Birimian crust was attached to Archean

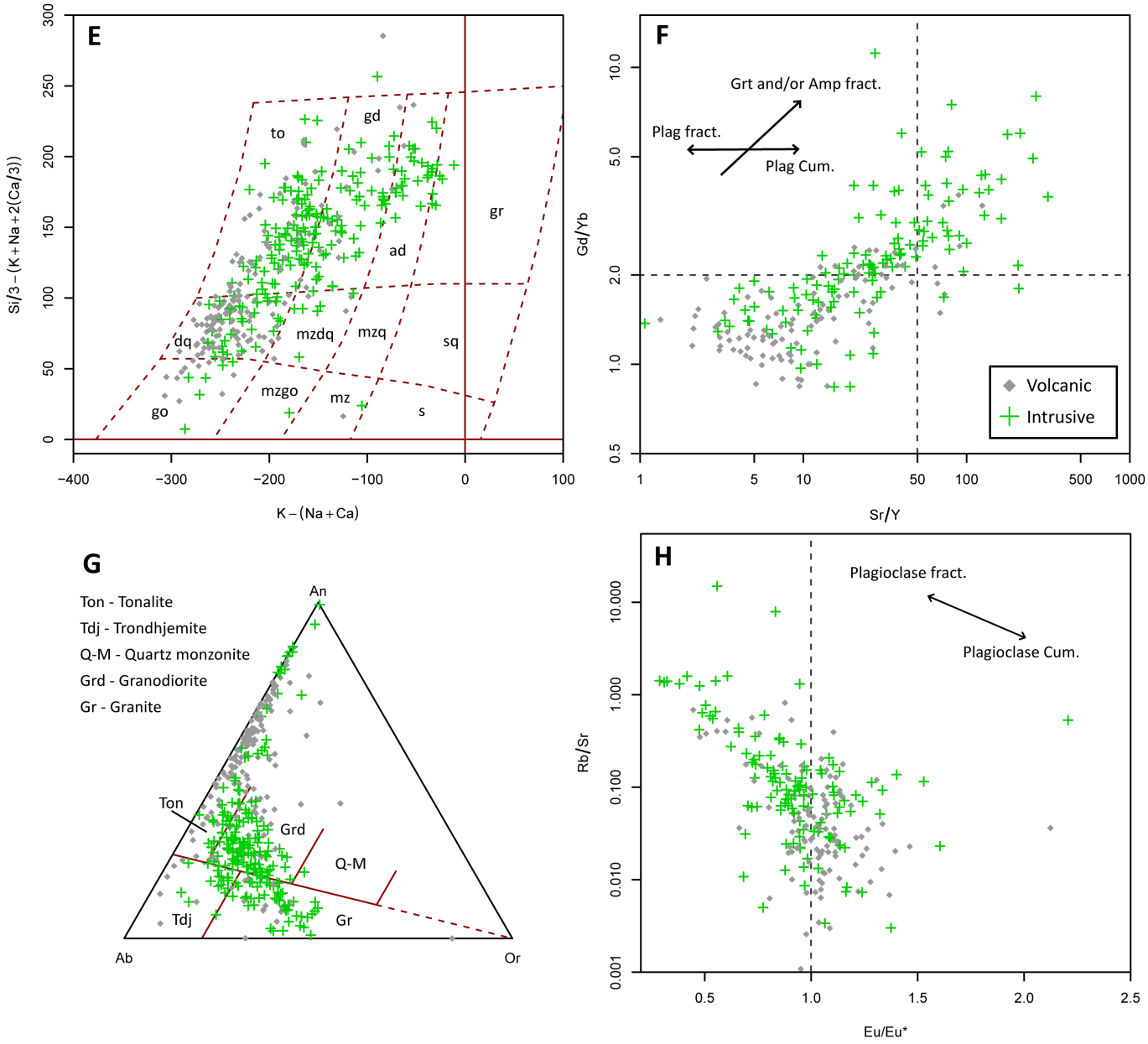

Fig. 10 continued. **E)** Millicationic P-Q diagram after Debon and Le Fort (1983) **(F)** log Gd/Yb vs. log Sr/Y. **G)** Ternary Albite-Anorthite-Orthoclase (CIPW norm) feldspar diagram after O'Connor (1965). **H)** log Rb/Sr vs. Eu/Eu* (Eu/√(Nd*Sm) after Kemp and Hawkesworth (2003).

crust in the present east of the Baoulé Mossi domain by 2.13 Ga at the latest. However, in the Amapá block, monzogranites were dated at 2218-2185 Ma (Pb-Pb on zircon) by Rosa-Costa et al. (2006) while Rosa-Costa et al. (2008) obtained similar ages from monazite in migmatitic gneisses. Because similar ages where present in the Birimian crust of the Paru domain (fig. 4) to the present southwest of the Amapá block, Rosa-Costa et al. (2008) suggested that the magmatic activity within the Amapá block may represent crustal reworking linked to arc building in the southwest. As discussed in section 4.3.1.1, the Birimian crust of the Paru domain and the Guasporé shield may have formed in an ocean basin separate from that in which the Baoulé Mossi domain formed. The ages obtained by Rosa-Costa et al. (2006, 2008) may therefore not record interaction between Birimian crust in the Baoulé Mossi domain (or rather its extension into the Amazon Craton).

However, possible involvement of older crust has also been indicated in supracrustal rocks from the Ashanti belt (Dampare et al. 2009) and the São Luís Craton (Klein et al. 2009) on the basis of Sm-Nd isotopic data. The rocks from the São Luís Craton have an assumed magmatic age of 2.24 Ga (Klein & Moura 2001) while those of the Ashanti belt should be older than circa 2.17 Ga, which is the age of intrusive rocks of that belt (e.g. Hirdes et al. 1992). While they may not represent definitive proof for the involvement of Archean crust and may simply represent incorporation of older Paleoproterozoic crust (Klein et al. 2009), they nevertheless provide an indication that the Birimian crust of the Baoulé Mossi domain may have interacted with Archean crust in the present-day east

as early as 2.24 Ga. The Archean crust may perhaps have acted as a backstop for accreting arcs. More coupled isotopic and geochronological data from magmatic rocks in the eastern Baoulé Mossi would be required to determine more precisely when Birimian and Archean crust may have begun to interact.

4.3.1.2.2 An extensional phase in Ghana and the São Luís Craton?

At least Ghana and the São Luís Craton may have experienced a period of extension between 2160-2150 Ma. Monzogranite emplacement in southern Ghana at this time was attributed by Feybesse et al. (2006) to infracrustal melting through thickening. However, these rocks are also coeval with emplacement of amphibole±clinopyroxene bearing diorites, tonalites and granodiorites (e.g. Loh & Hirdes 1999; Attoh et al. 2008; Klein et al. 2008). In the São Luís Craton, diorites from the Tromai suite which are spatially and temporally associated with the syenogranitic Areal granite (Klein et al. 2008) are tholeiitic. Meanwhile, the Areal granite has a composition which tends towards the ferroan field of the $FeO_t/(FeO_t+MgO)$ diagram of Frost et al. (2001). It also has a pronounced negative Eu-anomaly with unfractionated HREE. Such a composition may be caused by shallow infracrustal melting during crustal extension which leaves residual plagioclase and orthopyroxene (Patiño Douce 1997).

Taken together, the presence of both tholeiitic diorites and K-rich granites indicate that this region was under extension at 2160-2150 Ma. Large degree melting of upwelling mantle may have generated the diorites while heat from the mantle and intruding magma could have been sufficient to partially melt the Birimian crust, forming the K-rich granites. In addition to southern Ghana and the São Luís Craton, monzogranite magmatism also took place in the Bole belt at circa 2150 Ma (de Kock et al. 2009, 2011). Perrouty et al. (2012) identified extensional structures in the Ashanti belt which they interpreted to have formed during the EE phase. It may be speculated that this extension is connected with the magmatic activity at 2160-2150 Ma, although it may of course be related to other periods involving extensional tectonics. The EE phase was thus not all about accretion and compressional tectonics but also involved extension in a similar manner to modern accretionary orogens, with important implications for crustal growth and differentiation (Cawood et al. 2009).

4.3.1.2.3 Final amalgamation of Eoeburnean crust

By 2.15 Ga, the Eoeburnean crust within the Baoulé Mossi domain likely formed a continuous mass which is also favored by previous workers in more local studies (e.g. Feybesse et al. 2006; Baratoux et al. 2011). The coherence of the Eoeburnean crust is indicated by magmatic activity throughout the crust between 2.16-2.13 Ga but also by the fact the sedimentary basins which formed late during the EE phase as well as the EI phase are underlain by older Eoeburnean crust which requires that it was coherent before basin formation (e.g. Vidal & Alric 1994; Feybesse et al. 2006; Adadey et al. 2009; Baratoux et al. 2011; de Kock et al. 2012). Although there are only scattered occurrences of Eoeburnean crust in the EIIA domain (fig. 7) these may nevertheless correspond to the remnants of extended crust which have been overprinted by younger EIIA magmatism (see further discussion in section 4.3.3). The occurrence of such crust in the EIIA domain can be used to infer a connection between the Mako belt in the Kedougou-Kéniéba inlier (fig. 5) and the Eoeburnean crust in eastern Baoulé Mossi, which otherwise also show the same distribution of magmatic ages.

The amalgamated Eoeburnean crust was likely bordered to the west by an east-southeast dipping subduction zone. Such an orientation has also been favored by e.g. Vidal and Alric (1994) and de Kock et al. (2012) to account for structures which indicate east-west to northwest-southeast compression and/or extension. However, a east-southeast dipping subduction zone also appear to be required in order to account for the juxtaposition of the Archean crust in the Man domain with Birimian crust in the Baoulé Mossi domain. This is because there is no indication of a long-lived Birimian arc along the margin of the Man domain which instead appears to have corresponded to a passive margin. With that said, there are currently few ages from this region and the presence of a long-lived active margin cannot be entirely ruled out. Nevertheless, it will be assumed here that that the Man domain was fringed by passive margins leading up to the collision with the Birimian crust.

The Maluwe basin opened around 2.14-2.13 Ga as a result of crustal extension and was accompanied by the intrusion of amphibole-bearing granodiorites (de Kock et al. 2012). Magmatic activity within the Maluwe basin also continued into the EI phase. Opening of the Maluwe basin was preceded by what appears to be a small hiatus in magmatic activity between c. 2.15-2.14 Ga as there are few magmatic ages so far obtained from this period within the Baoulé Mossi domain. It is notable that detrital zircon ages (SHRIMP) obtained by Pigois et al. (2003) from the Tarkwa shallow water basin in the Ashanti belt show a peak at this time interval, indicating that magmatic activity may have been more important at this time than the currently available geochronological data suggest. However, there is also a possibility that the zircons are derived from somewhere outside of the currently exposed Birimian crust in the Man-Leo shield.

4.3.2 Eburnean I (2.13-2.10 Ga) — figure 11

The establishment of a coherent crustal mass by the end of the EE phase set the stage for the EI phase. It was likely flanked by an east-southeast dipping subduction zone to the west and possibly by Archean crust to the east. The EI phase in large parts represents a continuation of the EE phase but is distinguished by

the formation of several deep water and shallow water basins. The EI phase also covers the collision of the Archean crust of the Man domain with the Birimian crust. This collision occurred in the southern half of the Baoulé Mossi domain as well as its extension into the Guyana shield in the Amazon Craton.

Crustal domains established during the EI phase include the Boromo and Houndé-Haute Comoé sedimentary basins in northeastern Ivory Coast and western Burkina Faso as well as the Kumasi basin in southern Ghana. In addition, based on the age of the Ity-Toulépleu massif (Kouamelan et al. 1997) the Birimian crust in the southeastern Man domain is also assigned to this phase. This age is also the reason for assigning the Birimian overprint on the southeastern Man domain (e.g. Kouamelan et al. 1997; Pitra et al. 2010) to the EI phase although it likely also continued into the EII phase (see section 4.3.3). Magmatic and tectonothermal activity during the EI phase also affected the Eoeburnean crustal domains.

4.3.2.1 Deformation

The widespread deformation and shearing which took place during the EI phase shows that the crust which amalgamated during the EE phase had not yet stabilized and was now deforming internally. It is beyond the scope of this work to attempt to make a detailed reconstruction of the deformation during the EI phase and how it may relate to the formation of the sedimentary basins. The following section will therefore mainly highlight different aspects of this deformation.

The structural evolution of the Birimian crust during the EI phase was complex. As an example, the Kouare granite in eastern Burkina Faso (fig. 7) — dated at 2128±6 Ma (Pb-Pb on zircon, Castaing et al. 2003, in Vegas et al. 2008) — is interpreted to have been emplaced during northwest-southeast compression that generated north-northeast-trending sinistral shear zones (Vegas e al. 2008). The proximal and circa 10 Myr younger (dated at 2117±6 Ma, Pb-Pb on zircon, Castaing et al. 2003, in Vegas et al. 2008) Tenkodogo-Yamba monzogranite is instead interpreted to have been emplaced during dextral shearing along a northeast trending shear zone. The north-south trending sinistral Ouango-Fitini shear zone (e.g. Vidal & Alric 1994; Vidal et al. 1996) that runs along the Haute-Comoé basin (fig. 7) is constrained to around 2105-2095 Ma by intrusive rocks affected by shearing (Hirdes et al. 1996). To the west, movement along the N'Zi-Brabo is constrained by a maximum age of 2116 Ma. This age is obtained from the northwest-trending Kowara two-mica leucogranite which terminates at the contact with the leucocratic N'Zi granite that runs parallel with the N'Zi-Brabo shear zone (fig. 7, Gasquet et al. 2003).

Sinistral and dextral shearing therefore appears to have varied alternately over time, even in areas where the shear zones had roughly the same orientation. As will be further discussed in section 4.3.3, the Baoulé Mossi domain was also subjected to widespread sinistral shearing during the EII phase. While field observations enable reconstruction of the stress field that deformed the Birimian crust at a given time it is more problematic to determine the causes of primary stress. This is compounded by the fact that much of the Birimian crust in the WAC is covered by younger sediment and that crust that was once connected to the WAC is now displaced due to subsequent orogenic activity and plate movements. However, it seems likely that the Archean crust of the Man domain may have had some influence on the Birimian crust as it began to collide with the Birimian crust although it is likely hard to separate deformation that may have been caused by e.g. oblique subduction.

4.3.2.2 Basin formation

4.3.2.2.1 General models for basin formation

Most models for the formation of sedimentary basins involve rifting in an extensional or transtensional regime followed by sedimentation and inversion through transpression-compression (e.g. Vidal & Alric 1994; Vidal et al. 1996; Feybesse et al. 2006; de Kock et al. 2012; Perrouty et al. 2012). This accounts for the opening, sedimentation and subsequent folding and shearing of sedimentary rocks and synkinematic intrusive rocks. In western Burkina Faso, Baratoux et al. (2011) proposed that sedimentation may have occurred simultaneously with compression in foreland basins that developed as the Birmian crust was folded into crustal scale anti- and synforms. In a similar manner, Feybesse et al. (2006) also proposed that sedimentation in the deep water basins in southern Ghana may have partly overlapped with closure of the basins in a foreland-type setting.

4.3.2.2.2 Block rotation and the importance of the Ouango-Fitini shear zone

Vidal and Alric (1994) proposed that the Haute-Comoé basin, and other north-south trending sedimentary basins within the Baoulé Mossi domain, formed as oblique backarc basins behind a southeast dipping subducting slab. The margin of this subduction zone was located along the current GFB shear zone (fig. 7b), which in this model corresponds to a suture. In the model of Vidal and Alric (1994), the sedimentary basins opened during transtension and closed during a subsequent switch to transpression as the Birimian crust was subjected to northwest-southeast compression. Movement along the sinistral Ouango-Fitini shear zone established the "pinched" shape of the Haute-Comoé basin (see figure 7).

An interesting aspect of the Ouango-Fitini shear zone is that it appears to terminate in the northern part of the Comoé-Sunyani basin, which here serves as the southern limit of the EI domain that covers the Haute-Comoé basin (figure 11). This aspect of the Ouango-Fitini shear zone does not appear to have been dealt with in the presently available literature. However, it may offer a clue to how the sedimentary

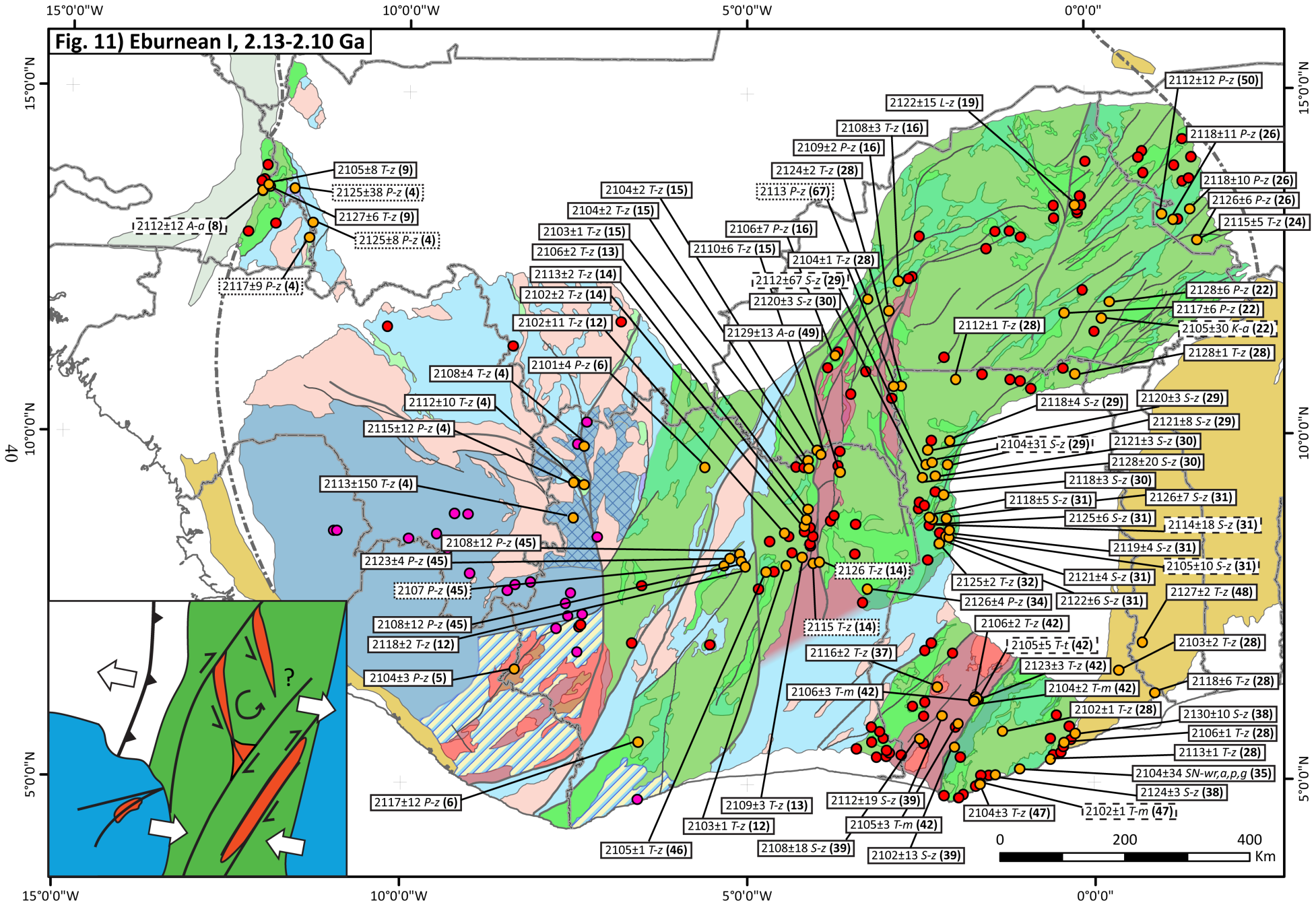
Fig. 11) Eburnean I, 2.13-2.10 Ga
15°0'0"W
10°0'0"W
5°0'0"W
0°0'0"
15°0'0"N
10°0'0"N
5°0'0"N
2112±12 P-z (50)
2122±15 L-z (19)
2108±3 T-z (16)
2109±2 P-z (16)
2124±2 T-z (28)
2113 P-z (67)
2118±11 P-z (26)
2118±10 P-z (26)
2126±6 P-z (26)
2115±5 T-z (24)
2105±8 T-z (9)
2125±38 P-z (4)
2127±6 T-z (9)
2125±8 P-z (4)
2112±12 A-a (8)
2117±9 P-z (4)
2104±2 T-z (15)
2104±2 T-z (15)
2103±1 T-z (15)
2106±2 T-z (13)
2113±2 T-z (14)
2102±2 T-z (14)
2102±11 T-z (12)
2106±7 P-z (16)
2110±6 T-z (15)
2104±1 T-z (28)
2112±67 S-z (29)
2120±3 S-z (30)
2129±13 A-a (49)
2128±6 P-z (22)
2117±6 P-z (22)
2105±30 K-a (22)
2112±1 T-z (28)
2128±1 T-z (28)
2108±4 T-z (4)
2101±4 P-z (6)
2112±10 T-z (4)
2115±12 P-z (4)
2113±150 T-z (4)
2118±4 S-z (29)
2120±3 S-z (29)
2121±8 S-z (29)
2104±31 S-z (29)
2121±3 S-z (30)
2128±20 S-z (30)
2118±3 S-z (30)
2118±5 S-z (31)
2126±7 S-z (31)
2125±6 S-z (31)
2114±18 S-z (31)
2119±4 S-z (31)
2105±10 S-z (31)
2121±4 S-z (31)
2122±6 S-z (31)
2108±12 P-z (45)
2123±4 P-z (45)
2107 P-z (45)
2108±12 P-z (45)
2118±2 T-z (12)
2104±3 P-z (5)
2126 T-z (14)
2125±2 T-z (32)
2126±4 P-z (34)
2127±2 T-z (48)
2115 T-z (14)
2106±2 T-z (42)
2105±5 T-t (42)
2116±2 T-z (37)
2103±2 T-z (28)
2123±3 T-z (42)
2118±6 T-z (28)
2106±3 T-m (42)
2104±2 T-m (42)
2102±1 T-z (28)
2130±10 S-z (38)
2106±1 T-z (28)
2113±1 T-z (28)
2104±34 SN-wr,a,p,g (35)
2124±3 S-z (38)
2102±1 T-m (47)
2104±3 T-z (47)
2112±19 S-z (39)
2109±3 T-z (13)
2103±1 T-z (12)
2105±3 T-m (42)
2108±18 S-z (39)
2102±13 S-z (39)
2105±1 T-z (46)
2117±12 P-z (6)
?
0
200
400
Km
40

Fig. 11. The spatial extent of Eburnean I crustal domains together with a compilation of geochronological data from the Eburnean I phase. See figure 7 for legend and references. Inset shows a schematic depiction of the geodynamic setting during the Eburnean I phase (2.13-2.10 Ga). During the Eburnean I phase, the Archean crust in the Man domain began to impinge on the Eoeburnean crust now present in the south-southeastern Baoulé Mossi domain and in the Maroni-Itacaiúnas domain in the Amazon craton (fig. 4). Meanwhile, an active subduction zone is still present in the northern part of the Baoulé Mossi domain. The collision in the present-day south may have triggered slab rollback in the north as the active subduction zone began to rotate against the Archean crust of the Man domain, leading to crustal extension in the north even as the southern areas where subjected to compression. The collision between the Archean crust of the Man domain and the Eoeburnean crust may led to the establishment of northeast trending dextral shear zones interconnected with north-south trending sinistral shear zones (such as the N'Zi-Brabo and Ouango-Fitini, see figure 7). During dextral shearing block rotation may have been responsible for the formation of an early set of sedimentary basins corresponding to Haute-Comoé and Boromo (fig. 7). Within this context, the Kumasi basin may have formed as a pull-apart basin on account of its orientation parallel to the inferred northeast-southwest trending dextral shear zones. The northeast-southwest trending dextral shear zones later acted as structures along which the Bandama-Banfora and Comoé-Sunyani sedimentary basins opened during northwest-southeast extension (see section 4.3.3 and figure 14). During the initial collision, the southeastern portion of the Man domain was subjected to a Birimian overprint leading to metacratonization with the development of shear zones and intrusion of the Ity-Toulepleu tonalite. This interaction may or may not have involved thrusting of Birimian crust onto the Archean continent (see further discussion in section 2.2.3).

basins formed during the EI phase as well as during the subsequent EIIB phase.

On most geological maps covering the Ivory Coast, the Ouango-Fitini shear zone is shown to have slightly sigmoid shape, bending towards the southwest in the south and towards the northeast in the north (figure 7, cf. Milési et al 1989; Feybesse & Milési 1994; Baratoux et al. 2011). This also applies to the N'Zi-Brabo shear zone which has the same general shape as Ouango-Fitini. In the north, both shear zones connect with the northeast-trending dextral GFB shear zone in Burkina Faso (fig. 7, Baratoux et al. 2011). As can be seen in figure 7, both the northern and southern ends of the N'Zi-Brabo and Ouango-Fitini shear zones connect with the northeast-southwest oriented EIIB crustal domains.

As will be discussed further in section 4.3.3.2, the Banfora-Bandama and Comoé-Sunyani basins which comprise the two EIIB crustal domains likely opened simultaneously. This may have taken place in response to rapid slab rollback in the present northwest triggered by the ongoing collision between the Man domain and the Birimian crust in the present-day southwest. Because of the similar orientation, and because they "bracket" both the N'Zi-Brabo and Ouango-Fitini shear zones, it may be speculated that when the Banfora-Bandama and Comoé-Sunyani basins opened they utilized preexisting northeast-southwest structures established during the EI phase that were connected to the north-south trending shear zones.

The Ouango-Fitini shear zone may therefore have been connected to a shear zone that ran parallel to the Comoé-Sunyani basin but which was destroyed when the latter opened. The same applies to the N'Zi-Brabo shear zone further to the southwest. Assuming that the N'Zi-Brabo and Ouango-Fitini and the northeast trending shear zones were interconnected, the latter must have been dextral in order to account for the sinistral shearing recorded along the former (Mortimer 1992b; Vidal & Alric 1994; Gasquet et al. 2003). This is in accordance with the dextral movement recorded along the GFB in western Burkina Faso (Baratoux et al. 2011). Such a structure suggests that the Birimian crust underwent some form of block rotation during the EI phase. This may help explain both the "pinched" shape of the Haute-Comoé basin as well as the sudden termination of the Ouango-Fitini shear zone in the south. In addition, it also provides an explanation for the location of the Banfora-Bandama and Comoé-Sunyani basins. However, it requires that the subduction zone was located to the northwest of the GFB shear zone unlike the model by Vidal and Alric (1994).

Since both the Haute-Comoé and Comoé-Sunyani basins are defined by low-grade metamorphism (e.g. Vidal & Alric 1994) there does not appear to have been any significant vertical displacements between them. This may indicate that there was a smooth transition from the opening of the Haute-Comoé basin and until the opening of the Comoé-Sunyani basin. Perhaps both basins remained submerged throughout this period, which would prevent a break in sedimentation, at least during the establishment of the Comoé-Sunyani basin.

The model presented above does not account for the Kumasi basin which, based on detrital and magmatic ages (e.g. Hirdes et al. 1992; Davis et al. 1994), was coeval with the Haute-Comoé basin. In fact, the orientation of the Kumasi basin appears to be parallel with the proposed shear zones along which the Banfora-Bandama and Comoé-Sunyani basins subsequently opened. Because of their similar orientation, it may be speculated that the Kumasi basin formed in a similar manner to the Banfora-Bandama and Comoé-Sunyani basins, i.e. by extension at a high angle to a northeast-striking shear zone. However, the Kumasi basin may perhaps also represent an elongate pull-apart basin formed during dextral shearing.

4.3.2.2.3 Lower crustal flow

Considering the high geotherm inferred for the Baoulé Mossi domain (see section 4.1.3) it might be possible that lower crustal flow may have been important during the Birimian event. A possible modern example of lower crustal flow can be found in Sundaland in SE Asia. Sundaland is located in the backarc region of subduction zones facing both the Indian and Pacific

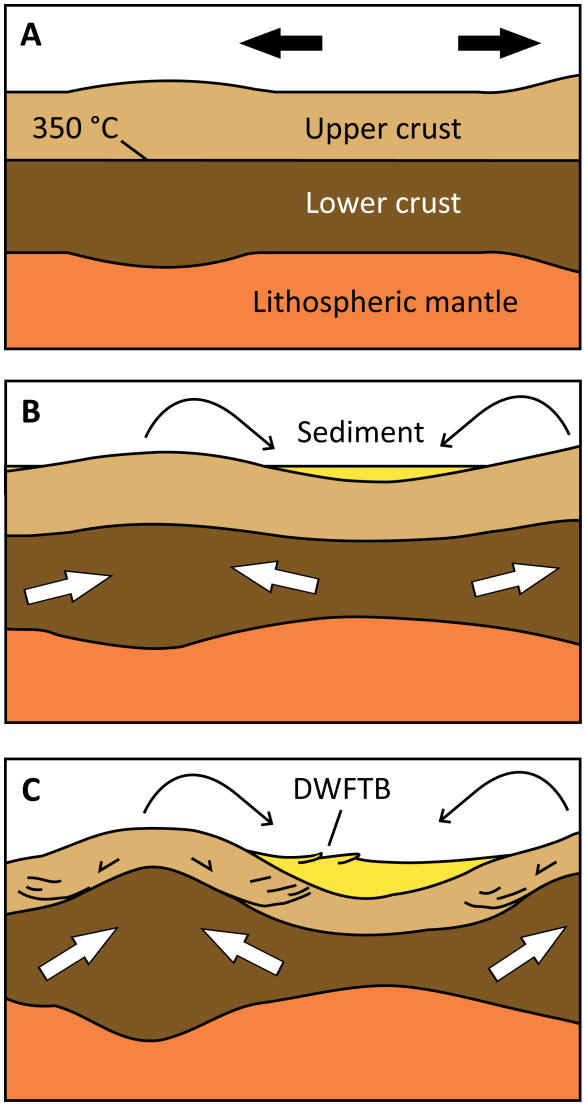

Fig. 12. Lower crustal flow in thin and hot lithosphere. Redrawn after Hall (2011), based on the model of Morley and Westaway (2006). **A)** Starting conditions in which thin and warm crust with a mild topography is divided into upper and lower crustal sections separated by a thermal boundary at 350°C. The crust is extended leading to the establishment of a muted topography. **B)** Sedimentation in depocentre leads to thermal blanketing which lowers the geotherm, thus shifting the upper/lower crust boundary downwards. Simultaneous erosion in the sediment source region leads to uplift of lower and warmer crust, shifting the upper/lower crust boundary upwards. This creates a lateral pressure gradient upon the lower crust which therefore flows from the depocentre towards the sediment source regions. In a non steady-state situation, this leads to crustal thinning under the depocentre. **C)** Lower crustal flow leads to vertical motion and uplift of in the source region. This creates a setting in which partially or fully gravity-driven deep water fold and thrust belts (DWFTB) can develop in the offshore depocentre.

oceans and is characterized by a high heat flow and a thin lithosphere (Currie & Hyndman 2006; Hall 2011). Within Sundaland, the establishment of superdeep (some with thicknesses exceeding 15 km) sedimentary basins has been attributed to lower crustal flow (Morley & Westaway 2006). The reason for this is that the amount of crustal extension is insufficient to account for the significant depth of the basins, unlike in conventional models for basin formation and sedimentation.

As envisioned for the Sundaland basins, lower crustal flow may be triggered by the cooling effect of sediment which shifts the temperature-dependent upper-lower crust boundary (at 350°C) downwards beneath the depocentre while it is simultaneously raised beneath the sediment source regions (fig. 12, Morley & Westaway 2006). This causes the lower crust to flow from the depocentre towards the source regions, thus creating accommodation space for more sediment within the basin.

Hall (2011) expanded on the model by Morley and Westaway (2006) to explain the presence of highlands in Sundaland (e.g. in northern Borneo) that exposes high-grade and mid-crustal intrusive rocks and which occur parallel with offshore sedimentary basins. Hall (2011) argued that these highlands could have been uplifted through lower crustal flow triggered by offshore sedimentation. He further suggested that uplift onshore may be responsible for the development of deep water fold and thrust belts in offshore sedimentary basin through gravity-driven compression.

For the Birmian crust, lower crustal flow carries the implication that extension may have been less important (although still needed for establishing a depocentre). In addition, lower crustal flow may also account for the uplift and exposure of granitoid-gneiss domains next to the basins. The possibility of gravity-driven fold and thrust belts also adds further complications when it comes to determine stresses during the Birimian event as structures may not record regional compression but only the (reverse) direction of lower crustal flow.

4.3.2.3 Juxtaposition of Man and Baoulé Mossi domains

The Archean crust of the Man domain likely began to collide with the Birimian crust during the EI phase. While shearing and opening of the sedimentary basins around 2.13-2.12 Ga may have been triggered by incipient collision between the Archean and Birimian crust, the main collisional phase with associated HP-HT metamorphism instead likely occurred during the late EI and early EII phases. The oldest Paleoproterozoic age from the Man domain is 2104±3 Ma (Pb-Pb on zircon) obtained by Kouamelan et al. (1997) from the tonalitic Ity-Toulépleu massif (fig. 11). As discussed in section 2.2.3 this age may correspond to a maximum or minimum age of what might be considered the main collisional phase depending on whether the Ity-Toulépleu massif is part of a Birimian klippe (Feybesse & Milési 1994) or is an intrusion whose emplacement was triggered by metacratonization of the Archean crust as it collided with the Birmian crust (Pitra et al. 2010).

Although it has been proposed that high-P

granulite facies metamorphism affected the southeastern Man domain around 2.05-2.03 Ga (Pitra et al. 2010) it will be argued in section 4.3.4 that it may instead have taken place around 2.10-2.09 Ga. The primary reason for this reinterpretation is that there is little tectonothermal or magmatic activity within the Baoulé Mossi domain at 2.05 Ga. It therefore seems unlikely that a high-grade metamorphic event took place in the southeastern Man domain at this time. 2.10-2.09 Ga instead seem as a more suitable time as this coincides with widespread tectonothermal and magmatic activity within the Baoulé Mossi domain (e.g. Feybesse et al. 2006; Pouclet et al. 2006; Vidal et al. 2009).

Assuming that the southeastern Man domain reached peak high-P granulite facies conditions around 2.10-2.09 Ga also places some constraints on when the Man domain may have collided with the Birimian crust as it would take some time following collision before peak conditions were reached. Peak metamorphic conditions at 2.10-2.09 Ga seem to fit better with the model of Pitra et al. (2010) in which the Ity-Toulépleu massif intrudes as the Archean crust is metacratonized. However, it is conceivable that the supracrustals within the Ity-Toulépleu domain may represent a klippe — as proposed by Feybesse and Milési (1994) — which was emplaced at an earlier stage. Future dating of detrital zircon from sediment among these supracrustals may help shed some light on their origin.

The current lack of ages from the Man domain and southwestern Baoulé Mossi domain is problematic and more detailed reconstructions of when and how the Man and Baoule Mossi domains became juxtaposed requires more geochronological data that records magmatism, metamorphism, sedimentation and cooling on both sides of the contact. This data may also help shed some light on the SASCA domain (fig. 5). At this point there is little information concerning where the Archean crust of the SASCA domain may have come from; whether it originally was a part of the Man domain or rather constituted a separate microcontinent.

4.3.2.4 EI magmatism

Magmatism during the EI phase shows a compositional range (fig. 13) equivalent to that of the EI phase (fig. 10). This is in line with the model by Baratoux et al. (2011) in which the period 2160-2120 Ma was characterized by emplacement of abundant TTG intrusions. Although the number of samples from volcanic rocks is significantly lower this does not reflect the relative proportion of volcanic rocks between the EE and EI phases, even though eruptive magmatism may have played a smaller part during the latter. The similar compositional range suggests that the Birimian crust of the Baoulé Mossi domain was close to the east-dipping subduction zone to the west during the EI phase. However, most of the samples that are plotted in figure 13 are from rocks which formed between circa 2.13-2.12 Ga and come from northwestern Ghana although samples from the Kedougou-Kéniéba inlier, Burkina Faso, Ivory Coast and Togo (fig. 1) are also included. The intrusion of the sanukitoid-like Palimé-Amlamé pluton in Togo at 2127±2 (TIMS on zircon, Agbossoumondé et al. 2007) and the 2121±4 (SHRIMP on zircon) high-Mg Bomburi granodiorite in the Maluwe basin (de Kock et al. 2009), together with the recent opening of the Maluwe basin (de Kock et al. 2012) indicate that the Birmian crust in the Baoulé Mossi domain at this point was undergoing extension.

There is a tendency among EI intrusive rocks to have higher Gd/Yb and Sr/Y (fig. 13f) compared with EE intrusive (and volcanic) rocks (fig. 10f). This may indicate magma generation at a greater depth within the stability field of garnet or a greater sedimentary (aluminous) component in the source of the magma that increases the stability of garnet at lower pressure (Moyen 2009). However, it may also reflect that the EI magmatic rocks were derived from sources with more fractionated HREE and Y or higher Sr and LREE-MREE compared with the EE rocks. The latter should not be ruled out as EE intrusive and supracrustal rocks would have provided the crustal source for later EI intrusive and volcanic rocks. However, the shift towards higher Gd/Yb and Sr/Y during the EI phase may also reflect a gradual thickening of the Birimian crust (e.g. Baratoux et al. 2011).

Following 2.12 Ga, there appears to be a shift towards more granitic and monzogranitic compositions among intrusive rocks in the eastern Baoulé Mossi domain. This includes the monzogranitic Tenkodogo-Yamba pluton (Naba et al. 2004) in eastern Burkina Faso dated to 2117±6 Ma (Pb-Pb on zircon, Castaing et al. 2003, in Vegas et al. 2008), the Tonton granite in the Kumasi basin dated to 2112±19 Ma (SHRIMP on zircon, Adadey et al. 2009) and the Winneba granite in southeastern Ghana dated to 2113±1 Ma (TIMS on zircon, Agyei Duodu et al. 2009). However, granodioritic intrusions, including minor trondhjemitic and monzogranitic components (Yao & Robb 2000), from the Kumasi basin have been dated to 2106-2104 Ma (TIMS on zircon and monazite, Oberthür et al. 1998) and show that more sodic magmatism was nevertheless present during the later part of the EI phase.

The more K-rich compositions of intrusive rocks in eastern Baoulé Mossi are contrasted by sodic (trondhjemite-tonalite) intrusive rocks in central Ivory Coast at around 2.12-2.10 Ga (Doumbia et al. 1998). This may indicate that the subduction zone had migrated to the (present day) west at this point, leaving the eastern part of the Baoulé Mossi domain in a distal backarc position. Establishing if this was indeed the case requires more coupled geochronological, petrological and geochemical data. However, support for the migration of the subduction zone towards the west is also provided by the absence of magmatic ages from the northeastern Baoulé Mossi domain after 2100 Ma (fig. 14), which requires that this area was gradu-

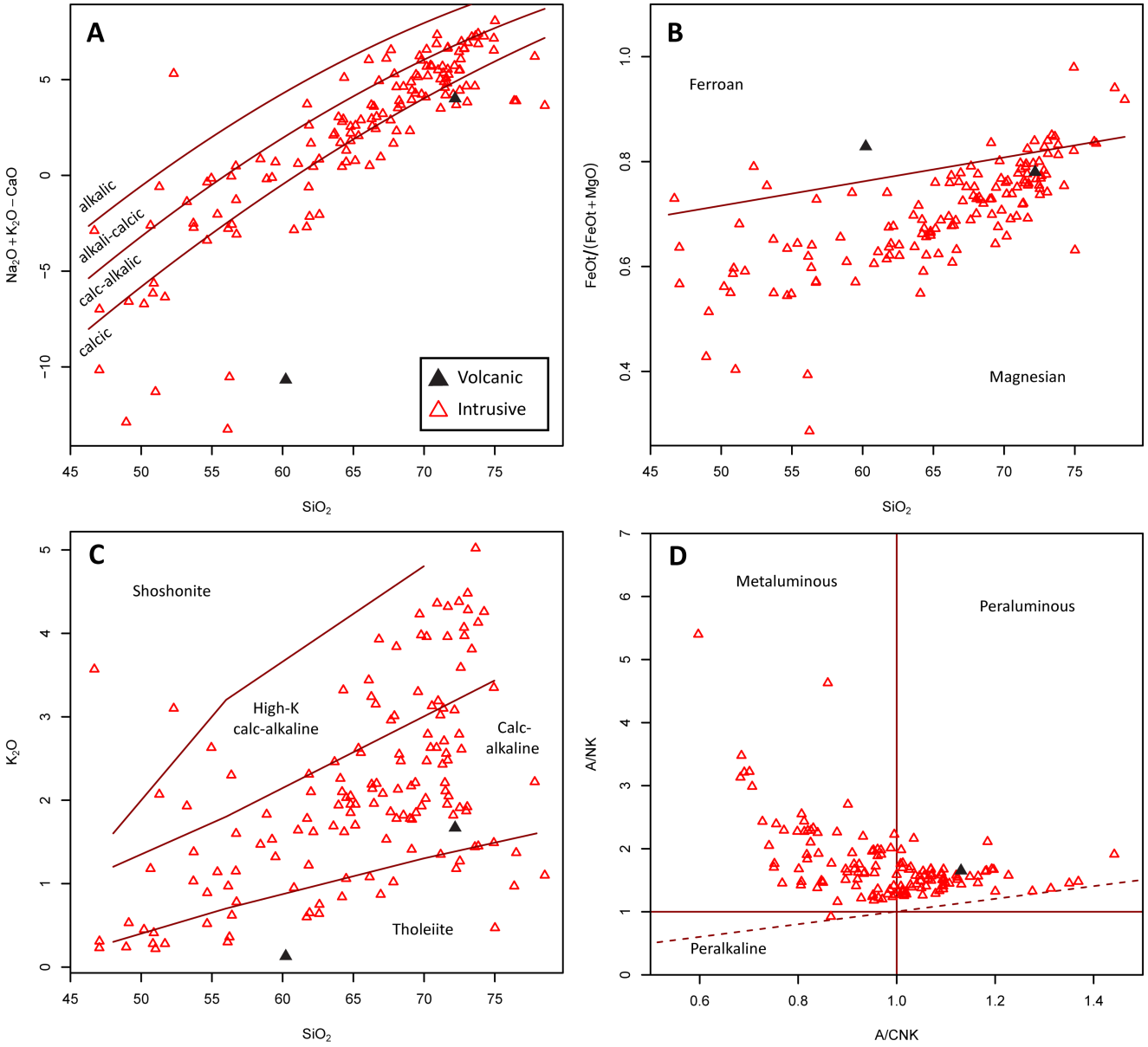

Fig. 13. Geochemical data for volcanic and intrusive rocks formed during the Eburnean I phase (2.13-2.10 Ga). **A)** Na_2O+K_2O-CaO vs. SiO_2 after Frost et al. (2001). **B)** FeOt/(FeOt+MgO) after Frost et al. (2001). **C)** K_2O vs. SiO_2 diagram after Peccerillo and Taylor (1976). **D)** A/NK vs. A/CNK after Shand (1943). Data from A. Scherstén (unpublished data), Kouamelan et al. (1997), Doumbia et al. (1998), Yao and Robb (2000), Gasquet et al. (2003), Naba et al. (2004), Dioh et al. (2006), Agbossoumondé et al. (2007), Vegas et al. (2008), Adadey et al. (2009), de Kock et al. (2009), Siegfried et al. (2009), Thomas et al. (2009) and Tapsoba et al. (2013).

ally removed from the influence of subduction processes.

The migration of the subduction zone towards the west may have been a continuation of extension during the late stage of the EE phase, which led to opening of the Maluwe basin around 2.14-2.13 Ga (de Kock et al. 2012). The migration likely continued throughout the EI phase as indicated by emplacement of lamprophyric dykes at 2108±12 Ma in central Ivory Coast (Pb-Pb on zircon, Doumbia et al. 1998) and dolerite dykes in the Kumasi basin (Yao & Robb 2000). The latter are cut by 2106-2104 Ma granodiorites dated by Oberthür et al. (1998, TIMS on zircon). A gabbro sill intruding the Tarkwa shallow water basin in the Ashanti belt was dated by Adadey et al. (2009) to 2102±13 (SHRIMP on zircon). The mainly volcaniclastic (with rare flows) Asankangrawa belt (fig. 7) within the Kumasi basin (Leube et al. 1990) has not been dated directly. However, Adadey obtained an age of 2142±24 Ma (SHRIMP on zircon) from andesite intercalated with sediment of the Kumasi basin. The age is the weighted average of two populations at circa 2.10 and 2.20 Ga, respectively. The age given by Adadey et al. (2009) thus appear to be a mixing age which likely does not reflect the magmatic age of the andesite. Instead, the younger population likely represents the magmatic component while the older is inherited (Adadey et al. (2009). The

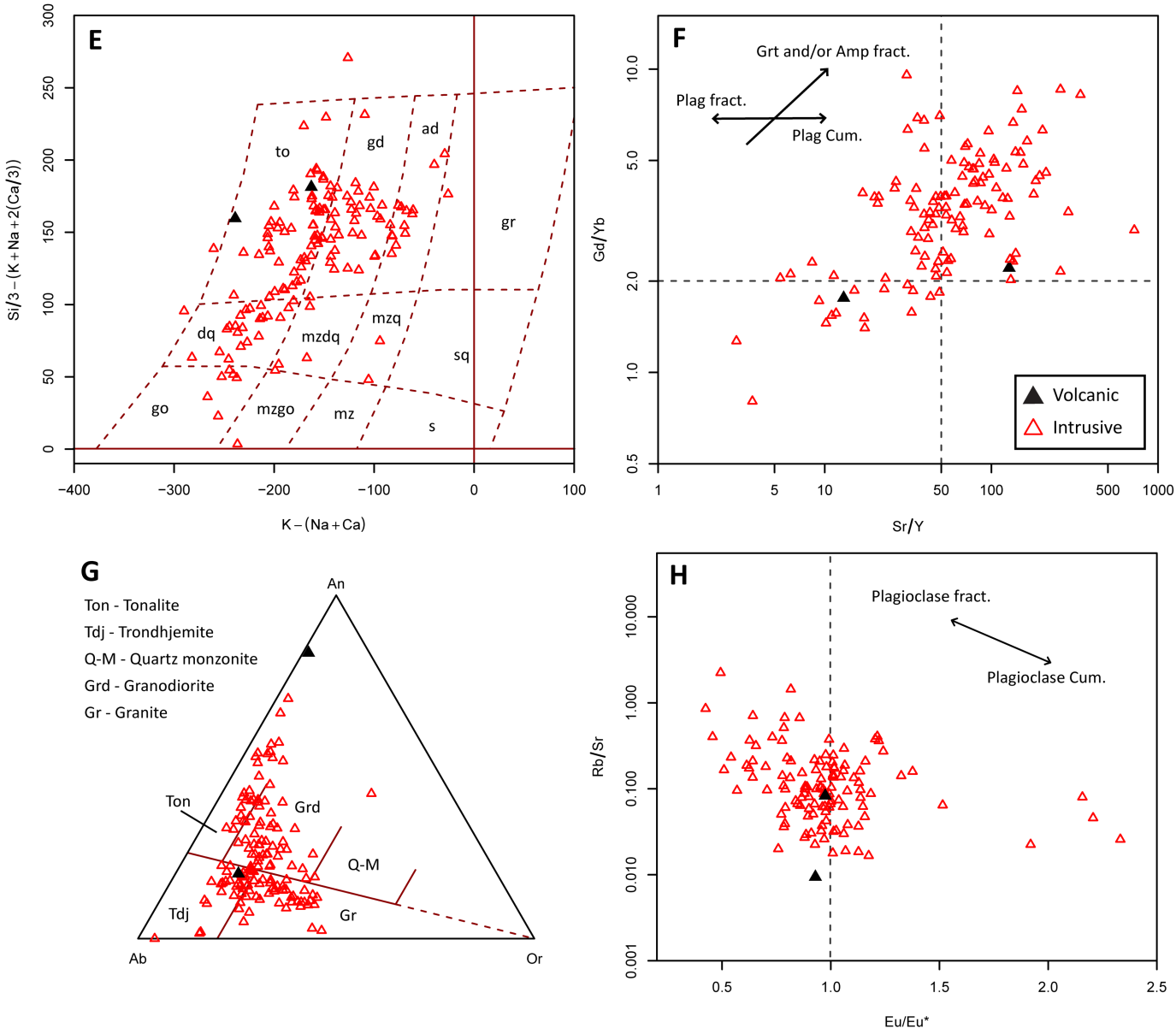

Fig. 13 continued. **E)** Millicationic P-Q diagram after Debon and Le Fort (1983) **(F)** log Gd/Yb vs. log Sr/Y. **G)** Ternary Albite-Anorthite-Orthoclase (CIPW norm) feldspar diagram after O'Connor (1965). **H)** log Rb/Sr vs. Eu/Eu* (Eu/√(Nd*Sm) after Kemp and Hawkesworth (2003).

younger population may thus provide a poorly constrained age for the Asankangrawa belt.

The spatial and temporal trends of magmatic rocks, the end of magmatic activity by circa 2.10 Ga in northeastern Baoulé Mossi and the formation of several sedimentary basins (see above) during the EI phase is consistent with crustal extension or transtension, as noted by several authors for this period of time (e.g. Vidal & Alric 1994; Feybesse et al. 2006; de Kock et al. 2012; Perrouty et al. 2012). This may most easily be explained by slab rollback along an eastward-dipping subduction in the present northwest of the Baoulé Mossi domain (fig. 11 and 14). It may be speculated that slab rollback during the EI phase was triggered by the collision of Archean and Birimian crust in the southwestern part of the Baoulé Mossi domain and its extension into the Amazon craton (fig. 4). As will be discussed in section 4.3.3.1, slab rollback may have become more rapid after 2.10 Ga leading to the formation of the EIIA and EIIB crustal domains (fig. 7, see section 4.3.3).

4.3.3 Eburnean II (2.10-2.07 Ga) — figure 14

The EII phase is divided into two parts; EIIA and EIIB. The crustal domain associated with the EIIA phase covers northwestern Ivory Coast, southwestern Mali, eastern Guinea and eastern Senegal in the Kedougou-Kéniéba Inlier (fig. 7). EIIB domains are present in the Ivory Coast and west-central Ghana. As for the EI phase, magmatic activity was not limited to the EII domain but also took place within older EE and EI domains. For the geochemical plots in figure 15, intrusions within EE-EI crustal domains to the east of the

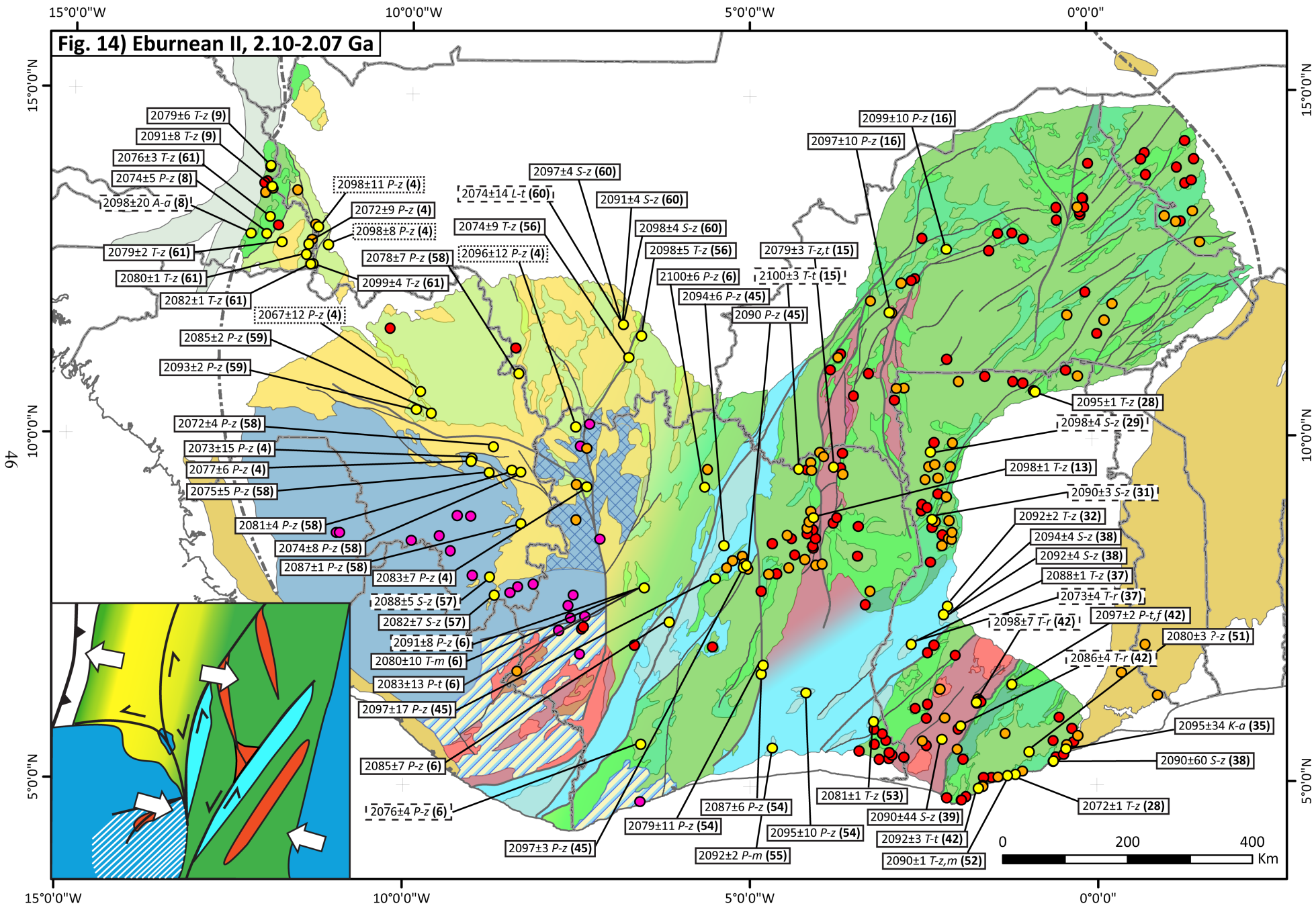
Fig. 14) Eburnean II, 2.10-2.07 Ga
15°0'0"W
10°0'0"W
5°0'0"W
0°0'0"
15°0'0"N
10°0'0"N
5°0'0"N
2079±6 T-z (9)
2091±8 T-z (9)
2076±3 T-z (61)
2074±5 P-z (8)
2098±20 A-a (8)
2079±2 T-z (61)
2080±1 T-z (61)
2082±1 T-z (61)
2098±11 P-z (4)
2072±9 P-z (4)
2098±8 P-z (4)
2067±12 P-z (4)
2085±2 P-z (59)
2093±2 P-z (59)
2072±4 P-z (58)
2073±15 P-z (4)
2077±6 P-z (4)
2075±5 P-z (58)
2081±4 P-z (58)
2074±8 P-z (58)
2087±1 P-z (58)
2083±7 P-z (4)
2088±5 S-z (57)
2082±7 S-z (57)
2091±8 P-z (6)
2080±10 T-m (6)
2083±13 P-t (6)
2097±17 P-z (45)
2085±7 P-z (6)
2076±4 P-z (6)
2074±14 L-t (60)
2097±4 S-z (60)
2091±4 S-z (60)
2074±9 T-z (56)
2098±4 S-z (60)
2098±5 T-z (56)
2096±12 P-z (4)
2078±7 P-z (58)
2099±4 T-z (61)
2100±6 P-z (6)
2094±6 P-z (45)
2090 P-z (45)
2097±3 P-z (45)
2087±6 P-z (54)
2079±11 P-z (54)
2095±10 P-z (54)
2092±2 P-m (55)
2079±3 T-z,t (15)
2100±3 T-t (15)
2099±10 P-z (16)
2097±10 P-z (16)
2095±1 T-z (28)
2098±4 S-z (29)
2098±1 T-z (13)
2090±3 S-z (31)
2092±2 T-z (32)
2094±4 S-z (38)
2092±4 S-z (38)
2088±1 T-z (37)
2073±4 T-r (37)
2098±7 T-r (42)
2097±2 P-t,f (42)
2080±3 ?-z (51)
2086±4 T-r (42)
2095±34 K-a (35)
2090±60 S-z (38)
2072±1 T-z (28)
2081±1 T-z (53)
2090±44 S-z (39)
2092±3 T-t (42)
2090±1 T-z,m (52)
0
200
400
Km
46

Fig. 14. The spatial extent of Eburnean II crustal domains together with a compilation of geochronological data from the Eburnean II phase. See figure 7 for legend and references. Inset shows a schematic depiction of the geodynamic setting during the Eburnean II phase (2.10-2.07 Ga). In a continuation from the developments of the Eburnean I phase, collision proceeded in the present-day south while extension was active in the north as a result of westward-directed slab rollback. As a result of ongoing collision, peak metamorphic (high-P granulitic) conditions may have been reached in the SE Man domain around 2.10-2.09 Ga (note that there is no geochronological data to support this, see discussion in section 4.3.4.1.3). Slab rollback in the present-day northwest triggered extension that led to the establishment of the EIIA and EIIB crustal domains. The EIIA crustal domain constitutes a wide area defined by high-K felsic intrusive and extrusive magmatism along with minor occurrences of basalts and komatiites (see section 4.3.3.1 and figure 15). It may perhaps represent the southern end of a wide extensional belt that stretches northwards to the Yetti and Eglab massifs in the Reguibat shield (fig. 1) that could potentially correspond to a Siliceous Large Igneous Province (see discussion in section 4.3.3.1.5). The formation of the EIIA domain separated Eoeburnean crust in the Mako belt (fig. 7) from other Eoeburnean crust in the east. Scattered Eoeburnean ages obtained from within the EIIA domain may represent remnants of a thinned and largely consumed Eoeburnean basement to the EIIA domain. The EIIB crustal domains correspond to the Sunyani-Comoé and Bandama-Banfora sedimentary basins (fig. 7). They may have opened along northeast-southwest oriented shear zones that were active during the Eburnean I phase (see figure 11 and section 4.3.2). Subsequent closure of the Sunyani-Comoé and Bandama-Banfora sedimentary basins during post-collisional sinistral transpressional shearing led to the emplacement of leucogranitic batholiths between 2095-2080 Ma. During sinistral transpressional shearing fragments of the Archean crust in the Man domain may have been transposed northwards along the Sassandra shear zone (fig. 7). The end of leucogranite emplacement in the Comoé-Sunyani basin at 2080 Ma may mark the end of transpressional shearing and switch to transtension-extension. There appears to have been little or no magmatic activity within the present northeastern part of the Baoulé Mossi domain. However, tectonothermal activity may still have affected crust in this area.

EIIA domain are grouped together with the EIIB rocks while those to the west are grouped as EIIA rocks. However, outside of the EII crustal domains, magmatic activity occurs primarily in the Ivory Coast and Ghana while there is a marked absence of activity in northeastern Baoulé Mossi.

The EII phase is the most complex phase during the Birimian event. In the present northwest, rapid slab rollback led to crustal thinning and the establishment of the EIIA domain. This led to widespread alkali-calcic, high-K extrusive and intrusive magmatism together with coeval mafic-ultramafic volcanic magmatism. Crustal extension separated the Mako belt from EE crustal domains in the east while the thinned EE crust within the EIIA domain was largely overprinted by younger intrusive and supracrustal rocks. Slab rollback was also responsible for opening the sedimentary basins, which constitute the EIIB domains. As discussed in sections 4.3.2.2 and 4.3.3.2, these basins may have opened along shear zones established during the EI phase.

EII phase coincided with peak collision at circa 2.10-2.09 Ga between Archean crust in the Man domain and Imataca complex on one side and the Amapá block on the other, separated by a belt of Birimian crust (fig. 4). The collision that had begun during the EI phase (see section 4.3.3) here reached its peak. Tectonothermal activity related to the collision will be covered more extensively in the section 4.3.4. However, lateral escape associated with this collision could provide an explanation for the continued development of shear zones within the Baoulé Mossi domain, e.g. the Sassandra and Banifin in western Baoulé Mossi (fig. 7).

The complex interplay between slab rollback in the northwest and collision in the south can be seen in the EIIB domains. Slab rollback — in response to collision in the south — was responsible for opening the Banfora-Bandama and Comoé-Sunyani basins, which constitute the EIIB domains (fig. 7). However, as collision in the south switched from normal compression to post-collisional transcurrent sinistral shearing around 2.10-2.09 Ga (see further discussion in section 4.3.4) the EIIB sedimentary basins closed while shearing induced crustal melting and emplacement of widespread leucogranites between 2095-2080 Ma. The collision between the Man domain and Birimian crust in the southern part of the Baoulé Mossi domain and its extension into the Guyana shield in Amazon Craton (fig. 4) thus had implications beyond the crustal areas, which were located between the converging crustal blocks.

4.3.3.1 Eburnean IIA

The EIIA domain includes the Dialé-Daléma basin in the Kedougou-Kéniéba Inlier and most of the Birmian crust within Guinea s well as southeastern Mali. The Plutonic belt (Egal et al. 2002) also form part of the EIIA domain but will be dealt with in separate subsection because of the Archean crust involved during its formation. Magmatic ages from the EIIA domain are predominantly younger than 2.10 Ga. Three Eoeburnean ages provide a notable exception to this pattern (see figure 8). A rhyodacite from the Niani volcanic suite was dated by Lahondère et al. (2002) to 2212±6 Ma (Pb-Pb on zircon) while a porphyritic granodiorite and a quartz-diorite in southwestern Mali were dated to 2131±5 Ma and 2132±5 Ma (LA-ICPMS on zircon), respectively, by MacFarlane et al. (2011). The limited ages available from detrital zircon in the EIIA domain, obtained by Milési et al. (1989), constrain the maximum depositional ages for sediment to circa 2.10 Ga. These ages could reflect inheritance, but they might also represent fragments of a thinned Eoeburnean and Eburnean I basement to the rocks which formed during the EII phase.

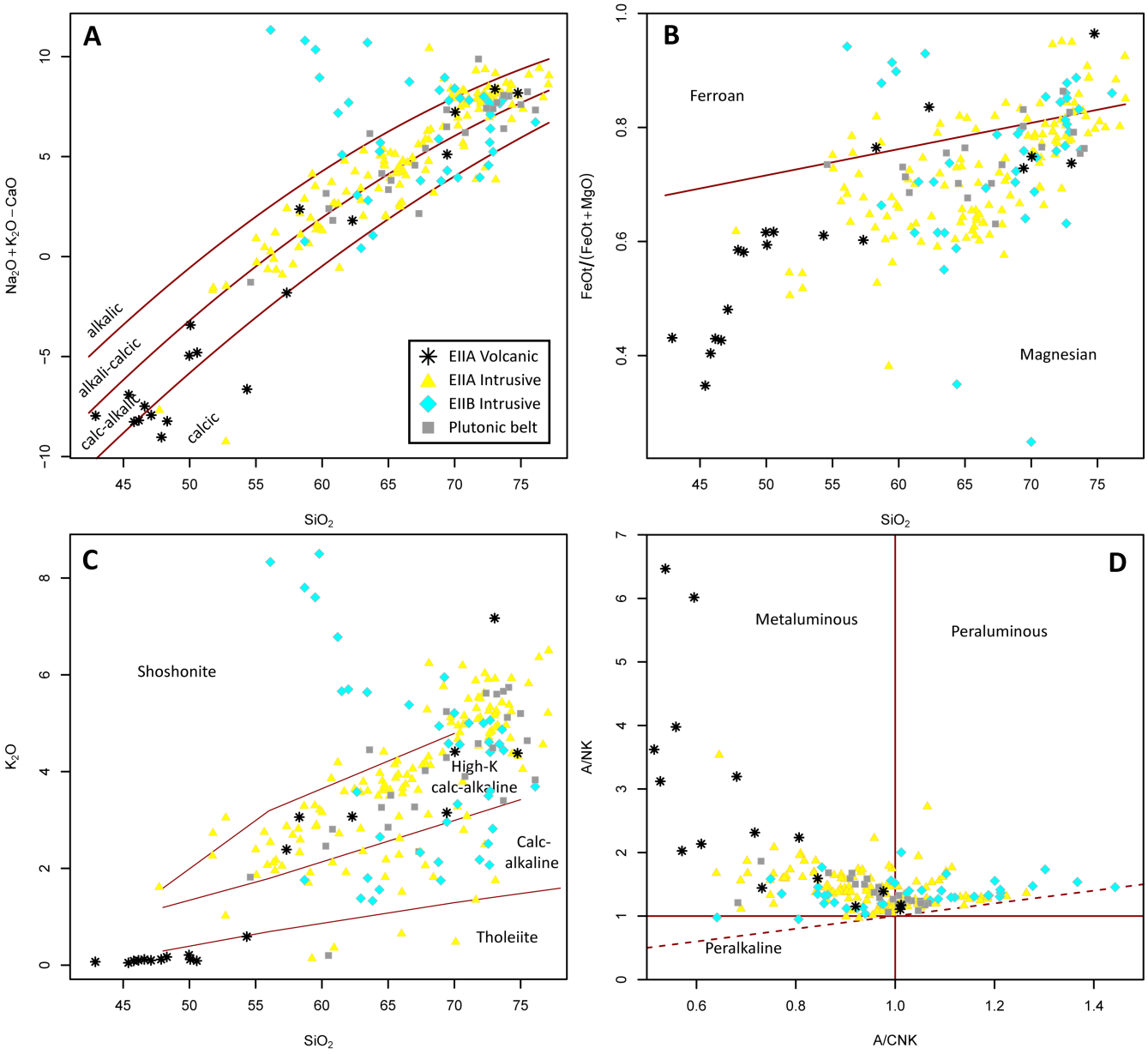

Fig. 15. Geochemical data for volcanic and intrusive rocks formed during the Eburnean II phase (2.10-2.07 Ga). These have been further divided between rocks from the EIIA and EIIB domains. Rocks from the Plutonic belt along the contact between the EIIA and Man domains are plotted as a separate from other EIIA rocks. **A)** Na_2O+K_2O-CaO vs. SiO_2 after Frost et al. (2001). **B)** FeOt/(FeOt+MgO) after Frost et al. (2001). **C)** K_2O vs. SiO_2 diagram after Peccerillo and Taylor (1976). **D)** A/NK vs. A/CNK after Shand (1943). Data from A. Scherstén (unpublished data), Tegyey and Johan (1989), Liégeois et al. (1991), Boher et al. (1992), Ndiaye et al. (1997), Doumbia et al. (1998), Loh and Hirdes (1999), Egal et al. (2002), Dioh et al. (2006), Pawlig et al. (2006), Klein et al. (2008), Adadey et al. (2009) and McFarlane et al. (2011).

4.3.3.1.1 EIIA magmatism

Available petrographic and geochemical data from intrusive and volcanic rocks in the EIIA domain (from southwestern Mali and the Dialé-Daléma basin) show that they have a more alkaline composition compared with the magmatism associated with the EE and EI phases (figure 15, compare with figures 9 and 10). In terms of chemical composition, these rocks are predominantly high-K and alkali-calcic and ranges from metaluminous to moderately peraluminous. Ferroan samples typically have high SiO_2 while those with lower SiO_2 are magnesian. However, there are nevertheless some ferroan samples with intermediate SiO_2 (fig. 15b).

In southwestern Mali, Liégeois et al. (1991) found that volcanic and intrusive rocks defined a composite trend evolving from diorite through monzogranite and granodiorite to syenogranite. Highly differentiated alkaline granites were also observed. Intermediate to mafic samples contain biotite, amphibole and occasional clinopyroxene while more evolved granites only contain biotite. Some granites investigated by Liégeois et al. (1991) contained mafic enclaves which in some parts display a hybrid relationship with the granites, indicative of magma mingling and mixing. These areas show signs of syn-magmatic

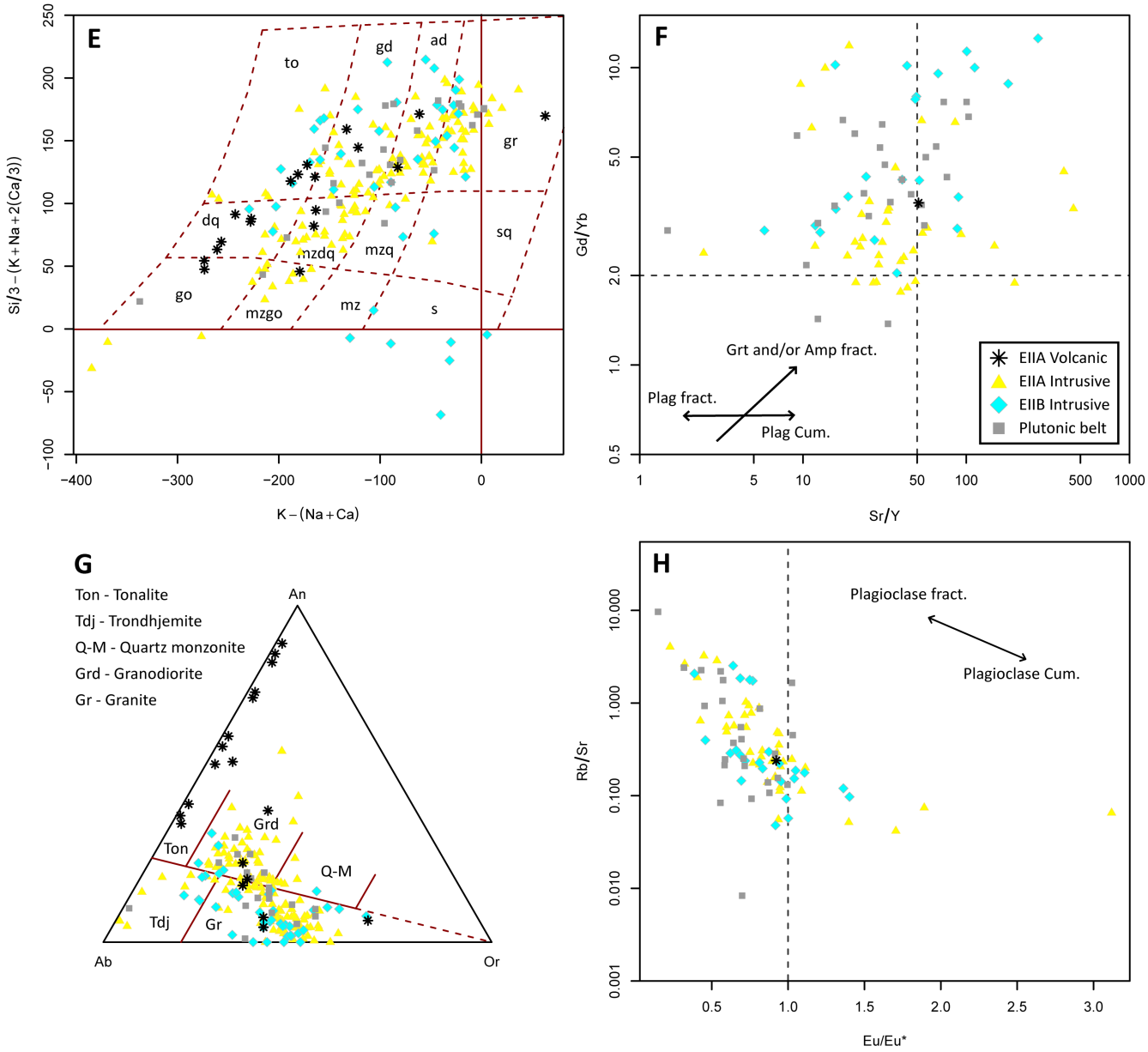

Fig.15 continued. Millicationic P-Q diagram after Debon and Le Fort (1983) **(F)** log Gd/Yb vs. log Sr/Y. **G)** Ternary Albite-Anorthite-Orthoclase (CIPW norm) feldspar diagram after O'Connor (1965). **H)** log Rb/Sr vs. Eu/Eu* (Eu/√(Nd*Sm) after Kemp and Hawkesworth (2003).

deformation, e.g. expressed as elongated, schlieren-like enclaves indicating the granites were subcontemporaneous with deformation (Liégeois et al. 1991).

As noted by Liégeois et al. (1991), the magmatic rocks in southwestern Mali are similar to those in the Dialé-Daléma basin. This area is characterized by K-rich intrusive rocks and felsic volcanics (Ndiaye et al. 1997; Hirdes & Davis 2002; Dioh et al. 2006) much like southwestern Mali. This includes two-mica syenogranites, biotite granites as well as clinopyroxene granodiorites, some of which have mafic enclaves. Small rounded and undeformed intrusions of two-pyroxene, K-feldspar-bearing gabbro to amphibole-bearing monzogranite have also been reported from the KKI (Dioh et al. 2006).

The Keniero and Niandan volcanic ranges in the southwestern part of the EIIA domain (fig. 7) are constrained to have formed between 2095-2085 Ma (Lahondère et al. 2002, and references therein). The Keniero range is composed of bimodal volcanics with a basal layer of basalt overlain by chemical and epiclastic sediment followed by rhyolites and pyroclastics. The basalts are reported have a composition similar to basalts formed in an intracontinental rift-environment. The Niandan range is comprised of a komatiite-basalt suite which includes pillow lavas and volcaniclastics (Tegyey & Johan 1989; Lahondère et al. 2002). The komatiites within this suite exhibit a spinifex texture and have MgO >20 wt% (Tegyey & Johan 1989). The Hérémakono and Falémé belts (fig. 7) are composed of intermediate to felsic volcanic and volcaniclastic rocks. In addition, the Siguiri (Lahondère et al. 2002) and Dialé-Daléma (Hirdes & Davis 2002) deep water basins in places also contain

large amounts of volcaniclastic rocks, indicating that they formed simultaneously with volcanic activity.

4.3.3.1.2 Crustal extension in the EIIA domain

The dominantly alkali-calcic nature of the magmatism within the EIIA domain, together with coeval eruption of mafic-ultramafic volcanics, suggests that it took place within an extensional environment with crustal thinning and mantle upwelling. The intrusive and volcanic rocks are not typical examples of "A-type" magmatism, which is more enriched in Zr-Y-Nb-REE in addition to being ferroan regardless of SiO_2 (e.g. Frost et al. 2001). Instead, it may be more favorable to compare them with the Caledonian post-collisional plutons of Frost et al. (2001), which are dominantly alkali-calcic and magnesian, only reaching ferroan compositions at high SiO_2.

The EIIA magmatism is coeval with widespread shearing along the Sassandra (Egal et al. 2002) and Banifin shear zones (Liégeois et al. 1991) as well as the collision between Archean and Birimian crust in the southern Baoulé Mossi domain and its extension into the Guyana shield in the Amazon Craton. It was also contemporaneous with ongoing subduction towards the west and the EIIA domain could thus still be influenced by subduction processes. Continued subduction may have led to the convergence of the Sarmatia-Man domain and Volgo-Uralia blocks (fig. 4) which appear to have been amalgamated around 2.05 Ga (Shchipansky et al. 2007; Bogdanova et al. 2008).

The older Eoeburnean rocks within the EIIA domain (Lahondère et al. 2002; McFarlane et al. 2011) would therefore correspond to the basement to the rocks formed during the EII phase. This is analogous to the situation in the Reguibat shield where 2.20-2.18 Ga orthogneisses occur as massifs among 2.09-2.07 Ga intrusive and volcanic rocks formed in response to crustal extension (Peucat et al. 2005). The similarities between the EIIA domain and the Reguibat shield are further discussed below in section 4.3.3.1.5.

Rifting within the Birimian crust has also been invoked by e.g. Milési et al. (1989) and Feybesse and Milési (1994) to account for the presence of e.g. the volcanics of the Keniero and Niandan volcanic ranges and sheeted dikes within sedimentary basins. The presence of both subduction- and rift-related mafic volcanics within the Baoulé Mossi domain explain some of controversy surrounding the Birimian lithostrathigraphy (see section 2.2.2.5), compounded by a lack of precise radiometric ages.

4.3.3.1.3 The Plutonic belt — an active continental margin?

Egal et al. (2002) proposed that the granodiorites and granites of the Plutonic belt in eastern Guinea formed along a short-lived (2.09-2.07 Ga) active continental margin analogous to the Andes (see also section 2.2.3.2). The participation of an evolved component in the source of the intrusive rocks of the Plutonic belt is indicated by their enriched composition, e.g. high REE, Zr, Th and K_2O/Na_2O (Egal et al. 2002). In addition, Boher et al. (1992) found that intrusive rocks from this region had an evolved Sm-Nd isotopic composition requiring derivation from an isotopically evolved source which is likely Archean considering the proximity to the Man domain.

While the participation of Archean crust in the formation of the Plutonic belt is thus well supported there are several problems with the interpretation of the Plutonic belt as the remnant of an active continental margin when considering it in context of the magmatic and tectonothermal activity elsewhere in the Man and Baoulé Mossi domains. These include the widespread and coeval magmatic-tectonothermal activity throughout the EIIA domain, the presence of coeval komatiites and continental basalts, the alkali-calcic character of magmatic rocks and the presence of scattered Eoeburnean rocks within a domain otherwise characterized by activity younger than 2.10 Ga. As discussed above, these characteristics can be more easily explained by a model involving rifting of Eoeburnean crust around 2.10 Ga.

Within the model presented here, it therefore seems more suitable to consider the magmatism in the plutonic belts as being a part of the magmatic activity seen elsewhere within the EIIA domain, although with the exception that it was partly sourced from Archean crust. As the Birimian crust of the EIIA domain was extended, upwelling mantle beneath would have been juxtaposed with the felsic Archean crust of the north-eastern Man domain, thus providing the necessary heat to initiate melting. The synkinematic nature of the early granodiorites and granites and the post-kinematic monzogranites constrain shearing along the Sassandra shear zone to 2090-2070 Ma (Egal et al. 2002). This is coeval with shearing along the Banifin shear zone (Liégeois et al. 1991) and is a further indicator that magmatism within the EIIA domain is related, even though the rocks near the Banifin shear zone are juvenile (Liégeois et al. 1991; MacFarlane et al. 2011).

The presence of relict clinopyroxene as cores in amphibole as well as mafic enclaves (although Egal et al. 2002 do not appear to distinguish between microgranular mafic enclaves indicative of magma mingling or xenoliths) in granodiorites and granites within the Plutonic belt indicate that the granitoids may contain a mafic mantle-derived component in addition to crustal sources, although the latter likely dominates (Egal et al. 2002). This mafic component could be derived from partial melting of upwelling mantle beneath the Birimian crust of the EIIA domain. The apparent subduction signature of the Plutonic belt, such as low HFSE and high LILE (Egal et al. 2002), may simply be attributed to inheritance (Arculus 1987; Roberts & Clemens 1993) from sources which were formed in an active arc, or to the effect of residual minerals during partial melting.

4.3.3.1.4 Archean crust in NW Ivory Coast — a marker of lateral displacement?

As discussed in section 2.2 the extent of Archean crust in northwestern Ivory Coast is uncertain (fig. 5). Nevertheless, Milési et al. (1989) obtained Archean ages from orthogneisses, some of which were mylonitic, close to the Sassandra shear zone thus showing that Archean crust is indeed present in this region. It is hard to say how extensive these occurrences of Archean crust are in this region.

Feybesse and Milési (1994) interpreted the Archean crust in northwestern Ivory Coast as exposed basement to allochthonous Birimian crust. However, the presence of widespread thrusting has since been challenged (Kouamelan et al. 1997; Egal et al. 2002). An alternative explanation for the presence of Archean crust in northwestern Ivory Coast may be that they represent crustal fragments separated from the main mass of Archean crust in the Man domain during sinistral shearing along the Sassandra and Banifin shear zones. This would in such a case imply a relative northwards displacement of at least 200-300 km (fig. 8).

While such a model would be compatible with the sinistral movement recorded along the Sassandra (Kouamelan et al. 1997; Egal et al. 2002) and Banifin (Liégeois et al. 1991) shear zones further radiometric dating of rocks on both sides of the shear zones is required to constrain the extent of Archean and Birmian crust, and to find out whether Archean crust is primarily located along the shear zones or form a larger domain to the east of the Sassandra and Banifin shear zones (fig. 7).

4.3.3.1.5 The EIIA and Yetti-Eglab domains — a Paleoproterozoic SLIP?

Coeval with the formation of the EIIA domain and the extensional-related alkali-calcic magmatism a similar development also took place in the Yetti and Eglab massifs in the eastern Reguibat Shield (Algeria) in the north of the WAC (fig. 1). Here, crustal extension between 2.09-2.07 Ga led to extrusive and intrusive high-K magmatism within a basement comprised of 2.20-2.18 Ga orthogneisses (Kahoui & Mahdjoub 2004; Peucat et al. 2005). Early magmatism during the period 2.09-2.07 Ga consisted of trondhjemite and tonalite intrusions together with calc-alkaline basalt-andesite-rhyolite. This was followed by more potassic magmatism including alkaline gabbros, syenites, monzogranites and a peralkaline ring complex as well as eruption of extensive ignimbrites around 2.07 Ga. The presence of tholeiitic to alkaline gabbros, tholeiitic Skaergaard-type layered intrusions and calc-alkaline lamprophyres indicate that both enriched and depleted mantle sources contributed to magmatism during this stage (Peucat et al. 2005).

Peucat et al. (2005) proposed a model for the Eglab massif in which subduction led to the development of a mature island arc between 2.20-2.18 Ga, corresponding to the orthogneisses now exposed in the Eglab massif. Following a long period of apparently low magmatic activity, subduction eventually led to collision at circa 2.1-2.09 Ga between the island arc and the Yetti massif, the latter exposed along the Algerian-Mauritanian border (fig. 1). Structures along the contact between the Eglab and Yetti massifs indicate transpression, which appear to have resulted in thrusting of the former massif on top of the latter. Subsequent extension between 2.09-2.07 Ga, possibly due to slab rollback or delamination, triggered the post-collisional bimodal magmatism in both the Eglab and Yetti massifs.

Peucat et al. (2005) noted several apparent differences between the Paleoproterozoic geodynamic evolution of the Reguibat and Man-Leo shields. These authors pointed to the lack of linear volcanic belts and sedimentary basins in the Reguibat shield. In addition, they also compared mafic rocks from the two shields and found that those from the Reguibat shield where more evolved compared to those of the Man-Leo shield. They argued that this reflected differences in maturity between island arcs, which came to form the crust in each respective shield. However, the comparisons by Peucat et al. (2005) were relatively broad and did not take into consideration variations exhibited by different regions within the Man-Leo shield.

As it stands, the model proposed by Peucat et al. (2005) for the Yetti-Eglab domain shares many similarities with that discussed above for the EIIA domain. Both regions underwent extension between circa 2.10-2.07 Ga, which led to extensive intrusive and extrusive magmatism spanning a compositional range from felsic to mafic (although felsic compositions appear to predominate) with an alkali-calcic affinity (fig. 16). This suggests that the two areas may be related — perhaps forming part of a more than 1500 km long and 400 km wide crustal domain that underwent extension between circa 2.10-2.07 Ga. Although it is hard to evaluate the prospect of such a model since the intervening crust is covered by the sediment of the Taoudeni basin it does not appear as to far-fetched, considering the compositional and temporal similarities between these two domains.

Even though the EIIA and the Yetti-Eglab domains may belong to the same crustal domain — subjected to extension at circa 2.10-2.07 Ga — there are nevertheless some differences between them in terms of magmatic style and composition at this time. The felsic rocks of the Reguibat shield have a more pronounced "A-type" characteristic (e.g. Whalen et al. 1987; Bonin 2007) compared to those in the EIIA domain with higher Fe*, Zr, Y, Nb and REE (fig. 16), along with the presence of rocks such as alkaline ring-complexes (Kahoui & Mahdjoub 2004; Peucat et al. 2005) or Rapakivi granites (Rocci et al. 1991). Ferrous samples with high-silica also exhibit quite prominent Eu-anomalies indicating that they formed through partial melting of quartzofeldsphatic crust at low pressure (<4 kbar) leaving residual plagioclase and orthopyroxene (Patiño Douce 1997; Frost & Frost 2011). Such

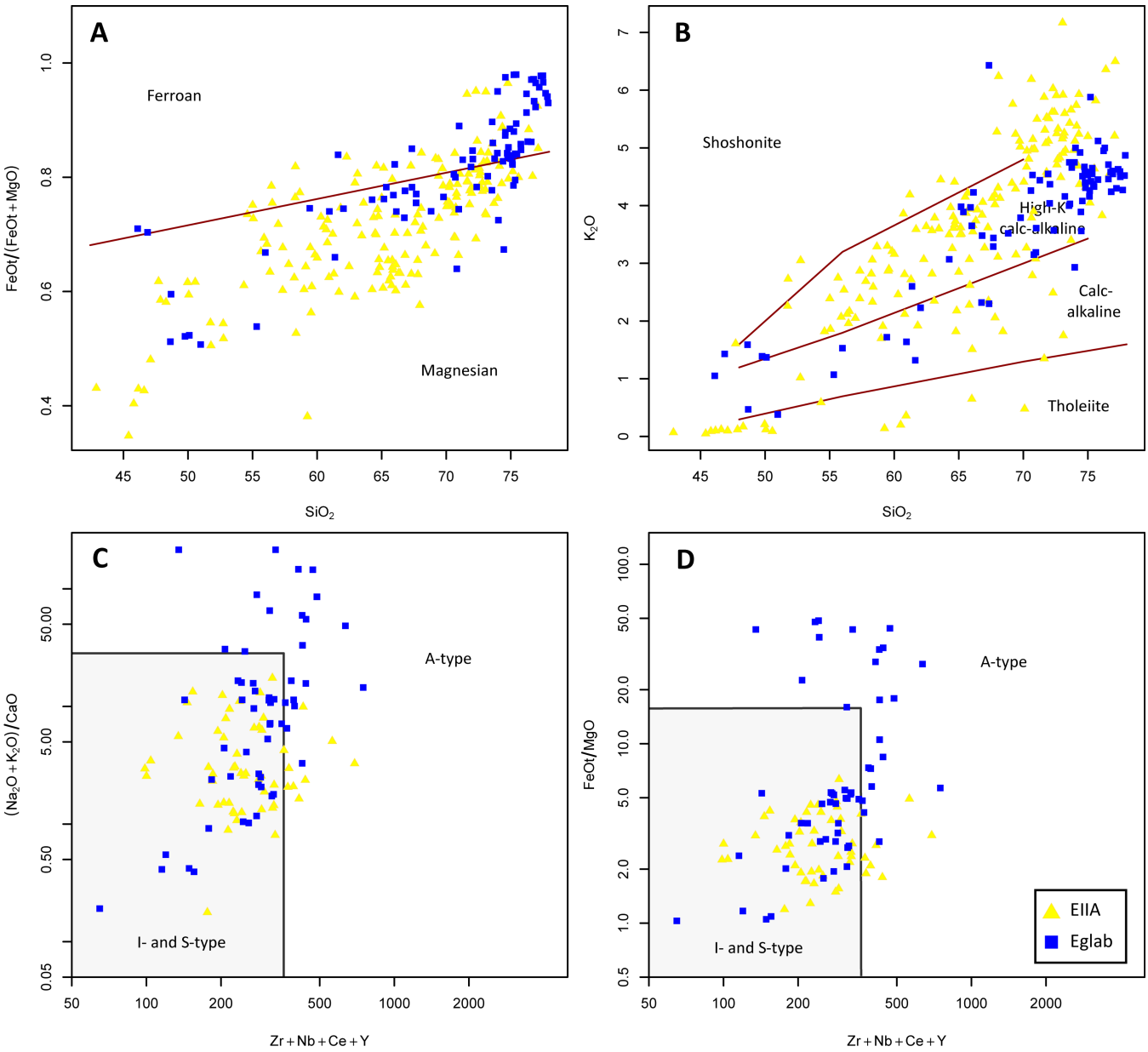

Fig. 16. Geochemical diagrams for combined volcanic and intrusive rocks from the EIIA domain (including the Plutonic belt) and the Reguibat Shield. **A)** FeOt/(FeOt+MgO) after Frost et al. (2001). **B)** K_2O vs. SiO_2 diagram after Peccerillo & Taylor (1976). **C)** $(Na_2O+K_2O)/CaO$ vs. Zr+Nb+Ce+Y after Whalen et al. (1987). **D)** FeOt/MgO vs. Zr+Nb+Ce+Y after Whalen et al. (1987). Data for EIIA domain from Tegyey and Johan (1989), Liégeois et al. (1991), Boher et al. (1992), Ndiaye et al. (1997), Egal et al. (2002), Dioh et al. (2006), Pawlig et al. (2006) and McFarlane et al. (2011). Data for the Reguibat shield from Kahoui & Mahdjoub (2004) and Peucat et al. (2005).

shallow melting requires a high heat flow, which is consistent with the period of crustal extension envisioned by Peucat et al. (2005). Komatiites, while present in the Niandan volcanic range in the EIIA domain (Milési et al. 1989; Tegyey & Johan 1989) have not been recognized in the Birimian crust of the Reguibat shield (Peucat et al. (2005).

Assuming that the samples from the Reguibat shield and the EIIA domain are representative of the magmatism in their respective regions during the EII phase then they show that these areas were defined by different magmatic processes. This cannot be attributed to differences in exposed crustal level as both the EIIA (e.g. Liégeois et al. 1991; Hirdes & Davis 2002; Lahondère et al. 2002) and Yetti-Eglab (Peucat et al. 2005) domains are characterized by at most greenschist-amphibolite facies conditions. The differences in magmatic style between these areas must therefore be related to other factors. Ferroan melts are hotter and drier compared to those that are magnesian (Frost & Frost 2011). The differences between the magmatism in the EIIA and Yetti-Eglab domains between 2.10-2.07 Ga could therefore be related to drier and hotter magmatism in the Yetti-Eglab domain to the north compared with the EIIA domain to the south. This could perhaps be related to a more proximal position of the EIIA domain relative to an active subduction zone, which could provide more water to the magmatic

system in this domain. Alternatively, the Yetti-Eglab domain may have experienced more extension compared to the EIIA domain, leading to the greater degrees of partial melting in upwelling mantle. In this setting, hot and dry mafic melts could either trigger crustal anatexis through dehydration melting or fractionate to form high-silica ferroan ("A-type") rocks (Patiño Douce 1997; Frost & Frost 2011).

If the EIIA and Yetti-Eglab domains are indeed connected along a northeast-southwest oriented belt that cuts across the WAC it could potentially correspond to a siliceous large igneous province (SLIP, Bryan 2007; Pankhurst et al. 2011; Bryan & Ferrari 2013). SLIPs typically form areally extensive (>0.1 Mkm2) linear belts defined by large volumes (>0.25 Mkm3) of extrusive and subvolcanic rocks formed during a fairly short period of time (<40 Ma). In particular, the SLIPs are characterized by large volumes of volcaniclastic rocks, such as ignimbrites. The magmatism is dominated by felsic compositions although mafic and intermediate compositions are also present. In terms of their chemical composition, magmatic rocks associated with SLIPs are transitional "arc" and "within-plate" signatures.

All these characteristics (spatial and temporal extent, type of magmatism) are exhibited by the magmatic activity in the EIIA and Yetti-Eglab domains during the EII phase. Although SLIPs have so far only been recognized from the Phanerozoic (Bryan 2007; Pankhurst 2011) the potential existence of a SLIP in the WAC would extend the record of SLIPs back to the Paleoproterozoic.

4.3.3.2 Eburnean IIB

The EIIB crustal domains correspond to the Bandama-Banfora basin in the central Ivory Coast and southwestern Burkina Faso as well as the Comoé-Sunyani basin in southeastern Ivory Coast and west-central Ghana (fig. 7). The maximum age of the Bandama-Banfora basin is constrained by handful of detrital zircon obtained by Doumbia et al. (1998), which yielded ages between 2133-2107 Ma (Pb-Pb on zircon). The Ferkéssédougou two-mica leucogranite that intrudes the Bandama-Banfora basin was dated by the same authors to 2094±6 Ma (Pb-Pb on monazite). The two-mica leucogranites within the Comoé-Sunyani basin have been dated by several authors to between 2095-2080 Ma (figs. 14 and 17). Vidal et al. (2009) proposed that the leucogranites within the Comoé-Sunyani basin were exposed at a shallower crustal level than the Ferkéssédougou batholith. At depth, the individual leucogranites in the Comoé-Sunyani would thus connect to form a similarly sized batholith.

While there is no detrital zircon available from the EIIB part of the Comoé-Sunyani basin the termination of the Ouango-Fitini shear zone, associated with a syn-kinematic tonalite dated by Hirdes et al. (1996) to 2110±6 Ma (TIMS on zircon), provides an upper age for the formation of the basin. Based on these temporal constraints both the Comoé-Sunyani and Bandama-Banfora basins actually straddle the transition between the EI and EII phases and likely began to open during the later EI phase. This highlights the fact that the Eburnean phases form part of a continuum rather than representing discrete events. However, magmatism appears to have taken place entirely within the EII phase which justifies their classification as EIIB domains.

Altogether, the similar composition, subparallel orientation, extent and coeval emplacement suggest that the leucogranites in the Bandama-Banfora and Comoé-Sunyani basins, and in extension the basins themselves, formed in response to the same event. The coeval presence of extension-related magmatism within the EIIA domain must also be considered, as will must collision between the Man domain and the Birmian crust, which reached its peak around 2.10-2.09 Ga. Assuming that a similar extensional regime affect the Eoeburnean crust in eastern Baoulé Mossi this would have provided a setting in which the EIIB basins could have opened. Preferentially oriented shear zones formed during the EI phase, such as the GFB shear zone, could have acted as nuclei for the basins.

The dominantly siliciclastic rocks of both the Bandama-Banfora (Doumbia et al. 1998; Pouclet et al. 2006) and Comoé-Sunyani basins (Vidal et al. 1996, 2009) have been gently compressed into northeast-southwest striking upright folds which pre-date the magmatic activity. Shearing also took place during the inversion of the basins (Pouclet et al. 2006; Feybesse et al. 2006; Vidal et al. 2009). This shows that the EII domains did not form entirely within a transtensional-extensional regime but that it also involved transpression-compression. This likely reflects the interplay between extension due to slab rollback followed by post-collisional transpression and sinistral shearing following peak collision between the Man domain and the Birmian crust in the south.

In west-northwest São Luís Craton, two-mica leucogranites belonging to the Tracuateua intrusive suite (Klein et al. 2008) have been dated by Palheta et al. (2009) to around 2090 Ma (Pb-Pb on zircon). Based on the pre-Atlantic reconstruction of Onstott et al. (1984, after Bullard et al. 1965) in figure 2, this part of the São Luís Craton is placed in a position in which the Tracuateua intrusive suite appear to form an extension of the coeval two-mica leucogranites within the Comoé-Sunyani basin. Exposed Birmian rocks to the southeast of the Tracuateua intrusive suite are compositionally and temporally similar to those of the Sefwi belt (compare e.g. Klein et al. 2008 with Hirdes et al. 1993 and Agyei Duodu et al. 2009). If correct, such a connection could be used as an additional tie-point in WAC and São Luís Craton reconstructions.

4.3.3.2.1 EIIB magmatism

The two-mica leucogranites within the Comoé-Sunyani (Hirdes et al. 1993; Vidal et al. 2009; Jessell et al. 2012) and Bandama-Banfora basins (Doumbia et al. 1998; Pouclet et al. 2006) are the most dominant

expressions of magmatism associated with the EIIB domains. The alkaline Ninakri massif intrudes the Bandama-Banfora basin close to the Ferkéssédougou batholith and is composed of nepheline and quartz syenites. Although the Ninakri massif has not been dated, and could therefore postdate the EII phase, it has nevertheless been included here. This is mainly because of the reported presence of alkali-calcic magmatism within the EIIA domain and Reguibat shield at this time.

Just like magmatism in the EIIA domain, the magmatism associated with the EIIB domain is distinct from that of the EE and EI phases. Analyzed samples from the EIIB domain, also including samples from rocks intruding into EE and EI domains, are high SiO_2 (>60 wt%), medium to high-K, calc-alkalic to alkali-calcic and dominantly magnesian, except for some differentiated samples (fig. 15). The only exception is samples from the alkaline Ninakri massif, which has lower SiO_2, is alkaline and ferroan. However, since these intrusions have been dated using any precise method, it is possible that they may be younger than the EII phase. Their inclusion in figure 15 is therefore only tentative.

The two-mica leucogranites in the EIIB domains are the only ones of this size in the Baoulé Mossi domain. The Ferkéssédougou batholith was interpreted by Doumbia et al. (1998) to have formed from water-saturated melting at 4-5 kbar and 600-700°C during syn-magmatic shearing, This is in line with general models for two-mica leucogranites which favor formation in a syn-kinematic setting where fluids are concentrated within shear zones triggering low temperature water-saturated melting (Barbarin 1996). Syn-kinematic magmatism may also weaken the crust, thus facilitating further shearing.

4.3.3.2.2 Emplacement of the two-mica leucogranites

Different models have been proposed regarding the style of emplacement for the two-mica leucogranites within the Comoé-Sunyani basin. The granites have an elongate shape in map view and Feybesse et al. (2006) proposed that they had been emplaced syn-kinematically during sinistral shearing. Vidal et al. (2009) also argued for synkinematic emplacement during sinistral shearing but also argued for the involvement of a vertical component in which the leucogranites rose relative to the surrounding sediment because of density contrasts. Jessell et al. (2012), based on finite element modelling, instead argued that the leucogranites were dominantly pre-kinematic and had acquired their distinct elongate shape during post-magmatic shearing, responsible for up to 400 km of lateral, possibly dextral, displacement along the Sefwi-Sunyani-Comoé shear zone (fig. 7).

A syn-kinematic origin for the two-mica leucogranites, in the Comoé-Sunyani as well as the Bandama-Banfora basin, is favored in the geodynamic model presented here. Dominantly pre-kinematic emplacement of the leucogranites, as proposed by Jessell et al. (2012), appears unlikely for several reasons. One reason is the coeval nature of the leucogranites in the Comoé-Sunyani and Bandama-Banfora basins. If the elongate shape of the granites within the Comoé-Sunyani basin was acquired after emplacement, then this should also be the case for the Ferkéssédougou leucogranite in the basin, which contrasts with the interpretation of Doumbia et al. (1998). As a consequence, both of the basins should have been subjected to extensive shearing each associated with up to 400 km of lateral displacement.

As discussed above, there is evidence for shearing along the Sassandra (Egal et al. 2002) and Banifin (Liégeois et al. 1991) shear zones in the western part of the Baoulé Mossi domain during the EII phase. This occurred during peak collision between Archean crust in the Man domain-Imataca complex-Amapá block (fig. 4) and the intervening Birimian crust (see further discussion in section 4.3.4.1). In this setting it would seem unlikely that the two-mica leucogranites within both the Comoé-Sunyani and Bandama-Banfora basins would have been unaffected by shearing, especially considering the weakening effect that melting would have had on the crust (Barbarin 1996).

An elongate shape is also not limited to the extensive two-mica leucogranites in EIIB domains but is also exhibited by other two-mica granites within the Baoulé Mossi domain although these are volumetrically smaller than those in the EIIB domains (fig. 17). The most prominent are the N'Zi and Kowara granites southeast of the Ferkéssédougou batholith (Doumbia et al. 1998; Gasquet et al. 2003) and the Awahikro granite in the Haute-Comoé basin (Vidal et al. 2009). All of these granites have an elongate shape and are associated with shear zones. The Kowara granite was interpreted as syn-kinematic by Doumbia et al. (1998). It is oriented in the same northeast-southwest direction as the leucogranites in the EIIB domains but is about 20-30 Myr older, dated to 2118±2 Ma (TIMS on zircon) by Gasquet et al. (2003). It is cut by the north-south oriented N´Zi granite, which was emplaced along the N'Zi-Brabo shear zone (Gasquet et al. 2003). Despite their different age and orientation, these two-mica granites nevertheless exhibit an elongate shape. These features are clearly not restricted to the leucogranites in the EIIB domains but rather appear typical for two-mica granites within the Baoulé Mossi domain.

Although it has been argued here that the elongate shape of the leucogranites is a primary feature established during their emplacement it is also recognized that the Birimian crust of the Baoulé Mossi was affected by shearing which post-dated the formation of these granites. This is for example recorded by the formation of the Ashanti lode-gold deposits that has been dated to 2063±7 Ma (SHRIMP on hydrothermal xenotime) by Pigois et al. (2003) and which was associated with sinistral shearing along the Ashanti fault (Perrouty et al. 2012). However, post-magmatic shear-

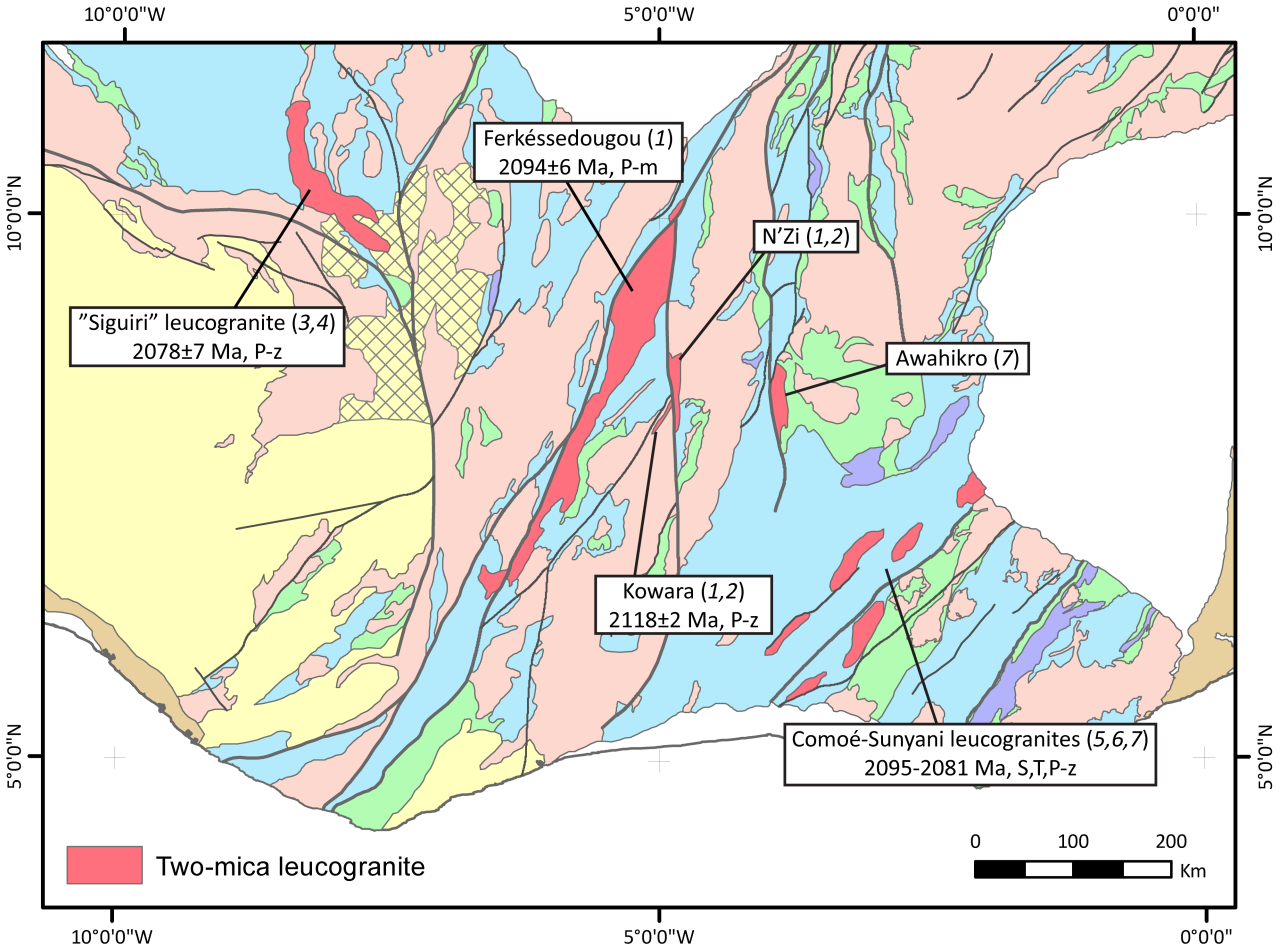

Fig. 17. Schematic map highlighting two-mica leucogranites within the Baoulé Mossi domain. See figure 5 for legend for other lithological units. Data compiled from the following sources: **1** - Doumbia et al. (1998); **2** - Gasquet et al. (2003); **3** - Egal et al. (2002); **4** - Tagini (1972); **5** - Vidal et al. (2009); **6** - Jessell et al. (2012); **7** - A. Scherstén, unpublished data. Abbreviations for geochronological data as in figure 7.

ing associated with the leucogranites would in such a case be less than the 400 km estimated by Jessell et al. (2012).

Sinistral shearing thus appears to have dominated the Birmian crust during the EII and EIII phases. This is also the case for the Guyana shield, which is considered to have been affected by prolonged sinistral shearing during this time period (Delor et al. 2003a). The sinistral movement would have stemmed from southward displacement of the Man domain as Archean crust in the east represented by the Amapá block (and likely older Paleoproterozoic crust in the east, see section 4.3.1.2.1), moved northwards, relative to the present day Baoulé Mossi domain. Lateral escape may also have been important during this period of sinistral transpression as the subduction zone to the west would have provided a free face for displaced crust (Redfield et al. 2007).

4.3.3.2.3 On the lack of magmatic activity in NE Baoulé Mossi

The lack of magmatism in northern Ghana and eastern Burkina Faso during the EII phase is notable (fig. 14). With the exception of a microdiorite dated to 2052±16 Ma (Pb-evaporation on zircon) by Abdou (1992, in Soumaila et al. 2008) and a K-feldspar phenocrystic granite-monzogranite from the Nangodi belt dated to 2095±1 Ma (TIMS on zircon) by Agyei Duodu et al. (2009) there are no rocks <2.10 Ga in this region. In the Bole belt and Maluwe basin in northeastern Ghana magmatic activity largely ceased at 2118 Ma with the intrusion of late alkaline granites and gabbros (de Kock et al. 2009, 2012; Siegfried et al. 2009; Thomas et al. 2009). After 2118 Ma, magmatic and tectonothermal activity in this area was limited to reactivation of shear zones, metamorphic growth on zircon (2.10-2.09 Ga) and intrusion of a few late but as of yet undated granitoids.

The apparent lack of magmatic activity after circa 2.10 Ga in the northeastern portion of the Baoulé Mossi domain — bounded by the Haute-Comoé-Houndé basin in the west and the Comoé-Sunyani basin to the south — contrast with the otherwise widespread magmatism seen elsewhere within this domain during the EII phase. A striking feature of the northeastern part of the Baoulé Mossi domain is the lack of the large, elongate sedimentary basins which otherwise define the central and southeastern parts of the Baoulé Mossi domain. These basins (in particular Banfora-Bandama and Comoé-Sunyani) are also characterized

by widespread magmatism during the EII phase.

The distribution of magmatism during the EII phase may be largely controlled by structures established during the EI phase. As discussed above, the Banfora-Bandama and Comoé-Sunyani basins (i.e. the EIIB crustal domains) may have opened along shear zones established during the EI phase synchronous with the opening of the Haute-Comoé-Houndé, Banfora and Kumasi basins. As the EII magmatic activity is located in or near EI and EIIB sedimentary basins it appears to be structurally controlled. The lack of magmatism in the northeastern Baoulé Mossi domain may therefore be a consequence of structures established already during the EI phase.

As the Birimian crust was subject to widespread extension during the EII phase the northeastern portion of the Baoulé Mossi domain would have remained largely unaffected as this extension, and any associated magmatism, would have been preferentially partitioned into existing EI structures or basins. The same may be assumed to have occurred during any subsequent deformational phases. Also, as the subduction zone migrated further to the west its influence would simultaneously decrease, eventually leading to the termination of subduction-related magmatic activity in the east.

4.3.4 Eburnean III (<2.07 Ga) — figure 18

As can be seen in figure 18 there was little magmatic activity within the Baoulé Mossi and Man domains after circa 2.07 Ga. However, three important features of the Birimian event can still be indentified in this last phase. Although they are discussed separately in the sections below, they all reflect the final convergence and stabilization of the Birimian crust in the Baoulé Mossi and Man domains.

The main feature of the EIII phase is the presence of circa 2.05-2.03 Ga crustal anatexis in the southeastern Man domain linked to high-P granulite metamorphism. As will be discussed below this is the crustal anatexis following peak convergence and crustal thickening around 2.10-2.09 Ga. However, this development was mostly restricted to the Guyana Shield in the Amazon Craton (figures 3 and 4), which requires a closer look at the geodynamic evolution for this shield.

The two other features of the EIII phase are related to the post-collisional evolution of the Birimian crust, which included late deformation and magmatism between 2.00-1.80 Ga together with gradual cooling of the Birimian crust between 2.05-1.90 Ga.

4.3.4.1 High-grade metamorphism and crustal anatexis in the SE Man domain

The main magmatic activity during the Eburnean III phase took place along the present southeastern portion of the Man domain which at this time underwent crustal anatexis linked to high-P granulite metamorphism (Hurley et al. 1971; Kouamelan et al. 1997; Cocherie et al. 1998; Triboulet & Feybesse 1998; Pitra et al. 2010). Radiometric ages from migmatites, leucogranite, syenite (SHRIMP and Pb-Pb on zircon, EMP on monazite) and metabasites (Sm-Nd isochron) in the southeastern portion of the Man domain fall between 2055-2020 Ma and record the tectonothermal and magmatic effect of this event.

The apparently localized presence of granulite metamorphism and crustal anatexis at 2.05 Ga may partly be attributed to a lack of geochronological data. However, no ages in this interval has been reported from more extensively studied areas such as the Bole belt and Maluwe basin (fig. 7), from which a relatively large number of precise (SHRIMP on zircon) ages have been obtained (de Kock et al. 2009, 2011). If it had been affected by this tectonothermal event it seems likely that it would have been recorded, for example as rims on zircon. The lack of ages in this interval from the Bole belt and Maluwe basin thus suggest that it remained unaffected by the event which did affect the southeastern Man domain.

The southeastern Man domain is the only known area in the Man and Baoulé Mossi domains which was affected by granulite facies conditions during the Birimian event. The peak HP-HT conditions obtained by Triboulet and Feybesse (1998) and Pitra et al. (2010) at 1000°C, 14 kbar and 850°C, 13 kbar, respectively, clearly stand out among the lower grade Birimian rocks of the Baoulé Mossi domain. Assuming that the peak P-T conditions reflect a Birimian (as opposed to Neoarchean, see section 2.2.3) overprint it is still unclear whether they are recorded by the radiometric ages obtained in this region (fig. 18) or if these ages rather correspond to the retrograde conditions (700-800°C, <7 kbar) recognized by Pitra et al. (2010).

The apparently localized effect of the circa 2.05 Ga tectonothermal and magmatic event in the Man domain may be explained by juxtaposing the WAC and Amazon Craton using the Midgardia configuration (fig. 4) of Johansson (2009). This places the Amazon Craton south of present day WAC, connecting the Imataca complex with the Man domain. Previous workers, such as Feybesse and Milési (1994) and Nomade et al. (2003), have also the placed the WAC and the Amazon Craton in this configuration, recognizing

Fig. 18. A compilation of geochronological data from the Eburnean III phase. See figure 7 for legend and references. Inset shows a schematic depiction of the geodynamic setting during the Eburnean III phase (<2.07 Ga). This phase was characterized by crustal relaxation and extension-transtension following the main collision between the Man domain and the Birmian crust. Relaxation led to uplift and retrograde metamorphism-crustal anatexis within the Archean crust that had been subjected to granulite facies metamorphism during the EII phase (however, for alternate possibilities see section 4.3.4.1.3). Magmatic activity during the Eburnean III phase was limited to anatexis within uplifted Archean crust and scattered intrusions within the Baoulé Mossi domain. Cooling ages from amphibole, biotite and muscovite indicate that the Birimian crust stabilized around 2.0 -1.9 Ga. Late deformation may have taken place in response to far-field tectonothermal events.

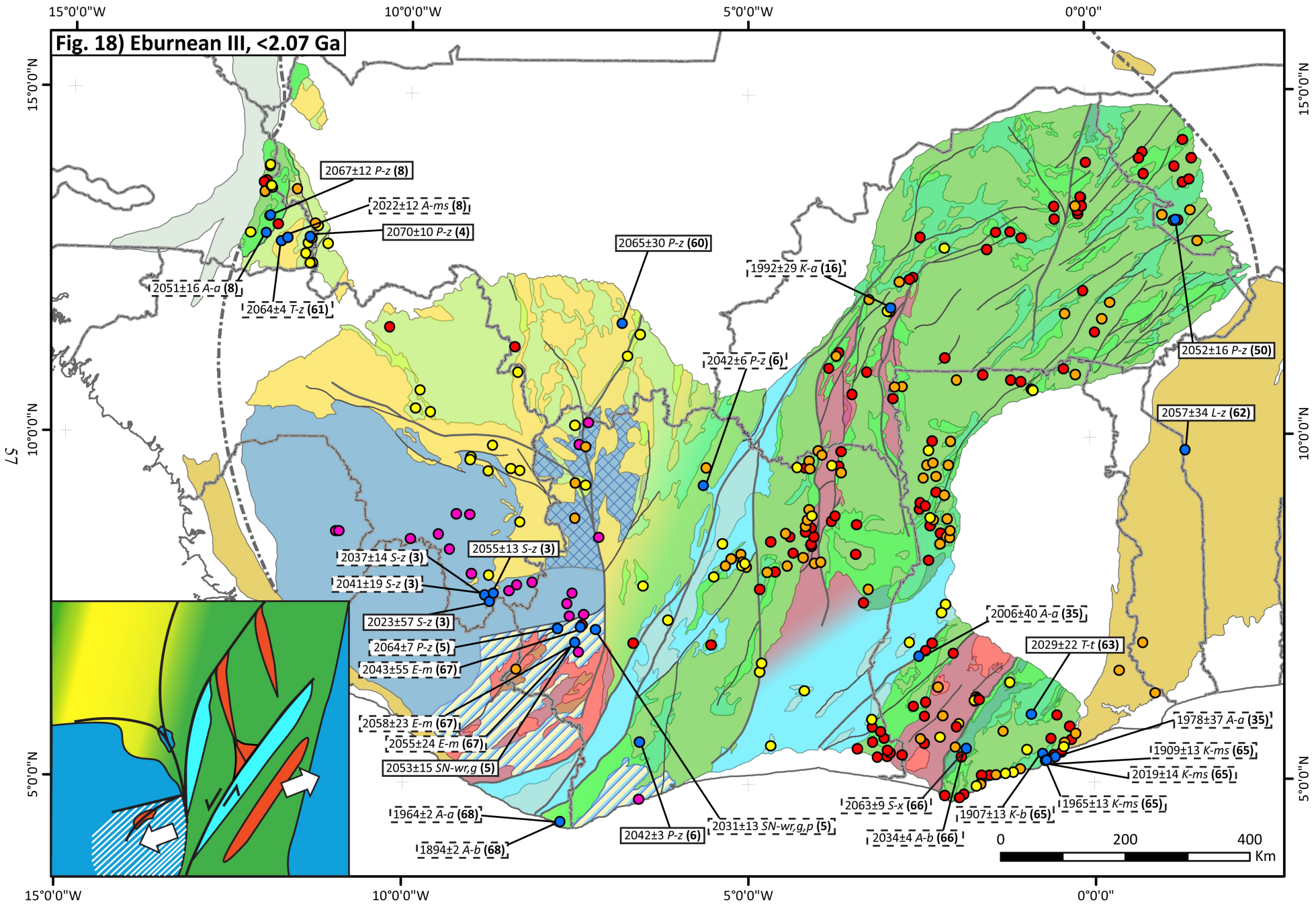
Fig. 18) Eburnean III, <2.07 Ga
15°0'0"W
10°0'0"W
5°0'0"W
0°0'0"
15°0'0"N
10°0'0"N
5°0'0"N
2067±12 P-z (8)
2022±12 A-ms (8)
2070±10 P-z (4)
2051±16 A-a (8)
2064±4 T-z (61)
2065±30 P-z (60)
1992±29 K-a (16)
2042±6 P-z (6)
2052±16 P-z (50)
2057±34 L-z (62)
2037±14 S-z (3)
2055±13 S-z (3)
2041±19 S-z (3)
2023±57 S-z (3)
2064±7 P-z (5)
2043±55 E-m (67)
2058±23 E-m (67)
2055±24 E-m (67)
2053±15 SN-wr,g (5)
1964±2 A-a (68)
1894±2 A-b (68)
2042±3 P-z (6)
2031±13 SN-wr,g,p (5)
2006±40 A-a (35)
2029±22 T-t (63)
1978±37 A-a (35)
1909±13 K-ms (65)
2019±14 K-ms (65)
1965±13 K-ms (65)
2063±9 S-x (66)
1907±13 K-b (65)
2034±4 A-b (66)
0
200
400
Km
S7

the convergence between the Archean crust in the southeastern Amazon Craton (including the Amapà block) with the Archean crust of the Man domain. This configuration will form the foundation for the discussion below regarding the geodynamic setting of the Birimian granulites. It follows that this assumes that the configuration is "correct" and actually reflects the position of the WAC and Amazon Craton during the Birimian event.

4.3.4.1.1 Granulite occurrences in Midgardia

The following section will present a short overview of granulite-facies domains in the WAC and the Guyana shield in the Amazon Craton. The locations of these domains within the Midgardia-configuration are shown in figure 19. Unlike the WAC, where granulites are only present in the Man domain, there are more widespread occurrences of granulites in the Guyana shield. These are, from northwest to southeast, the Imataca complex, Bakhuis UHT-granulite belt and the Amapá block.

4.3.4.1.1.1 Man domain and Imataca complex

In the Midgardia-configuration of Johansson (2009) the Man domain in the WAC connects with the Archean Imataca complex in the Guyana Shield (fig. 4). The Imataca complex is comprised of migmatized ortho- and paragneisses, occasional anatectic granitoids and quartzofeldsphatic granulites (Swapp & Onstott 1989; Tassinari et al. 2004). These gneisses appear to have been derived from granite-greenstone protoliths with Sm-Nd model ages between 3.7-2.8 Ga. Like the Man domain, the Imataca complex was also subjected to a Neoarchean (2.8 Ga) tectonothermal event (Tassinari et al. 2004). However, unlike the Man domain, juvenile additions occur in the Imataca complex (although the limited data available data from the Man domain means that Neoarchean juvenile additions cannot be ruled out)

As discussed above, P-T conditions in the Man domain record HP-HT conditions (700-1000°C at 13-14 kbar) interpreted to have been associated with crustal anatexis between 2055-2020 Ma. Lower grade conditions have been reported from the Imataca complex were Swapp and Onstott (1989) and Tassinari et al. (2004) obtained peak P-T conditions at 750-800°C, 8-8.5 kbar and 750-800°C, 6-8 kbar, respectively. Tassinari et al. (2004) obtained an age of 2055±28 Ma (SHRIMP on zircon) from a zircon rim which they proposed may lay close to peak metamorphism. However, because of the thin zircon rims the possibility of mixing could not be ruled out. Other methods (e.g. Sm-Nd isochrons) yield slightly younger ages around 2.0 Ga and the Birimian overprint was broadly constrained by Tassinari et al. (2004) to 2.05-1.98 Ga.

Granulite facies conditions were interpreted by Tassinari et al. (2004) to have developed when the Imataca complex collided with the Birimian crust of

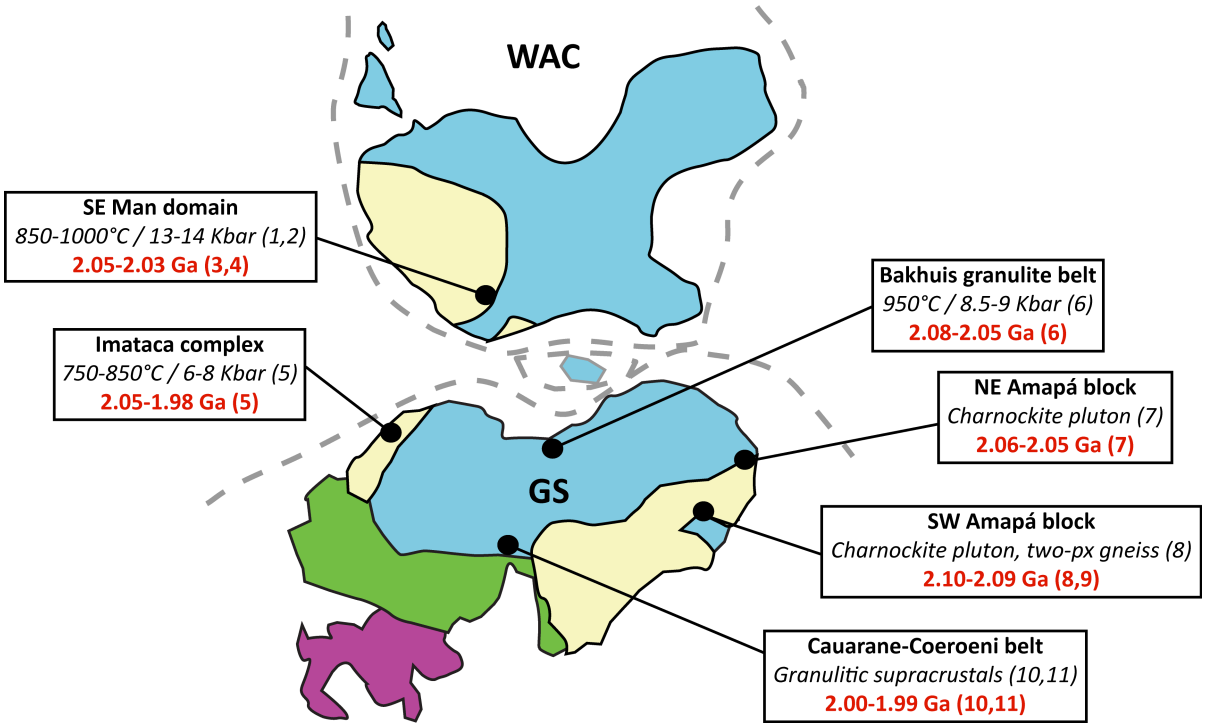

Fig. 19. Location of reported occurrences of 2.10-1.98 Ga granulites in the Man-Leo and Guyana shields shown here in a pre-Pan African-Brasiliano position following Onstott et al. (1984) and Johansson (2009). See figure 3 for legend. Timing and indicators of granulite conditions (P-T data or, if lacking, lithological associations) after the following references; **1** - Pitra et al. 2010; **2** - Triboulet & Feybesse 1998; **3** - Kouamelan et al. 1997; **4** - Cocherie et al. 1998; **5** - Tassinari et al. 2004; **6** - Roever et al. 2003; **7** - Avelar et al. 2003, and references therein; **8** - Rosa-Costa et al. 2006; **9** - Rosa-Costa et al. 2008; **10** - Fraga et al. 2009a; **11** - Fraga et al. 2009b. Simplified tectonic maps after Macambira et al. (2009, with modifications from Rosa Costa et al. 2006) and Baratoux et al. (2011).

the Maroni-Itacaiunas province. This led to crustal thickening through crustal imbrication. Subsequent transpression led to the sinistral shearing along the Guri fault which marks the contact between the Imataca complex and Birimian crust of the Maroni-Itacaiunas province (Swapp & Onstott 1989; Tassinari et al. 2004). The Guri fault is considered to form an extension of the sinistral Sassandra shear zone in the Man-Leo shield (Onstott et al. 1984). The model for the Imataca complex, involving thrusting followed by shearing in a transpressional regime, is equivalent to the model by Feybesse and Milési (1994) for the contact between the Man and Baoulé Mossi domains but differs from that of Kouamelan et al. (1997) and Pitra et al. (2010) who do not recognize thrusting.

4.3.4.1.1.2 Bakhuis UHT-granulite belt

The Bakhuis UHT-granulite belt is 40 km wide and 100 km long belt located in the north-central part of the Maroni-Itacaiunas province, near the Atlantic coast. The Bakhuis belt is composed of granulitic ortho- and paragneisses intruded by syn- to early post-tectonic charnockites and dolerites (Roever et al. 2003). Doleritic dykes are relatively common within the core of the Bakhuis belt, some of which are folded together with their host rocks whereas others are undeformed. However, all dolerites are affected by granulite facies metamorphism and are thus linked to the metamorphism.

Radiometric ages (Pb-Pb zircon) obtained by Roever et al. (2003) from gneisses, metadolerites, charnockites and pegmatites fall within the period of 2085-2050 Ma with inherited ages up to 2150 Ma. Interpretation of these ages, and how they relate to peak metamorphism, is somewhat ambiguous. Roever et al. (2003) proposed that the radiometric data could be interpreted in terms of high-grade metamorphism between 2090-2070 Ma followed by magmatism around 2065-2055 Ma. Alternatively, high-grade metamorphism and magmatism may have been largely coeval and occurred around 2070-2055 Ma whereas older ages reflect inherited components. No Archean rocks have been recognized in the Bakhuis belt, either through inherited zircon ages or evolved isotopic compositions (Roever et al. 2003). The Bakhuis belt therefore stand out among the other granulite occurrences in the WAC and Amazon Craton in that it was developed in Birimian — as opposed to Archean — protoliths.

Some rare occurrences of UHT-metamorphism have been reported from the Bakhuis belt (Roever et al. 2003). These are comprised of quartzites and pelitic gneisses with orthopyroxene-sillimanite-quartz assemblages in which orthopyroxene contain up to 10% Al_2O_3. Sapphirine and corundum occur in quartz-rich rocks. Roever et al. (2003) noted the consistent lack of garnet within the Bakhuis UHT-assemblages which is otherwise present in many other UHT-occurrences worldwide. These authors suggested that the lack of garnet might be due to high oxygen fugacities. From petrological studies, Roever et al. (2003) proposed that the UTH mineral assemblages had formed during a counter-clockwise P-T path with peak conditions at 900-1000°C and 8.5-9 kbar, followed by isobaric cooling.

The Bakhuis belt occurs within a dome structure, which Roever et al. (2003) proposed developed coevally with the intrusion of an anorthosite pluton dated by the same authors to 1980±5 Ma (Pb-Pb on zircon). The late — in relation to peak metamorphism at 2.08-2.05 Ga — formation of the dome structure and consequent uplift of the granulite belt was required due to the isobaric cooling of the UHT granulites.

4.3.4.1.1.3 Amapá block

The Amapá block is located in the southeastern part of the Guyana Shield. It is composed of an approximately west-northwest and east-southeast oriented 100 km wide belt of Archean rocks surrounded to the north and south by Birimian crust (Avelar et al. 2003; Rosa Costa et al. 2006, 2008). The Archean crust formed mainly during the Paleo- and Mesoarchean (3.3-2.8 Ga). The Amapá block was reworked during the Neoarchean (2.8-2.6 Ga) and subjected to tectonothermal and magmatic activity during the Birimian event.

While there does not appear to be any quantitative P-T data available from the Amapá block the presence of charnockites and granulitic gneisses nevertheless indicate that it has been subjected to granulite-facies conditions. In its northeastern part, charnockitic plutons have been dated to 2.06-2.05 Ga while Sm-Nd whole rock-garnet isochrons have yielded ages between 2.03-2.00 Ga (Avelar et al. 2003, and references therein). In the southeastern Amapá block, U-Th-Pb monazite and Pb-Pb zircon ages from granulitic gneisses and charnockite intrusions indicate that this area was subjected to granulite-facies metamorphism and crustal anatexis around 2.10-2.09 Ga (Rosa Costa et al. 2006, 2008). Further anatexis and emplacement of monzo- and syenogranites around 2.06-2.03 Ga was associated with retrogression to amphibolite-facies conditions.

Based on structural relationships, Rosa Costa et al. (2008) argued that the 2.10-2.09 Ga granulite facies metamorphism in the SW Amapá block was contemporaneous with the development of a transpressional thrust system. Retrogression to amphibolite facies conditions with associated crustal anatexis between 2.06-2.03 Ga was associated with shearing along strike-slip shear zones. The emplacement of granites and development of migmatites along strike-slip corridors during this period was interpreted by Rosa Costa et al. (2008) as marking a post-collisional stage in the Amapá block.

4.3.4.1.2 Previous geodynamic models for granulite facies metamorphism

Delor et al. (2003a) proposed a model for the Guyana shield in which the granulite domains formed during

the final convergence between Archean continents — represented by the Imataca complex and Amapá block — and the intervening Birmian crust. Widespread sinistral shearing, granitic magmatism and development of pull-apart basins took place between 2.11-2.08 Ga. This was followed by sinistral shearing between 2.07-2.05 Ga. According to Delor et al. (2003a), this late shearing led to the development of crustal-scale boudins. The three granulite domains of the Guyana shield developed within the necks of these boudins as upwelling mantle provided a heat source for (UHT) granulite facies metamorphism.

Radiometric dating by Rosa Costa et al. (2008) on rocks from the SW Amapá block showed that the granulite facies metamorphism in this granulite domain (2.10-2.09 Ga) predated the ages interpreted to record granulite facies metamorphism in the Bakhuis belt (2.08-2.05, Roever et al. 2003), the Imataca complex (2.05-1.98, Tassinari et al. 2004) and the Man domain (2.05-2.03 Ga, Kouamelan et al. 1997; Pitra et al. 2010). Rosa Costa et al. (2008) therefore proposed that granulite facies metamorphism during the late stage of the Birimian event in the Guiana and Man-Leo shields had been diachronous, beginning earlier in the Amapá block before being progressively developed within the Bakhuis and Imataca complex-Man domain. As such, this temporal trend is at odds with the model of Delor et al. (2003a) in which the granulite domains are coeval.

Rosa Costa et al. (2008) noted the contemporaneous nature of the UHT granulite facies metamorphism in the Bakhuis belt and the post-collisional retrogression to amphibolite facies condition and crustal anatexis within the southwestern Amapá block and proposed that they formed during the same stage. This would correspond to the late shearing recognized by Delor et al. (2003a) within the Guyana shield. 2.06-2.05 Ga charnockites in northeastern Amapá block (Avelar et al. 2003) would also be related to this event (Rosa Costa et al. 2008).

4.3.4.1.3 On the timing of granulite facies metamorphism in SE Man domain

As discussed above, the EIII phase is characterized by limited magmatic activity, as can be seen in the compilation of radiometric ages in figure 18. Within this context, the high-P granulite metamorphism within the southeastern Man domain (Kouamelan et al. 1997; Triboulet & Feybesse 1998; Pitra et al. 2010) appears out of place. Indeed, such an event would rather be expected to be associated with widespread tectonothermal and magmatic activity, such as took place during the 2.10-2.07 Ga EII phase.

The geochronological data that has been used to constrain the timing of granulite metamorphism in the Man domain is ambiguous. Most ages (U-Th-Pb on monazite, SHRIMP on zircon) have been obtained from migmatitic gneisses, anatectic veins or granites (Cocherie et al. 1998; Thiéblemont et al. 2004) and thus date crustal anatexis. It is not immediately clear at what point during the P-T evolution of the Man domain that anatexis occurred; in other words, does the magmatic ages of the above rocks record peak P-T conditions in the Man domain.

Pitra et al. (2010) recognized two metamorphic assemblages in a metabasite from the southeastern Man domain; M1 (850°C, 13 kbar) and M2 (700-800°C, <7 kbar). The metabasitic sample upon which Pitra et al. (2010) performed their thermobarometric study had previously been dated by Kouamelan et al. (1997) to 2031±13 Ma using a Sm-Nd four-point isochron (whole rock, two garnet and plagioclase). Pitra et al. (2010) argued that this age, together with the ages from Cocherie et al. (1998) and Thiéblemont et al. (2004), recorded the Birimian overprint on the Archean crust of the Man domain. In their discussion, Pitra et al. (2010) recognized that the Sm-Nd age obtained from their sample may record either their M1 or M2 assemblage, considering that the cooling age of garnet straddles the conditions recognized for the respective assemblages. However, because of the tight clustering of ages (2055-2030 Ma) in the Man domain Pitra et al. (2010) argued that the M1 and M2 assemblages had both developed during this short period of time.

Although the geochronological data would thus seem to indicate that the Birimian high-P granulitic overprint was developed between 2.05-2.03 Ga, the lack of activity elsewhere within the Baoulé Mossi domain at this time seems incompatible with such an interpretation. The same can be said about the geodynamic evolution in the equivalent crust of the Guyana shield in which the main magmatic and tectonothermal activity ended by 2.05 Ga (e.g. Delor et al. 2003a; Rosa Costa et al. 2008). The model by Rosa Costa et al. (2008) in which the granulites of the Bakhuis belt and the uplift, retrogression and crustal anatexis within the Amapá block occurred in a post-collisional setting (between circa 2.08-2.03 Ga) is also at odds with the development of essentially coeval high-P granulites within the Man domain.

When compared with the Amapá block it is interesting to note that the crustal anatexis within the Man domain, as recorded by migmatites (Cocherie et al. 1998) and emplacement of granites (Thiéblemont et al. 2004), is coeval with the migmatization and emplacement of granites within the Amapá block which are associated with retrogression from granulite to amphibolite facies conditions (Rosa Costa et al. 2006, 2008). Meanwhile, the granulite facies metamorphism took place between 2.10-2.09 Ga (Rosa Costa et al. 2008). When considering the overall magmatic and tectonothermal evolution of the Baoulé Mossi domain it is clear that a similar age for the granulite facies metamorphism in the southeastern Man domain would fit better.

It must be pointed out that there is no age from the Man domain, which could be taken to support such an interpretation. Instead, it relies entirely on circumstantial evidence, such as the lack of extensive mag-

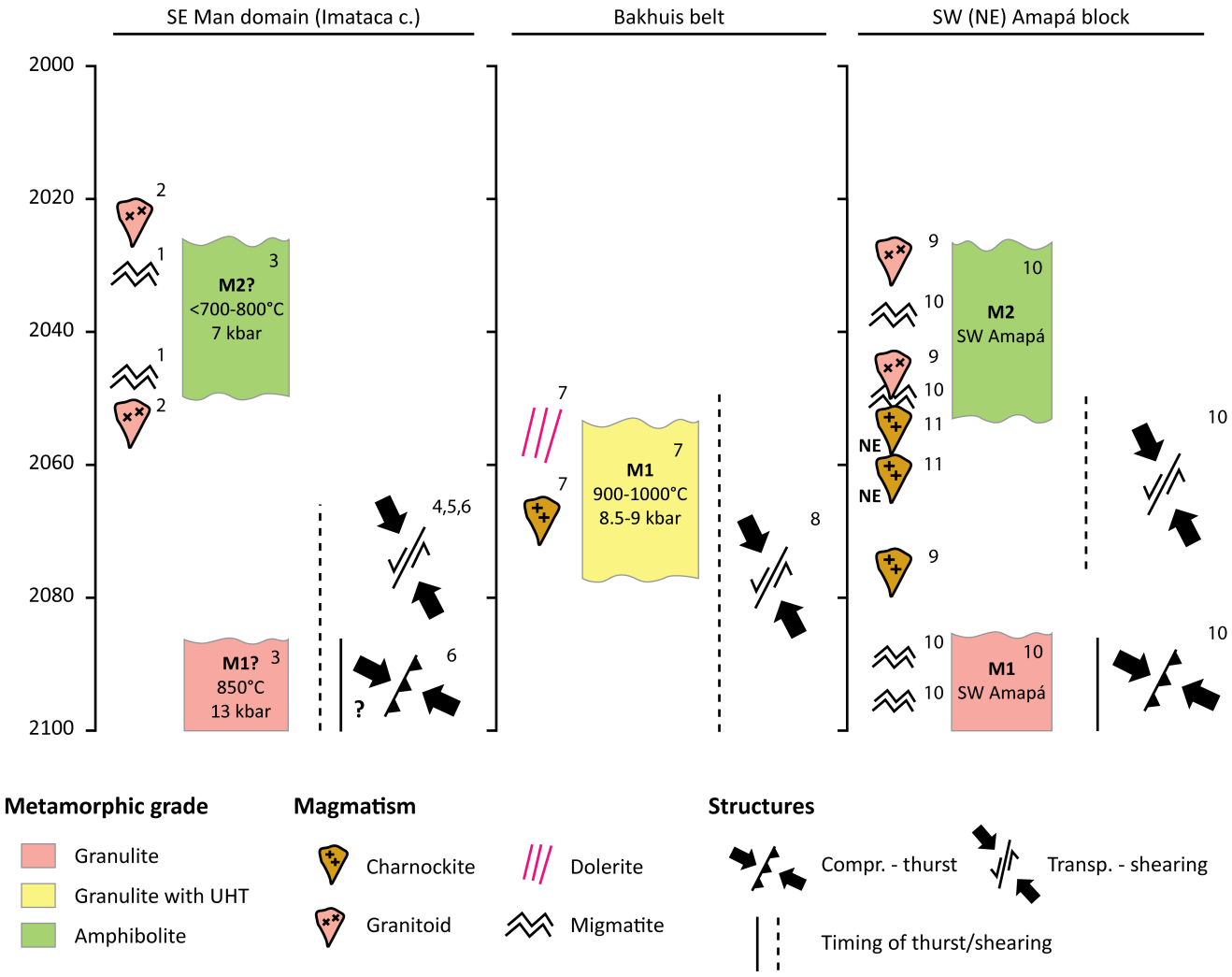

Fig. 20. A proposed simplified stratigraphy for magmatic and tectonothermal events in the granulite domains of SE Man domain -Imataca complex, Bakhuis belt and Amapá block for the period 2.10-2.00 Ga. References for the events are given by a number to the upper right of each symbol; **1** - Cocherie et al. (1998); **2** - Thiéblemont et al. (2004); **3** - Pitra et al. (2010); **4** - Kouamelan et al. (1997); **5** - Egal et al. (2002); **6** - Tassinari et al. (2004); **7** - Roever et al .(2003); **8** - Delor et al. (2003a); **9** - Rosa Costa et al. (2006); **10** - Rosa Costa et al. (2008); **11** - Avelar et al. (2003). Note that the timing of granulite and amphibolite facies metamorphism in the SE Man domain-Imataca complex is based on a reinterpretation of the available tectonothermal and magmatic data from the Man and Baoulé Mossi domains. See discussion in section 4.3.4.1 for further details.

matic or tectonothermal activity during the period 2.05-2.03 Ga (fig. 18). This is clearly problematic and requires further high-precision geochronological investigations (SHRIMP or LA-ICP-MS) on granulitic rocks from this area to firmly establish whether granulitic metamorphism actually occurred around circa 2.10 Ga. However, it should also be remembered that the currently available geochronological data from the Man domain is limited and is, in the view of the author, compatible with granulite facies metamorphism taking place at 2.10 Ga.

Based on the above discussion it proposed here that the high-P granulite metamorphism within the southeastern Man domain (M1 of Pitra et al. 2010) developed between 2.10-2.09 Ga, coevally with that in the Amapá block. The migmatization and emplacement of granites recorded between 2055-2030 Ma (Cocherie et al. 1998; Thiéblemont et al. 2004) would in that case have taken place in a post-collisional setting. This would correspond to the M2 of Pitra et al. (2010).

4.3.4.1.4 A proposal for the tectonic setting of granulite facies metamorphism

The purpose of this section is to present a model for the development of the granulite domains in the Man-Leo and Guyana shields. This model is based on the assumption outlined above that granulite facies metamorphism in the southeastern Man domain, and in extension the Imataca complex, took place around 2.10-2.09 Ga. Post-collisional retrogression and crustal anatexis occurred between 2055-2030 Ma, again contemporaneously with the Amapá block.

A schematic tectono-stratigraphic chart for the granulite domains in the Man domain-Imataca complex, Bakhuis belt and Amapá block is shown in figure 20. This stratigraphic chart shows the timing metamorphism within each belt, as well as the timing and type

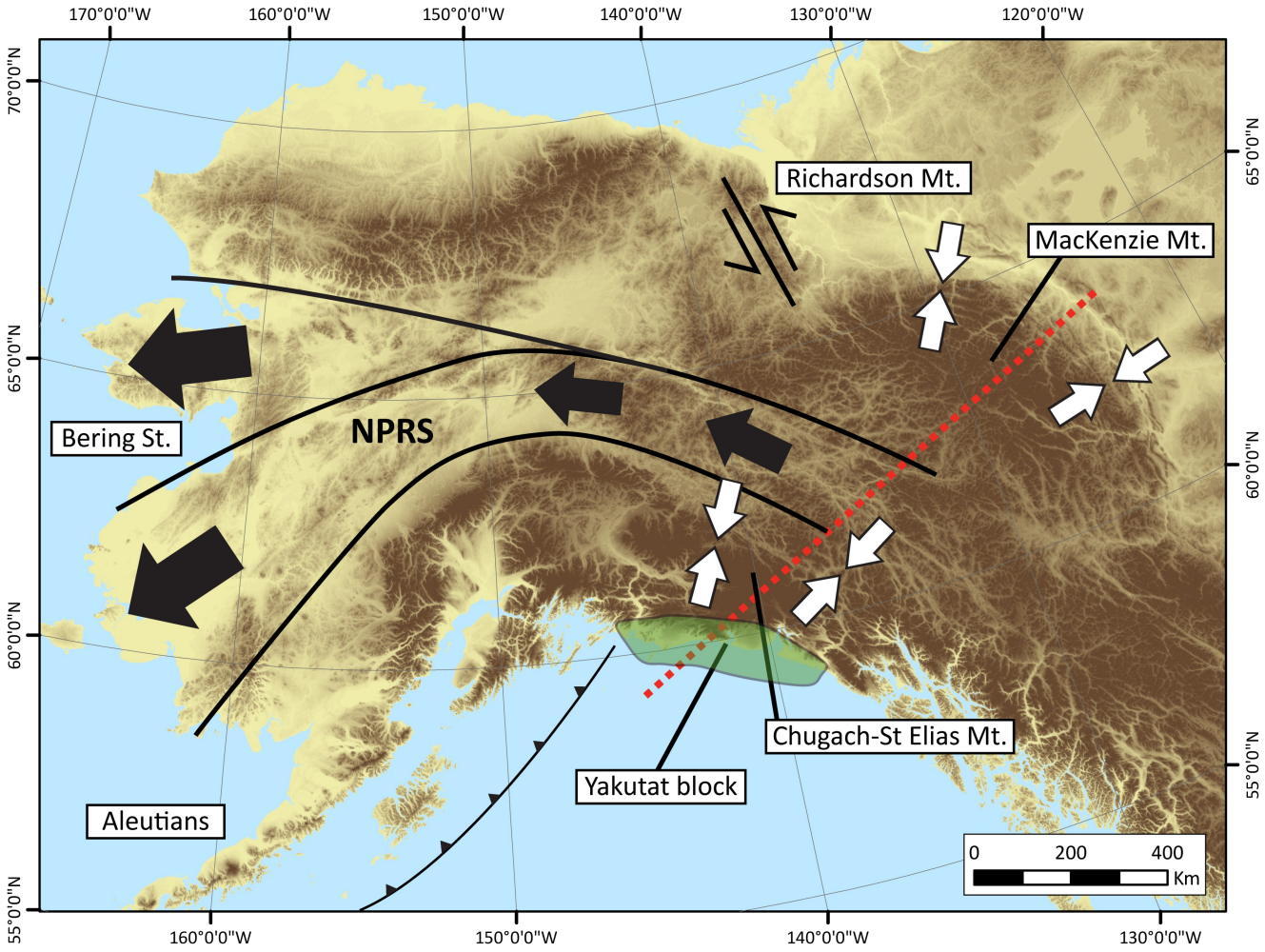

Fig. 21. Overview of the North American Cordilleras showing elevation (high-dark, low-light), lateral escape along the North Pacific Rim Orogenic Stream (NPRS, after Redfield 2007) and stress field resulting from convergence between the Yakutat block and the Cordilleran crust (after Mazotti & Hyndman 2002). Elevation data from USGS/EROS GTOPO30 (lta.cr.usgs.gov/GTOPO30, last accessed 05-07-2013). Displayed using the NAD 1927 Alaska Albert projection and the North American 1927 datum.

of magmatic activity and deformation during the relevant time period. For the Man domain and Imataca complex, it shows the timing of the M1 and M2 assemblages of Pitra et al. (2010) at 2.10-2.09 Ga and 2.05-2.03 Ga, as discussed above. While not shown in the stratigraphic chart, granulites in the Imataca was subjected to lower pressure at 6-8.5 kbar (Swapp & Onstott 1989; Tassinari et al. 2004) compared with those of the Man domain (fig. 19).

The stratigraphic chart displays a striking relationship between the granulite domains in which early (2.10-2.09 Ga) granulite facies metamorphism in the Amapá block and Man domain-Imataca complex is followed by UHT-granulite facies metamorphism in the intervening Bakhuis belt and coeval emplacement of charnockites in the northeastern Amapá block. The granulite facies metamorphism in the Bakhuis belt is in turn followed by retrogression within the former granulite domains with associated crustal anatexis. It is of importance to note that Birimian crust in the Guyana shield which occurs in between the granulite domains is characterized by greenschist facies metamorphism, with locally developed amphibolite facies conditions near intrusions (Voicu et al. 2001).

In comparison, the Man domain-Imataca complex and Amapá block show a strikingly similar evolution, despite being separated by a circa 1000 km wide belt of Birimian crust. The uncertainties regarding the timing of metamorphism within the Man domain-Imataca complex and the absence of P-T from the Amapá block are obviously problematic when making such comparisons. The risk for developing a circular reasoning should also not be ignored, considering that the timing of metamorphism in the Man domain-Imataca complex is partly based (see above) on the timing of metamorphism within the Amapá block. However, as discussed previously, there are also good reasons for placing the timing of metamorphism in the Man domain-Imataca complex the way it is shown in figure 20. Therefore, assuming that the similarities between these two domains are real, there is a need for a model which can explain the setting in which this

occurred and that accounts for the UTH-granulites in Bakhuis belt as well as the intervening, low grade Birimian crust. It is proposed here that the setting in which this took place may be comparable to the recent development in the northern Cordilleras of North America

The northern Cordilleras are characterized by a thin and hot lithosphere typical of modern backarcs (e.g. Hyndman et al. 2005; Currie & Hyndman 2006). Lower crustal temperatures reach 700-800°C with Moho temperatures at 800-900°C. The total lithospheric thickness is 50-60 km while the crust itself is typically less than 35 km thick. These conditions extend for hundreds of kilometers into the interior of North America.

In the Gulf of Alaska, a small composite oceanic and continental terrane called the Yakutat block (fig. 21) has been colliding with Cordilleran crust for the last 20 Ma (Mazzotti & Hyndman 2002; Hyndman 2010). This has led to crustal thickening and the uplift of the Chugach-St Elias Mountains in the Cordilleran forearc (fig. 21). However, simultaneously with the formation of these mountains, a foreland belt represented by the MacKenzie and Richardson Mountains has been developed, 800 km to the northeast of the Chugach-St Elias Mountains. These two mountain ranges are separated by the main northern Cordillera which has a lower elevation and thinner lithosphere. A cross-section between the Chugach-St Elias and MacKenzie Mountains is shown in figure 22.

Based on the concept of orogenic float (Oldow et al. 1990), Mazzotti and Hyndman (2002) argued that the simultaneous formation of the two separate mountain ranges was made possible by the development of a lower crustal detachment zone within the intervening thin and hot Cordilleran crust (fig. 22). This lower crustal detachment zone would allow the upper crust to float above it, transferring strain from the collision between the Yakutat block and the Cordilleran in the forearc into the foreland region. Thus, while crustal thickening through thrusting has led to the development of mountain ranges along the margins of the more rigid blocks, the intervening area of hot and thin crust has not been significantly deformed or thickened and has instead acted as a zone of strain transfer.

Using the northern Cordilleras as an analogue, it could therefore be envisaged that the apparently coeval (as proposed here) granulite facies metamorphism in the Archean crust of Amapá block and Man domain-Imataca complex could have formed through the collision between these domains and the Birimian crust between them. Given the assumed thin, hot and consequently weak Birimian crust (see section 4.1.3) it would behave similarly to the crust of the northern Cordillera during collision, transferring strain from the collision zone at the margin of the Amapá block to the margin of the Man domain-Imataca complex, or vice versa, depending on which of these areas assumed a forearc or foreland position during collision.

Such a model could therefore explain the simultaneous development of granulite facies metamorphism through crustal thickening by thrusting (Feybesse & Milési 1994; Tassinari et al. 2004) or, according to Pitra et al. (2010), to homogenous thickening of weak continental crust. Regardless, the intervening Birimian crust would not have been significantly thickened, thus providing an explanation for the low grade metamorphic conditions of volcanic and sedimentary rocks between the granulite belts (Voicu et al. 2001). The recognition of isobaric cooling paths within both the Bakhuis belt (Delor et al. 2003a; Roever et al. 2003) and in greenschist facies metasediment in French Guiana (Delor et al. 2003b) reflects a

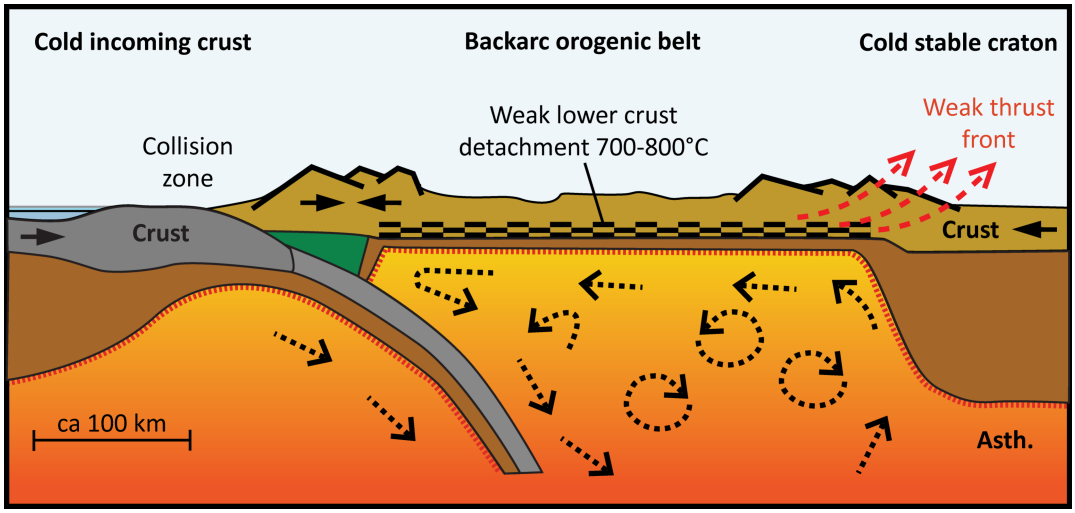

Fig. 22. A cross section of the North American Cordilleras approximately located along the dashed red line in figure 21. The figure illustrates the forearc collision between the Yakutat block and the Cordilleran crust. This has led to uplift of the Chugach-St Elias Mt. but also to strain transfer across the thin, hot and weak Cordilleran crust to the Cordilleran foreland where the McKenzie Mt. has developed along the margin of the stable North American continent. Strain transfer is facilitated by lower crustal detachment which allows the upper crust to be displaced against the foreland without undergoing significant thickening. Redrawn after Hyndman et al. (2005) and Hyndman (2010) with minor modifications.

lack of crustal thickening within the Birimian crust.

Roever et al. (2003) reconstructed a counter-clockwise (CCW) P-T path for the Bakhuis belt for the UHT-granulite facies metamorphism. This P-T path involved a slight pressure increase before peak conditions were reached. This suggest that the UHT conditions developed in a transpressional setting although, considering the presence of metamorphosed syn- to post-kinematic dolerites indicate that this transpression switched to transtension sometime between 2080-2055 Ma.

From the example of the northern Cordilleras, it is interesting to note that the thin crust that acts as strain transfer zone between the Chugach-St Elias and MacKenzie Mountains is also currently undergoing lateral escape towards the northwest along the North Pacific Rim orogenic stream (NPRS, Redfield et al. 2007) as shown in figure 21. This lateral escape is facilitated by crustal-scale strike-slip faults and may have been ongoing for at least 50 Myr (Redfield et al. 2007). This shows that lateral escape and development of strike-slip faults/shear zones can occur coevally with collision in a zone undergoing lower crustal detachment. As such, it can account for the formation of shear zones within the Baoulé Mossi domain during the EI and EII phases, coeval with the peak collision between Archean crust in the Man domain-Imataca complex and Amapá block.

As proposed by Rosa Costa et al. (2008), the development of the Bakhuis UHT-granulite belt, emplacement of charnockites in the northeastern Amapá block, and retrogression from granulite to amphibolite facies conditions took place in a post-collisional setting. In the Guyana shield, this was associated with crustal-scale sinistral shearing (Delor et al. 2003a). It is interesting to note that the formation of the Bakhuis belt granulites (2.08-2.05 Ga) began before crustal anatexis (2.06-2.03 Ga) within the Man domain-Imataca complex and Amapá block (fig. 20). In the case of the latter, magmatism in turn lasted for another 30 Myr after the development of granulite facies metamorphism within the Bakhuis belt. However, there is also an overlap between the youngest ages obtained from the Bakhuis belt (2060-2055 Ma, Roever et al. 2003) and the oldest ages (2060-2050 Ma) obtained from the Man domain-Imataca complex (Cocherie et al. 1998; Thiéblemont et al. 2004) and the Amapá block (Rosa Costa et al. 2008). Also, as discussed above, the emplacement of leucogranites within the EIIB domains span the interval between the end of the granulite facies metamorphism in the Man domain-Imataca complex and Amapá block and the beginning of UTH metamorphism in the Bakhuis belt.

The presence of syn- to post-kinematic dolerites — all of which have been metamorphosed — within the Bakhuis belt (Roever et al. 2003) indicate that it formed within an extensional setting (Delor et al. 2003a). Ages obtained from the Bakhuis belt, including discordant metadolerites, granulitic gneisses and charnockites, are coeval with the formation of the Ashanti lode gold deposit in southern Ghana which was dated to 2063±7 Ma (SHRIMP on hydrothermal xenotime) by Pigois et al. (2003). According to Perrouty et al. (2012), the Ashanti lode-gold deposit is associated with late sinistral shearing along the Ashanti fault (their D4). The timing and associated sinistral shearing of the Ashanti lode-gold deposit suggests that it also formed in response to a switch from compression of the Birimian crust between the Man domain-Imataca complex and the Amapá block to post-collisional transtension.

4.3.4.2 Late deformation and magmatism in the Baoulé Mossi domain

Even as the main magmatic and tectonothermal activity in the Baoulé Mossi domain appear to have ceased at about 2.07 Ga there are nevertheless reports of younger intrusive magmatism as well as deformational events associated with isotopic resetting from across the Baoulé Mossi domain.

Liégeois et al. (1991) found that the Banifin shear zone in southeastern Mali had been reactivated at around 1980 Ma. This reactivation was expressed as dextral movement (as opposed to sinistral shearing during the EIIA phase) under ductile but retrograde greenschist facies conditions. While this event was not associated with intrusive or extrusive magmatism Liégeois et al. (1991) proposed that percolation of fluids in the Banifin shear zone in association with this movement was responsible for resetting the Rb-Sr isotopic composition of spatially associated volcanic and intrusive rocks. From the calculated mean of three such reset Rb-Sr ages, Liégeois et al. (1991) obtained an age of 1984±30 Ma, which they interpreted as dating this late deformation.

The period around 1.98 Ga coincide with the intrusion of the gold-hosting Caxias biotite microtonalite in the São Luís Craton, dated by Klein et al. (2002) to 1985±4 Ma (Pb-Pb on zircon), as well as the anorthosite intruding into the Bakhuis UHT-granulite belt, in turn dated to 1980±5 Ma (Pb-Pb on zircon) by Roever et al. (2003). As discussed above, the anorthosite of the Bakhuis belt was intruded as the Bakhuis belt underwent a phase of doming during which the UTH-granulites were exhumed to their present crustal level, a process interpreted by Roever et al. (2003) to have occurred before cratonization of that part of the Guyana shield.

While magmatic activity around 1.98 Ga is limited within the Baoulé Mossi domain it is more widespread in the Guyana shield, including the Maroni-Itacaiunas and the Ventuari-Tapajós provinces (fig. 4). At this time, the Ventuari-Tapajós province constituted an accretionary orogen facing an extensive Paleoproterozoic ocean while the Birimian Maroni-Itacaiunas province assumed a backarc position (Cordani & Teixeira 2007). With this environment in mind, the magmatic and tectonothermal activity seen in the Baoulé Mossi domain is likely far-field effects related to the activity seen in the Amazon Craton.

Late alkaline intrusions dated at 1.89-1.82 Ga have been reported from Burkina Faso (Casting et al. 2003, in Vegas et al. 2008). However, during the course of this work it has not been possible to access the original publications (i.e. Castaing et al. 2003) and no further information is available regarding the location of these intrusions or the method used for dating them. As for the magmatism and tectonothermal activity around 1.98 Ga it seems reasonable to ascribe this magmatism to far-field effects related to ongoing activity along accretionary orogens in e.g. the Amazon Craton. The Caurane-Coeroeni granulite belt, located between the Maroni-Itacaiunas and Ventúari-Tapajos domains of the Guyana shield (figs. 4 and 13), formed around 2.00-1.99 Ga (Fraga et al. 2009a, 2009b) and could represent such a far-field event which could have had an impact on the recently amalgamated Birimian crust.

It is interesting to note that the magmatic and tectonothermal activity discussed above is coeval with biotite and muscovite cooling ages from elsewhere within the Baoulé Mossi domain (see also next section). This shows that while some areas of the Baoulé Mossi domain were cooling off and stabilizing magmatism and tectonothermal activity nevertheless persisted elsewhere. The "end" of the tectonothermal activity and magmatism was thus diachronous on the scale of the Baoulé Mossi domain and the Amazon Craton.

4.3.4.3 Cooling of the Baoulé Mossi domain

Cooling of the Baoulé Mossi domain is constrained by K-Ar and $^{40}Ar/^{39}Ar$ ages on amphibole, biotite and muscovite to have occurred between circa 2050-1900 Ma (e.g. Chalokwu et al. 1997; Feybesse et al. 2006; Gueye et al. 2007). Amphibole tends to record the oldest cooling ages while those of biotite and muscovite are progressively younger, reflecting their lower closure temperatures. Ages are mainly available from southeastern Ghana and the Kedougou-Kéniéba Inlier with only a few ages from southeastern Liberia and western Burkina Faso.

On the basis of the ages given in figure 18 it might be argued that Ghana in the southeastern corner of the Baoulé Mossi domain cooled later compared to the Kedougou-Kéniéba Inlier in the northwest. In southeastern Ghana, K-Ar muscovite and biotite cooling ages around 1920-1900 Ma have been obtained from a two-mica granite and pegmatite by Chalokwu et al. (1997), while in the Kedougou-Kéniéba Inlier, the youngest cooling age is dated to 2022±12 Ma ($^{40}Ar/^{39}Ar$) by Gueye et al. (2007) on muscovite from an episyenite.

However, the significance of this difference can be questioned considering the scarcity of available cooling ages and the fact that the ages that are available have been obtained by different workers in different regions using different methods. Also, as shown by the detailed study of Rosa Costa et al. (2009) from the Archean Amapá block and adjacent Birimian crust in the southeastern Guyana shield (fig. 4), the cooling history at the end of the Birimian event may vary between terranes within relatively restricted areas (<100 km). The lack of younger cooling ages in northwestern Baoulé Mossi may therefore be real but only reflecting local — instead of regional — variations.

With that said, younger ages in the southeastern part of the Baoulé Mossi domain would not be unexpected considering the presence of late magmatism in that region expressed by the 2029±22 (TIMS on titanite) age obtained by Delor et al. (2004) on diamond-bearing autoclastic tuffisite dykes from the Cape Coast basin in southeastern Ghana (fig. 7) or the 1985±4 Ma (Pb-Pb on zircon) Caxias microtonalite in the São Luís Craton (Klein et al. 2002). In addition, Onstott et al. (1984) obtained $^{40}Ar/^{39}Ar$ ages of 1964±2 and 1894±2 on amphibole and biotite, respectively, from amphibolites in southeastern Liberia close to the contact between the Man and Baoulé Mossi domains. As in southeastern Ghana, this area was also proximal to late magmatic activity during the Birimian event (e.g. Kouamelan et al. 1997; Cocherie et al. 1998; Thiéblemont et al. 2001).

5 The Birimian event in a global context

As the discussion in the previous section have focused largely on the relationship and geodynamic setting of Birimian crust in the WAC and Amazon Craton there is a need to place these cratons within a global context that looks at their relationship with other cratons or orogenic belts in Africa, South America, Europe and elsewhere within the framework of global plate tectonics. This will provide to a deeper understanding of the Birmian event and how it may relate to the events during the Paleoproterozoic, including the assembly of the supercontinent Columbia (Rogers & Santosh 2002; Zhao et al. 2004), the oxygenation of the atmosphere (Canfield 2005; Holland 2006) and the positive $\delta^{13}C$ excursion during the Rhyacian Lomagundi-Jatuli Event (Karhu & Holland 1996; Melezhik et al. 2013).

5.1 Regional trends during assembly of Atlantica-Midgardia

When considered in the context of the Archean and Paleoproterozoic evolution of the proposed Atlantica (Rogers 1996) and Midgardia (Johansson 2009) paleocontinents (figures 3 and 4) it can be seen that the circa 2.35-2.05 Ga crust formed during the Birimian event in the WAC, Amazon Craton and São Luís Craton is among the oldest from the Proterozoic. Juvenile crust of equivalent age is also present in other cratons and mobile belts in South America, such as the São Francisco Craton and the Rio de la Plata Craton (Cordani & Teixeira 2007; Brito Neves 2011). Crust of this age is also found in the East European Craton (Bogdanova et al. 2008). However, it appears to be less common in other African cratons and mobile belts where magmatic activity when present is usually comprised of crustal reworking (Neves 2011), such as 2.3 Ga

syenites from Gabon in northwestern Congo Craton (Tchameni et al. 2001).

The relationship between the early (Siderian to Rhyacian) and later (Orosirian) crust is most evident in the Midgardia configuration of Johansson (2009) which is based on the relative position of the constituent cratons during the Paleoproterozoic. Here, the Siderian to Rhyacian crust, together with amalgamated Archean cratons, act as a nucleus to younger Paleoproterozoic (<2.05 Ga) accretionary orogens (fig. 4). Fraga et al. (2009b) proposed that the collision between Archean and Birimian crust in the Guyana shield caused a switch in subduction at circa 2.00 Ga leading to the development of an accretionary orogen running along the margin of the recently amalgamated Archean and Birimian crust in the Amazon Craton.

A similar switch in orientation of orogenic belts also occurred in Sarmatia in the East European Craton (Bogdanova et al. 2008, and references therein). Here, north-south (present day orientation) orientated 2.2-2.0 Ga belts forming sutures between Archean crustal domains changes into a northeast-southwest oriented 2.0-1.95 Ga accretionary orogen developed on the margin of the amalgamated Archean and Birimian crust in Sarmatia. According to Bogdanova et al. (2008), this belt also extends further northeast along the margin of northwestern Volgo-Uralia which was sutured with Sarmatia around 2.05 Ga.

The above mentioned orogens developed in an "outboard" position relative to the "inboard" Rhyacian to Siderian accretionary orogens in the WAC and Amazon Craton developed during the Birimian event. The transition between the Rhyacian and Orosirian periods at circa 2.05 Ga appears to be an important crossover point where magmatic activity ceased within the Siderian-Rhyacian nucleus but began in the outboard orogens.

5.2 Atlantica-Midgardia — analogous to Gondwana?

The Birimian event, and in extension the Paleo- to Mesoproterozoic evolution of the Atlantica-Midgardia paleocontinent, appear to be similar to the assembly of Gondwana during the early Cambrian with the subsequent development of the Terra Australis accretionary orogen (fig. 23) outboard to that continent (Cawood & Buchan 2007). Cawood and Buchan (2007) argued that termination of subduction zones during the assembly of Gondwana would have required the initiation of new subduction zones elsewhere in order to maintain the constant radius of the Earth. The Terra Australis accretionary orogen would in that case have been a response to the assembly of Gondwana and the closure of subduction zones located between the amalgamated continents which it came to be formed of; now marked by the Pan-African-Brasiliano, East African and Kuunga orogens (fig. 23).

5.3 Is the Birimian event equivalent to the East African Orogen?

The East African Orogen (EAO) formed during the Neoproterozoic Pan-African orogenic cycle as a suture between the cratons and orogenic belts of proto-West and East Gondwana to form the "Greater Gondwana" continent (Stern 1994; Johnson et al. 2011; Fritz et al. 2013). Current exposures of the EAO stretch from Egypt and Saudi-Arabia in the north to Mozambique and Zambia in the south. Parts of the EAO are also preserved in Madagascar, western India and Antarctica. The orogen has a total length of more than 6000 km with a width commonly exceeding a 1000 km. The EAO can be divided into a northern and southern part corresponding to the Arabian-Nubian Shield (ANS) and Mozambique belt (MB), respectively (fig. 23). The ANS is composed of low-grade juvenile crust formed from amalgamated arc terranes. In contrast, the MB is contains more evolved crust metamorphosed at granulite-facies conditions during a continent-continent collision.

The juvenile crust of the ANS formed as island arcs in the Mozambique Ocean, which opened following the breakup of Rodinia around 0.9 Ga (Stern 1994; Stern et al. 2010; Johnson et al. 2011). The Mozambique Ocean was progressively closed between 800-630 Ma leading to the amalgamation of these island arcs to form a progressively larger mass of juvenile crust. This amalgamation culminated with the 680-640 Ma Nabitah Orogeny during which the core of the juvenile crust in the ANS was finally assembled (Johnson et al. 2011). As the Mozambique Ocean finally closed around 630 Ma the juvenile crust of the ANS was caught between rigid crustal blocks belonging to proto-West and East Gondwana (fig. 23), initiating the final phase of the EAO.

During the final phase of the EAO, lasting between 650-540 Ma (Johnson et al. 2011; Fritz et al. 2013), convergence between the continents of proto-West and East Gondwana led to the development of a continent-continent collision in the MB (Stern 1994; Johnson et al. 2011; Fritz et al. 2013) with nappe-stacking and granulite-facies metamorphism. The convergence simultaneously triggered lateral escape in the juvenile crust of the ANS which was subjected to orogen-parallel extension as it moved towards an oceanic free-face in the north (fig. 23). The uneven distribution of juvenile crust between the ANS and MB likely reflect a smaller oceanic basin in the south which may be the result of a hinge-like opening an closure of the Mozambique Ocean during dispersal of Rodinia and subsequent assembly of Gondwana (Hoffman 1991; Johnson et al. 2011).

The geodynamic evolution of the ANS during the final phase of the EAO was characterized by the development extensive shear zones, formation of marine and terrestrial sedimentary basins, uplift of middle crustal gneisses in domes and belts and a transition from dominantly sodic to increasingly alkalic intrusive

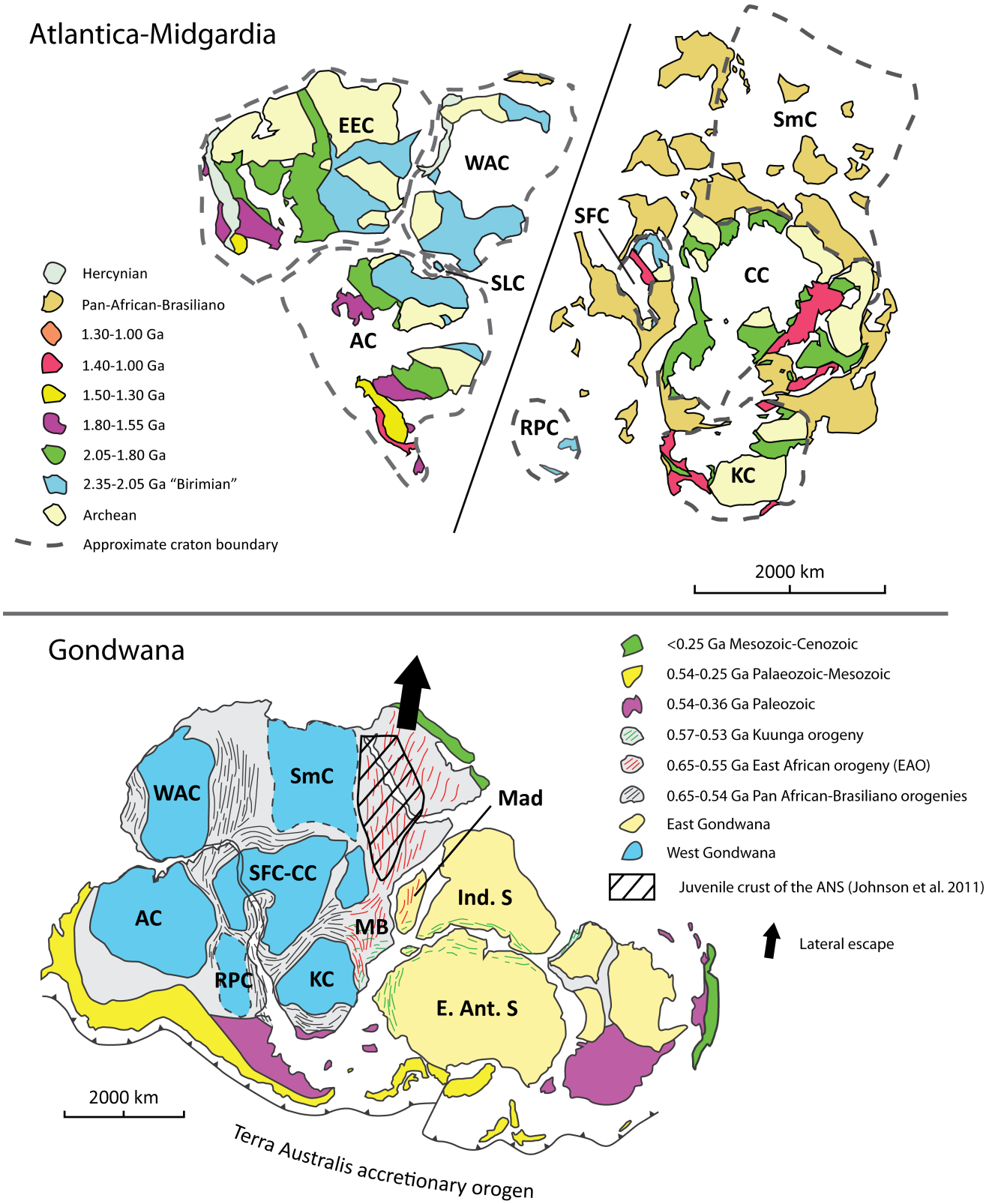

Fig. 23. Schematic tectonic maps of Atlantica-Midgardia and Gondwana. Atlantic-Midgardia map after references given in figures 3 and 4. The WAC, EEC and AC are shown in the Midgardia configuration of Johansson (2009). Due to the lack of paleogeographic data for other cratons in Africa and South America these are shown in their present-day relative positions but displaced relative to the Midgardia-block. Gondwana map redrawn after Gray et al. (2007) with modifications by Meert & Lieberman (2008). Ages for the East African, Kuunga and Proterozoic orogens refer to the timing of peak collisional tectonics. Ages after Villeneuve & Cornée (1994), Abdelsalam et al. (2002), Liégeois et al. (2003) and Johnson et al. (2011). The solid black arrow shows the general direction of lateral escape of crust in the EAO during collision between proto-West and East Gondwana. Abbreviations; **ANS** - Arabian-Nubian Shield, **MB** - Mozambique Belt, **Mad** - Madagascar, **Ind. S** - Indian Shield, **E Ant. S** - East Antarctic Shield. For others, see figures 3 and 4. Terra Australis accretionary orogen after Cawood & Buchan (2007).

magmatism (Johnson et al. 2011). Throughout this period the ANS was subjected to alternating compression and extension which caused inversion and uplift of sedimentary basins and controlled the formation of gneiss domes and belts.

The Birimian crust of the WAC (and its extension into the Maroni-Itacaiunas province of the Amazon Craton, fig. 4) has many similarities with the EAO, including timing of tectonothermal and magmatic activity as well as the presence of a vast area of juvenile crust. Together with the broad similarities between the assembly of Atlantica-Midgardia and Gondwana it is tempting to place the Birimian event in the WAC and Amazon Craton in the same position as the EAO assumed during the assembly of Gondwana. In the same way as the ANS formed through the accretion of juvenile arc terranes in the Mozambique Ocean separating West and East Gondwana the juvenile Birimian crust may have formed in a large ocean separating the continental blocks which came to form the western and eastern parts of the Atlantica-Midgardia paleocontinent (relative to the Birmian crust in the WAC and Amazon Craton).

The western parts would in that case be comprised of continents made up of the Archean crust in the Reguibat shield, Volgo-Uralia, Sarmatia, Man domain and Imataca complex (fig. 4). Meanwhile, the eastern part would be comprised of continents now preserved as Archean crust in the São Francisco-Congo Craton and Saharan Metacraton (fig. 23). The position of the Rio de la Plata Craton is unclear, but since it contains Rhyacian crust (2.20-2.05 Ga, Oyhantçabal et al. 2011) it seems reasonable that it should be positioned close to the WAC and the Amazon Craton.

Much as the assembly of Gondwana was comprised of multiple temporally overlapping orogens (Meert & Lieberman 2008; Fritz et al. 2013) a similar development may also be envisioned for the formation of the Atlantica-Midgardia continent, which continued to grow after the end of activity in the WAC. The Tanzania Craton (now in the eastern portion of the Congo Craton, see figure 3) was accreted against the "proto-Congo Craton" at 2.0-1.9 Ga (Hanson 2003; De Waele et al. 2008; Fernandez-Alonso et al. 2012). Since the Congo Craton and the São Francisco Craton remained connected until the breakup of Pangea and the opening of the Atlantic (Torquato & Cordani 1981; Trompette 1994; Fernandez-Alonso et al. 2012) there is a "temporal bridge" between the dominantly Siderian to early Orosirian (2.35-2.00 Ga) tectonothermal and magmatic activity in the São Francisco Craton (e.g. Rosa Sexias et al. 2012; Santos-Pinto et al. 2012) and the partially overlapping Orosirian (2.10-1.95 Ga) activity associated with accretion of the Tanzania Craton (Hanson 2003; De Waele et al. 2008). The temporal and spatial distribution of magmatic activity seen among cratons of Atlantica-Midgardia is thus similar to the overlapping ages among Pan-African-Brasiliano-Kuungan orogenic belts during the assembly of Gondwana (fig. 23).

5.4 Atlantica-Midgardia in relation to other Paleoproterozoic continents

The above discussion has only concerned the cratons which have traditionally been considered part of Atlantica (in addition Sarmatia and Volgo-Uralia in the East European Craton, fig. 4). This section will therefore be devoted to briefly examine the configuration and geodynamic setting of other paleocontinents that have been proposed to exist during the Paleoproterozoic.

The following discussion will use the three paleocontinental configurations Nena, Atlantica and Ur as a starting point. These are the Precambrian paleocontinents envisioned by Rogers (1996) and subsequently used by Rogers and Santosh (2002) as the three main constituent blocks in their reconstruction of the Paleo- to Mesoproterozoic supercontinent Columbia (fig. 24a).

5.4.1 Geological vs. paleomagnetic fits

It is necessary at this point to comment on the reasons for using the Nena, Atlantica and Ur configurations in the following discussion. These configurations where constructed using correlatable orogens or supracrustal units of different continental blocks (Rogers 1996). However, the use of only geological fits in paleogeographic reconstructions has been criticized because such fits are non-unique. Instead, the use of paleomagnetic data together with magmatic barcodes from Large Igneous Provinces are considered as a more reliable methods for paleogeographical reconstructions, capable of yielding unique fits between now separate continental blocks (e.g. Li et al. 2008; Ernst & Bleeker 2010).

Even though geological fits may not be suitable for reconstructing the exact position of different continental blocks relative to each other in deep time, they can nevertheless be used to identify continental blocks that share a common geological history during a specified time period. In essence, geological and paleomagnetic fits thus work on two different levels of detail. The two approaches differ in that the geological approach is only capable of making broad and qualitative reconstructions while those derived from the paleomagnetic approach are more detailed and quantitative.

The two approaches (i.e. geological and paleomagnetic fits) may be compared with solving a puzzle — which depicts a scene comprised of a number of different components, e.g. a forest, a house and a lake — either by fitting all the pieces together one by one (the paleomagnetic approach) or by sorting the pieces based on their colors and patterns (the geological approach). While the paleomagnetic approach is obviously capable of solving the puzzle, it nevertheless requires information regarding how all the pieces relate to each other — which may be a time-consuming and challenging task to acquire. On the other hand,

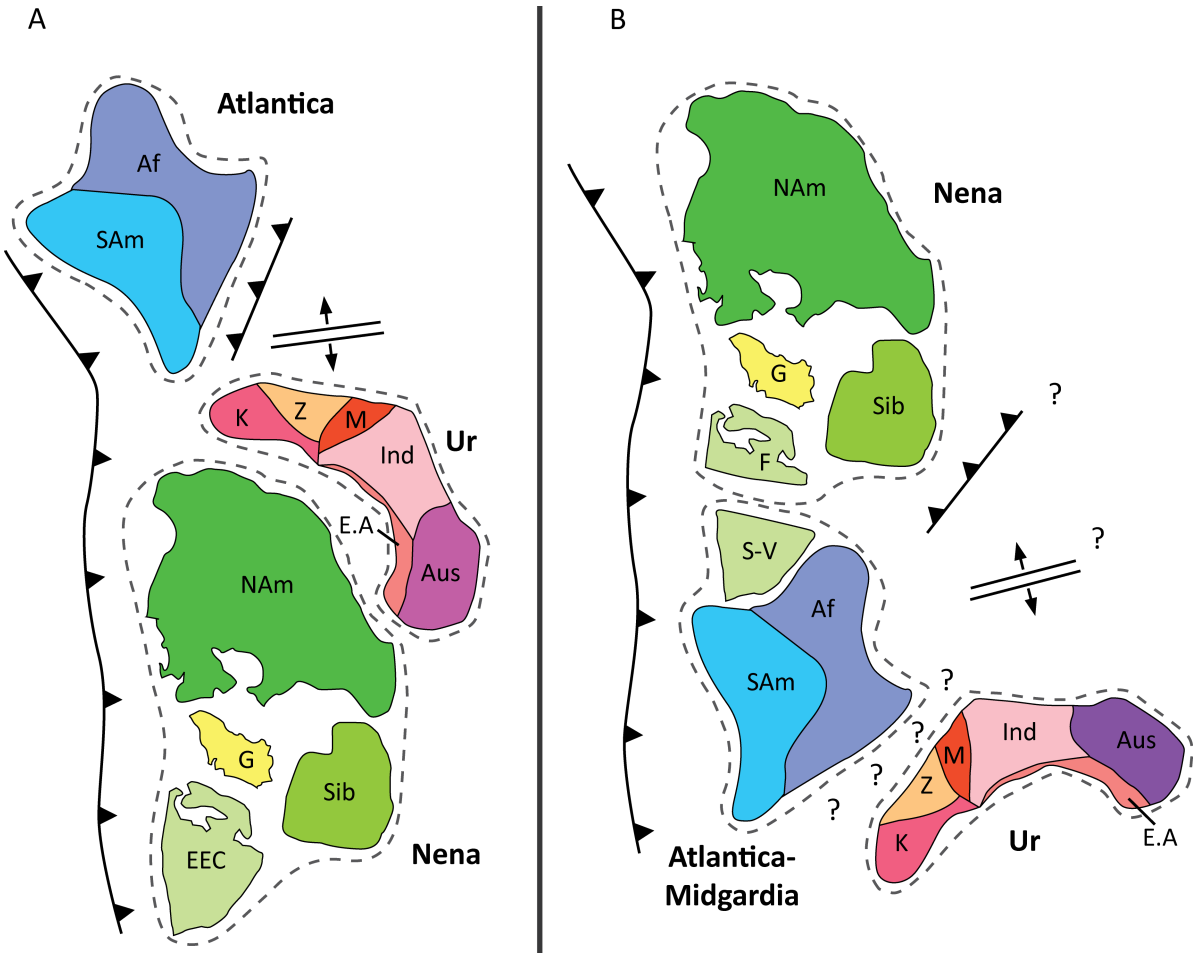

Fig. 24. **A)** The original Columbia configuration of Rogers & Santosh (2002). Redrawn with minor modifications. **B)** A proposed alternative Columbia configuration which incorporates the SAMBA-configuration of Johansson (2009) and places Ur next to Atlantica-Midgardia. See text for further discussion. Abbreviations: **Af** - Africa; **SAm** - South America; **NAm** - North America; **G** - Greenland; **EEC** - East European Craton; **Sib** - Siberian Craton; **K** - Kaapvaal; **Z** - Zimbabwe; **M** - Madagaskar; **Ind** - India; **Aus** - Australia; **E.A** - East Antarctica; **F** - Fennoscandia; **S-V** - Sarmatia–Volgo-Uralia.

while the geological approach cannot solve the puzzle by itself, it can be used to make a broad reconstruction of the scene that it depicts — by assigning the pieces to its different components based on their colors and patterns. As some pieces will undoubtedly contain parts of two or more components, it will also be possible to determine how the different components relate to each other. Unlike the paleomagnetic approach, the geological approach does not require that any pieces of the puzzle are actually put together.

Even though the geological approach is not capable of solving the puzzle by itself, it can nevertheless provide a rough image of how it looks. It represents a more ”quick and dirty” method compared with the paleomagnetic approach. However, the two approaches are not mutually exclusive. Indeed, the true potential instead lies in combining them by using the geological approach to identify broad patterns of the puzzle while the paleomagnetic approach can then be used to fit the pieces together in a more exact position.

The following discussion will be based on a geological approach. The focus will therefore lie on the geodynamic setting (accretionary orogenic, collisional orogenic, extensional or passive) recorded over time by the various continental blocks that comprised Nena, Ur and Atlantica. In this context, the exact paleogeographical configurations of the different blocks that comprise Nena, Ur and Atlantica is of secondary importance. These paleocontinental configurations will instead be considered as groups of continental blocks that share a common geological history (regarding timing of accretionary and collisional orogenies, or rifting) during the Paleoproterozoic. Since the Nena, Ur and Atlantica configurations of Rogers (1996) are based on geological data (as opposed to paleomagnetic) they are well suited for the discussion in the following sections.

While the position of certain blocks within Nena, Ur and Atlantica may prove to be incorrect, it is not central to the following discussion. As long as these blocks share a common geological history they will nevertheless still belong to the same group of continental blocks (i.e. Nena, Ur or Atlantica). The relative position of continental blocks within these configurations — as depicted in the figures within this text — should be viewed only as possible configurations. The important aspect is instead the behaviour and position of Nena, Ur and Atlantica among themselves

and relative to each other.

Some modifications to the Nena, Ur and Atlantica configurations are required to account for new data that has emerged since the work of Rogers (1996) and Rogers and Santosh (2002). This primarily concerns the separate early Paleoproterozoic history of Fennoscandia and Sarmatia–Volgo-Uralia in the East European Craton (Bogdanova et al. 2008), the SAMBA configuration of Johansson (2009, see section 2.1.2) and the different geological history of the Precambrian Cratons of Australia (Payne et al. 2009). This will be discussed further in the sections below.

In the following three sections, the Paleoproterozoic history of continental blocks within Nena, Ur and Atlantica will be outlined briefly. The purpose of the following discussion is not to make a detailed and exhaustive review of the geological history of the various blocks that are included in these configurations. The purpose is instead to highlight broad differences and similarities between the paleocontinents in terms of the geodynamic setting that defined them through the Paleoproterozoic.

5.4.2 Nena

Nena, as used by Rogers and Santosh (2002), include the Archean and Proterozoic crust now present in North America, Greenland, Siberian Craton and the East European Craton (fig. 24a). However, the inclusion of the East European Craton should be revised to only include Fennoscandia as Sarmatia and Volgo-Uralia instead formed a part of Atlantica-Midgardia (see section 2.1.2 and below) until 1.8-1.7 Ga (Bogdanova et al. 2008; Johansson 2009).

During the early Paleoproterozoic (circa 2.45-2.00 Ga), Archean crust in the above regions was characterized by rifting and continental breakup as recorded by deposition of passive margin sequences and/or intrusion of diabase dike swarms in North America (Aspler & Chiarenzelli 1998; Whitmeyer & Karlstrom 2007; Ernst & Bleeker 2010), Greenland (Lahtinen et al. 2008; Nilsson et al. 2013), Fennoscandia (Bogdanova et al. 2008; Lahtinen et al. 2008) and the Siberian Craton (Rosen et al. 1994; Urmantseva & Turkina 2009). The Archean crust was subsequently amalgamated along extensive circa 2.10-1.80 Ga accretionary orogenic belts which are present in all regions (see above references). Both the North Australian Craton and the Proterozoic Mawson Continent (including the Gawler Craton in Australia and the Adélie Craton in Antarctica) record tectonothermal, magmatic and depositional inactivity during the early Paleoproterozoic that was followed by rifting and sedimentation (Payne et al. 2009). These continental blocks have been linked with crust in Laurentia because of their correlative Archean and Paleoproterozoic history (e.g. Zhao et al. 2004; Payne et al. 2009) and may therefore also be considered as part of Nena rather than Ur as proposed by Rogers and Santosh (2002).

5.4.3 Atlantica

The Atlantica paleocontinent of Rogers and Santosh (2002) contain the blocks outlined in section 2.1.2 but should also include the Sarmatia and Volgo-Uralia blocks of the East European Craton, a configuration that is from here on referred to as Atlantica-Midgardia. As discussed above, this paleocontinent was amalgamated along circa 2.35-1.95 Ga orogens. This was followed by development of accretionary orogens outboard to this paleocontinent, which remained active from circa 2.0 Ga and through the Paleo- and Mesoproterozoic.

5.4.4 Ur

As envisioned by Rogers (1996) and Rogers and Santosh (2002) the paleocontinental configuration of Ur contains Archean and Proterozoic crust now found in the Kalahari craton, Madagascar, India, Australia and the coastal regions of East Antarctica (fig. 24a). As discussed in section 5.3.1, the North Australian Craton and the Mawson Continent are here considered as part of Nena, leaving the West Australian Craton as part of Ur.

Rhyacian and early Orosirian (2.2-2.0 Ga) accretionary and collisional orogenic activity is recorded in both the Kheis-Okwa-Magondi belt and Limpopo belt of the Kalahari Craton (Hanson 2003; Master et al. 2010) as well as in the Ophthalmian and Glenburgh orogenies in the Capricorn orogen of the West Australia Craton (Johnson et al. 2011). The Ophthalmian orogeny records an accretionary stage between circa 2.23-2.14 Ga that was followed by the Glenburgh orogeny around 2.00-1.95 Ga, during which the Yilgarn and Pilbara blocks were accreted.

Mikhalsky et al. (2010) proposed that the Ruker Province currently exposed in the southern Prince Charles Mountains of East Antarctica may be correlative with the Capricorn orogen of Western Australia, based on the similarities between Archean and Paleoproterozoic rocks in these regions. In India, Mahonty (2013) also proposed that the Satpura belt (Central Indian Tectonic Zone) was involved in a collisional orogen at circa 2.2-2.1 Ga, which might also be correlated with the Capricorn orogen. Madagascar appears to be the only region which does not record any significant activity before 2.0 Ga. All the constituent continental blocks of Ur record magmatic and tectonothermal activity during the later part of the Paleoproterozoic (Orosirian-Statherian).

5.5 Supercontinent cycles and iterations

5.5.1 Proterozoic and Phanerozoic supercontinent cycles

The review in section 5.4 is admittedly brief but its main purpose is to highlight the general Paleoproterozoic history of the paleocontinents Nena, Atlantica-Midgardia and Ur (fig. 24) and to illustrate the contrasting history between Nena on one hand and that of

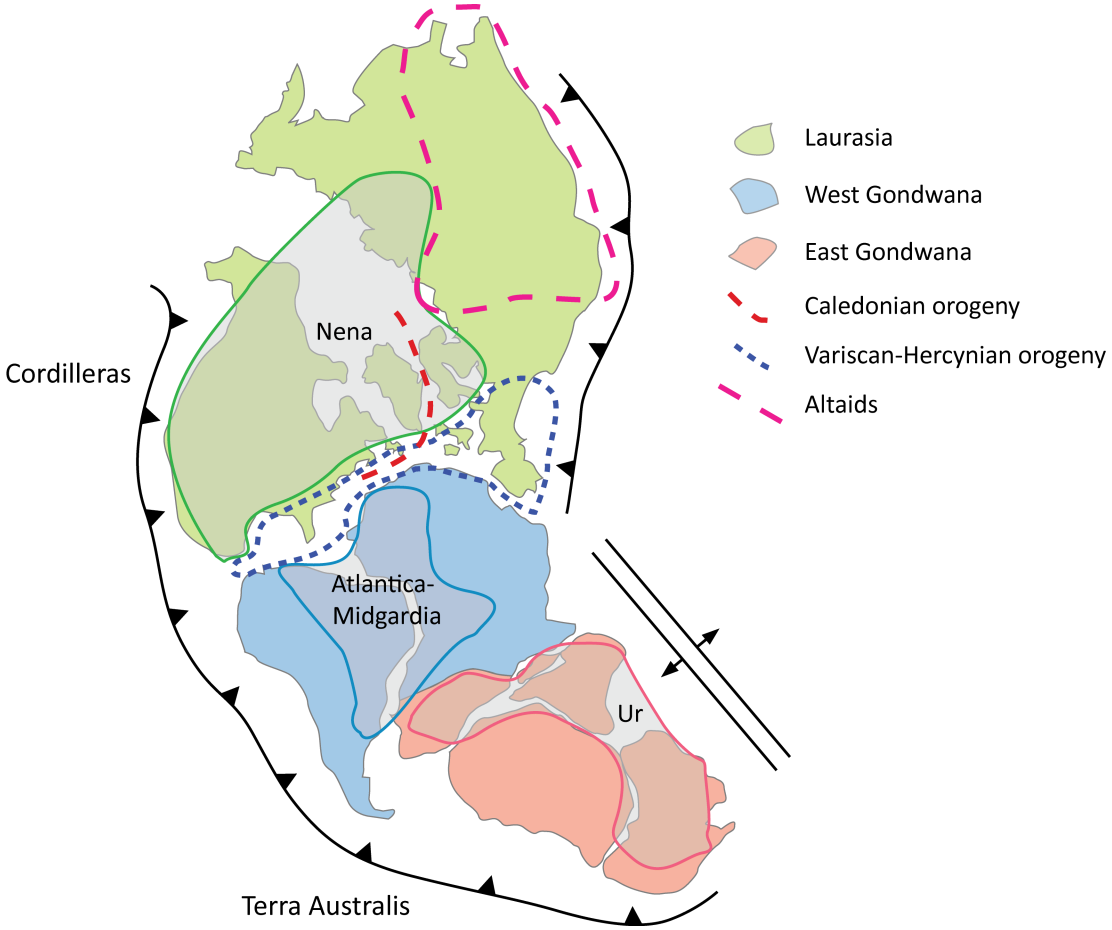

Fig. 25. Position of Nena, Atlantica-Midgardia and Ur within Pangea. Redrawn after Rogers & Santosh (2002) with modifications to show the approximate extent of the Caledonide and Variscan-Hercynian orogenies (Nance et al. 2010; Stampfli et al. 2013) as well as the Altaids (Wilhelm et al. 2012). Notice how Nena, Atlantica-Midgardia and Ur each form part of Laurasia, West Gondwana and East Gondwana (Rogers & Santosh 2002) in the same relative position as they do in the proposed Columbia configuration in figure 24b.

Atlantica-Midgardia-Ur on the other — following a geological approach, as described in section 5.4.1.

While the constituent blocks of Nena are characterized by inactivity, rifting and sedimentation during the early Paleoproterozoic (2.45-2.00 Ga), the regions within Atlantica-Midgardia and Ur are instead characterized by accretion and amalgamation of Archean cratons along with Paleoproterozoic crust. This diachronous behavior was recognized by Aspler and Chiarenzelli (1998) who noted that the WAC, Amazon, São Francisco and Congo cratons amalgamated at the same time as most of the cratons on the current northern hemisphere (i.e. Nena) were in the process of breaking up. After ca 2.0 Ga, all continents record accretion. However, while accretion in Nena involves amalgamation of Archean cratons (as it did for Atlantica-Midgardia and Ur before 2.0 Ga) this is not the case for Atlantica-Midgardia, which is instead characterized by long-lived orogens which did not involve accretion of Archean crust, as can be seen in the Amazon Craton (Cordani & Teixeira 2007).

Given the similarities between Atlantica-Midgardia and Gondwana outlined in section 5.2, it is interesting to note that the relationship between Atlantica-Midgardia and Nena (i.e. assembly vs. dispersal) is analogous to that between the assembly of Gondwana in the Neoproterozoic-early Paleozoic and the simultaneous rifting of Laurentia (North America and Greenland in Nena) and the East European Craton from the WAC and Amazon Craton, which took place during the final stages of Rodinia breakup (e.g. Johansson 2009; Nance et al. 2010; Stampfli et al. 2013). This led to the opening of the Iapetus and Rheic oceans and dispersal of Laurentia and the East European Craton as the WAC and Amazon Craton remained to form part of West Gondwana.

Following the assembly of Gondwana (fig. 25) by circa 600-500 Ma (e.g. Meert & Lieberman 2008; Fritz et al. 2013) the Iapetus Ocean closed during the circa 420 Ma Caledonian orogeny when Laurentia and the East European Craton joined to form Laurussia (fig. 25, Nance et al. 2010; Stampfli et al. 2013). The Rheic ocean closed during the circa 300 Ma Variscan-Hercynian orogeny when Laurussia merged with the WAC and Amazon Craton in West Gondwana. This also coincided with the final assembly of the Altaids in the Central Asian Orogenic Belt when multiple terranes and microcontinents, including the Siberian Craton, were accreted against the East European Craton in Laurussia (Şengör et al. 1993; Wilhelm et al. 2012).

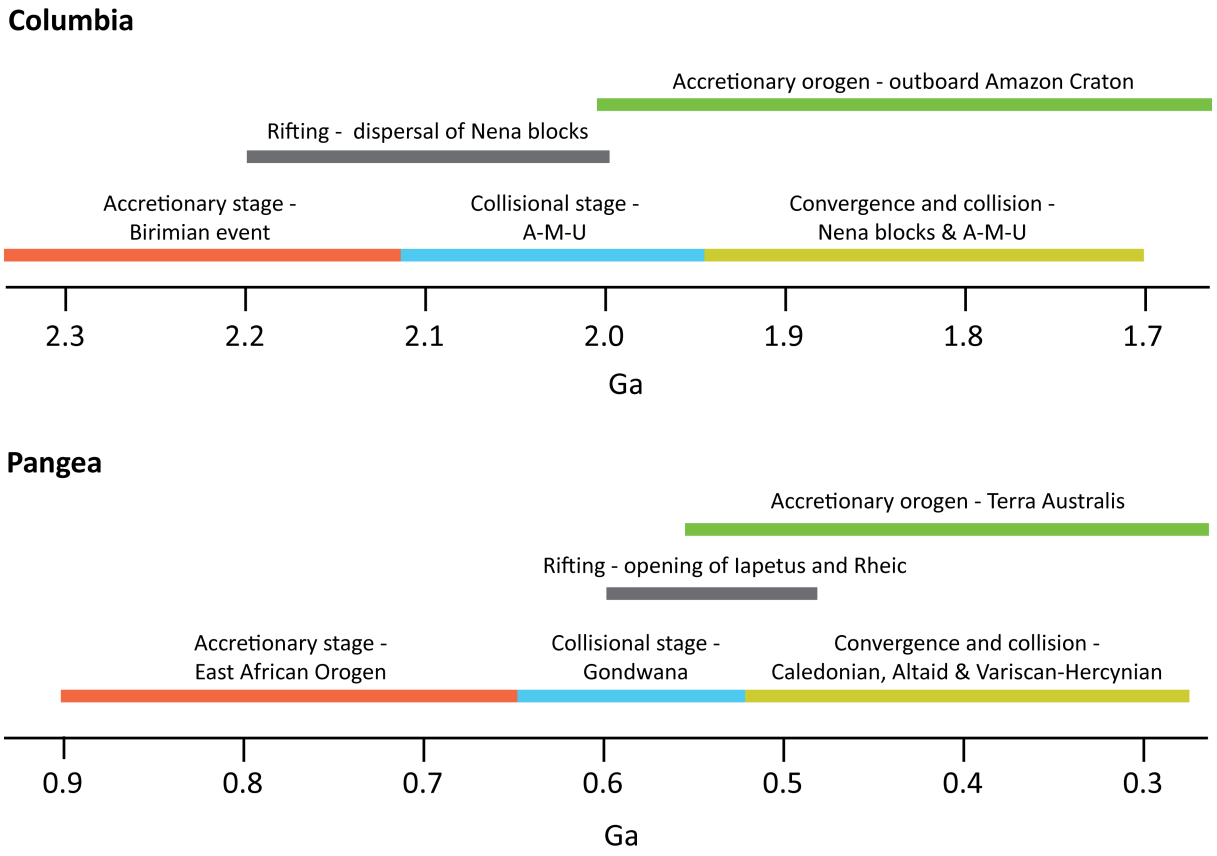

Fig. 26. Comparison of the temporal extent of tectonic events on different paleocontinents during the assembly of Columbia and Pangea. Timing of events related to the assembly of Columbia as discussed in the text. Accretionary stage of the EAO and collisional stage of Gondwana after Meert & Lieberman (2008), Johnson et al. (2011) and Fritz et al. (2013). Convergence and collision in Laurasia after Nance et al. (2010), Wilhelm et al. (2012) and Stampfli et al. (2013). Rifting and opening of Iapetus and Rheic oceans after Nance et al. (2010). Terra Australis accretionary orogen after Cawood & Buchan (2007).

Together, the Variscan-Hercynian orogeny and assembly of the Altaids ultimately led to the formation of the supercontinent Pangea (fig. 25).

It could be argued that the assembly of Columbia shares many similarities with the assembly of Pangea, assuming that North America (Laurentia) was connected with the Atlantica-Midgardia continent as proposed in the SAMBA-configuration (fig. 24b). The above sequence of events, starting with the opening of the Iapetus Ocean, would thus be comparable with rifting and dispersal of the Archean crust within Nena around 2.0 Ga even as Atlantica-Midgardia was in the process of being amalgamated. Subsequent assembly of Archean cratons in Nena between 2.1-1.8 Ga would be comparable with the Caledonian-Variscan-Hercynian-Altaid orogenies. The collision between Fennoscandia and Volgo-Uralia–Sarmatia around 1.8-1.7 Ga (Bogdanova et al. 2008) would by analogy correspond to the point when Columbia reached maximum packing by docking of Nena and Atlantica-Midgardia (including Ur, see discussion below). However, this would be some 200-50 Myr later than the timing (1.90-1.85 Ga) of maximum packing for Columbia proposed by Rogers and Santosh (2009).

It is interesting to note that circa 2.05 Ga bimodal magmatism, comprised of granites and dolerite dikes, is recorded in the Birmian basement of the Anti-Atlas inliers along the northern margin of the WAC (fig. 1; Walsh et al. 2002; Kouyaté et al. 2013). Kouyaté et al. (2013) proposed that this period of magmatism may have been triggered by a mantle plume associated with the breakup of an Archean continent. The authors noted that dikes of comparable age to those found in the Anti-Atlas inliers are present in the North Atlantic Craton in Greenland (Nilsson et al. 2013) as well as the Superior Craton in North America (Ernst & Bleeker 2010) and suggested that these areas may have been connected around 2.05 Ga. Breakup at this time, as record by the dolerites and granites, could perhaps be related to the opening of an ocean equivalent to the Neoproterozoic Iapetus Ocean — Nena being equivalent to Laurentia and the East European Craton while the WAC would be equivalent to West Gondwana, as discussed above.

The preceding discussion has largely omitted Ur and focused on Atlantica-Midgardia and Nena, leaving the question of where this continent should be located in a Columbia-configuration unanswered. In their original configuration of the supercontinent Columbia, Rogers and Santosh (2002) placed Ur next to the current western margin of North America (fig. 24a), which is also the position it has been given in other Columbia reconstructions (e.g. Zhao et al. 2004; Rogers & Santosh 2009). Nevertheless, considering

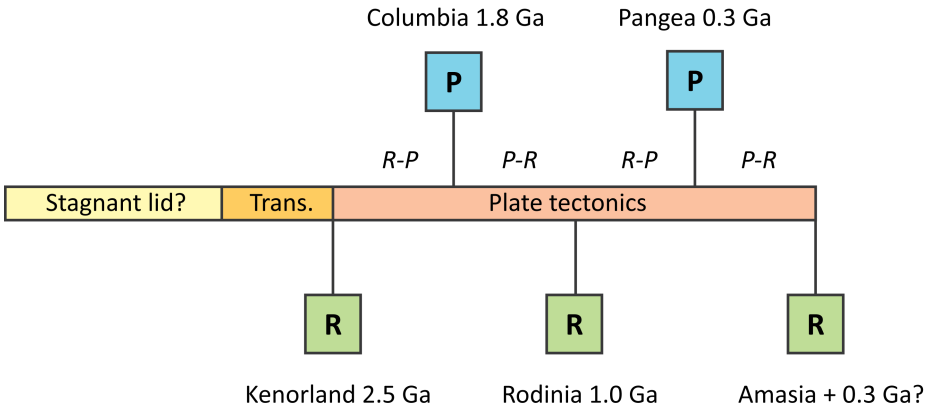

Fig. 27. Conceptual diagram showing the evolution from stagnant lid to plate tectonics and the timing of Pangea- (P) and Rodinia- (R) type supercontinents. As discussed in the text, the transition from plume to plate tectonics may have ended with the assembly of a first supercontinent in the late Archean, here called Kenorland after Williams et al. (1991). This was a Rodinia-type supercontinent and was followed by assembly of the first Pangea-type supercontinent — Columbia (Rogers & Santosh 2002) — during the first supercontinent cycle. The subsequent supercontinent cycle led to the formation of new iterations of the Pangea- and Rodinia-type supercontinents with the assembly of Rodinia (Li et al. 2008) and Pangea (Stampfli et al. 2013). In this model, the next supercontinent Amasia (Yoshida & Santosh 2011) should be a Rodinia-type. Supercontinent cycles alternate between going from Rodinia- to Pangea-type supercontinents (R-P) and vice versa (P-R).

the similarity in timing of orogenic activity in continental blocks from Ur and Atlantica-Midgardia it is here proposed that Ur should instead be placed adjacent to Atlantic-Midgardia, with the implication that these continents were assembled together (fig. 24b). Atlantica-Midgardia and Ur may in such a case be considered as two parts of the same continent.

Because of the long-lived accretionary margin that developed outboard to the Amazon Craton, it would seem reasonable to place Ur on the opposite side of Atlantica-Midgardia, next to the Congo Craton and Saharan Metacraton. Following the analogy between Atlantic-Midgardia and Gondwana, Ur should therefore be an equivalent of East Gondwana, whereas Atlantica-Midgardia is equivalent to West Gondwana. In the following text, this configuration will be referred to as Atlantica-Midgardia-Ur and will be considered as a Paleoproterozoic equivalent of Gondwana. However, it must be emphasized that this is a highly speculative fit based only on equivocal geological data and remains to be tested against robust paleomagnetic and more detailed geological data.

The positioning of Nena and Atlantica-Midgardia according to the SAMBA-configuration (Johansson 2009) — and with Ur next to Atlantica-Midgardia as shown in figure 24b — would be near identical to how their respective crustal blocks were positioned in Pangea (fig. 25). Rogers and Santosh (2002) noted that their reconstruction of Columbia had the same geometry as Pangea (cf. figures 24 and 25), with a long-lived subduction zone on one margin and the presence of both spreading centres and subduction zones on the other, along which a transfer of terranes took place. However, in the configuration by Rogers and Santosh (2002), the relative position of Nena, Ur and Atlantica differed between Columbia and Pangea (cf. figures 24a and 25).

In the configuration shown in figure 24b, the constituent blocks of these paleocontinents would have assumed the same relative position in Columbia as they did in Pangea. In addition, they would also have been assembled in the same order, beginning with Atlantica-Midgardia-Ur and Gondwana, respectively, as the continental blocks of Nena and Laurasia were dispersing. Subsequent assembly of these continents and their docking with Atlantica-Midgardia-Ur and Gondwana led to the formation of the supercontinents Columbia and Pangea, respectively. The assembly of Atlantica-Midgardia-Ur and Gondwana — as well as the dispersal and assembly of Nena and Laurasia — had more or less the same temporal extent (fig. 26).

If the above configuration is correct, it would mean that amalgamation of Columbia in the late Paleoproterozoic and Pangea in the late Paleozoic occurred on the same timescales and in the same relative sequence of events, were the involved crustal blocks largely assumed the same relative positions. This has several implications for supercontinent cycles, mantle dynamics and plate tectonics.

The model implies that supercontinent cycles, involving breakup of one supercontinent (following Meert 2012, a supercontinent contains at least 75% of the preserved continental crust at maximum packing) and the subsequent assembly of another, is far from a random process. Indeed, the similarities between Columbia and Pangea suggest that these supercontinents actually represent two iterations of a certain type of supercontinent, from here on referred to as Pangea-type (fig. 27). If both Columbia and Pangea represent one type, then it seem logical that Rodinia (e.g. Li et al. 2008) would represent another, perhaps together with a possible late Archean supercontinent (here referred to as Kenorland after Williams et al. 1991), as well as the proposed next supercontinent, Amasia (e.g. Yoshida & Santosh 2011). It is considered here that these supercontinents may represent three iterations of a supercontinent-type that differed from the Pangea-type (fig. 27). This assumption is largely based on the

different configuration of Rodinia compared with Pangea (e.g. Hoffman 1991; Li et al. 2008) and the unlikely situation that there might be a Pangea-type supercontinent which has formed twice in Earth's history but which is separated by three individually distinct supercontinents. In addition, it is also supported by the similar behaviour of $^{87}Sr/^{86}Sr$ and $\delta^{13}C$ in the Paleo- and Neoproterozoic (as will be discussed in the next section). This type of supercontinent will here be referred to as Rodinia-type supercontinents.

It follows from the recognition of two alternately occurring types of supercontinents — Pangea- and Rodinia-type — that supercontinent cycles will involve the breakup of a Rodinia-type and assembly of a Pangea-type supercontinent, or vice versa, in an alternating fashion (fig. 27). Together, two such cycles would record the full revolution from breakup to reassembly of the same type of supercontinent, be it a Rodinia- or Pangea-type. Possible connections between these types of supercontinent cycles and environmental perturbations throughout the Earth's history will be further explored in the next section.

5.5.2 Geochemical traces of supercontinent cycles

The oxygenation of Earth's atmosphere is believed by most workers to have been stepwise, involving both increases and decreases (e.g. Canfield 2005; Holland 2006; Campbell & Allen 2008; Bekker & Holland 2012; Partin et al. 2013). Two steps appear to have been of particular importance (fig. 28a). The first took place during the early Paleoproterozoic and is known as the Great Oxidation Event (GOE, Holland 2006; Och & Shields-Zhou 2012). It has been broadly constrained to about 2.5-2.0 Ga and corresponds to the period when Earth's atmosphere first became oxygenated, which was a significant shift from the anoxic conditions that prevailed in the Archean. The second step occurred during the late Neoproterozoic between circa 0.8 Ga to 0.5 Ga and has been referred to as both the Second Great Oxidation Event (Campbell & Squire 2010) and the Neoproterozoic Oxygenation Event (NOE, Och & Shields-Zhou 2012); the latter will be used in this text. The increase in the concentration of oxygen in the atmosphere was significantly larger during the NOE compared to the GOE and also coincided with the Cambrian explosion (Holland 2006; Campbell & Squire 2010; Och & Shields-Zhou 2012). The similarities between the biogeochemical cycling of elements such as C, Fe and P during the GOE and NOE have been interpreted as indicating that the fundamental causes for the rise in atmospheric oxygen were the same during both events (Papineau 2010).

Several explanations have been put forward to account for the rise of oxygen during the GOE and NOE. These include the emergence of oxygenic photosynthesis, changes in the redox state of volcanic gases or loss of hydrogen to space (Canfield 2005; Holland 2006; Bekker & Holland 2012; Kasting 2013). Of these, oxygenic photosynthesis is one of the most commonly evoked explanations for the rise in oxygen (e.g. Canfield 2005; Kasting 2013). Oxygen form as a product of photosynthesis — together with reduced carbon in the form organic matter — in the reversible reaction $CO_2+H_2O \leftrightarrow CH_2O + O_2$. An increase in oxygen thus requires that organic matter is removed from the atmosphere-ocean system (e.g. buried in sediment) to prevent it from back-reacting with oxygen (e.g. Des Marais 1994; Karhu & Holland 1996; Campbell & Squire 2010; Kasting 2013; Melezhik et al. 2013). Long-term burial of organic matter would be ultimately controlled by tectonic processes.

A review of the different hypotheses behind the rise of oxygen during the GOE and NOE is beyond both the scope and purpose of this section. The aim is instead to investigate possible connections between the oxygenation of the atmosphere-ocean system and the supercontinent cyclicity discussed in the previous section. The following discussion will therefore be based on the assumption that the GOE and NOE are linked to tectonic processes where burial of organic matter was an important factor.

The focus here will lie on the secular evolution of $^{87}Sr/^{86}Sr$ and $\delta^{13}C$ ($^{13}C/^{12}C$ of a sample relative to the V-PBD standard) in marine sedimentary carbonates. Since the Neoarchean, both $^{87}Sr/^{86}Sr$ and $\delta^{13}C$ are characterized by a fluctuating pattern with pronounced and long-lived peaks of the same magnitude recorded in both the Paleoproterozoic and the Neoproterozoic (fig. 28b). While the peak of the positive $\delta^{13}C$ excursions coincides with both the GOE and NOE, maximum $^{87}Sr/^{86}Sr$ occurs instead at the end of both events. In both occasions, $\delta^{13}C$ peak some 200 Myr prior to $^{87}Sr/^{86}Sr$. The smoother shapes of the Paleoproterozoic excursions reflect less abundant data from this period — coupled with poorer temporal constraints — compared with the Neoproterozoic (Shields & Viezer 2002; Melezhik et al. 2013).

The $^{87}Sr/^{86}Sr$ of marine carbonates is generally considered to reflect the relative importance of river runoff — controlled by chemical weathering of the continents — against mantle input, in turn controlled by alteration of oceanic crust (Shields 2007). Average river runoff is considered to have high $^{87}Sr/^{86}Sr$, reflecting the generally radiogenic composition of continental crust. However, this is only a maximum value as weathering of juvenile crust will give less radiogenic river runoff that would be closer to the unradiogenic $^{87}Sr/^{86}Sr$ of the mantle (Shields 2007; Spencer et al. 2013). The peaks of $^{87}Sr/^{86}Sr$ shown in figure 28b may thus reflect increased continental weathering, weathering of particularly radiogenic crust, decreasing mantle input, high levels of CO_2 in the atmosphere, or a combination of any or all of these factors (Shields 2007; Och & Shields-Zhou 2012). However, increased continental weathering appear to be the most widely evoked explanation.

Sustained burial of organic matter — which is enriched in ^{12}C and therefore have a negative $\delta^{13}C$ — through sedimentation is commonly invoked to ex-

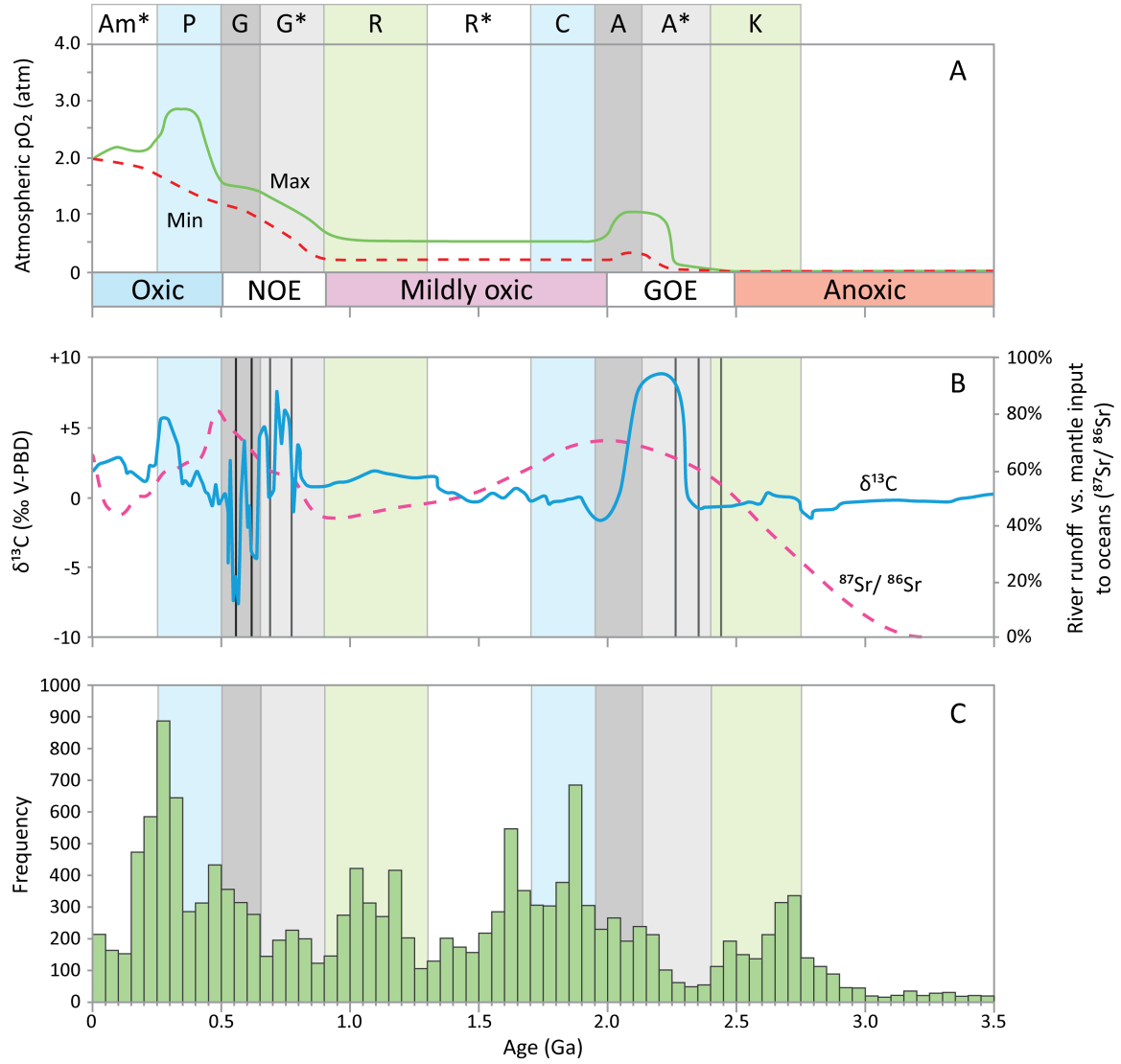

Fig. 28. **A)** Estimation of the maximum (solid green) and minimum (dashed red) pO_2 in the atmosphere during the past 3.5 Gyr. After Bekker & Holland (2012). Timing of Great Oxidation Event (GOE) and Neoproterozoic Oxygenation Event (NOE) after Och & Shields-Zhou (2012). **B)** $\delta^{13}C$ (solid blue) and $^{87}Sr/^{86}Sr$ (dashed purple) evolution of seawater. $\delta^{13}C$-curve after Campbell & Allen (2008) except the time interval between 2.5-1.9 Ga which is based on the "least-assumption" reconstruction of Melezhik et al. (2013). The $^{87}Sr/^{86}Sr$-curve is after Shields (2007) and shows the varying dominance of river runoff on the Sr-isotopic composition of seawater (increasing percentage) vs. mantle input. Vertical black lines mark Proterozoic glacial epochs. Timing of Neoproterozoic glacial epochs after Campbell & Allen (2008), Paleoproterozoic ditto after Hoffman (2013). **C)** Histogram of U-Pb zircon ages shown in 50 Myr bins. The ages are compiled from data in Campbell and Allen (2008) and Belousova et al. (2010) which have been derived primarily from detrital sources. The duration of different stages during supercontinent cycles are shown as vertical bars and include both assembly and maximum packing of supercontinents as well as intervening stages. Duration of Kenorland (K) after Campbell & Allen (2008), Accretionary stage (A*) and collisional stage (A) of Atlantica-Midgardia-Ur as discussed in section 5, Columbia assumed to have assembled by 1.7 Ga based on collision between Fennoscandia and Volgo-Uralia-Sarmatia (Bogdanova et al. 2008). Transitional period between Columbia and Rodinia marked as R*. Rodinia (R) after Li et al. (2008). Accretionary stage (G*) and collisional stage (G) of Gondwana after Meert & Lieberman (2008), Johnson et al. (2011) and Fritz et al. (2013). Pangea after Nance et al. (2010) and Stampfli et al. (2013). Transition period from breakup of Pangea until present marked as Am*.

plain the positive $\delta^{13}C$ excursions during both the Paleoproterozoic (Karhu & Holland 1996; Bekker & Holland 2012; Melezhik et al. 2013) and the Neoproterozoic (Och & Shields-Zhou 2012). Long-lived excursions such as those in the Paleo- and Neoproterozoic require stable tectonic settings in which the buried organic matter is not uplifted and eroded, or at the very least does not exceed the amount that is simultaneously buried (Campbell & Squire 2010; Bekker & Holland 2012; Melezhik et al. 2013). It should be noted that other explanations for the generation of positive $\delta^{13}C$ excursions that are not controlled by tectonic processes have also been suggested (Hayes & Waldbauer 2006; Melezhik et al. 2013). However, burial of organic matter appears to be the most widely accepted mechanism and it will be assumed here that it is indeed responsible for the $\delta^{13}C$ excursions. This can also explain the general coincidence of the GOE and

NOE with positive excursions of $\delta^{13}C$, as burial of organic matter would lead to an increase in oxygen (e.g. Des Marais 1994; Karhu & Holland 1996; Melezhik et al. 2013).

Assuming that the positive excursions of $\delta^{13}C$ in the Precambrian are both controlled by burial of organic matter — and therefore by tectonic processes — then they may be used in conjunction with $^{87}Sr/^{86}Sr$ as proxies for tectonic events. Both $^{87}Sr/^{86}Sr$ (Shields 2007) and $\delta^{13}C$ (Karhu & Holland 1996; Melezhik et al. 2013) of well-preserved sedimentary carbonates are generally considered to record the composition of Earth's oceans. $^{87}Sr/^{86}Sr$ and $\delta^{13}C$ thus present proxies which are less sensitive to preservation and sampling bias compared with e.g. detrital zircons or high-grade rocks (Cawood et al. 2013). While high relative input of river runoff may be taken to reflect periods of extensive collisional orogeny (Shields 2007; Campbell & Squire 2010) the positive $\delta^{13}C$ may instead be interpreted to reflect relatively stable periods lacking collisional orogens (e.g. Bekker & Holland 2012). The end of positive $\delta^{13}C$ excursions may thus be taken as an indicator for collisional orogens involving uplift and erosion of previously deposited organic matter.

In figure 28 curves reflecting the secular evolution of atmospheric oxygen (after Bekker & Holland 2012, based on various proxies), $\delta^{13}C$ and $^{87}Sr/^{86}Sr$ has been plotted against different stages of the supercontinent cycles discussed above. These stages correspond to the assembly and maximum packing of Kenorland, Columbia, Rodinia and Pangea as well as intervening periods involving breakup and assembly of these supercontinents. The intervening periods includes the accretionary and collisional phases of the assembly of Atlantica-Midgardia-Ur (fig. 24b) and Gondwana. A compilation of mainly detrital zircon (fig. 28c) shows that peaks broadly coincide with different supercontinents, as noted by Campbell and Allen (2008). This has been attributed to increased preservation of rocks during supercontinent assembly (e.g. Hawkesworth et al. 2009; Cawood et al. 2013).

Both the accretionary stage of Atlantica-Midgardia-Ur and Gondwana coincide with the peak of the $\delta^{13}C$ curve while their collisional stage instead coincides with the return to unfractionated values at the same time as the $^{87}Sr/^{86}Sr$ values are increasing. $^{87}Sr/^{86}Sr$ values of marine carbonates reach their peak at the end of the collisional phases of Atlantica-Midgardia-Ur and Gondwana. The positive excursions of $^{87}Sr/^{86}Sr$ and $\delta^{13}C$ both occur during a supercontinent cycle involving the breakup of a Rodinia-type supercontinent and the subsequent assembly of a Pangea-type (fig. 28). During both cycles, the excursions occur in the same order, are of the same magnitude and have the same duration. It is also notable that similar excursions do not occur during Pangea- to Rodinia-type cycles.

The repetitive pattern of the excursions recorded by $^{87}Sr/^{86}Sr$ and $\delta^{13}C$ in sedimentary marine carbonates and their correlation with the same type of tectonic events during Rodinia- to Pangea-type supercontinent cycles strongly suggest that there is a link between them, i.e. the isotopic signals are indeed tectonically controlled. By extension, it also implies that if there is a link between increasing atmospheric oxygen and burial of organic matter (Karhu & Holland 1996; Campbell & Squire 2010; Bekker & Holland 2012; Och & Shields-Zhou 2012) then the GOE and NOE are linked to Rodinia- to Pangea-type supercontinent cycles (fig. 28), rather than supercontinent cycles in general (e.g. Campbell & Allen 2008). The preceding discussion has assumed that there was a supercontinent during the Neoarchean (Williams et al. 1991) as opposed to multiple continents (Aspler & Chiarenzelli 1998; Bleeker 2003). The similar behavior of $^{87}Sr/^{86}Sr$ and $\delta^{13}C$ during the Paleo- and Neoproterozoic may be taken as further evidence in support for such model, assuming that the excursions were caused by the same factors and are indeed controlled by tectonic processes.

The positive $\delta^{13}C$ excursion during the Paleoproterozoic, also known as the Lomagundi-Jatuli Event (LJE, Karhu & Holland 1996; Melezhik et al. 2013), has been attributed to either burial of organic matter on tectonically stable shelves or continental rifts (Bekker & Holland 2012; Melezhik et al. 2013) or at convergent margins (Lindsey & Brasier 2002). However, as highlighted in the above discussion, accretionary orogens, passive margin sedimentation and continental rifting characterize the period between 2.3-2.0 Ga during which the excursion takes place. Black shales with $\delta^{13}C$ around -30 to -20‰ (typical for Precambrian organic matter, e.g. Des Marais 1994) have been reported from several localities in the Baoulé Mossi domain, which are constrained to between circa 2.2-2.1 Ga (Leube et al. 1990; Hirdes et al. 1993; Kříbek et al. 2008). This suggests that deposition in the accretionary setting that this domain constituted may at least have contributed to the positive $\delta^{13}C$ excursion. However, there seems to be no reason why deposition of organic matter would not have taken place at passive margins or rift basins as well, even though there is an absence of such rocks in the geological record (e.g. Melezhik et al. 2013). A more plausible tectonic explanation for the positive $\delta^{13}C$ excursions may instead be that they form during a period when the global plate tectonic framework is characterized by an absence of collisional orogens, at the same time as passive margins, rift basins, backarc basins and accretionary wedges are formed in regions undergoing dispersal or accretion.

If the Paleo- and Neoproterozoic positive $\delta^{13}C$ excursions are caused by burial of organic matter then the end of these events should correspond to uplift and erosion of the sediment in which it is buried (Bekker & Holland 2012). The simultaneous rise in $^{87}Sr/^{86}Sr$ as $\delta^{13}C$ is decreasing occurs during the collisional stage of both Atlantica-Midgardia-Ur and Gondwana (fig. 28). It therefore seems reasonable to connect this pattern to increased continental weathering. However,

closure of ocean basins along with oceanic ridges may also contribute, in the sense that the relative mantle input decreases. As $^{87}Sr/^{86}Sr$ peak at the end of the collisional stage of Atlantica-Midgardia-Ur and Gondwana it would appear as if the assembly of Columbia and Pangea exert less relative control on $^{87}Sr/^{86}Sr$, perhaps because oceanic ridges are more widespread at this time. At least for Gondwana, rifting of crustal blocks initiated shortly after its assembly and should have led to the formation of ocean ridges whose input of low $^{87}Sr/^{86}Sr$ to the oceans may perhaps have helped to counteract the effect of continental weathering during the assembly of Pangea.

Also shown in figure 28 is the timing of widespread glaciations during the Paleoproterozoic and Neoproterozoic (fig. 28b) of which at least some are believed to have had a global extent, the so called "Snowball Earths" (Hoffman 2002, 2013; Melezhik 2005; Och & Shields-Zhou 2012). These glaciations have been attributed to the loss of greenhouse-conditions during the oxygenation of the atmosphere but may also be the result of multiple causes. Although the temporal constraints for the Paleoproterozoic glaciations are somewhat uncertain, they nevertheless appear to occur earlier relative to the Rodinia- to Pangea-type supercontinent cycle compared with the Neoproterozoic glaciations. It may be speculated that the relative delay of glaciations in the Neoproterozoic may somehow be related to different atmospheric starting conditions in the Paleoproterozoic — which was anoxic or only weakly oxidized — compared with conditions during the Neoproterozoic when oxygen was already present (fig. 28, Holland 2006; Bekker & Holland 2012). A further discussion is beyond the scope of this work, but the example serves to highlight how environmental changes caused by a supercontinent cycle may change the starting conditions of a subsequent cycle. In a similar manner to glaciations, the behavior of $\delta^{13}C$ also appears to change in the Phanerozoic following the Cambrian radiation. Positive excursions in $\delta^{13}C$ around 400 and 300 Ma (fig. 28b) coincide with the Variscan-Hercynian and Caledonian orogenies, respectively. This differs from the Paleo- and Neoproterozoic positive excursions, which instead appear to have preceded collisional orogens. In this case, the radiation of Metazoans and emergence of land plants may have changed how $\delta^{13}C$ responded to collisional orogens (e.g. Campbell & Squire 2010).

5.5.3 Rodinia- to Rodinia-type supercontinent cycles

5.5.3.1 Onset and nature of supercontinental cycles

If plate tectonics began to operate in the Mesoarchean (e.g. Condie & Kröner 2008; Næraa et al. 2012) then Kenorland should have been the first supercontinent to have formed in a plate tectonic regime (fig. 27). However, the existence of a Neoarchean supercontinent incorporating the majority of Archean crust has been questioned by authors who propose that the Archean crust at this time may instead have been distributed in two or more separate paleocontinents, leaving Columbia as the first true supercontinent (e.g. Aspler & Chiarenzelli 1998; Rogers & Santosh 2002; Bleeker 2003). Nevertheless, because of the similarities between the assembly of Columbia and Pangea (fig. 26), coupled with the behavior of $^{87}Sr/^{86}Sr$ and $\delta^{13}C$ in the Paleo- and Neoproterozoic (fig. 28), it is inferred here not only that Kenorland was a Rodinia-type supercontinent but also that the breakup of this continent in the Paleoproterozoic mirrored that of Rodinia in the Neoproterozoic.

At this stage it is pertinent to ask what constitutes a supercontinental cycle. Assuming that Kenorland was the first supercontinent to have formed in a plate tectonic regime — and that it was the first iteration of a Rodinia-type supercontinent — the supercontinental cycle may be considered as the breakup of Kenorland and the subsequent assembly of the next supercontinent Columbia (i.e. a Rodinia- to Pangea-type supercontinental cycle, see section 5.5.1). However, the real supercontinental cycle should correspond to a Rodinia- to Rodinia-type cycle, which records the breakup of a given Rodinia-type iteration and the subsequent assembly of the next. This will correspond to either the Paleo- to Mesoproterozoic breakup of Kenorland and assembly of Rodinia or the Neoproterozoic-Phanerozoic breakup of Rodinia and (ongoing) assembly of Amasia. In this context, Pangea-type supercontinents (i.e. Columbia or Pangea) only correspond to transient stages during a Rodinia- to Rodinia-type cycle at which time enough continental crust (>75%, Meert 2012) is amalgamated to form a supercontinent. The proposed Neoproterozoic supercontinent Pannotia (Dalziel 1997) — that may have existed following the assembly of East and West Gondwana but before the opening of the Iapetus Ocean — would be another example of such a transient supercontinental stage.

5.5.3.2 Breakup of Rodinia and assembly of Gondwana-Pangea

Because of the similarities between the periods corresponding to the breakup of Rodinia in the Neoproterozoic and the inferred breakup of Kenorland in the Paleoproterozoic (figures 26 and 28), it is assumed here that models for the breakup of Rodinia should also be applicable for the breakup of Kenorland. Indeed, as will be discussed below, the breakup of Kenorland and subsequent assembly of Columbia (with a configuration as in figure 24b, see also discussion in section 5.5.1) can be broadly explained using the reconstructions of Hoffman (1991) and Dalziel (1997) for the breakup of Rodinia and assembly of Gondwana and Pangea.

In the reconstructions of Hoffman (1991) and Dalziel (1997), Rodinia began to break up as the continental blocks that came to form East Gondwana rifted from the margin of Laurentia (fig. 29a). The blocks of

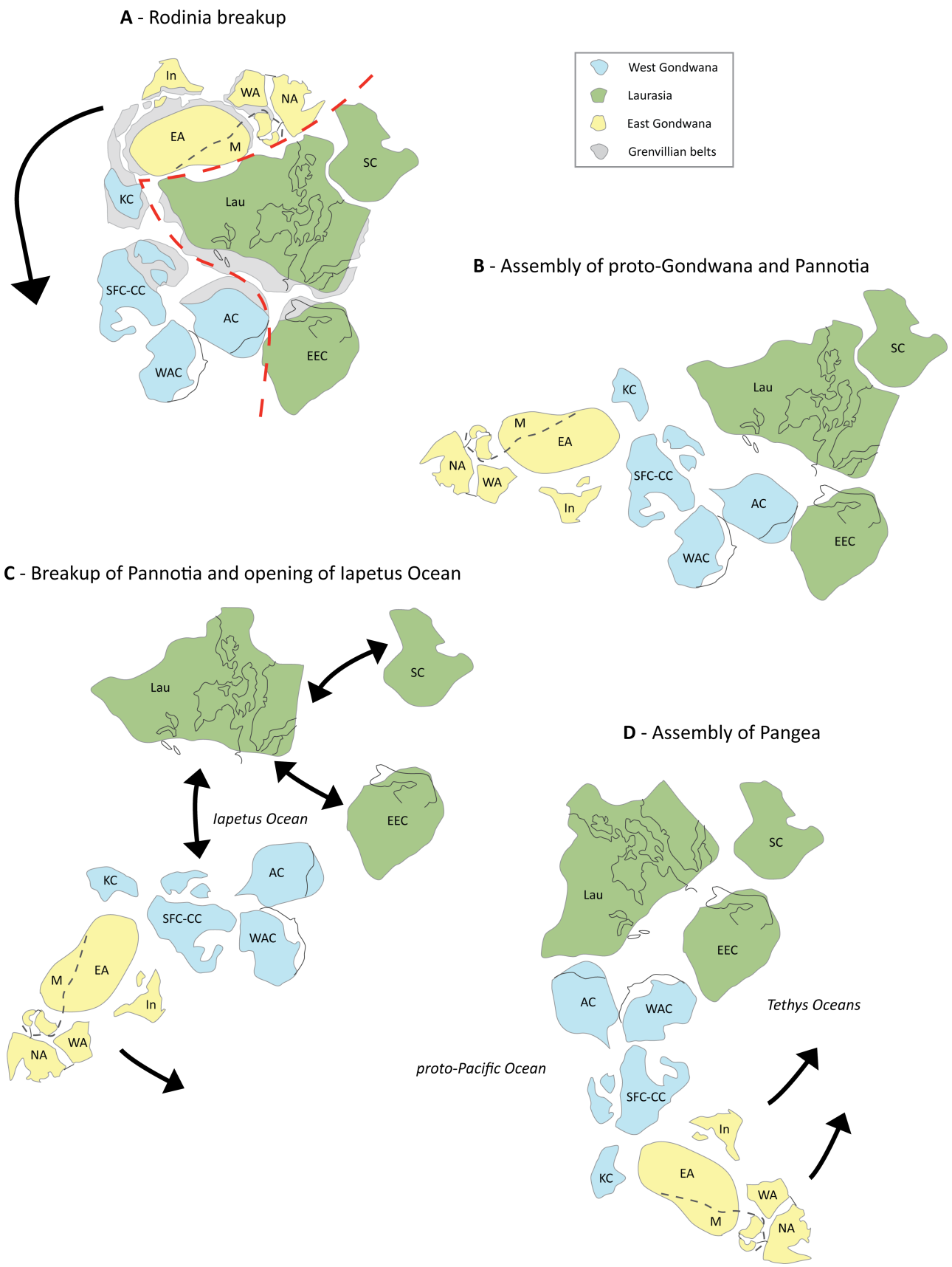

Fig. 29. Schematic depiction of the breakup of Rodinia and assembly of Gondwana and Pangea. After Hoffman (1991) and Dalziel (1997). Breakup of East Gondwana after Metcalfe (2013) and Stampfli et al. (2013). Abbreviations for continental blocks: **EA** - East Antarctica**; KC** - Kalahari Craton; **In** - India; **WA** - West Australian Craton; **SFC-CC** - São Francisco Craton -Congo Craton; **WAC** - West African Craton; **AC** - Amazon Craton; **EEC** - East European Craton; **Lau** - Laurentia; **SC** - Siberian Craton; **M** - Mawson continent; **NA** - North Australian Craton. Rodinia configuration redrawn after Hoffman (1991).

proto-East Gondwana were subsequently accreted against proto-West Gondwana (fig. 29b). This led to the formation of Pannotia as proto-West Gondwana at this point remained in contact with Laurentia. As Gondwana was assembled Laurentia, the East European Craton and Siberia rifted and began to drift relative to each other as the Iapetus Ocean opened (fig. 29c). At this time, Gondwana also rotated counterclockwise relative to the Laurasian blocks. This had the effect that when Laurasia and Gondwana merged to form Pangea (fig. 29d), the margin of proto-West Gondwana that had faced Laurentia in Rodinia was now facing the proto-Pacific ocean. As Pangea was assembled through collision between West Gondwana and Laurussia, terranes began to rift from East Gondwana from where they were carried across the Tethys Oceans to be accreted against Laurasia (e.g. Metcalfe 2013; Stampfli et al. 2013). Apart from Antarctica, the continental blocks of East Gondwana are now accreted or in the process of being accreted to Asia.

5.5.3.3 The Kenorland to Rodinia supercontinental cycle

If the breakup of Kenorland played out in the same manner as for Rodinia, the challenge lies in how to account for the breakup of one Rodinia-type supercontinent (i.e. Kenorland) following the sequence of events in figure 29 and from there assemble another Rodinia-type supercontinent (i.e. Rodinia "*sensu stricto*"). There are at least three important aspects that need to be accounted for in this cycle. The first is the relative rotation of Laurentia from the Mesoproterozoic to today, which has caused a switch of the site of accretionary growth from the present East Coast to the West Coast (i.e. the North American Cordilleras, e.g. Williams et al. 1991; Dalziel 1997). The second is the 180° rotation of East Gondwanan continental blocks from their relative position in Rodinia (as shown in Hoffman 1991, fig. 29a) to their relative position today (assuming that Antarctica moves northwards and is accreted outboard of India-SE Asia-Australia). The third is not an aspect as much as an assumption, namely that the current North and South American Cordilleras are equivalent to the long-lived accretionary orogens which formed outboard to Laurentia, Fennoscandia and the Amazon Craton and whose closure in the late Mesoproterozoic led to the assembly of Rodinia (e.g. Li et al. 2008; Johansson 2009). However, this it is also required if Amasia is to be the third iteration of a Rodinia-type supercontinent (see section 5.5.1).

With this in mind, the assembly of Rodinia may be run in reverse through Columbia back to Kenorland. Proposed reconstructions of Columbia (as shown in figure 24b) and Kenorland, together with the configuration of Rodinia by Hoffman (1991), are shown in figure 30a, while a six-stage schematic depiction of the breakup of Kenorland through to the assembly of Rodinia is shown in figure 30b. Because of the 180° rotation of the continental blocks that constituted East Gondwana from Rodinia to the present day, a similar 180° rotation should also have taken place among these blocks from Kenorland to Rodinia. This places these blocks, which correspond to East Atlantica-Midgardia-Ur (see section 5.5.1) on the margin of Nena in the same relative position as they have today (fig. 30a). Mimicking the breakup of Rodinia, the breakup of Kenorland should have involved rifting of these blocks in the Paleoproterozoic from the margin of Nena followed by their gradual accretion towards the crustal blocks corresponding to West Atlantica-Midgardia-Ur (see section 5.4.1) and illustrated by stage 2 in figure 30b. This coincided with the rifting and drifting of blocks within Nena (stages 2-3, fig. 30b), which largely coincided with the assembly of Atlantica-Midgardia-Ur (section 5.5.1). During stages 2-3 (fig. 30b), and leading up to stage 4, the Atlantica-Midgardia-Ur continent rotated relative to the Nena blocks in the same manner as Gondwana did relative to Laurasia in the Neoproterozoic-Paleozoic (fig. 29c).

The rotation of Atlantica-Midgardia-Ur had the effect that when Columbia assembled around 1.8-1.7 Ga (stage 4, fig. 30b) by collision between Fennoscandia and Sarmatia-Volgo-Uralia (see discussion in section 5.5.1) the margin of Atlantica-Midgardia-Ur that had faced the Nena blocks in Kenorland was now instead facing an extensive ocean, which is evidenced by the development of long-lived accretionary orogens along this margin (e.g. Cordani & Teixeira 2007, see also discussion in section 5.1). These long-lived accretionary orogens correspond to those found in the Amazon Craton (Cordani & Teixeira 2007) and Fennoscandia (Bogdanova et al. 2008). Following the assembly of Columbia, long-lived accretionary orogens also developed on the margin of Laurentia (Whitmeyer & Karlstrom 2007; Johansson 2009) which had previously been connected with the blocks which comprised East Atlantica-Midgardia-Ur. Together, these accretionary orogens faced a Proterozoic proto-Pacific Ocean.

The continental blocks in Nena that participated in the collisional orogeny associated with the assembly of Columbia (i.e. Fennoscandia and perhaps the Siberian Craton, following the reconstruction of Evans & Mitchell 2011) should also have been in contact with the continental blocks of West Atlantica-Midgardia-Ur in Kenorland prior to its breakup. This would be analogous with how Grenvillian belts in Laurentia (on the East Coast of present-day North America) formed part of the Variscan-Hercynian orogeny (fig. 25). This provides some constraints for the position of Fennoscandia in Kenorland (fig. 30a). Evans and Mitchell (2011) suggested that the Siberian Craton was adjacent to Volgo-Uralia and (present-day) northern Laurentia in the late Paleoproterozoic and Mesoproterozoic (1.9-1.3 Ga). It should therefore also have been close to Fennoscandia in Kenorland, as shown in figure 30a.

Simultaneously with the collision between Fennoscandia and the Sarmatia–Volgo-Uralia continental blocks should have begun to rift from East Atlantica-

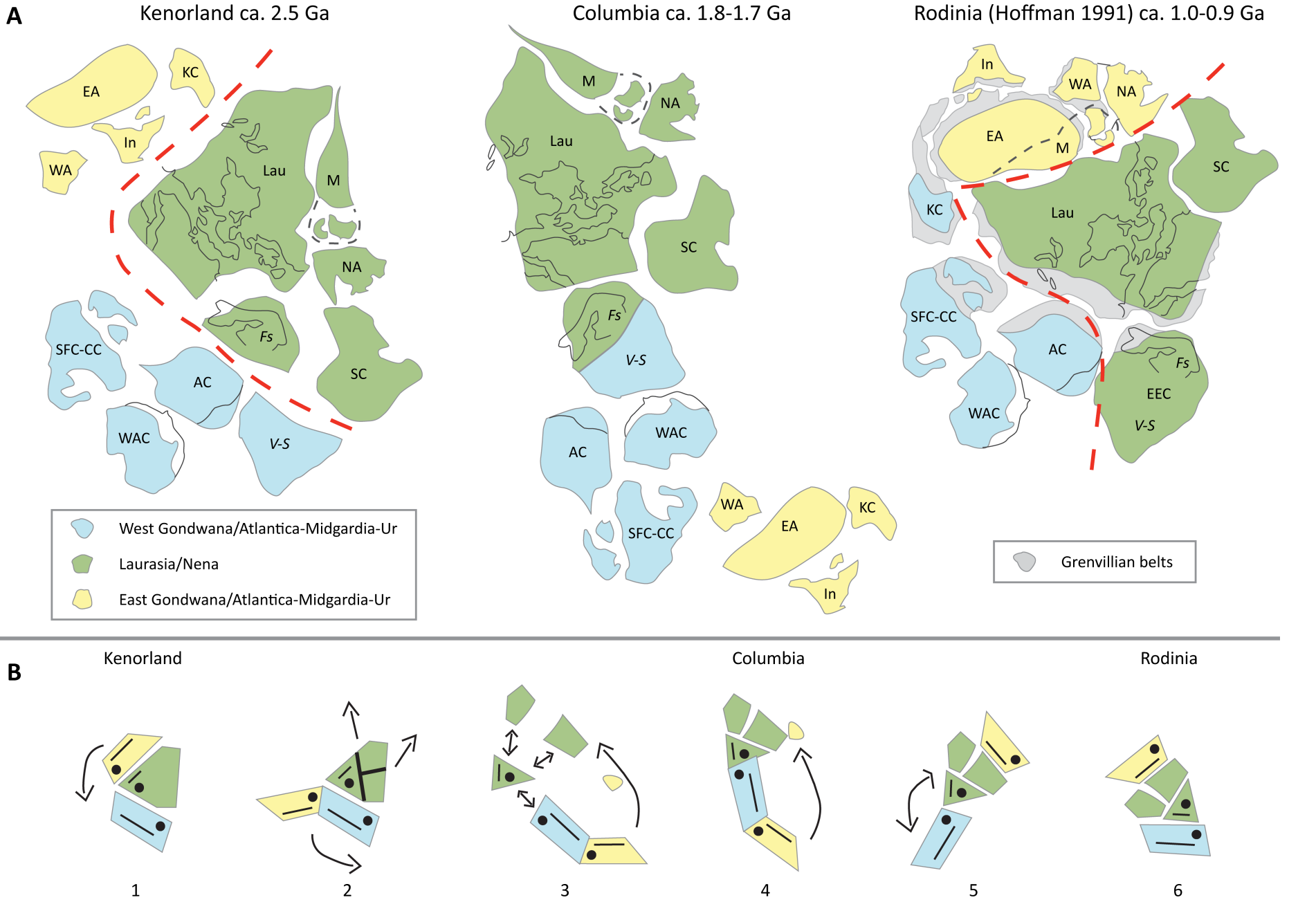
A
Kenorland ca. 2.5 Ga
Columbia ca. 1.8-1.7 Ga
Rodinia (Hoffman 1991) ca. 1.0-0.9 Ga
EA
KC
In
WA
Lau
M
NA
Fs
SFC-CC
AC
SC
WAC
V-S
West Gondwana/Atlantica-Midgardia-Ur
Laurasia/Nena
East Gondwana/Atlantica-Midgardia-Ur
Grenvillian belts
B
Kenorland
Columbia
Rodinia
1
2
3
4
5
6

Midgardia-Ur (stage 4, fig. 30b) in the same way as blocks did from East Gondwana in the Paleozoic (e.g. Metcalfe 2013, see also figure 29d). The West Australian Craton appears to have been accreted to the North Australian Craton and the Mawson Continent around 1.80-1.75 Ga (Payne et al. 2009) indicating that this process was occurring at the same time as West Atlantica-Midgardia-Ur and Nena collided. The North Australian Craton and the Mawson Continent would thus at this point have been equivalent to the Asian foreland during the Paleozoic accretion of continental blocks derived from East Gondwana (cf. figures 29d and 30a). During the Mesoproterozoic, the lead up to the assembly of Rodinia would have involved gradual accretion of blocks from East Atlantica-Midgardia-Ur to one side of Nena while the long-lived accretionary orogens along West Atlantica-Midgardia-Ur and Nena's other side began to close in on each other (stages 5-6, fig. 30b). This culminated with the Grenvillian orogeny (e.g. Li et al. 2008; Johansson 2009) and the assembly of Rodinia in the late Mesoproterozoic to early Neoproterozoic (fig. 30a and stage 6 in figure 30b).

The combined effect of the rotation of Atlantica-Midgardia-Ur and the subsequent collision between the accretionary orogens along the Amazon Craton and Fennoscandia on one hand and Laurentia on the other during the assembly of Rodinia (e.g. Johansson 2009) caused Nena (including Laurentia) to rotate counter-clockwise relative to its position in Kenorland (compare Kenorland and Rodinia in figure 30a and stages 1 and 6 in figure 30b). This can account for the shift in accretionary orogenic activity seen today in North America, but also why the same is not seen in e.g. the Amazon Craton in South America (e.g. Brito Neves 2011). As Rodinia broke up along the Grenvillian belts which formed during the collision between Nena and West Atlantica-Midgardia-Ur these came to form continental margins facing the Iapetus and Rheic oceans (e.g. Nance et al. 2010). However, because Gondwana rotated counter-clockwise relative to Laurentia closure of the Iapetus and Rheic oceans did not lead to a reassembly of matching Grenvillian belts. Instead, the same Grenvillian margin of Laurentia accreted against northwestern Africa while its matching margin in West Gondwana came to face the proto-Pacific ocean (fig. 29d). A new long-lived accretionary orogen (essentially a Phanerozoic version of the Paleo- to Mesoproterozoic orogen on the East Coast of North America) formed on the West Coast where it developed into the present-day North American Cordilleras. The counter-clockwise rotation of Gondwana during breakup of Rodinia ensured that the Paleo- to Mesoproterozoic belts in the Amazon Craton were turned to face the Pacific, allowing for continued accretionary orogenic activity.

The six-stage conceptual model presented in figure 30b shows that there are several transient moments during the Kenorland to Rodinia supercontinental cycle where enough crust may have been assembled to constitute a supercontinent (containing >75% of the available continental crust, Meert 2012). An early such supercontinental stage may have occurred after East Atlantica-Midgardia-Ur rifted from Nena but before West Atlantica-Midgardia-Ur had done the same (stage 2). This would correspond to a direct equivalent of Pannotia in the Neoproterozoic (Dalziel 1997). Likewise, the assembly of Columbia at 1.8-1.7 Ga (stage 4) would be equivalent to the assembly Pangea and would represent a new supercontinental stage. Depending on the rate of rifting versus accretion of continental blocks from East Atlantica-Midgardia-Ur against Nena (stages 3-5) it may be envisioned that a supercontinent existed through stages 4-6 which spanned the late Paleo- and Mesoproterozoic, up and until the assembly of Rodinia. This is consistent with the recognition of a long-lived Columbia supercontinent (e.g. Zhao et al. 2004). However, it is important to recognize that although there is such a long-lived supercontinental stage the supercontinent itself was

Fig. 30. **A**) Schematic reconstructions of Kenorland, Columbia and Rodinia showing the cells that the constituent continental blocks belong to. The participating continental blocks can be grouped into three cells (yellow, blue and green) based on their behavior during the supercontinental cycle (see section 5.5.3.5 for further discussion). The yellow cell is equivalent to East Gondwana in the Neoproterozoic-Phanerozoic or East Atlantica-Midgardia-Ur in the Proterozoic. The green cell is equivalent to Laurasia in the Neoproterozoic-Phanerozoic and Nena in the Proterozoic. The blue cell is equivalent to West Gondwana in the Neoproterozoic-Phanerozoic and West Atlantica-Midgardia-Ur in the Proterozoic. The breakup of Kenorland is based on the "inside-out" model of Hoffman (1991) for the breakup of Rodinia during the Neoproterozoic. The Rodinia configuration is redrawn after Hoffman (1991). **Note** that while the continental blocks for Rodinia are also used for the Kenorland and Columbia configurations, they may contain crust that is younger than these supercontinents. For example, large parts of the WAC and AC would not have existed in the actual Kenorland supercontinent. However, the Archean crust within these blocks would have assumed a similar position. The dashed red lines in the Kenorland and Rodinia reconstructions shows the lines along which these supercontinents broke up into different cells. As shown by the behavior of KC, V-S, M, and NA, continental blocks may be transferred from one cell to another between two Rodinia- to Rodinia-type supercontinent cycles (see section 5.5.3.5 for further discussion). Abbreviations for continental blocks: **EA** - East Antarctica**; KC** - Kalahari Craton; **In** - India; **WA** - West Australian Craton; **SFC-CC** - São Francisco Craton-Congo Craton; **WAC** - West African Craton; **AC** - Amazon Craton; ***V-S*** - Volgo-Uralia–Sarmatia; ***Fs*** - Fennoscandia; **EEC** - East European Craton; **Lau** - Laurentia; **SC** - Siberian Craton; **M** - Mawson continent; **NA** - North Australian Craton. **B**) A six-stage conceptual reconstruction of a Rodinia-Rodinia type supercontinental cycle based upon the breakup of Kenorland and subsequent assembly of Rodinia. Stages 1, 4 and 6 correspond to Kenorland, Columbia and Rodinia, respectively. The movement of the cells is based on the breakup of Rodinia as depicted by Hoffman (1991) and Dalziel (1997). Note how, from Kenorland to Rodinia, the yellow cell rotates 180° while the green cell is rotated counter-clockwise. The blue cell does not rotate. Also compare with the relative position of continental blocks between the Kenorland and Rodinia reconstructions in A). See section 5.5.1 for further discussion.

not stable and reorganization of crust took place throughout this period. For example, the reconstruction of Columbia in Zhao et al. (2004) would be largely equivalent to stage 5 (fig. 30b) but clearly differs from that in stage 4. These two configurations might either be seen as a continuum of one supercontinent (i.e. Columbia) or as separate entities. During the Kenorland-Rodinia cycle, the only period during which there was no supercontinent present appears to have been during stage 3 (and perhaps part of stage 2, fig. 30b), which largely corresponds to the middle-late Paleoproterozoic (2.0-1.8 Ga).

What sets the Kenorland-Rodinia supercontinental cycle apart from the present Rodinia-Amasia cycle is the apparent absence of an oceanic basin equivalent to the Atlantic Ocean. This has been the elephant in the room in the preceding discussion and clearly has to be accounted for if the model of Rodinia- to Rodinia supercontinental cycles is to be considered viable. Opening of the Atlantic Ocean during the breakup of Pangea led to the separation of crust from Laurasia and West Gondwana. The next supercontinent Amasia has been proposed to assemble through closure of either the Pacific or Atlantic Ocean (e.g. Yoshida & Santosh 2011). Following the model outlined here, Amasia should assemble by closure of the Atlantic Ocean and subsequent collision between the South and North American Cordilleras through the rotation of these accretionary orogens against each other. By accreting Antarctica outboard to Asia, this would lead to the assembly of another Rodinia-type supercontinent. While no equivalent to the Atlantic Ocean appear to have formed during the Paleo- and Mesoproterozoic, both Nena and Atlantic-Midgardia-Ur appear to have been affected by extension and rifting during the Mesoproterozoic (e.g. Zhao et al. 2004; Ernst et al. 2013; El Bahat et al. 2013). Although speculative, it could be imagined that this rifting at least in part corresponded to unsuccessful attempts at opening a Proterozoic Atlantic-type ocean. Although an oceanic basin was not established it was not for a lack of trying, but must have been due to other factors.

Finally, it must be noted that although the continental blocks in Rodinia are also used for the Kenorland and Columbia configurations in figure 30, they contain crust that is younger than these supercontinents. For example, large parts of the WAC and Amazon Craton would not have existed in the actual Kenorland supercontinent. However, the Archean crust within these blocks would nevertheless have assumed a similar position in both Kenorland and Rodinia. The usage of Rodinia continental blocks for Kenorland and Columbia might therefore be largely an issue of presentation and does not impact on the fundamental concept of Rodinia- to Rodinia-type supercontinental cyclicity. A more pressing issue is the validity of the Rodinia-reconstruction used here (from Hoffman 1991). Although there are several configurations of Rodinia, that of Hoffman (1991) does not differ significantly from the recent consensus configuration given by Li et al. (2008), nor does it appear to be incompatible with the SAMBA-configuration of Johansson (2009). The use of the Rodinia-configuration of Hoffman (1991) thus seem to be sufficient for the purposes of this work. However, more detailed reconstructions of Rodinia- to Rodinia-type supercontinental cycles will require the use of a more detailed Rodinia configuration. If the model outlined above holds, it would indeed appear as if Rodinia is the key to Kenorland.

5.5.3.4 Supercontinental cycles and mantle dynamics

It has been proposed that there is a strong link between plate tectonics, supercontinent cycles and mantle dynamics (e.g. Anderson 1982, 2001; Gurnis 1988; Yoshida & Santosh 2011; Murphy & Nance 2013; Nance et al. 2014). It therefore seems reasonable to assume that the supercontinent cycles and recurring iterations discussed above should also be reflected in mantle dynamics, with the implication that convection within the mantle should be fairly ordered. In contrast, it may be speculated that the transition from the onset of plate tectonics to the assembly of the first supercontinent (here assumed to be Kenorland in the Neoarchean) corresponded to a period of turbulence, as it would have involved the switch from one tectonic regime (plume dominated stagnant-lid or intermittent subduction? See further discussion in section 1) to another dominated by modern-style subduction of oceanic crust (van Hunen et al. 2008; Sizova et al. 2010). This transition was presumably gradual as the right conditions for subduction to occur may not have been reached simultaneously across the surface of the Earth (Condie & Kröner 2008).

It seems reasonable to assume that the assembly of the first supercontinent Kenorland marked the end of the turbulent transition period. The assembly of Kenorland should have marked a point when most, if not all, continental crust was aggregated in one place. This should have corresponded to a geoid-low formed were subducted oceanic crust was collecting in the mantle (Gurnis 1988; Anderson 2001; Murphy & Nance 2013). Outside of Kenorland, upwelling mantle would have represented geoid-highs. The assembly of the first supercontinent may therefore have had a stabilizing effect on the crust-mantle system through the establishment of geoid-highs and lows related to a supercontinent that included most if not all continental crust. Assuming that Kenorland had the same shape as the Rodinia (fig. 30) it is interesting to note that this corresponds to what is essentially a circular aggregation of crust (based on the reconstructions by Hoffman 1991 and Li et al. 2008). Although it is beyond the scope of this work, the round shape of Kenorland may provide clues for the distribution of crust during the transition period and how it played out following the establishment of modern-style plate tectonics, leading up to the aggregation of Kenorland.

Because of the insulating effect of large conti-

nents, the mantle beneath Kenorland would have gradually heated up and expanded, turning the geoid-low into a geoid-high comprised of warm and buoyant mantle (Anderson 1982, 2001; Gurnis 1988; Murphy and Nance 2013). The establishment of the geoid-high would have caused Kenorland to begin to break up as outlined in section 5.5.3.3 and shown in figure 30. The behavior of different crustal blocks during the Kenorland to Rodinia supercontinental cycle (i.e. whether they formed part of Nena, Ur or Atlantica-Midgardia) would have been conditioned by their relative position in Kenorland. The same can of course also be said about how they behaved following the breakup of Rodinia and the ongoing assembly of Amasia.

The silicate Earth thus appear to be a self-organizing system in which modern-style plate tectonics established a Rodinia- to Rodinia-type supercontinental cycle when the thermal conditions could no longer sustain the pre-plate tectonic regime (Sizova et al. 2010). This would indicate that mantle convection is controlled by plate tectonics in what may be equivalent to a "top-down" geodynamic setting (Gurnis 1988; Anderson 2001; Murphy & Nance 2013). However, "top-down" geodynamic models involve consumption of exterior oceans as continents disperse above geoid highs and aggregate above geoid lows (Murphy & Nance 2013). As Rodinia- to Rodinia-type supercontinent cycles involves both consumption of exterior and interior oceans (illustrated by stages 1-2 and 3-4 in figure 30b, respectively) the full story is undoubtedly more complex.

Assuming that the Paleoproterozoic accretionary orogens formed along subduction zones, then the similar time-scales of the assembly of Columbia and Pangea (fig. 26) indicate that plate tectonics operated much the same in the Paleoproterozoic as it did in the Neoproterozoic and Paleozoic (and by inference today). Differences between the Paleoproterozoic and Phanerozoic geological record, e.g. the absence of HP-LT metamorphic rocks (Stern 2005), may perhaps best be accounted for by a higher geotherm (e.g. Condie & Kröner 2008; van Hunen et al. 2008) but would in such case not have had a significant impact on how plate tectonics operated. However, when reviewing the Precambrian bedrock of North America, Williams et al. (1991) noted that there was a trend towards larger continental plates over time as smaller Archean fragments were amalgamated into larger blocks. It could be speculated that an increase in lithospheric plate size could be a way for the silicate Earth — acting as a system — to maintain regular supercontinent cycles in response to secular cooling, which would represent a change imposed upon the system. In this situation, plate tectonics may have been operating differently in the Proterozoic in response to a higher geotherm (for example by having a greater global ridge length and more plates, e.g. Hargraves 1986) even as supercontinent cycles operated on the same time scales as in the Phanerozoic.

5.5.3.5 Continental cells and transfer of blocks

Since the continental blocks appear to have had largely the same role and behavior in the Kenorland-Rodinia as in the Rodinia-Amasia cycle (see discussion in section 5.5.1) the blocks of West Gondwana/Atlantica-Midgardia-Ur, East Gondwana/Atlantica-Midgardia-Ur and Laurasia/Nena may be considered as forming three separate "continental cells" (fig. 30a). These cells are characterized by the same behavior since the onset of the first Rodinia- to Rodinia-type supercontinent cycle, following the breakup of Kenorland.

This is similar to the long-lived paleocontinents Arctica (Nena), Ur and Atlantica proposed by Rogers (1996, see also section 5.4), which he suggested had remained intact following their formation in the Neoarchean-Paleoproterozoic up and until their breakup in the Mesozoic. However, the concept of continental cells does not require that the continental blocks remain amalgamated throughout a given Rodinia- to Rodinia-type supercontinental cycle. Indeed, the behavior of for example the East Gondwana/Atlantica-Midgardia-Ur cell is instead characterized by successive breakup and amalgamation during such a cycle. As such, it is more dynamic than the long-lived continents envisioned by Rogers (1996). It also assumes that all continental blocks must belong to either one of the three cells, which is different from the paleocontinents proposed by Rogers (1996). These paleocontinents instead acted as nucleuses which interacted with other "independent" continental blocks.

Rogers (1996) suggested two ways in which continental blocks might have been transferred between the paleocontinents Arctica (Nena), Ur and Atlantica; docking or rifting, drifting and accretion. Docking takes place when two continents are amalgamated and upon breakup does not rift along the original suture, leading to the transfer of a part of one continent to the other. Rifting, drifting and accretion simply involves the rifting of a block from one continent and its accretion against another continent, through consumption of intervening oceanic crust. While transfer of continental blocks may be used to describe the history of the paleocontinents proposed by Rogers (1996), can it also be used to describe the behavior of continental blocks in the context of Rodinia- to Rodinia-type supercontinent cycles where all continental blocks form part of a cell?

If all continental blocks belong to a given cell then transfer should correspond to the movement of a given block from one cell to another, with a consequent change in the behavior of that block during a Rodinia- to Rodinia-type supercontinental cycle. While rifting and drifting of continental blocks take place, for example during the breakup of East Gondwana/Atlantica-Midgardia-Ur, this movement is actually a part of how the cell behaves during a supercontinent cycle and will not lead to the transfer of the block from one cell to another. In the context of Rodinia- to Rodinia-type supercontinent cycles involving conti-

nental cells, docking therefore appears to be the only viable mechanism for transfer of continental blocks from one cell to another. In addition, transfer through docking should only occur during the transition from one supercontinent cycle to another (i.e. during the breakup of a Rodinia-type supercontinent) as this corresponds to the transition period when the continental cells are in contact and in the process of breaking up to initiate a new supercontinental cycle.

The apparent change in behavior of the Kalahari Craton, the Volgo-Uralia–Sarmatia blocks, the Mawson Continent and the North Australian Craton from the Kenorland-Rodinia to the Rodinia-Amasia cycle (fig. 30a) are examples of transfer of crustal blocks between different continental cells through docking. While the Mawson Continent and the North Australian Craton belonged to the Laurasia/Nena cell during the Kenorland-Rodinia cycle (see section 5.4.1), they instead formed part of the East Gondwana/Atlantica-Midgardia-Ur cell following the breakup of Rodinia (compare the Kenorland and Rodinia reconstructions in figure 30a). The same situation applies to Volgo-Uralia–Sarmatia, which formed part of the West Gondwana/Atlantica-Midgardia-Ur cell in the Kenorland-Rodinia cycle but joined the Laurasia/Nena cell during in the Rodinia-Amasia cycle. Finally, while the Kalahari Craton belonged to the East Gondwana/Atlantica-Midgardia-Ur cell during the Kenorland-Rodinia cycle, it was part of the West Gondwana/Atlantica-Midgardia-Ur cell (based on Hoffman 1991 and Gray et al. 2007) after the breakup of Rodinia (compare Kenorland and Rodinia in figure 30a).

The relationship between the Kalahari Craton, the Volgo-Uralia–Sarmatia blocks, the Mawson Continent and the North Australian Craton suggest that the transfer of blocks is a dynamic process wherein the Laurasia/Nena cell "lost" the Mawson Continent and the North Australian Craton to the East Gondwana/Atlantica-Ur cell but at the same time "gained" Volgo-Uralia–Sarmatia from the West Gondwana/Atlantica cell. Meanwhile, the Kalahari Craton was transferred to the West Gondwana/Atlantica-Midgardia-Ur cell from the East Gondwana/Atlantica-Midgardia-Ur cell. These relationships indicate that as a given cell "loses" a continental block(s) to one cell, it will at the same time "gain" a block(s) from the other remaining cell. As a consequence, there is rotation of continental blocks between the different cells, even as their size remains essentially constant.

The long-lived nature of the cells, as well as the transfer of crust between them, raises several questions regarding plate tectonics and mantle dynamics. For example, what is the relationship between the continental (lithospheric) cells and the underlying asthenosphere? Is it possible that the asthenospheric mantle is to some extent connected with the cells and has been so since the breakup of Kenorland? The breakup of East Gondwana/Atlantica-Midgardia-Ur during a Rodinia– to Rodinia-type supercontinent cycle do indicate that oceanic crust may form a transient part of these "continental" cells. If the cells also include oceanic crust, and perhaps part of the asthenospheric mantle, it would perhaps be more suitable to call them *convective cells*, rather than continental. Finally, is the transfer of crust between the continental cells from the Kenorland-Rodinia to the Rodinia-Amasia cycle an attempt to preserve the breakup-angles between the cells (shown as dashed red lines in figure 30a, after the "inside-out" model for the breakup of Rodinia by Hoffman 1991)? If that is the case, is this shift related to a different position of the geoid-high during breakup of Rodinia compared with Kenorland?

The above discussion has only briefly touched on some of the differences between the Kenorland-Rodinia and the Rodinia-Amasia supercontinental cycles such as the absence of an Atlantic-type ocean during the Kenorland-Rodinia cycle or the transfer of continental blocks between different cells form one cycle to another. As is evident from these examples, no Rodinia- to Rodinia-type supercontinental cycle can ever be expected to play out in exactly the same way. The combined effect of crustal growth and subduction erosion (Scholl & Von Huene 2009; Stern 2011; Cawood et al. 2013) together with the apparent tendency towards larger lithospheric plates over time (Williams et al. 1991) will also have the consequence that different supercontinental cycles should not be expected to involve similarly sized or shaped continental blocks. These features are in turn superimposed on the secular cooling of the Earth, which originally led to the establishment of modern-style plate tectonics (van Hunen et al. 2008; Herzberg et al. 2010; Sizova et al. 2010).

Despite these differences, the fundamental cyclicity that governs plate movements and mantle convection nevertheless appear to be the same during both the Kenorland-Rodinia and the Rodinia-Amasia supercontinental cycles. This cyclicity can ultimately be traced back to the assembly and subsequent breakup of Kenorland. Changes during the operation of these cycles are only superimposed on the original fundamental (first-order?) cyclicity but mean that successive Rodinia- to Rodinia-type supercontinental cycles will gradually diverge from the original cycle (i.e. the Kenorland-Rodinia cycle). The opening of the Atlantic Ocean during the Rodinia-Amasia cycle is a good example of this, as it contrasts with the assumed failed attempts to open a similar ocean during the Kenorland-Rodinia cycle. Although they may vary in detail, the concept of Rodinia- to Rodinia-type supercontinental cycles can provide a framework for understanding plate movements during successive cycles.

6 Synthesis

6.1 The Birimian event in the Baoulé Mossi domain

The model presented above for the evolution of the Man and Baoulé Mossi domains during the Birimian

event is an attempt to synthesize presently available data from these domains and place it in a realistic — albeit undoubtedly simplistic — and internally consistent model. While it represents one possible interpretation there are certainly others which may be equally valid. Due to the scarcity of good data from many parts of the Birimian crust in the WAC the model by necessity only covers the broadest aspects of the geodynamic evolution. The geodynamic model also suffers from a lack of structural data. Future developments should attempt to incorporate detailed tectonothermal data and attempt to connect this with the broad aspects of the geodynamic evolution within the Baoulé Mossi domain.

The geodynamic evolution of the Baoulé Mossi domain can be broadly characterized by an early accretionary stage followed by collision as the Birimian crust is juxtaposed with the Archean crust of the Man domain. The Archean crust in southeastern Ghana (and perhaps the Amapá block) appears to have been accreted earlier. This two-stage (accretionary-collisional) evolution has previously been recognized by workers in different parts of the Baoulé Mossi domain (e.g. Feybesse & Milési 1994; Vidal et al. 1996; Hirdes & Davis 2002; Feybesse et al. 2006; Baratoux et al. 2011).

However, the geodynamic model presented here emphasizes the diverse geodynamic settings within the Baoulé Mossi domain during the Eburnean phases which involve both collisional and accretionary settings. This is particularly true for the EII phase during which the southern part of the Baoulé Mossi domain (and its extension into the Guyana shield) is subjected to compression due to collision with the Man domain while central-northwestern Baoulé Mossi is subjected to extension in response to slab rollback. Meanwhile, northeastern Baoulé Mossi experienced little magmatic activity during or after the EII phase and appears to have been effectively shut off from the (magmatic, but perhaps also tectonothermal) activity affecting other parts of the Baoulé Mossi domain at this stage.

During the EII phase, the EIIB crustal domains (i.e. the Bandama-Banfora and Comoé-Sunyani sedimentary basins) assume an intermediate position between areas affected by extension and compression. Opening of the sedimentary basins may have been triggered by slab rollback were extension preferentially occurred along older structures established during the EI phase. Subsequent closure of these basins and emplacement of leucogranites within them may be attributed to post-collisional sinistral shearing. The leucogranites (2095-2080 Ma) assume a temporally intermediate position between peak metamorphism and late UTH-metamorphism in the Bakhuis belt (fig. 20). The apparent end of leucogranite emplacement at 2080 Ma may mark the point in time when the Baoulé Mossi domain began to experience post-collisional extension.

The Eburnean phases are characterized by the interaction between Archean and Birimian crust during a collision in which part of the eastward dipping subduction zone along the western margin of the Birimian crust remained active. As this collision may well have triggered slab rollback in the still active subduction zone (perhaps similar to the Banda arc following collision between Australia and Southeast Asia, e.g. Hall 2011) it would also have been a major factor in the geodynamic evolution of the areas outside of the immediate collision zone, such as the EII crustal domains.

Birimian magmatic and tectonothermal activity in the Baoulé Mossi domain can be explained largely by modern-style plate tectonic processes and may be comparable to modern settings that are defined by a high heat flow due to long-lived subduction, e.g. Sundaland (Hall 2011) in Southeast Asia or the North American Cordilleras (Hyndman et al. 2005; Hyndman 2010). However, the presence of komatiites in the Niandan range suggests that the Birimian crust was nevertheless characterized by a higher geotherm than modern accretionary orogens. Using the terminology of Chardon et al. (2009), the Birimian event in the Baoulé Mossi domain and the Guiana shield would correspond to a mix of ultra-hot and mixed hot orogenic styles. The former corresponds to the accretionary stage of the Birimian event while the latter records the interaction between cooler and more rigid Archean crust with hot and weak Birimian crust during the collisional stage.

Many aspects of the Birimian event in the Baoulé Mossi domain remains poorly constrained. This includes the timing of high-P granulite metamorphism in southeastern Man domain, timing of collision between Archean and Birimian crust in eastern Baoulé Mossi as well as the extent of Archean crust in northwestern and southeastern (SASCA domain) Ivory Coast. Also, more constraints are needed on the coupled P-T-t-D history of Birmian crust within the Baoulé Mossi domain. Extension appears to have been important throughout the Birimian event and its effect could potentially be traced with coupled P-T-t-D data. The sedimentation history (transgressions, retrogressions etc.) and environment (lacustrine, marine or transitional) of the sedimentary basins may also yield further insight into the geodynamic history of the Baoulé Mossi domain.

The geodynamic model accounts for many characteristics of the Birimian event in the Baoulé Mossi domain and its extension into the Guiana shield. This includes the spatial and temporal distribution of magmatism as well as the broad aspects of the tectonothermal activity experienced by these areas. The model may form the basis for future geodynamic models, which take into account more detailed lithological, structural, metamorphic, geochemical and geochronological data.

6.2 The Birimian event in a global context

The Birimian event has been largely overlooked in the

literature regarding its role in supercontinent cycles and Paleoproterozoic environmental perturbations. However, it is important to recognize that the event culminates with the assembly of a continent between 2.10-1.95 Ga involving crustal blocks now located in Africa and South America but also (as discussed in sections 5.4 and 5.5.1) crust now present in East Antarctica, Western Australia and India. Equally important is to recognize that this collisional phase was preceded by long accretionary orogenic activity, perhaps extending as far back as 2.40 Ga.

The comparison between the assembly of Atlantica-Midgardia-Ur during the Birimian event and the assembly of Gondwana stems from the similarities between the Birimian crust in the WAC and Amazon Craton and the East African Orogen. These areas have extensive tracts of juvenile crust as well as accretionary and collisional stages of equivalent temporal extent. In addition, the development of accretionary orogens outboard to at least the "Midgardia-section" (e.g. Fraga et al. 2009b; Johansson 2009) of Atlantica-Midgardia-Ur is reminiscent of the Terra Australis accretionary orogeny, which developed outboard to Gondwana in the Neoproterozoic (Cawood & Buchan 2007). The diachronous assembly of Atlantica-Midgardia-Ur is also similar to the assembly of Gondwana were collisional orogens in the west began and ended earlier than those in the east, although they partly overlapped (e.g. Meert & Lieberman 2008; Fritz et al. 2013). Further comparisons between Atlantica-Midgardia-Ur and Gondwana requires more detailed reconstructions of the former, incorporating lithological, structural, metamorphic, geochemical and paleomagnetic data.

If accepting that Atlantica-Midgardia-Ur assembled in the same manner as Gondwana, then the breakup of Archean crust now present in North America, Greenland, Fennoscandia and Siberia during the Paleoproterozoic (e.g. Lahtinen et al. 2008; Ernst & Bleeker 2010) can be considered as equivalent to the breakup between Laurentia, the East European Craton, WAC and Amazon Craton during the Neoproterozoic, which coincided with the amalgamation of Gondwana (e.g. Johansson 2009; Nance et al. 2010; Stampfli et al. 2013). The subsequent assembly of the Archean continental blocks in North America, Greenland, Fennoscandia and Siberia along 2.10-1.80 Ga accretionary orogenic belts (e.g. Lahtinen et al. 2008; Whitmeyer & Karlstrom 2007) would by analogy be equivalent to the assembly of Laurasia. Amalgamation of the Fennoscandian crustal block with Volgo-Uralia-Sarmatia between 1.8-1.7 Ga (Bogdanova et al. 2008) may be equivalent with the Variscan-Hercynian orogeny when Laurasia and Gondwana merged to form Pangea (e.g. Stampfli et al. 2013).

The similarities between the assembly of Columbia and Pangea form the basis for the hypothesis that there are only two types of supercontinents — a Rodinia- and a Pangea-type — which form in alternately occurring iterations. As indicated by the similarities between Columbia and Pangea different supercontinent iterations assemble in the same sequence of events, played out over the same timescales and in which the participating crustal blocks assume largely the same relative positions. The hypothesis only considers the broad features of the assembly and breakup of a given supercontinent. Differences between subsequent iterations of a particular supercontinent type, such as the size and shape of crustal blocks, have evidently existed (see section 5.5.3.5).

Placing Ur next to Atlantic-Midgardia as shown in figure 24b may be somewhat forced, considering that it is here only based on limited — and admittedly selective — geological data. However, as discussed above, the idea of supercontinent iterations requires that the crustal blocks assume largely the same relative position in subsequent iterations. For this reason, crustal blocks that formed part of East Gondwana (largely corresponding to Ur, see figure 25 and section 5.4.3) should also have been present east of Atlantica-Midgardia. However, transfer of crustal blocks (see section 5.5.3.5) between different supercontinent iterations mean that not all crust in East Gondwana formed part of an East Atlantica-Midgardia paleocontinent. Determining the paleogeographic location of the continental blocks that constituted West Atlantica-Midgardia-Ur and East Atlantica-Midgardia-Ur will require more detailed geological and paleomagnetic data.

The correlation between positive excursions of $\delta^{13}C$ and $^{87}Sr/^{86}Sr$ and the accretionary and collisional stages of Gondwana and Atlantica-Midgardia-Ur (fig. 28) can be taken as further support for supercontinent cycles involving Rodinia- and Pangea-type supercontinents. It also suggests that there is a connection between Rodinia- to Pangea-type supercontinent cycles and oxygenation events during the early and late Proterozoic.

The similarities between the tectonic evolution during the assembly of Columbia in the Paleoproterozoic and Pangea in the Neoproterozoic-Paleozoic (fig. 26) — coupled with the coeval and equivalent environmental perturbations during these periods (fig. 28) — suggests that the processes related to the breakup of Rodinia can also be applied, with some modifications, to the breakup of Kenorland in the Neoarchean. This assumes that there was indeed one Neoarchean supercontinent as opposed to several smaller continents (Rogers 1996; Aspler & Chiarenzelli 1998; Bleeker 2003).

If Kenorland was the first supercontinent, "true" supercontinent cycles should correspond to the breakup of one Rodinia-type supercontinent and the assembly of the subsequent iteration of a Rodinia-type supercontinent. In this context, supercontinents such as Columbia, Pangea or Pannotia only represent transient stages during which enough crust (>75%, see Meert 2012) is aggregated to form a supercontinent. Even though they are here referred to as cycles, no Rodinia- to Rodinia-type supercontinent cycle is exactly the

same (exemplified by the apparent absence of an Atlantic-type ocean during the Kenorland- Rodinia cycle). However, they reflect the same underlying behavior and cyclicity, which can be traced back to the breakup of Kenorland in the Paleoproterozoic.

Because of the consistent behavior of continental blocks since the breakup of Kenorland, they may be grouped into three cells. These cells correspond to West Gondwana, Laurasia and East Gondwana during the Rodinia-Amasia cycle and their equivalents West Atlantica-Midgardia-Ur, Nena and East Atlantic-Midgardia-Ur during the Kenorland-Rodinia cycle. Transfer of continental blocks between cells may occur during the breakup of a given Rodinia-type supercontinent iteration, which correspond to the transition between two Rodinia- to Rodinia-type supercontinent cycles. Transfer occurs through docking and appears to be a dynamic process in which a given cell "loses" a continental block(s) to one cell but at the same time "gains" a block(s) from the other cell. This lead to a rotation of continental blocks between the cells, even as the size of the cells remains essentially constant.

A problem with this hypothesis is that there is so far only four possible supercontinents recognized, a fifth — Amasia — is currently being assembled. Assuming that there was one Neoarchean supercontinent this means that there has been two iterations each of a Rodinia- and Pangea-type supercontinent. There are therefore too few supercontinents to form an identifiable trend which obviously presents a problem when trying to identify cycles and iterations among them. However, there is not much that can be done regarding this aspect. While the lack of an identifiable trend is problematic it may be attributed to insufficient time passing since the supercontinent cycles were established in the late Neoarchean (fig. 27) to allow for the formation of multiple (>3) iterations of each supercontinent type and multiple Rodinia- to Rodinia-type supercontinent cycles. The lack of a trend is therefore not evidence for the absence of supercontinent cycles and iterations.

As it stands, the idea of supercontinent cycles involving only two alternating types of supercontinents (i.e. Rodinia or Pangea) is based primarily on the similarities between the assembly of Columbia in the late Paleoproterozoic and Pangea in the late Paleozoic. However, it is further supported by the behavior of $\delta^{13}C$ and $^{87}Sr/^{86}Sr$. More data is needed from the proposed Rodinia-type supercontinents (Kenorland, Rodinia and Amasia) to test the hypothesis. Despite uncertainties regarding the Rodinia-type supercontinents and the position of Ur, the simplicity of the hypothesis is by itself appealing. If correct, the idea of Rodinia- and Pangea-type supercontinents and iterations have the potential of providing constraints regarding the paleogeographic position of continental blocks going back to at least the Neoarchean, but also into the future.

The depictions of how continental blocks moved during the Kenorland-Rodinia and ongoing Rodinia-Amasia cycles are largely conceptual. While the reconstructions used in this work may be detailed enough to convey broad movements and trends during supercontinental cycles, they are also vague enough not to hinge on specific details regarding e.g. the exact position and orientation of continental blocks. However, this "vagueness" is of course also a weakness, as the model remains unproven. Time-dependent reconstructions — which account for all continental blocks and associated tectonothermal and magmatic activity — coupled with sedimentological, paleoclimatic and paleomagnetic data will be required to further test the validity of Rodinia- to Rodinia-type supercontinent cycles.

7 Conclusions

- The geodynamic evolution of Birimian crust in the southern West African Craton can be divided into four phases which; the Eoeburnean (EE, >2.13 Ga), Eburnean I (EI, 2.13-2.10 Ga), Eburnean II (EII, 2.10-2.07 Ga) and Eburnean III (EIII, <2.07 Ga). Although they have distinct characteristics, the phases nevertheless form part of a continuum and their temporal extent is only approximate. The Eburnean phases are equivalent to the Eburnean orogeny (e.g. Feybesse et al. 2006, Pouclet et al. 2006 and de Kock et al. 2012) and exerted the strongest control on the structure of the Birimian crust; this particularly applies to the first two phases.
- The EE phase corresponds to a period of juvenile crustal growth but also involved Archean crust at an early stage, perhaps as early as 2.20 Ga. The geochemical composition of volcanic and intrusive rocks indicates that this took place in an intra-oceanic accretionary orogenic setting. Emplacement of granites along with coeval deformation at 2.20-2.19 and 2.16-2.15 Ga indicate a complex geodynamic history, which involved both compression and extension within an accretionary orogenic setting. Such events may have been triggered by collision between arc terranes, changes in global plate geometry or a transition from flat to steep subduction (or vice versa).
- The EE crust in the Baoulé Mossi domain might have amalgamated around 2.15 Ga although subduction and accretion remained active outboard of this nucleus to its current west. The last 20 Myr constituted a transition period between the EE and EI phases, which may have involved west-directed subduction rollback with early basin opening.
- During the EI phase Birimian crust of the southernmost Baoulé Mossi domain and its extension in the Amazon Craton began to be squeezed between Archean and Siderian-early Rhyacian crust in the present-day east and the

Archean crust of the Man domain in the west. However, the rest of the Baoulé Mossi domain saw continued slab rollback, which may have provided an extensional force for opening of sedimentary basins. The structures established in the Baoulé Mossi domain during the EI phase may record block rotation and represent the interaction between slab rollback and early collision.

- Intrusions of K-rich rocks in eastern Baoulé Mossi during the later part of the EI phase such as the Winneba (sample 001A, Appendix A), Tonton (Adadey et al. 2009) and Tenkodogo-Yamba (Naba et al. 2004) plutons may record the progressive movement of the trench towards the west due to slab rollback. Rollback may have been triggered by early oblique impingement of the Archean crust in the Man domain on the Birimian crust.
- The geodynamic evolution in different parts of the Baoulé Mossi domain during the Eburnean II phase was very diverse. Different areas of the Baoulé Mossi domain was subject to both compression (EE, EI and EIIB domains in Ivory Coast and Ghana) and extension (EIIA domain in Guinea and Senegal) even as some areas were largely unaffected, at least by magmatic activity (EE and EI domains in Burkina Faso). The contrasting geodynamic histories of different areas of the Baoulé Mossi domain reflect an interplay between stresses applied upon the thin, hot and weak Birmian crust as it converged with more rigid Archean cratons in the south while subduction rollback occurred in the northwest. In some cases, structures established during earlier stages of convergence controlled the location of subsequent deformation and/or magmatism.
- The formation of the EIIA domain with associated alkali-calcic magmatism and komatiite-basalt volcanics indicate that the area was subjected to a large degree of extension. This may be attributed to slab rollback in response to the collision of the Archean crust of the Man domain with the Birimian crust of the Baoulé Mossi domain, which at this time reached its peak. The EIIA domain may perhaps be connected with the Eglab and Yetti massifs in the Reguibat shield, which together may constitute an example of a Paleoproterozoic siliceous large igneous province.
- Cooling and stabilization of the Birimian crust in the Baoulé Mossi domain characterized the EIII phase. Crustal anatexis in the southeastern Man domain took place in response to post-collisional relaxation following the orogenic peak during the EII phase. Late alkaline intrusions and reactivation of shear zones may be far-field effects of accretionary orogens outboard of the amalgamated Birmian crust in the Baoulé Mossi domain, e.g. in the Amazon Craton.
- The formation of the Birimian crust may be accounted for by processes which take place in modern tectonic setting that have a high geotherm. A key aspect is that modern backarcs are defined by a high heat flow and thin lithosphere (e.g. Hyndman et al. 2005). If the interpretation that the Birimian crust originated as amalgamated arc terranes is correct it follows that the crust should also have the characteristics of modern backarcs, reflecting long-lived subduction. Modern backarcs such as Sundaland in SE Asia (Hall 2011) or the North American Cordilleras (Hyndman 2010) show that such areas may be affected by widespread shearing, intraplate deformation, lower crustal flow or detachment and vertical motions; all owing to the weak and hot nature of the lithosphere. However, the presence of komatiites, traditionally associated with hot mantle plumes, in the Baoulé Mossi domain nevertheless indicates that the geotherm was indeed higher compared to modern backarcs.
- From a plate tectonic perspective there are several similarities between the assembly of the Atlantica-Midgardia continent and that of Gondwana in the late Neoproterozoic-early Paleozoic, both in terms of geometry, timescales and the crustal blocks involved. In particular, the Birimian crust in the West African Craton and Amazon Craton shows many similarities with the Neoproterozoic East African Orogen which might indicate that these areas assumed the same relative position during the assembly of Atlantica-Midgardia and Gondwana, respectively.
- Similarities between Columbia and Pangea hint at a supercontinent cyclicity in which there is two fundamental supercontinent types — Rodinia and Pangea — that occur alternately in cycles going from a Rodinia to Pangea-type, or vice versa. Different iterations of the supercontinents involve largely the same crustal blocks in the same relative positions. Rodinia- to Pangea- cycles are associated with the Paleoproterozoic Great Oxidation Event and the Neoproterozoic Oxygenation Event which indicate that this type of cycles may have exerted a strong control on the evolution of Earth's atmosphere and, by extension, the rise of metazoans in the Phanerozoic.
- The first supercontinent to have formed appears to have been Kenorland in the late Neoarchean. Therefore, supercontinental cycles involving the breakup of one Rodinia-type supercontinent and the subsequent assembly of the next Rodinia-type supercontinent (i.e. Kenorland-Rodinia and Rodinia-Amasia) represent "true" supercontinent cycles. In this context, supercon-

tinents such as Columbia, Pannotia or Pangea are only transient stages during which enough crust is aggregated to constitute a supercontinent.

- Based on the similarities between the assembly of Columbia and Pangea, breakup of Kenorland and assembly of Rodinia in the Paleo- and Mesoproterozoic probably mirrored the "inside-out" breakup of Rodinia (Hoffman 1991) and the ongoing assembly of Amasia. During the Kenorland-Amasia cycle, Atlantica-Midgardia, Nena and Ur (see section 5.4) therefore assumed the same relative role as West Gondwana, Laurasia and East Gondwana, respectively, in the current Rodinia-Amasia cycle,
- The consistent behavior of most continental blocks since the breakup of Kenorland suggests that they may be divided into "continental cells" comprising the continental blocks in West Gondwana/Atlantica, Laurasia/Nena and East Gondwana/Atlantica (Ur). Each cell is characterized by a particular behavior during a Rodinia- to Rodinia-type supercontinent cycle. Transfer of continental blocks between cells may take place during the breakup of a Rodinia-type supercontinent. Transfer appear to occur in a dynamic fashion in which a given cell "loses" a block to one cell but at the same time "gains" a block from another cell.
- Although there are differences between the Kenorland-Rodinia and Rodinia-Amasia cycles — exemplified by the apparent absence of an Atlantic-type ocean during the Proterozoic — they are still controlled by the same fundamental cyclicity that was established during the breakup of Kenorland.

8 Future work

- Continue to collect published geochronological and geochemical (whole rock and isotopic) data from Birimian crust in the WAC, preferably in GIS based databases, and expand this to include published metamorphic and structural data. Metamorphic data should include quantitative P-T estimates as well as metamorphic index minerals and mineral assemblages.
- Using the GIS databases together with published geological maps to digitize a new, GIS-based geological map (scale 1:2,000,000?) for the Baoulé Mossi and Man domains, which should also include a simplified metamorphic map. This should be done using lithological divisions which can be extrapolated to Birimian crust elsewhere, such as the São Luís Craton, Reguibat shield and Amazon Craton. This will allow for better comparative studies between these areas.
- The lithological divisions for such a new geological map should try to incorporate the compositional variety among intrusive rocks (for example using the classification system of Le Maitre et al. 2002 in a similar manner to Stephens et al. 2009) and the different depositional environments (deep or shallow water, marine or lacustrine, cf. Johnson et al. 2011) and magmatic styles of the sedimentary basins. Recognizing the spatial (and temporal) extent of these characteristics is essential for further refined geodynamic models for the Birimian event.
- Define geological domains based on lithological, structural, chemical and geochronological data for which lithostratigraphic columns may be constructed. These may subsequently form the basis for comparative studies between these different domains.
- GIS databases should also be expanded to cratons and orogenic belts outside of the WAC which contain Birimian crust. Such databases should at least include geochronological and isotopic (Sm-Nd) data as well as the timing and extent of granulite and eclogite (if and were present) facies metamorphism, as a marker for collisional orogens. This can subsequently be used to trace the assembly of the Atlantica-Midgardia-Ur continent.
- Considering other cratons and orogenic belts outside of the WAC, a particular focus should be placed on the Amazon Craton because of its relatively well constrained relationship with the WAC (e.g. Onstott et al. 1984; Nomade et al. 2003), its large exposures of Birimian and Archean crust, and its importance for understanding the geodynamic evolution within the Baoulé Mossi domain.
- The importance of working on now separate cratons in order to understand the geodynamic evolution during the Birimian event requires accurate plate tectonic reconstructions. Plate reconstruction software such as GPlates (Williams et al. 2012) is compatible with common GIS file formats. This makes it possible to combine GIS datasets, containing e.g. geochronological and metamorphic data, together with geological maps (with a common legend, see above) from different cratons to make more geometrically accurate plate reconstructions.
- Make a more detailed comparative study between the Birimian event in the WAC-Amazon Craton and the East African Orogen in particular and the assembly of Atlantica-Midgardia-Ur and Gondwana in general. Here, the focus should be on similarities or differences relating to the timing, duration and style of tectonothermal and magmatic activity. Robust paleomagnetic data, were available, should also be incorporated. This should subsequently be related to the environmental perturbations which took place during the assembly of these respective

paleocontinents (i.e. the Paleoproterozoic Great Oxidation Event and the Neoproterozoic Oxygenation Event, see figure 28).

- Further investigations into supercontinent cycles and iterations should include detailed compilation of the geological history of continental blocks across the Earth which — together with robust paleomagnetic data — can be used to make reconstructions of their movements during Rodinia- to Rodinia-type supercontinent cycles. Ultimately, since supercontinent cycles and iterations are global and span at least the Proterozoic and Phanerozoic, further investigations will eventually require global datasets including lithological, geochronologic, isotopic, paleomagnetic and paleoclimatic data.
- Petrological studies investigating the differences between magmatism during different phases and areas of the Birimian event regarding features such as contributing sources and P-T conditions at the time of melting. This could for example take the shape of a comparative study between the Kumasi, Sunyani and Maluwe basins to identify secular trends in magmatic style.
- Cataloguing the spatial and temporal distribution of (black) shales within the Birimian crust to determine whether the relative abundance of shales can account for the positive carbon-isotope excursion during the Lomagundi-Jatuli Event. Re-Os dating on black shales may be able to provide accurate temporal constraints on the age of deposition, as could intrusive and stratigraphic relationships with other dated rocks.
- Locate Birimian carbonates that can be analyzed for carbon isotopes. The presence of extrusive and intrusive rocks within the Birimian crust may present opportunities to date more precisely the depositional age of such carbonates that can improve the temporal resolution of the Lomagundi-Jatuli Event (e.g. Melezhik et al. 2013).

9 Acknowledgements

I would like to take this opportunity to thank my supervisor Anders Scherstén for initially giving me the opportunity to work on the Birmian event as a Bachelor thesis project and to continue this work through my Master thesis. He is also thanked for providing suggestions, criticisms and corrections which significantly improved both the content and readability of the thesis.

This work is largely derived from the compilation and study of literature data. It would not have been possible to make if it had not been for the data and observations made available through the effort of many workers through the years.

Finally, the excellent geochemical software GCDkit 3.0 (Janoušek et al. 2006) has been used for plotting the geochemical diagrams presented in this text.

10 References

Abdelsalam, M.G., Liégeois, J.P. & Stern, R.J., 2002: The Saharan Metacraton. *Journal of African Earth Sciences 34*. 119-136.

Abdou, A., Blin, G., Kadey, B.D., Hirbec, Y., Regnoult, J.M. & Younfa, I., 1992: *Mise en execution du plan de développement mineral du Niger*. Unpublished report, Ministry of Mines and Energy of Niger, Niamey.

Abdou, A., Bonnot, H., Kadey, B.D., Chalamet, D., Saint Martin, M. & Younfa, I., 1998: *Notice explicative des cartes géologiques du Liptako à 1/100000 et 1/200000*. Direction de la Recherche Géologique et Minière, Ministère du Mines de la Géologie, Niamey, Niger.

Abouchami, W., Boher, M., Michard, A. & Albarède, F., 1990: A major 2.1 Ga event of mafic magmatism in West Africa: An early stage of crustal accretion. *Journal of Geophysical Research 95*. 17605-17629.

Adadey, K., Théveniaut, H., Clarke, B., Urien, P., Delor, C., Roig, R.J. & Feybesse, J.L., 2009: *Geological map explanation - map sheet 0503B (1:100000)*. CGS/BRGM/Geoman/GSD. 156 pp.

Agbossoumondé, Y., Ménot, R-P., Paquette, J.L., Guillot, S., Yéssoufou & Perrache, C., 2007: Petrological and geochronological constraints on the origin of the Palimé-Amlamé granitoids (south Togo, West Africa): A segment of the West African Craton Paleoproterozoic margin reactivated during the Pan-African collision. *Gondwana Research 12*. 476-488.

Agyei Duodu, J., Loh, G.K., Hirdes, W., Boamah, K.O., Baba, M., Anokwa, Y.M., Asare, C., Brakohiapa, E., Mensah, R.B., Okla, R., Toloczyki, M., Davis, D.W. & Glück, S., 2009: *Geological Map of Ghana 1:1000000*. BGS/GGS, Accra, Ghana/Hannover, Germany.

Ama-Salah, I., Liégeois, J.-P. & Pouclet, A., 1996: Evolution d´un arc insulaire océanique birimien précoce au Liptako nigérien (Sirba): géologie, géochronologie et géochimie. *Journal of African Earth Sciences 22*. 235-254.

Anderson, D.L., 1982: Hotspots, polar wander, Mesozoic convection and the geoid. *Nature 297*. 391-393.

Anderson, D.L., 2001: Top-down tectonics? *Science 293*. 2016-2018.

Arculus, R.J., 1987: The significance of source versus process in the tectonic controls of magma genesis. *Journal of Volcanology and Geothermal Research 32*. 1-12.

Arculus, R.J. 1994: Aspects of magma genesis in arcs. *Lithos 33*.189-208.

Asiedu, D.K., Kutu, J.M., Manu, J. & Hayford, E.K., 2009: Geochemistry and provenance of metagrey-

wackes from the Konongo area, southwestern Ghana. *African Journal of Science and Technology 10*. 37-44.

Aspler, L.B. & Chiarenzelli, J.R., 1998: Two Neoarchean supercontinents? Evidence from the Paleoproterozoic. *Sedimentary Geology 120*. 75-104.

Assie, K.E., 2008: *Lode gold mineralization in the Paleoproterozoic (Birimian) volcano-sedimentary sequence of Afema gold district, southeastern Côte d'Ivoire*. Phd thesis, Technical University of Clausthal. Germany. 166 pp.

Attoh, K., 1982: Structure, gravity models and stratigraphy of an early Proterozoic volcanic-sedimentary belt in northeastern Ghana. *Precambrian Research 18*. 275-290.

Attoh, K.., Evans, M.J. & Bickford, M.E., 2006: Geochemistry of an ultramafic-rodingite rock association in the Paleoproterozoic Dixcove greenstone belt, southwestern Ghana. *Journal of African Earth Sciences 45*. 333-346.

Avelar, V.G., Lafon, J.M., Delor, C., Guerrot, C. & Lahondère, D., 2003: Archean crustal remnants in the easternmost part of the Guiana Shield: Pb-Pb and Sm-Nd geochronological evidence for Mesoarchean versus Neoarchean signatures. *Géologie de la France 2-3-4*. 83-99.

Baratoux, L., Metelka, V., Naba, S., Jessell, M.W., Grégoire, M. & Ganne, J., 2011: Juvenile Paleoproterozoic crust evolution during the Eburnean orogeny (2.2-2.0 Ga), western Burkina Faso. *Precambrian Research 191*. 18-45.

Barbarin, B., 1996: Genesis of the two peraluminous granitoids. *Geology 24*. 295-298.

Bard, J.P & Lemoine, S., 1976: Phases tectoniques superposes dans les metasediments Precambriens du domaine cotier occidental de la Cote d'Ivoire. *Precambrian Research 3*. 209-229.

Barley, M.E., Bekker, A. & Krapež, B., 2005: Late Archean to early Paleoproterozoic global tectonics, environmental change and the rise of atmospheric oxygen. *Earth and Planetary Science Letters 238*. 156-171.

Barth, M.G., Rudnick, R.L., Carlson, R.W., Horn, I. & McDonough, W.F., 2002: Re-Os and U-Pb geochronological constraints on the eclogite-tonalite connection in the Archean Man shield, West Africa. *Precambrian Research 118*. 267-283.

Bea, F., Montero, P., Haissen, F. & El Archi, A., 2013: 2.46 Ga kalsilite and nepheline syenites from the Awsard pluton, Reguibat Rise of the West African Craton, Morocco. Generation of extremely K-rich magmas at the Archean-Proterozoic transition. *Precambrian Research 224*. 242-254.

Beckinsale, R.D., Gale, N.H., Pankhurst, R.J., MacFarlane, A., Crow, M.J., Arthurs, J.W. & Wilkinson, A.F., 1980: Discordant Rb-Sr and Pb-Pb whole rock isochron ages for the Archaean basement of Sierra Leone. *Precambrian Research 13*. 63-76.

Bédard, J.H., 2006: A catalytic delamination-driven model for coupled genesis of Archaean crust and sub-continental lithospheric mantle. *Geochimica et Cosmochimica Acta 70*. 1188-1214.

Bekker, A. & Holland, H.D., 2012: Oxygen overshoot and recovery during the early Paleoproterozoic. *Earth and Planetary Science Letters 317-318*. 295-304.

Belousova, E.A., Kostitsyn, Y.A., Griffin, W.L., Begg, G.C., O'Reilly, S.Y. & Pearson, N.J., 2010: The growth of the continental crust: Constraints from zircon Hf-isotope data. *Lithos 119*. 457-466.

Béziat, D., Bourges, F., Debat, P., Lompo, M., Martin, F. & Tollon, F., 2000: A Paleoproterozoic ultramafic-mafic assemblage and associated volcanic rocks of the Boromo greenstone belt: fractionates originating from island-arc volcanic activity in the West African craton. *Precambrian Research 101*. 25-47.

Billa, M., Feybesse, J.L., Bronner, G., Lerouge, C., Milési, J.P., Traoré, S. & Diaby, S., 1999: Les formations à quartzites rubanés ferrugineux de Mont Nimba et du Simandou: des unites empilées tectoniqument, dur un soubassement plutonique Archéen (craton de Kénéma-Man), lors de l'orogène Éburnéen. *Comptes Rendus de l'académie des sciences à Paris, Sciences de la terre et des planetès 329*. 287-294.

Black, R., 1980: Precambrian of West Africa. *Episodes 4*. 3-8.

Bleeker, W., 2003: The late Archean record: A puzzle in ca. 35 pieces. *Lithos 71*. 99-134.

Bogdanova, S.V., Bingen, B., Gorbatschev, R., Kheraskova, T.N., Kozlov, V.I., Puchkov, V.N. & Volozh, Yu.A., 2008: The East European Craton (Baltica) before and during the assembly of Rodinia. *Precambrian Research 160*. 23-45.

Boher, M., Abouchami, W., Michard, A., Albarède, F. & Arndt, N.T., 1992: Crustal growth in West Africa at 2.1 Ga. *Journal of Geophysical Research 97*. 345-369.

Bonin, B., 2007: A-type granites and related rocks: Evolution of a concept, problems and prospects. *Lithos 97*. 1-29.

Bossière, G., Bonkoungou, I., Peucat, J.J. & Pupin, J.P., 1996: Origin and age of Paleoproterozoic conglomerates and sandstones of the Tarkwaian Group in Burkina Faso, West Africa. *Precambrian Research 80*. 153-172.

Brito Neves, B.B., 2011: The Paleoproterozoic in the South-American continent: Diversity in the geological time. *Journal of South American Earth Sciences 32*. 270-286.

Brown, M., 2008: Characteristic thermal regimes of plate tectonics and their metamorphic imprint throughout Earth history: When did Earth first adopt a plate tectonics mode of behavior? *In* K.C. Condie & V. Pease (eds.): *When did plate tectonics begin on planet Earth?*, 97-128. The Geological Society of America Special Paper 440.

Bryan, S., 2007: Silicic large igneous provinces. *Epi-*

sodes 30. 20-31.

Bryan, S.E. & Ferrari, L., 2013: Large igneous provinces and silicic large igneous provinces: Progress in our understanding over the last 25 years. *GSA Bulletin 125*. 1053-1078.

Bullard, E., Everett, J.E. & Gilbert Smith, A., 1965: The fit of the continents around the Atlantic. *Philosophical Transactions of the Royal Society London A 258*. 41-51.

Campbell, I.H. & Allen, C.M., 2008: Formation of supercontinents linked to increases in atmospheric oxygen. *Nature Geoscience 1*. 554-558.

Campbell, I.H. & Squire, R.J., 2010: The mountains that triggered the Late Neoproterozoic increase in oxygen: The Second Great Oxidation Event. *Geochimica et Cosmochimica Acta 74*. 4187-4206.

Canfield, D.E., 2005: The early history of atmospheric oxygen: Homage to Robert M. Garrels. *Annual Review of Earth and Planetary Sciences 33*. 1-36.

Caby, R., Delor, C. & Agoh, O., 2000: Lithologie, structureet métamorphisme des formations birimiennes dans la region d'Odienné (Côte d'Iovire): Rôle majeur du diapirisme des plutons et des décrochements en bordure du craton de Man. *Journal of African Earth Sciences 30*. 351-374.

Caen-Vachette, M., 1988: Le craton oust-africain et le bouclier guyanais: Un seul craton au Protérozoïque inférieur?. *Journal of African Earth Sciences 7*. 479-488.

Castaing, C., Billa, M., Milési, J.-P., Thiéblemont, D., Le mentour, J., Egal, E., Donzeau, M., Guerrot, C., Cocherie, A., Chèvremont, P., Tegyey, M., Itard, Y., Zida, B., Ouedraogo, I., Kote, S., Kabore, B.E., Ouedraogo, C., Ki, J.C. & Zunino, C., 2003: *Notice explicative de la carte géologique et miniére du Burkina Faso à 1/1000000*. BRGM, BUMIGEB. 147 pp.

Cawood, P.A., Kröner, A. & Pisarevsky, S., 2006: Precambrian plate tectonics: Criteria and evidence. *GSA today 16*. 4-11.

Cawood, P.A. & Buchan, C., 2007: Linking accretionary orogenesis with supercontinent assembly. *Earth-Science Reviews 82*. 217-256.

Cawood, P.A., Kröner, A., Collins, W.J., Kusky, T.M., Mooney, W.D. & Windley, B.F., 2009: Accretionary orogens through Earth history. *In* P.A. Cawood & A. Kröner (eds.): *Earth accretionary systems in space and time*, 1-36. The Geological Society of London Special Publication 318.

Cawood, P.A., Hawkesworth, C.J. & Dhuime, B., 2013: The continental record and the generation of continental crust. *Geological Society of America Bulletin 125*. 14-32.

Chalokwu, C.I., Ghazi, M.A. & Foord, E.E., 1997: Geochemical characteristics and K-Ar ages of rare-metal bearing pegmatites from the Birimian of southeastern Ghana. *Journal of African Earth Sciences 24*. 1-9.

Chardon, D., Gapais, D. & Cagnard, F., 2009: Flow of ultra-hot orogens: A view from the Precambrian, clues for the Phanerozoic. *Tectonophysics 477*. 105-118.

Cheilletz, A., Barbey, P., Lama, C., Pons, J., Zimmermann, J.L. & Dautel, D., 1994: Age de refroidissement de la croûte juvenile Birimienne d'Afrique de l'Ouest. Donnés U-Pb, Rb-Sr et K-Ar sur les formations à 2.1 Ga du SW Niger. *Comptes Rendues de l'Académie des Sciences série II, Sciences de la terre et des planètes 319*. 435-442.

Cocherie, A., Legendre, O., Peucat, J.-J. & Kouamelan, A.N., 1998: Geochronology of polygenetic monazites constrained by in situ microprobe Th-U-total lead determination: Implications for lead behavior in monazite. *Geochimica et Cosmochimica Acta 62*. 2475-2497.

Condie, K.C., 1989: Geochemical changes in basalts and andesites across the Archean-Proterozoic boundary: Identification and significance. *Lithos 23*. 1-18.

Condie, K.C., 2008: Did the character of subduction change at the end of the Archean? Constraints from convergent-margin granitoids. *Geology 36*. 611-614.

Condie, K.C. & Kröner, A., 2008: When did plate tectonics begin? Evidence from the geologic record. *In* K.C. Condie & V. Pease (eds.): *When did plate tectonics begin on planet Earth?*, 281-294. The Geological Society of America Special Paper 440.

Condie, K.C., O´Neill, C. & Aster, R.C., 2009: Evidence and implications for widespread magmatic shutdown for 250 My on Earth. *Earth and Planetary Science Letters 282*. 294-298.

Condie, K.C., Bickford, M.E., Aster, R.C., Belousova, E. & Scholl, D.W., 2011: Episodic zircon ages, Hf isotopic composition, and the preservation rate of continental crust. *Geological Society of America Bulletin 123*. 951-957.

Cordani, U.G. & Teixeira, W., 2007: Proterozoic accretionary belts in the Amazonian Craton. *In* R.D. Hatcher Jr., M.P. Carlson, J.H. McBride & J.R. Martínez Catalán (eds.): *4-D framework of continental crust*, 297-320. The Geological Society of America Memoir 200.

Currie, C.A. & Hyndman, R.D., 2006: The thermal structure of subduction zone back arcs. *Journal of Geophysical Research 111*. B08404

Dalziel, I.W.D., 1997: Neoproterozoic-Paleozoic geography and tectonics: Review, hypothesis, environmental speculation. *GSA Bulletin 109*. 16-42.

Dampare, S., Shibata, T., Asiedu, D. & Osae, S., 2005: Major-element geochemistry of Proterozoic Prince´s Town granitoid from the southern Ashanti belt, Ghana. *Okayama University Earth Science Reports 12*. 15-30.

Dampare, S.B., Shibata, T., Asiedu, D.K., Osae, S. & Banoeng-Yakubo, B., 2008: Geochemistry of Paleoproterozoic metavolcanic rocks from the southern Ashanti volcanic belt, Ghana: Petrogenetic and tectonic setting implications. *Precam-*

brian Research 162. 403-423.

Dampare, S., Shibata, T., Asiedu, D., Koano, O., Manu, J. & Sakyi, P., 2009: Sr-Nd isotopic compositions of Paleoproterozoic metavolcanic rocks from the southern Ashanti volcanic belt, Ghana. *Okayama University Earth Science Reports 16*. 9-28.

Davis, D.W., Hirdes, W., Schaltegger, U. & Nunoo, E.A., 1994: U-Pb age constraints on deposition and provenance of Birimian and gold-bearing Tarkwaian sediments in Ghana, West Africa. *Precambrian Research 67*. 89-107.

Debat, P., Nikiéma, S., Mercier, A., Lompo, M., Béziat, D., Bourges, F., Roddaz, M., Salvi, S., Tollon, F. & Wenmenga, U., 2003: A new metamorphic constraint for the Eburnean orogeny from Paleoproterozoic formations of the Man shield (Aribinda and Tampelga countries, Burkina Faso). *Precambrian Research 123*. 47-65.

Debon, F. & Le Fort, P., 1983: A chemical-mineralogical classification of common plutonic rocks and associations. *Transactions of the Royal Society of Edinburgh; Earth and Environmental Science 73*. 135-149.

de Kock, G.S., Botha, P.M.W., Théveniaut, H. & Gyapong, W., 2009: *Geological map explanation - map sheet 0803B (1:100000)*. CGS/BRGM/Geoman/GSD. 354 pp.

de Kock, G.S., Armstrong, R.A., Siegfried, H.P. & Thomas, E., 2011: Geochronology of the Birim supergroup of the West African craton in the Wa-Bolé region of west-central Ghana: Implications for the stratigraphic framework. *Journal of African Earth Sciences 59*. 1-40.

de Kock, G.S., Théveniaut, H., Botha, P.M.W. & Gyapong, W., 2012: Timing the structural events in the Paleoproterozoic Bolé-Nangodi belt terrane and adjacent Maluwe basin, West African craton, in central-west Ghana. Journal *of African Earth Sciences 65*. 1-24.

Delor, C., Siméon, Y., Vidal, M., Zéadé, Z., Koné, Y., Adou, M., Dibouahi, J., Bi-Irié, D., Yao, B.D., N'Da, D., Pouclet, A., Konan, G., Diaby, I., Chiron, J.C., Dommanget, A., Kouamelan, A., Peucat, J.J., Cocherie, A. & Cautru, J.P., 1995: *Carte géologique de la Côte-d'Ivoire 1/200000, feuille de Nassian*. Ministère des Mines et de l'Energie. DMG, Abidjan, Côte d'Ivoire.

Delor, C., Roever, E.W.F., Lafon, J.M., Lahondère, D., Rossi, P., Cocherie, A., Guerrot, C. & Potrel, A., 2003a: The Bakhuis ultrahigh-temperature granulite belt (Suriname): II. Implications for late Transamazonian crustal stretching in a revised Guiana Shield framework. *Géologie de la France 2-3-4*. 207-230.

Delor, C., Lahondère, D., Egal, E., Lafo, J.M., Cocherie, A., Guerrot, C., Rossi, P., Truffert, C., Théveniaut, H., Phillips, D. & Avelar, V.G., 2003b: Transamazonian crustal growth and reworking as revealed by the 1:500,000-scale geological map of French Guiana (2nd edition). *Géologie de la France 2-3-4*. 5-57.

Delor, C., Milesi, J.P., Lafon, J.M. & Krymsky, R., 2004: *The Akwatia diamond-bearing tuffisite dykes swarm (Ghana): Syntectonic products of deep mantle origin emplaced during the final stages of the Eburnian orogeny (2050-2000 Ma)*. Abstracts volume 20th Colloquium of African Geology – Orleans, France. 128 pp.

Des Marais, D.J., 1994: Tectonic control of the crustal organic carbon reservoir during the Precambrian. *Chemical Geology 114*. 303-314.

De Waele, B., Johnson, S.P. & Pisarevsky, S.A., 2008: Palaeoproterozoic to Neoproterozoic growth and evolution of the eastern Congo Craton: Its role in the Rodinia puzzle. *Precambrian Research 160*. 127-141.

Dewey, J.F., 2007: The secular evolution of plate tectonics and the continental crust: An outline. *In* R.D. Hatcher Jr., M.P. Carlson, J.H. McBride & J.R. Martínez Catalán (eds.): *4-D framework of continental crust*, 1-7. The Geological Society of America Memoir 200.

Dia, A., 1988: *Caractère et signification des complexes magmatiques et métamorphiques du secteur de Sandikounda-Laminia (nord de la boutonnière de Kédougou, est du Sénégal); une modéle géodynamique du Birimien de l'Afrique de l'ouest*. Unpublished Phd thesis, University of Dakar, Sénégal. 350p.

Dia, A., Van Schmus, W.R. & Kröner, A., 1997: Isotopic constraints on the age and formation of a Paleoproterozoic volcanic arc complex in the Kedougou Inlier, eastern Senegal, West Africa. *Journal of African Earth Sciences 24*. 197-213.

Dilek, Y. & Furnes, H., 2011: Ophiolite genesis and global tectonics: Geochemical and tectonic fingerprinting of ancient oceanic lithosphere. *Geological Society of America Bulletin 123*. 387-411.

Dioh, E., Béziat, D., Debat. P., Grégoire, M. & Ngom, P.M., 2006: Diversity of the Paleoproterozoic granitoids of the Kédougou inlier (eastern Sénégal): Petrographical and geochemical constraints. *Journal of African Earth Sciences 44*. 351-371.

Doumbia, S., Pouclet, A., Kouamelan, A., Peucat, J.J., Vidal, M. & Delor, C., 1998: Petrogenesis of juvenile-type Birimian (Paleoproterozoic) granitoids in central Côte d'Ivoire, West Africa: geochemistry and geochronology. *Precambrian Research 87*. 33-63.

Egal, E., Thiéblemont, D., Lahondére, D., Guerrot, C., Costea, C.A., Iliescu, D., Delor, D., Goujou, J-C., Lafon, J.M., Tegyey, M., Diaby, S. & Kolié, P., 2002: Late Eburnean granitization and tectonics along the western and northwestern margin of the Archean Kénéma-Man domain (Guinea, West African Craton). *Precambrian Research 117*. 57-84.'

Eisenlohr, B.N. & Hirdes, W., 1992: The structural

development of the early Proterozoic Birimian and Tarkwaian rocks of southwest Ghana, West Africa. *Journal of African Earth Sciences 14*. 313-325.

El Bahat, A., Ikenne, M., Söderlund, U., Cousens, B., Youbi, N., Ernst, R., Soulaimani, A., El Janati, M. & Hafid, A., 2013: U-Pb baddeleyite ages and geochemistry of dolerite dykes in the Bas Drâa inlier of the Anti-Atlas of Morocco: Newly identified 1380 Ma event in the West African Craton. *Lithos 174*. 85-98

Ennih, N. & Liégeois, J.P., 2008: The boundaries of the West African Craton, with special reference to the basement of the Moroccan metacratonic Anti-Atlas belt. *In* N. Ennih & J.P. Liégeois (eds.): *The boundaries of the West African Craton*, 1-17. The Geological Society of London Special Publication 297.

Ernst, R. & Bleeker, W., 2010: Large igneous provinces (LIPs), giant dyke swarms, and mantle plumes: Significance for breakup events within Canada and adjacent regions from 2.5 Ga to the Present. *Canadian Journal of Earth Sciences 47*. 695-739.

Ernst, R.E., Bleeker, W., Söderlund, U. & Kerr, A.C., 2013: Large Igneous Provinces and supercontinents: Toward completing the plate tectonic revolution. *Lithos 174*. 1-14.

Evans, D.A.D. & Mitchell, R.N., 2011: Assembly and breakup of the core of Paleoproterozoic-Mesoproterozoic supercontinent Nuna. *Geology 39*. 443-446.

Fernandez-Alonso, M., Cutten, H., De Waele, B., Tack, L., Tahon, A., Baudet, D. & Barritt, S.D., 2012: The Mesoproterozoic Karagwe-Ankole Belt (formerly the NE Kibaran belt): The result of prolonged extensional intracratonic basin development punctuated by two short-lived far-field compressional events. *Precambrian Research 216-219*. 63-86.

Feybesse, J.L., Milési, J.P., Verhaeghe, P. & Johan, V., 1990: Le domaine de Toulépleu-Ity (Côte-d'Ivoire): Une unite "birrimienne" charriée sur les gneiss archeéens du domiane de Kénéma-Man lors des premiers stades de l'orogène éburnéen. *Comptes Rendus de l'Académie des sciences à Paris série II 310*. 285-291.

Feybesse, J.L. & Milési, J.-P., 1994: The Archean/Paleoproterozoic contact zone in West Africa: a mountain belt of décollement thrusting and folding on a continental margin related to 2.1 Ga convergence of Archean cratons? Precambrian *Research 69*. 199-227.

Feybesse, J.L., Billa, M., Guerrot, C., Duguey, E., Lescuyer, J.L., Milési, J.P. & Bouchot, V., 2006: The Paleoproterozoic Ghanaian province: Geodynamic model and ore controls, including regional stress modeling. *Precambrian Research 149*. 149-196.

Fraga, L.M., Macambira, M.J.S., Dall'Agnol, R. & Costa, J.B.S., 2009a: 1.94-1.93 Ga charnockitic magmatism from the central part of the Guyana Shield, Roraima, Brazil: Single-zircon evaporation data and tectonic implications. Journal *of African Earth Sciences 27*. 247-257.

Fraga, L.M., Reis, N.J. & Dall'Agnol, R., 2009b: *Cauarane-Coeroeni belt - the main tectonic feature of the central Guyana shield, northern Amazonian Craton*. Extended abstract. Simpósio de Geologia da Amazônia 11, Manaus, Amazonas.

Fritz, H., Abdelsalam, M., Ali, K.A., Bingen, B., Collins, A.S., Fowler, A.R., Ghebreab, W., Hauzenberger, C.A., Johnson, P.R., Kusky, T.M., Macey, P., Muhongo, S., Stern, R.J. & Viola, G., 2013: Orogen styles in the East African Orogen: A review of the Neoproterozoic to Cambrian tectonic evolution. *Journal of African Earth Sciences 86*. 65-106.

Frost, C.D. & Frost, R.B., 2011: On ferroan (A-type) granitoids: Their compositional variability and modes of origin. *Journal of Petrology 52*. 39-53.

Frost, R.B., Barnes, C.G., Collins, W.J., Arculus, R.J., Ellis, D.J. & Frost, C.D., 2001: A geochemical classification for granitic rocks. *Journal of Petrology 42*. 2033-2048.

Furnes, H., Dilek, Y. & de Wit, M., 2013: Precambrian greenstone sequences represent different ophiolite types. Gondwana Research, *In Press*. *http://dx.doi.org/10.1016/j.gr.2013.06.004*.

Galipp, K., Hirdes, W. & Klemd, R., 2003: Metamorphism and geochemistry of the Paleoproterozoic Birimian Sefwi volcanic belt, Ghana, West Africa. *Geologisches Jahrbuch Reihe D 111*. 151-191.

Ganne, J., De Andrade, V., Weinberg, R.F., Vidal, O., Dubacq, B., Kagambega, N., Naba, S., Baratoux, L., Jessell, M. & Allibon, J., 2012: Modern-style plate subduction preserved in the Palaeoproterozoic West African craton. *Nature Geoscience 5*. 60-65.

Gasquet, D., Barbey, P., Adou, M. & Paquette, J.L., 2003: Structure, Sr-Nd isotope geochemistry and zircon U-Pb geochronology of the granitoids of the Dabakala area (Cõte d´Ivoire): evidence for a 2.3 Ga crustal growth event in the Paleoproterozoic of West Africa? *Precambrian Research 127*. 329-354.

Gradstein, F.M., Ogg, J.M., Smith, A.G., Bleeker, W. & Lourens, L.J., 2004: A new geologic time scale, with special reference to Precambrian and Neogene. *Episodes 27*. 83-100.

Gray, D.R., Foster, D.A., Maas, R., Spaggiari, C.V., Gregory, R.T., Goscombe, B. & Hoffmann, K.H., 2007: Continental growth and recycling by accretion of deformed turbidite fans and remnant ocean basins: Examples from Neoproterozoic and Phanerozoic orogens. *In* R.D. Hatcher Jr., M.P. Carlson, J.H. McBride & J.R. Martínez Catalán (eds.): *4-D framework of continental crust*, 63-92. The Geological Society of America Memoir 200.

Gueye, M., Siegesmund, S., Wemmer, K., Pawlig, S.,

Drobe, M., Nolte, N. & Layer, P., 2007: New evidences for an early Birimian evolution in the West African Craton: An example from the Kedougou-Kéniéba inlier, southeast Senegal. *South African Journal of Geology 110*. 511-534.

Gueye, M., Ngom, P.M., Diène, M., Thiam, Y., Siegesmund, S., Wemmer, K. & Pawlig, S., 2008: Intrusive rocks and tectono-metamorphic evolution of the Mako Paleoproterozoic belt (eastern Senegal, West Africa). *Journal of African Earth Sciences 50*. 88-110.

Gurnis, M., 1988: Large-scale mantle convection and the aggregation and dispersal of supercontinents. *Nature 332*. 695-699.

Hall, R., 2011: Australia-SE Asia collision: Plate tectonics and crustal flow. *In* R. Hall, M. Cottam and M.E.J. Wilson (eds.): *The SE Asian gateway: History and tectonics of the Australia-Asia collision*, 75-109. The Geological Society of London Special Publication 355.

Hamilton, W.B., 2007: Earth´s first two billion years - The era of internally mobile crust. *In* R.D. Hatcher Jr., M.P. Carlson, J.H. McBride & J.R. Martínez Catalán (eds.): *4-D framework of continental crust*, 233-296. The Geological Society of America Memoir 200.

Hanson, R.E., 2003: Proterozoic geochronology and tectonic evolution of southern Africa. *In* M. Yoshida, B.F. Windley & S. Dasgupta (eds.): *Proterozoic east Gondwana: Supercontinent assembly and breakup*, 427-463. The Geological Society of London Special Publication 206.

Harcoüet, V., Guillou-Frottier, L., Boneville, A., Bouchot, V. & Milesi, J.P., 2007: Geological and thermal conditions before the major Palaeoproterozoic gold-mineralization event at Ashanti, Ghana, as inferred from improved thermal modeling. *Precambrian Research 154*. 71-87.

Hargraves, R.B., 1986: Faster spreading or greater ridge length in the Archean? *Geology 14*. 750-752.

Hayes, J.M. & Waldbauer, J.R., 2006: The carbon cycle and associated redox processes through time. *Philosophical Transactions of the Royal Society London B 361*. 931-950.

Hawkesworth, C., Cawood, P., Kemp, T., Storey, C. & Dhuime, B., 2009: A matter of preservation. *Science 323*. 49-50.

Hein, K.A.A., 2010: Succession of structural events in the Goren greenstone belt (Burkina Faso): Implications for West African tectonics. *Journal of African Earth Sciences 56*. 83-94.

Herzberg, C., Condie, K. & Korenaga, J., 2010: Thermal history of the Earth and its petrological expression. *Earth and Planetary Science Letters 292*. 79-88.

Hirdes, W. & Davis, D.W., 1998: First U-Pb zircon age of extrusive volcanism in the Birimian Supergroup of Ghana/West Africa. *Journal of African Earth Sciences 27*. 291-294.

Hirdes, W. & Davis, D.W., 2002: U-Pb geochronology of Paleoproterozoic rocks in the southern part of the Kedougou-Kéniéba Inlier, Senegal, West Africa: Evidence for diachronous accretionary development of the Eburnean Province. *Precambrian Research 118*. 83-99.

Hirdes, W., Davis, D.W. & Eisenlohr, B.N., 1992: Reassessment of Proterozoic granitoid ages in Ghana on the basis of U/Pb zircon and monazite dating. *Precambrian Research 56*. 89-96.

Hirdes, W., Senger, R., Adjei, J., Efa, E., Loh, G. & Tettey, A., 1993: *Explanatory notes for the geological map of southwest Ghana 1:100000: sheets Wiawso (0603D), Asafo (0603C), Kukuom (0603B), Goaso (0603A), Sunyani (0703D) and Berekum (0703C)*. Geologisches Jahrbuch Reihe B, Heft 83. 139 pp.

Hirdes, W., Davis, D.W., Lüdtke, G. & Konan, G., 1996: Two generations of Birimian (Paleoproterozoic) volcanic belts in northeastern Côte d'Ivoire (West Africa): Consequences for the "Birimian controversy". *Precambrian Research 80*. 173-191.

Hirdes, W., Konan, K.G., N'Da, D., Okou, A., Sea, P., Zamble, Z.B. & Davis, D.W., 2007: *Geology of the Northern Portion of the Oboisso Area, Cote d'Ivoire. Sheets 4A, 4B, 4B BIS, 4*. Direction de la Geologie, Abidjan, Cote d'Ivoire and Bundesanstalt fur Geowissenschaften und Rohstoffe, Hannover. 180 pp.

Hoffman, P.F., 1991: Did the breakout of Laurentia turn Gondwanaland inside-out?. *Science 252*. 1409-1412.

Hoffman, P.F., 2002: Stratigraphic and tectonic settings of Proterozoic glaciogenic rocks and banded iron formations: Relevance to the snowball Earth debate. *Journal of African Earth Sciences 35*. 451-466.

Hoffman, P.F., 2013: The Great Oxidation Event and a Siderian snowball Earth: MIF-S based correlation of Paleoproterozoic glacial epochs. Chemical Geology, *In Press. http: //dx.doi.org/10.1016/ j.chemgeo.2013. 04.018*.

Holland, H.D., 2006: The oxygenation of the atmosphere and oceans. *Philosophical Transactions of the Royal Society London B 361*. 903-915.

Hurley, P.M., Leo, G.W., White, R.W. & Fairbairn H.W., 1971: Liberian age provinces (2,700 m.y.) and adjacent provinces in Liberia and Sierra Leone. *GSA bulletin 82*. 3483-3490.

Hyndman, R.D., Currie, C.A., & Mazzotti, S.P., 2005: Subduction zone backarcs, mobile belts, and orogenic heat. *GSA Today 15*. 4-10.

Hyndman, R.D., 2010: The consequences of Canadian Cordillera thermal regime in recent tectonics and elevation: A review. *Canadian Journal of Earth Sciences 47*. 621-632

Janoušek, V., Farrow, C.M. & Erban, V., 2006: Interpretation of whole-rock geochemical data in igneous geochemistry: Introducing Geochemical Data Toolkit (GCDkit). *Journal of Petrology 47*. 1255-

1259.

Jessell, M.W., Amponsah, P.O., Baratoux, L., Asiedu, D.K., Loh, G.K. & Ganne, J., 2012: Crustal-scale transcurrent shearing in the Paleoproterozoic Sefwi-Sunyani-Comoé region, West Africa. *Precambrian Research 212-213*. 155-168.

Johansson, Å., 2009: Baltica, Amazonia and the SAMBA connection - 1000 million years of neighborhood during the Proterozoic?. *Precambrian Research 175*. 221-234.

John, T., Klemd, R., Hirdes, W. & Loh, G., 1999: The metamorphic evolution of the Paleoproterozoic (Birimian) volcanic Ashanti belt (Ghana, West Africa). *Precambrian Research 98*. 11-30.

Johnson, P.R., Andresen, A., Collins, A.S., Fowler, A.R., Fritz, H., Ghebreab, W., Kusky, T. & Stern, R.J., 2011: Late Cryogenian-Ediacaran history of the Arabian-Nubian Shield: A review of depositional, plutonic, structural, and tectonic events in the closing stages of the northern East African Orogen. *Journal of African Earth Sciences 61*. 167-232.

Johnson, S.P., Sheppard, S., Rasmussen, B., Wingate, M.T.D., Kirkland, C.L., Muhling, J.R., Fletcher, I.R. & Belousova, E.A., 2011: Two collisions, two sutures: Punctuated pre-1950 Ma assembly of the West Australian Craton during the Ophthalmian and Glenburgh Orogenies. *Precambrian Research 189*. 239-262.

Kahoui, M. & Mahdjoub, Y., 2004: An Eburnian alkaline-peralkaline magmatism in the Reguibat rise: The Djebel Drissa ring complex (Eglab Shield, Algeria). Journal *of African Earth Sciences 39*. 115-122.

Kalsbeek, F., Affaton, P., Ekwueme, B., Frei, R. & Thrane, K., 2012: Geochronology of granitoid and metasedimentary rocks from Togo and Benin, West Africa: Comparisons with NE Brazil. *Precambrian Research 196-197*. 218-233.

Karhu, J.A. & Holland, H.D., 1996: Carbon isotopes and the rise of atmospheric oxygen. *Geology 24*. 867-870.

Karikari, F., Ferrière, L., Koeberl, C., Reimold, W.U. & Mader, D., 2007: Petrography, geochemistry, and alteration of country rocks from the Bosumtwi impact structure, Ghana. *Meteoritics & Planetary Science 42*. 513-540.

Kasting, J.F., 2013: What caused the rise of atmospheric O_2? *Chemical Geology 362*. 13-25.

Keller, C.B. & Schoene, B., 2012: Statistical geochemistry reveals disruption in secular lithospheric evolution about 2.5 Gyr ago. *Nature 485*. 490-493.

Kemp, A.I.S. & Hawkesworth, C.J., 2003: Granitic perspectives on the generation and secular evolution of the continental crust. *In* R.L. Rudnick (ed.): *The crust*, 349-410. Treatise on Geochemistry Vol.3 (eds. H.D. Holland & K.K. Turekian).

Kerr, A.C., 2003: Oceanic plateaus. *In* R.L. Rudnick (ed.): *The crust*, 537-565. Treatise on Geochemistry Vol.3 (eds. H.D. Holland & K.K. Turekian).

Klein, E.L. & Moura, A.V. 2001: Age constraints on granitoids and metavolcanic rocks of the Sao Luis Craton and Gurupi Belt, northern Brazil: Implications for lithostrathigraphy and geological evolution. *International Geology Review 43*. 237-253.

Klein, E.L., Koppe, J.C. & Moura, C.A.V., 2002: Geology and geochemistry of the Caxias gold deposit, and geochronology of the gold-hosting Caxias microtonalite, São Luís Craton, northern Brazil. *Journal of South American Earth Sciences 14*. 837-849.

Klein, E.L., Moura, C.A.V., Krymsky, R.S. & Griffin, W.L., 2005a: The Gurupi belt, northern Brazil: Lithostrathigraphy, geochronology, and geodynamic evolution. *Precambrian Research 141*. 83-105.

Klein, E.L., Moura, C.A.V. & Pinheiro, B.L.S., 2005b: Paleoproterozoic crustal evolution of the Sao Luis craton, Brazil: Evidence from zircon geochronology and Sm-Nd isotopes. *Gondwana Research 8*. 177-186.

Klein, E.L., Luzardo, R., Moura, C.A.V. & Armstrong, R., 2008: Geochemistry and zircon geochronology of Paleoproterozoic granitoids: Further evidence on the magmatic and crustal evolution of the Sao Luis cratonic fragment, Brazil. *Precambrian Research 165*. 221-242.

Klein, E.L., Luzardo, R., Moura, C.A.V., Lobato, D.C., Brito, R.S.C. & Armstrong. R., 2009: Geochronology, Nd isotopes and reconnaissance geochemistry of volcanic and metavolcanic rocks of the São Luís Craton, northern Brazil: Implications for tectonic setting and crustal evolution. *Journal of South American Earth Sciences 27*. 129-145.

Klockner, I.A., 1991: *Carthographie géologie du sillon de Téra, Étude géochronologique*. Unpublished report, Ministry of Mines and Energy of Niger, Niamey.

Klemd, R., Hünken, U. & Olesch, M., 2002: Metamorphism of the country rocks hosting gold-sulfide-bearing quartz veins in the Paleoproterozoic southern Kibi-Winneba belt (SE-Ghana). *Journal of African Earth Sciences 35*. 199-211.

Koeberl, C., Reimold, W.U., Blum, J.D. & Chamberlain, C.P., 1998: Petrology and geochemistry of target rocks from the Bosumtwi impact structure, Ghana, and comparison with Ivory Coast tektites. *Geochimica et Cosmochimica Acta 62*. 2179-2196.

Kouamelan, A.N., 1996: *Géochronologie et géochimie des formations Archéenes et Protérozoïques de la dorsale de Man en Côte d´Ivoire: Implication pour la transition Archéen-Protérozoïque*. Mémoires de Géosciences Rennes 73. 290 pp.

Kouamelan, A.N., Delor, C. & Peucat, J.-J., 1997: Geochronological evidence for reworking of Archean terrains during the early Proterozoic (2.1 Ga) in the western Côte d´Ivoire (Man Rise-West African Craton). *Precambrian Research 86*. 177-199.

Kouyaté, D., Söderlund, U., Youbi, N., Ernst, R., Hafid, A., Ikenne, M., Soulaimani, A., Bertrand, H., El Janati, M. & Chaham, K.R., 2013: U-Pb baddeleyite and zirconages of 2040 Ma, 1650 Ma and 885 Ma on dolerites in the West African Craton (Anti-Atlas inliers): Possible links to break-up of Precambrian supercontinents. *Lithos 174*. 71-84.

Kříbek, B., Sýkorová, I., Machovič, V. & Laufek, F., 2008: Graphitization of organic matter and fluid-deposited graphite in Paleoproterozoic (Birimian) black shales of the Kaya-Goren greenstone belt (Burkina Faso, West Africa). *Journal of Metamorphic Petrology 26*. 937-958.

Lahondère, D., Thiéblemont, D., Tegyey, M., Guerrot, C. & Diabate, B., 2002: First evidence of early Birimian (2.21 Ga) volcanic activity in Upper Guinea: the volcanics and associated rocks of the Niani suite. *Journal of African Earth Sciences 35*. 417-431.

Lahtinen. R, Garde, A.A. & Melezhik, V.A., 2008: Paleoproterozoic evolution of Fennoscandia and Greenland. *Episodes 31*. 1-9.

Leake, M.H., 1992: *The petrogenesis and structural evolution of the early Proterozoic Fettekro greenstone belt, Dabakala region, NE Côte d'Ivoire*. Unpublished thesis, University of Portsmouth, U.K., 315 pp.

Ledru, P., Johan, V., Milési, J.P. & Tegyey, M., 1994: Markers of the last stages of the Paleoproterozoic collision: Evidence for a 2 Ga continent involving circum-South Atlantic provinces. *Precambrian Research 69*. 169-191.

Le Maitre, R.W., Streckeisen, A., Zanettin, B., Le Bas, M.J., Bonin, B., Bateman P., Bellieni, G., Dudek, A., Efremova, S., Keller, J., Lameyre, J., Sabine, P.A., Schmid, R., Sorensen, H. & Woolley, A.R., 2002: *Igneous rocks: A classification and glossary of terms recommendations of the International Union of Geological Sciences Subcommission on the systematics of igneous rocks*. Cambridge University Press. 252 pp.

Lemoine, S., 1988: *Evolution géologique de la région de Dabakala (NE de la Côted'Ivoire) au Protérozoïque. Possibilités d'extension au reste de la Côte-d'Ivoire et au Burkina Faso: similitudes et différences; les lineaments de Greenville-Ferkéssédougou et Grand-Cess-Niakaramandougou*. Thèse ès Sciences, Universite Clermont-Ferrand. 388 pp.

Lerouge, C., Feybesse, J.L., Guerrot, C., Billa, M. & Diaby, S., 2004: Reaction textures in Proterozoic calcsilicates from northern Guinea: A record of the fluid evolution. *Journal of African Earth Sciences 39*. 105-113.

Leube, A., Hirdes, W., Mauer, R. & Kesse, G.O., 1990: The early Proterozoic Birimian Supergroup of Ghana and some aspects of its associated gold mineralization. *Precambrian Research 46*. 139-165.

Li, Z.X., Bogdanova, S.V., Collins, A.S., Davidson, A., De Waele, B., Ernst, R.E., Fitzsimons, I.C.W., Fuck, R.A., Gladkochub, D.P., Jacobs, J., Karlstrom, K.E., Lu, S., Natapov, L.M., Pease, V., Pisarevsky, S.A., Thrane, K. & Vernikovsky, V., 2008: Assembly, configuration and break-up history of Rodinia: A synthesis. *Precambrian Research 160*. 179-210.

Liégeois, J.P., Claessens, W., Camara, D. & Klerkx, J., 1991: Short-lived Eburnian orogeny in southern Mali. Geology, tectonics, U-Pb and Rb-Sr geochronology. *Precambrian Research 50*. 111-136.

Liégeois, J.P., Latouche, L., Boughrara, M., Navez, J. & Guiraud, M., 2003: The LATEA Metacraton (Central Hoggar, Tuareg shield, Algeria): Behavior of an old passive margin during the Pan-African orogeny. *Journal of African Earth Sciences 37*. 161-190.

Lin, S., 2005: Synchronous vertical and horizontal tectonism in the Neoarchean: Kinematic evidence from a synclinal keel in the northwestern Superior craton, Canada. *Precambrian Research 139*. 181-194.

Lindsay, J.F. & Brasier, M.D., 2002: Did global tectonics drive early biosphere evolution? Carbon isotope record from 2.6-1.9 Ga carbonates of Western Australian basins. *Precambrian Research 114*. 1-34.

Lompo, M, 1991: *Etude structural et géologique des séries birimiennes de la region de Kwademen, Burkina Faso, Afrique de l'Ouest. In: Evolution et controle structural des minéralisations sulfurées et auriferes pendant l'Eburnéen*. Université de Clermont Ferrand, France. 192pp.

Lompo, M., 2009: Geodynamic evolution of the 2.25-2.0 Ga Paleoproterozoic magmatic rocks in the Man-Leo shield of the West African Craton. A model of subsidence of an oceanic plateau. *In* S.M. Reddy, R. Mazumder, D.A.D. Evans & A.S. Collins (eds.): *Paleoproterozoic supercontinents and global evolution*, 231-254. The Geological Society of London Special Publication 323.

Lompo, M., 2010: Paleoproterozoic structural evolution of the Man-Leo shield (West Africa). Key structures for vertical and transcurrent tectonics. *Journal of African Earth Sciences 58*. 19-36.

Lüdtke, G., Hirdes, W., Konan, K.G., Koné, Y., N'Da, D., Traoré, Y. & Zamblé, Z.B., 1992: *Geology of the Haute Comoé south area, geological map 1: 100000, sheets Dabakala 2b, d and 4b, d, 1st ed*. Ivorian-German Geological Cooperation Project (1995–1996).

Lüdtke, G., Hirdes,W., Konan, G., Koné, Y., Yao, C. & Zamblé, Z., 1998a: *Géologie de la région Haute Comoé Nord. Ministère des ressources minières et pétrolières de Côte d'Ivoire*, Direction de la Géologie Abidjan. Bulletin. 178 pp.

Lüdtke, G., Hirdes, W., Konan, G., Kone, Y., Yao, C., Diarra, S. & Zamble, Z., 1998b: *Geologie de la region Haute Comoe Nord—feuilles Kong (4b et*

4d) et Tehini-Bouna (3a a 3d). Direction de la Geologie Abidjan Bulletin. 178 pp.

Macambira, M.J.B., Vasquez, M.L., Silva, D.C.C., Galarza, M.A., Barros, C.E.M., & Camelo, J.F., 2009: Crustal growth of the central eastern Paleoproterozoic domain, SW Amazonian craton: juvenile accretion vs. reworking. *Journal of South American Earth Sciences 27*. 235-246.

Mahonty, S., 2013: Spatio-temporal evolution of the Satpura Mountain Belt of India: A comparison with the Capricorn Orogen of Western Australia and implication for evolution of the supercontinent Columbia. *Geoscience Frontiers 3*. 241-267.

Master, S., Bekker, A. & Hofmann, A., 2010: A review of the stratigraphy and geological setting of the Paleoproterozoic Magondi Supergroup, Zimbabwe — Type locality for the Lomagundi carbon isotope excursion. Precambrian *Research 182*. 254-273.

Mazzotti, S. & Hyndman R.D., 2002: Yakutat collision and strain transfer across the northern Canadian Cordillera. *Geology 30*. 495-498.

McFarlane, C.R.M., Mavrogenes, J., Lentz, D., King, K., Allibone, A. & Holcombe, R., 2011: Geology and intrusion-related affinity of the Morila gold mine, southeast Mali. *Economic Geology 106*. 727-750.

Meert, J.G., 2012: What's in a name? The Columbia (Paleopangea/Nuna) supercontinent. *Gondwana Research 21*. 987-993.

Meert, J.G., & Lieberman, B.S., 2008: The Neoproterozoic assembly of Gondwana and its relationship to the Ediacaran-Cambrian radiation. *Gondwana Research 14*. 5-21.

Melezhik, V.A., 2005: Multiple causes for Earth´s earliest global glaciations. *Terra Nova 18*. 130-137.

Melezhik, V.A., Fallick, A.E., Martin, A.P., Condon, D.J., Kump, L.R., Brasier, A.T. & Salminen 2013: The Paleoproterozoic perturbation of the global carbon cycle: the Lomagundi-Jatuli isotopic event. *In* V.A. Melezhik, L.R. Kump, A.E. Fallick, H. Strauss, E.J. Hanski, A.R. Prave & A. Lepland (eds.): *Reading the archives of Earths oxygenation. Volume 3: Global events and the Fennoscandian arctic Russia — drilling early earth project*, 1111-1150. Springer-Verlag, Berlin. 505 pp.

Metcalfe, I., 2013: Gondwana dispersion and Asian accretion: Tectonic and paleogeographic evolution of eastern Tethys. *Journal of African Earth Sciences 66*. 1-33.

Milési, J.P., Feybesse, J.L., Ledru, P., Dommanget, A., Ouedraogo, M.F., Tegyey, M., Calvez, J.Y. & Lagny, P., 1989: Les minéralisations aurifères de l'Afrique de l'Ouest; leur evolution lithostructurale au Protérozoique inférieur. *Chronique de la Recherche Minière 497*. 3-98.

Milési, J.P., Ledru, P., Feybesse, J.L., Dommanget, A. & Marcoux, E., 1992: Early Proterozoic ore deposits and tectonics of the Birimian orogenic belt, West Africa. *Precambrian Research 58*. 305-344.

Milési, J.P., Feybesse, J.L., Pinna, P., Deschamps, Y., Kampunzu, A.B., Muhongo, S., Lescuyer, J.L., Le Goff, E., Delor, C., Ralay, F. & Heinry, C., 2004: *Géologie et principaux gisements d'Afrique — Carte et SIG à 1/10 000 000*. Abstracts volume 20th Colloquium of African Geology – Orleans, France. 128 pp.

Mikhalsky, E.V., Henjes-Kunst, F., Belyatsky, B.V., Roland, N.W. & Sergeev, S.A., 2010: New Sm-Nd, Rb-Sr, U-Pb and Hf isotope systematics for the southern Prince Charles Mountains (East Antarctica) and its tectonic implications. *Precambrian Research 182*. 101-123.

Morley, C.K. & Westaway, R., 2006: Subsidence in the super-deep Pattani and Malay basins of Southeast Asia: A coupled model incorporating lower-crustal flow in response to post-rift sediment loading. *Basin Research 18*. 51-84.

Mortimer. J., 1992a: The Kan River Gneiss terrane of central Côte d´Ivoire: Mylonitic remnants of an ancient magmatic arc? *Journal of African Earth Sciences 15*. 353-367.

Mortimer. J., 1992b: Lithostrathigraphy of the early Proterozoic Toumodi Volcanic Group in central Côte d´Ivoire: Implications for Birrimian stratigraphic models. *Journal of African Earth Sciences 14*. 81-91.

Moyen, J.F., 2009: High Sr/Y and La/Yb ratios: The meaning of the "adakitic signature". *Lithos 112*. 556-574.

Moyen, J.F. & Martin, H., 2012: Forty years of TTG research. *Lithos 148*. 312-336.

Murphy, J.B. & Nance, R.D., 2013: Speculations on the mechanisms for the formation and breakup of supercontinents. *Geoscience Frontiers 4*. 185-194.

Mücke, A. Dzigbodi-Adjimah, K. & Annor, A., 1999: Mineralogy, petrography, geochemistry and genesis of the Paleoproterozoic Birimian manganese-formation of Nsuta/Ghana. *Mineralium Deposita 34*. 297-311.

Naba, S., Lompo, M., Debat, P., Bouchez, J.L. & Béziet, D., 2004: Structure and emplacement model for late-orogenic Paleoproterozoic granitoids: the Tenkodogo-Yamba elongate pluton. *Journal of African Earth Sciences 38*. 41-57.

Nance, R.D., Gutiérrez-Alonso, G., Keppie, J.D., Linnemann, U., Murphy, J.B., Quesada, C., Strachan, R.A. & Woodcock, N.H., 2010: Evolution of the Rheic Ocean. *Gondwana Research 17*. 194-222.

Nance, R.D., Murphy, J.B. & Santosh, M., 2014: The supercontinent cycle: A retrospective essay. *Gondwana Research 25*. 4-29.

Næraa, T., Scherstén, A., Rosing, M.T., Kemp, A.I.S., Hoffmann, J.E., Kokfelt, T.F. & Whitehouse, M.J., 2012: Hafnium isotope evidence for a transition in the dynamics of continental growth 3.2 Gyr ago. *Nature 485*. 627-630.

Ndiaye, P.M., Dia, A., Vialette, Y., Diallo, D.P., Ngom, P.M., Sylla, M., Wade, S. & Dioh, E.,

1997: Données pétrographiques, géochimiques et géochronologiques nouvelles sur les granitoids du Paléoproterozoïque du supergroupe de Dialé-Daléma (Sénégal Oriental): Implications pétrogénétiques et géodynamique. *Journal of African Earth Sciences 25*. 193-208.

Nilsson, M., Klausen, M.B., Söderlund, U. & Ernst, R.E., 2013: Precise U-Pb ages and geochemistry of Paleoproterozoic mafic dykes from southern West Greenland: Linking the North Atlantic and the Dharwar cratons. *Lithos 174*. 255-270.

Neves, S.P., 2011: Atlantica revisited: New data and thoughts on the formation of a long-lived continent. *International Geology Review 53*. 1377-1391.

Ngom, P.M., Cordani, U.G., Teixeira, W. & Assis Janasi, V., 2010: Sr and Nd isotopic geochemistry of the early ultramafic-mafic rocks of the Mako bimodal volcanic belt of the Kedougou-Kéniéba inlier (Senegal). *Arabian Journal of Geosciences 3*. 49-57.

Nomade, S., Chen, Y., Pouclet, A., Féraud, G., Théveniaut, H., Daouda, B.Y., Vidal, M. & Rigolet, C., 2003: The Guiana and the West African Shield Paleoproterozoic grouping: New paleomagnetic data for French Guiana and the Ivory Coast. *Geophysical Journal International 154*. 677-694.

Oberthür, T., Vetter, U., Davis, D.W. & Amanor, J.A., 1998: Age constraints on gold mineralization and Paleoproterozoic crustal evolution in the Ashanti belt of southern Ghana. *Precambrian Research 89*. 129-143.

Och, L.M. & Shields-Zhou, G.A., 2012: The Neoproterozoic oxygenation event: Environmental perturbations and biogeochemical cycling. *Earth-Science Reviews 110*. 26-57.

O'Connor, J.T., 1965: A classification for Quartz-rich igneous rocks based on feldspar ratios. *USGS Professional Paper 525-B*. 79-84.

Oldow, J.S., Bally, A.W. & Avé Lallement, H.G., 1990: Transpression, orogenic float, and lithospheric balance. *Geology 18*. 991-994.

Onstott, T.C., Hargraves, R.B., York, D. & Hall, C., 1984: Constraints on the motions of South American and African shields during the Proterozoic: I. $^{40}Ar/^{39}Ar$ and paleomagnetic correlations between Venezuela and Liberia. *Geological Society of America Bulletin 95*. 1045-1054.

Opare-Addo, E., 1992: *Aspects of early Proterozoic granitoids and migmatites in southern Ghana: Implications for crustal evolution*. Unpublished PhD thesis. University of Cambridge. 164 pp.

Opare-Addo, E., Browning, P. & John, B.E., 1993: Pressure-temperature constraints on the evolution of an Early Proterozoic plutonic suite in southern Ghana, West Africa. *Journal of African Earth Sciences 17*. 13-22.

Oyhantçabal, P., Siegesmund, S. & Wemmer, K., 2011: The Rio de la Plata Craton: A review of units, boundaries, ages and isotopic signature. *International Journal of Earth Sciences 100*. 201-220.

Palheta, E.S.M., Abreu, F.A.M. & Moura, C.A.V., 2009: Granitóides proterozóicos como marcadores da evolução geotectônica da região nordeste do Pará, Brasil. *Revisita Brasileira de Geosciências 39*. 647-657.

Pankhurst, M.J., Schaefer, B.F. & Betts, P.G., 2011: Geodynamics of rapid voluminous felsic magmatism through time. *Lithos 123*. 92-101.

Papineau, D., 2010: Global biogeochemical changes at both ends of the Proterozoic: Insights from phosphorites. *Astrobiology 10*. 165-181.

Partin, C.A., Bekker, A., Planavsky, N.J., Scott, C.T., Gill, B.C., Li, C., Podkovyrov, V., Maslov, A., Konhauser, K.O., Lalonde, S.V., Love, G.D., Poulton, S.W. & Lyons, T.W., 2013: Large-scale fluctuations in Precambrian atmospheric and oceanic oxygen levels from the record of U in shales. *Earth and Planetary Science Letters 369-370*. 284-293.

Patiño Douce, A.E., 1997: Generation of metaluminous A-type granites by low-pressure melting of calc-alkaline granitoids. *Geology 25*. 743-746.

Patiño Douce, A.E., 1999; What do experiments tell us about the relative contributions of crust and mantle to the origin of granitic magmas? *In* A.F. Fernández & J.L. Vigneresse (eds.): *Understanding granites: Integrating new and classical techniques*. 55-75. The Geological Society of London Special Publication 168.

Pawlig, S., Gueye, M., Klischies, R., Schwarz, S., Wemmer, K. & Siegesmund, S., 2006: Geochemical and Sr-Nd isotopic data on the Birimian of the Kedougou-Kéniéba Inlier (eastern Senegal): Implications on the Paleoproterozoic evolution of the West African Craton. *South African Journal of Geology 109*. 411-427.

Payne, J.L., Hand, M., Barovich, K.M., Reid, A. & Evans, D.A.D., 2009: Correlations and reconstruction models for the 2500-1500 Ma evolution of the Mawson Continent. *In* S.M. Reddy, R. Mazumder, D.A.D. Evans & A.S. Collins (eds.): *Paleoproterozoic supercontinents and global evolution*, 319-355. The Geological Society of London Special Publication 323.

Pearce, J.A., Harris, N.B.W. Tindle, A.G., 1984: Trace element discrimination diagrams for the tectonic interpretation of granitic rocks. Journal *of Petrology 25*. 956-983.

Pearce, J.A., 2008: Geochemical fingerprinting of oceanic basalts with applications to ophiolite classification and the search for Archean oceanic crust. *Lithos 100*. 14-48.

Peccerillo, A. & Taylor, S.R., 1976: Geochemistry of Eocene calc-alkaline volcanic rocks from the Kastamonu area, Northern Turkey. *Contribution to Mineralogy and Petrology 58*. 63-81.

Perrouty, S., Aillères, L., Jessell, M.W., Baratoux, L., Bourassa, Y. & Crawford, B., 2012: Revised Eb-

urnean geodynamic evolution of the gold-rich southern Ashanti belt, Ghana, with new field and geophysical evidence of pre-Tarkwaian deformations. *Precambrian Research 204-205*. 12-39.

Persits, F., Ahlbrandt, T., Tuttle, M., Charpentier, R., Brownfield, M. & Takahashi, K., 2002: *Map showing geology, oil and gas fields and geological provinces of Africa, ver. 2.0*. USGS Open File Report 97-470A, http://pubs.usgs.gov/of/1997/ofr-97-470/OF97-470A/index.html, last accessed 06-07-2013.

Peucat, J.-J., Capdevila, R., Drareni, A., Mahdjoub, Y. & Kahoui, M., 2005: The Eglab massif in the West African Craton (Algeria), an original segment of Eburnean orogenic belt: Petrology geochemistry and geochronology. *Precambrian Research 136*. 309-352.

Pigois, J.-P., Groves, D.I., Fletcher, I.R., McNaughton, N.J. & Snee, L.W., 2003: Age constraints on Tarkwaian paleoplacer and lode-gold formation in the Tarkwa-Damang district, SW Ghana. *Mineralium Deposita 38*. 695-714.

Pitra, P., Kouamelan, A.N., Ballèvre, M. & Peucat, J.J., 2010: Paleoproterozoic high-pressure granulite overprint of the Archean continental crust: Evidence for homogenous crustal thickening (Man Rise, Ivory Coast). *Journal of Metamorphic Geology 28*. 41-58.

Potrel, A., Peucat, J.J., Fanning, C.M., Auvray, B., Burg, J.P. & Caruba, C., 1996: 3.5 Ga old terranes in the West African Craton, Mauritania. Journal *of the Geological Society 153*. 507-510.

Potrel, A., Peucat, J.J. & Fanning, C.M., 1998: Archean crustal evolution of the West African Craton: Example of the Amsaga area (Reguibat Rise). U-Pb and Sm-Nd evidence for crustal growth and recycling. *Precambrian Research 90*. 107-117.

Pouclet, A., Vidal, M., Delor, C., Simeon, Y. & Alric, G., 1996: Le volcanisme Birimien du nord-est de la Côte d'Ivoire, mise en évidence de deux phases volcano-tectonique distinctes dans l'evolution géodynamique du Paléoprotérozoïque. *Bulletin de la Societe Geologique de France 167*. 529-541.

Pouclet, A., Doumbia, S. & Vidal, M., 2006: Geodynamic setting of the Birimian volcanism in central Ivory Coast (western Africa) and its place in the Palaeoproterozoic evolution of the Man shield. *Bulletin de la Societe Geologique de France 177*. 105-121.

Rapela, C.W., Fanning, C.M., Casquet, C., Pankhurst, R.J., Spalletti, L., Poiré, D. & Baldo, E.G., 2011: The Rio de la Plata craton and the adjoining Pan-African/Brasiliano terranes: Their origins and incorporation into south-west Gondwana. *Gondwana Research 20*. 673-690.

Redfield, T.F., Scholl, D.W., Fitzgerald, P.G. & Beck Jr., M.E., 2007: Escape tectonics and the extrusion of Alaska: Past, present, and future. *Geology 35*. 1039-1042.

Roberts, M.P. & Clemens, J.D., 1993: Origin of high-potassium, calc-alkaline, I-type granitoids. *Geology 21*. 825-828.

Robinson, P.T., Malpas, J., Dilek, Y. & Zhou, M.-F., 2008: The significance of sheeted dike complexes in ophiolites. *GSA Today 18*. 4-10.

Rocci, G., Bronner, G. & Deschamps, M., 1991: Crystalline basement of the West African Craton. *In* R.D. Dallmeyer & J.P. Lecorché (eds.): *The West African orogens and Circum-Atlantic correlatives*, 31-61. IGCP-project 233. Springer, Berlin.

Roever, E.W.F., Lafon, J.M., Delor, C., Cocherie, A., Rossi, P., Guerrot, C. & Potrel, A., 2003: The Bakhuis ultrahigh-temperature granulite belt (Suriname): I. Petrological and geochronological evidence for a counterclockwise P-T path at 2.07-2.05 Ga. *Géologie de la France 2-3-4*. 175-205.

Rogers, J.J.W., 1996: A history of the continents in the past three billion years. *The Journal of Geology 104*. 91-107.

Rogers, J.J.W. & Santosh, M., 2002: Configuration of Columbia, a Mesoproterozoic Supercontinent. *Gondwana Research 5*. 5-22.

Rogers, J.J.W. & Santosh, M., 2009: Tectonics and surface effects of the supercontinent Columbia. *Gondwana Research 15*. 373-380.

Rollinson, H.R. & Cliff, R.A., 1982: New Rb-Sr age determinations on the Archaean basement of eastern Sierra Leone. *Precambrian Research 17*. 63-72.

Rollinson, H.R., 1993: *Using geochemical data: Evaluation, presentation, interpretation*. Pearson Education Limited, Harlow, England. 352 pp.

Rosa Costa, L.S., Lafon, J.M. & Delor, C., 2006: Zircon geochronology and Sm-Nd isotopic study : Further constraints for the Archean and Paleoproterozoic geodynamical evolution of the southwestern Guiana Shield, north of Amazonian Craton, Brazil. *Gondwana Research 10*. 277-300.

Rosa Costa, L.S., Lafon, J.M., Cocherie, A. & Delor, C., 2008: Electron microprobe U-Th-Pb monazite dating of the Transamazonian metamorphic overprint on Archean rocks from the Amapá Block, southeastern Guiana Shield, northern Brazil. *Journal of South American Earth Sciences 26*. 445-462.

Rosa Costa, L.S., Monié, P., Lafon, J.M. & Arnaud, N.O., 2009: ^{40}Ar-^{39}Ar geochronology across Archean and Paleoproterozoic terranes from southeastern Guiana Shield (north of Amazonian Craton, Brazil): Evidence for contrasting cooling histories. *Journal of South American Earth Sciences 27*. 113-128.

Rosa Sexias, L.A., David, J. & Stevenson, R., 2012: Geochemistry, Nd isotopes and U-Pb geochronology of the 2350 Ma TTG suite, Minas Gerais, Brazil: Implications for the crustal evolution of the southern São Francisco craton. *Precambrian Research 196-197*. 61-80.

Rosen, O.M., Condie, K.C., Natapov, L.M. & Nozhkin, A.D., 1994: Archean and early Protero-

zoic evolution of the Siberian Craton: A preliminary assessment. *In* K.C. Condie (ed.): *Archean crustal evolution*, 411-459. Developments in Precambrian Geology 11.

Santos, T.I.S., Fetter, A.H., Van Schmus, W.R. & Hackspacher, P.C., 2009: Evidence for 2.35 to 2.30 Ga juvenile crustal growth in the northwest Borborema Province, NE Brazil. *In* S.M. Reddy, R. Mazumder, D.A.D. Evans & A.S. Collins (eds.): *Paleoproterozoic supercontinents and global evolution*, 271-281. The Geological Society of London Special Publication 323.

Santos-Pinto, M., Peucat, J.J., Martin, H., Barbosa, J.S.F., Manning, C.M., Cocherie, A. & Paquette, J.L., 2012: Crustal evolution between 2.0 and 3.5 Ga in the southern Gavião block (Umburanas-Brumado-Aracatu region), São Francisco Craton, Brazil: A 3.5-2.8 Ga proto-crust in the Gavião block? *Journal of South American Earth Sciences 40*. 129-142.

Siegfried, P., Aggenbach, A., Clarke, B., Delor, C. & Roig, J-Y., 2009: *Geological map explanation - map sheet 0903D (1:100 000)*. CGS/BRGM/Geoman/GSD. 225 pp.

Schwartz, M.O. & Melcher, F., 2003: The Perkoa zinc deposit, Burkina Faso. *Economic Geology 98*. 1463-1485.

Schofield, D.I., Horstwood, M.S.A., Pitfield, P.E.J., Gillespie, M., Darbyshire, F., O´Connor, E.A. & Abdouloye, T.B., 2012: U-Pb dating and Sm-Nd isotopic analysis of granitic rocks from the Tiris Complex: New constraints on key events in the evolution of the Reguibat Shield, Mauritania. *Precambrian Research 204-205*. 1-11.

Scholl, D.W. & Von Huene, R., 2009: Implications of estimated magmatic additions and recycling losses at the subduction zones of accretionary (non-collisional) and collisional (suturing) orogens. *In* P.A. Cawood & A. Kröner (eds.): *Earth accretionary systems in space and time*, 105-125. The Geological Society of London Special Publication 318.

Şengör, A.M.C., Natal'in, B.A. & Burtman, V.S., 1993: Evolution of the Altaid tectonic collage and Palaeozoic crustal growth in Eurasia. *Nature 364*. 299-307.

Shand, J.S., 1943: *Eruptive rocks: Their genesis, composition, and classification, with a chapter on meteorites*. 2nd ed. J Wiley & Sons, New York and London. 444 pp.

Shchipansky, A.A., Samsonov, A.V., Petrova, A.Yu. & Larionova, Yu.O., 2007: Geodynamics of the eastern margin of Sarmatia in the Paleoproterozoic. *Geodynamics 41*. 38-62.

Shields, G.A., 2007: A normalized seawater strontium isotope curve: Possible implications for Neoproterozoic-Cambrian weathering rates and the further oxygenation of the Earth. *eEarth 2*. 35-42.

Shields, G. & Viezer, J., 2002: Precambrian marine carbonate isotope database: Version 1.1. *Geochemistry, Geophysics, Geosystems 3*. 1-12.

Shiery, S.B. & Richardson, S.H., 2011: Start of the Wilson cycle at 3 Ga shown by diamonds from the subcontinental mantle. *Science 333*. 434-436.

Shirey, S.B., Kamber, B.S., Whitehouse, M.J., Mueller, P.A. & Basu, A.R., 2008: A review of the isotopic and trace element evidence for mantle and crustal processes in the Hadean and Archean: Implications for the onset of plate tectonic subduction. *In* K.C. Condie & V. Pease (eds.): *When did plate tectonics begin on planet Earth?*, 1-29. The Geological Society of America Special Paper 440.

Siméon, Y., Delor, C., Zéade, Z., Kone, Y., Yao, B.D., Vidal, M., Diaby, I., Konan, G., Bi Irié, D., N'Da, Dommanget, A., Cautru, J.P., Guerrot, C., Chiron, J.C., 1995: *Notice explicative de la carte géologique de la Côte d'Ivoire à 1/200000, feuille de Agnibilékrou-Kouamé-Dari, Mémoire n° 8*, Ministère des Mines et de l'Energie, Direction de la Géologie, Abidjan, Côte d'Ivoire.

Sizova, E., Gerya, T:, Brown, M. & Perchuk, L.L., 2010: Subduction styles in the Precambrian: Insight from numerical experiments. *Lithos 116*. 209-229.

Soumaila, A., Henry, P., Garba, Z. & Rossi, M., 2008: REE patterns, Nd-Sm and U-Pb ages of the metamorphic rocks of the Diagorou-Darbani greenstone belt (Liptako, SW Niger): Implication for Birimian (Paleoproterozoic) crustal genesis. *In* N. Ennih & J.P. Liégeois (eds.): *The boundaries of the West African Craton*, 19-32. The Geological Society of London Special Publication 297.

Spencer, C.J., Hawkesworth, C., Cawood, P.A. & Dhuime, B., 2013: Not all supercontinents are created equal: Gondwana-Rodinia case study. *Geology 41*. 795-798.

Stampfli, G.M., Hochard, C., Vérard, C., Wilhelm, C. & von Raumer, J., 2013: The formation of Pangea. *Tectonophysics 593*. 1-19.

Stephens, M.B., Ripa, M., Lundström, I., Persson, L., Bergman, T., Ahl, M., Wahlgren, C.H., Persson, P.H. & Wickström, L., 2009: *Synthesis of the bedrock geology in the Bergslagen region, Fennoscandian Shield, south-central Sweden*. Geological survey of Sweden Ba58. 259 pp.

Stern, R.J., 1994: Arc assembly and continental collision in the Neoproterozoic East African Orogen: Implications for the consolidation of Gondwanaland. *Annual Review of Earth and Planetary Sciences 22*. 319-51.

Stern, R.J., 2005: Evidence from ophiolites, blueschists, and ultrahigh-pressure metamorphic terranes that the modern episode of subduction tectonics began in Neoproterozoic time. *Geology 33*. 557-560.

Stern, R.J., Ali, K.A., Liégeois, J.P., Johnson, P.R., Kozdroj, W. & Kattan, F.H., 2010: Distribution and significance of pre-Neoproterozoic zircons in juvenile Neoproterozoic igneous rocks of the Arabian-Nubian Shield. *American Journal of Science*

310. 791-811.

Stern, C.R., 2011: Subduction erosion: Rates, mechanisms, and its role in arc magmatism and the evolution of the continental crust. *Gondwana Research 20*. 284-308.

Sun, S.S. & McDonough, W.F., 1989: Chemical and isotopic systematics of oceanic basalts: implications for mantle composition and processes. *In* A.D. Saunders & M. Norry (eds.): *Magmatism in Ocean Basins*, 313-345. The Geological Society of London Special Publication 42.

Swapp, S.M. & Onstott, T.C., 1989: P-T-time characterization of the Transamazonian orogeny in the Imataca complex, Venezuela. *Precambrian Research 42*. 293-314.

Sylvester, P.J. & Attoh, K., 1992: Lithostrathigraphy and composition of 2.1 Ga greenstone belts of the West African Craton and their bearing on crustal evolution and the Archean-Proterozoic boundary. *Journal of Geology 100*. 377-392.

Tagini, B., 1972: *Carte geologique de la Côte d'Ivoire à 1/4000000*. SODEMI, Abidjan.

Tapsoba, B., Lo, C.-H., Jahn, B.-M., Chung, S.-L., Wenmenga, U. & Iizuka, Y., 2013: Chemical and Sr-Nd isotopic compositions and zircon U-Pb ages of the Birimian granitoids from NE Burkina Faso, West African Craton: Implications on the geodynamic setting and crustal evolution. *Precambrian Research 224*. 364-396.

Tatsumi, Y., 2005: The subduction factory: How it operates in the evolving Earth. *GSA today 15*. 4-10.

Tchameni, R., Mezger, K., Nsifa, N.E. & Pouclet, A., 2001 - Crustal origin of Early Proterozoic syenites in the Congo Craton (Ntem Complex), South Cameroon. *Lithos 57*. 23-42.

Tegyey, M. & Johan, V., 1989: Une sequence komatiitique dans le Protérozoïque inférieur de Guinée (Afrique de l'Ouest): Caractèrs pétrographiques, minéralogiques et géochimiques. *Comptes rendus de l'Académie des sciences. Série 2, Mécanique, physique, chimie, sciences de l'univers, sciences de la t*erre. 1984-1993.

Thiéblemont, D., Delor, C., Cocherie, A., Lafon, J.M., Goujou, J.C., Baldé, A., Bah, M., Sané, H. & Fanning, C.M., 2001: A 3.5 Ga granite-gneiss basement in Guinea: Further evidence for early Archean accretion within the West African Craton. *Precambrian Research 108*. 179-194.

Thiéblemont, D., Goujou, J.C., Egal, E., Cocherie, A., Delor, C., Lafon, J.M. & Fanning, C.M., 2004: Archean evolution of the Leo Rise and its Eburnean reworking. *Journal of African Earth Sciences 39*. 97-104.

Thomas, E., Baglow, N., Viljoen, J. & Siaka, Z., 2009: *Geological map explanation — map sheet 0903B (1:100 000)*. CGS/BRGM/Geoman/GSD. 185 pp.

Torquato, J.R. & Cordani, U.G., 1981: Brazil-Africa geological links. *Earth Science Reviews 17*. 155-176.

Toure, S., Caen-Vachette, M. & Tempier, P., 1987: Nouvelles données pétrographiques, géochimiques et géochronologiques du massif "granitique" de Bondoukou (Côte d'Ivoire) mise en evidence d'un âge Burkinien, par isochrone Rb/Sr sur roches totals. *Journal of African Earth Sciences 6*. 269-274.

Triboulet, C. & Feybesse, J.L., 1998: Les métabasites birimiennes et archéennes de la région de Toulépleu-Ity (Côte d'Ivoire): Des roches portées à 8 kbar (≈24 km) et 14 kbar (≈ 42 km) au Paléoproterozoïque. *Comptes Rendus de l'Académie des sciences à Paris, Sciences de la terre et des planetès 327*. 61-66.

Trompette, R., 1994: *Geology of western Gondwana (2000-500 Ma)*. A A Balkema, Rotterdam. 364 pp.

Tshibubudze, A., Hein, K.A.A. & Marquis, P., 2009: The Markoye shear zone in NE Burkina Faso. *Journal of African Earth Sciences 55*. 245-256.

Turner, P., Hall, R.P., Hughers, D.J. & Whalley, J.S., 1993: The sediment-dominated Boundiali-Bagoé supracrustal belt and neighbouring granitic rocks, northern Côte d'Ivoire, West Africa: A Tarkwaian connection? *Journal of African Earth Sciences 17*. 1-11.

Urmantseva, L. & Turkina, O., 2009: Paleoproterozoic, high-metamorphic, metasedimentary units of Siberian Craton. Acta *Geologica Sinica (English edition) 83*. 875-883.

van Hunen, J., van Keken, P.E., Hynes, A. & Davies, G.F., 2008: Tectonics of early Earth: Some geodynamic considerations. *In* K.C. Condie & V. Pease (eds.): *When did plate tectonics begin on planet Earth?*, 157-171. The Geological Society of America Special Paper 440.

van Hunen, J. & Moyen, J.F., 2012: Archean Subduction: Fact or fiction? *The Annual Review of Earth and Planetary Sciences 40*. 195-219.

Van Kranendonk, M.J., Collins, W.J., Hickman, A. & Pawley, M.J., 2004: Critical tests of vertical vs. horizontal tectonic models for the Archaean east Pilbara granite-greenstone terrane, Pilbara Craton, Western Australia. *Precambrian Research 131*. 173-211.

Vasquez, M.L., Macambira, M.J.B. & Armstrong, R.A., 2008: Zircon geochronology of granitoids from the western Bacajá domain, southeastern Amazonian craton, Brazil: Neoarchean to Orosirian evolution. *Precambrian Research 161*. 279-302.

Vegas, N., Naba, S., Bouchez, J.L. & Jessell, M., 2008: Structure and emplacement of granite plutons in the Paleoproterozoic crust of eastern Burkina Faso: rheological implications. *International Journal of Earth Sciences 97*. 1165-1180.

Vidal, M. & Alric, G., 1994: The Paleoproterozoic (Birimian) of Haute-Comoé in the West African Craton, Ivory Coast: A transtensional back-arc basin. *Precambrian Research 65*. 207-229.

Vidal, M., Delor, C., Pouclet, A., Simeon, Y. & Alric,

G., 1996: Evolution géodynamique de l'Afrique de l'Ouest entre 2.2 Ga et 2 Ga: Le style archéen des ceintures vertes et des ensembles sédimentaires birimiens du nord-est de la Côte-d'Ivoire. *Bulletin de la Societe Geologique de France 167*. 307-319.

Vidal, M., Gumiaux, C., Cagnard, F., Pouclet, A., Ouattara, G. & Pichon, M., 2009: Evolution of a Paleoproterozoic "weak type" orogeny in the West African Craton (Ivory Coast). *Tectonophysics 477*. 145-159.

Villeneuve, M., 2005: Paleozoic basins in West Africa and the Mauritanide thrust belt. *Journal of African Earth Sciences 43*. 166-195.

Villeneuve, M. & Cornée, J.J., 1994: Structure, evolution and paleogeography of the West African Craton and bordering belts during the Neoproterozoic. *Precambrian Research 69*. 307-326.

Voicu, G., Bardoux, M. & Stevenson, R., 2001: Lithostrathigraphy, geochronology and gold metallogeny in the northern Guiana Shield, South America: A review. *Ore Geology Reviews 18*. 211-236.

Walsh, G.J., Aleinikoff, J.N., Benziane, F., Yazidi, A. & Armstrong, T.R., 2002: U-Pb zircon geochronology of the Paleoproterozoic Tagragra de Tata inlier and its Neoproterozoic cover, western Anti-Atlas, Morocco. *Precambrian Research 117*. 1-20.

Whalen, J.B., Currie, K.L. & Chappell, B.W., 1987: A-type granites: Geochemical characteristics, discrimination and petrogenesis. *Contributions to Mineralogy and Petrology 95*. 407-419.

Whitmeyer, S.J. & Karlstrom, K.E., 2007: Tectonic model for the Proterozoic growth of North America. *Geosphere 3*. 220-259.

Wilhelm, C., Windley, B.F. & Stampfli, G.M., 2012: The Altaids of Central Asia: A tectonic and evolutionary innovative review. *Earth-Science Reviews 113*. 303-341.

Williams, H., Hoffman, P.F., Lewry, J.F., Monger, J.W.H. & Rivers, T., 1991: Anatomy of North America: Thematic geologic portrayals of the continent. *Tectonophysics 187*. 117-134.

Williams, S.E., Müller, R.D., Landgrebe, T.C.W. & Whittaker, J.M., 2012: An open-source software environment for visualizing and refining tectonic reconstructions using high-resolution geological and geophysical data sets. *GSA Today 22*. 4-9.

Windley, B.F. & Garde, A.A., 2009: Arc-generated blocks with crustal sections in the North Atlantic craton of West Greenland: Crustal growth in the Archean with modern analogues. *Earth-Science Reviews 93*. 1-30.

Yao, B.D., Delor, C., Siméon, Y., Diaby, I., Gadou, G., Kohou, P., Okou, A., Konaté, S., Konan, G., Vidal, M., Cocherie, A., Dommanget, A., Cautru, J.P. & Chiron, J.C., 1995: *Carte géologique de la Côte-d'Ivoire 1/200000, feuille Dimbokro*. Direction des mines et de la géologie, Abidjan, Côte-d'Ivoire. 21 pp.

Yao, Y. & Robb, L.J., 2000: Gold mineralization in Paleoproterozoic granitoids at Obuasi, Ashanti region, Ghana: Ore geology, geochemistry and fluid characteristics. *South African Journal of Earth Science 103*. 255-278.

Yoshida, M. & Santosh, M., 2011: Supercontinents, mantle dynamics and plate tectonics: A perspective based on conceptual vs. numerical models. *Earth-Science Reviews 105*. 1-24.

Zhao, G., Sun, M., Wilde, S.A. & Li, S., 2004: A Paleo-Mesoproterozoic supercontinent: Assembly, growth and breakup. *Earth-Science Reviews 67*. 91-123.

Zitzmann, A., 1997: *Geological, geophysical and geochemical investigations in the Bui belt area in Ghana*. Geologisches Jahrbuch Reihe B, Heft 83. 269 pp.

Appendix A

Sample locations shown on a simplified geological map after Agyei Duodu et al (2009) with modifcations by Adadey et al. (2009), Baratoux et al. (2011) and field obervations by A. Scherstén. Projected using Ghana Metre Grid (Leigon datum). ASGH prefix is omitted from the sample ID.

Sample data is given in table 1 (brief descriptive data), 2 (radiometric data) and 3 (whole-rock geochemistry).

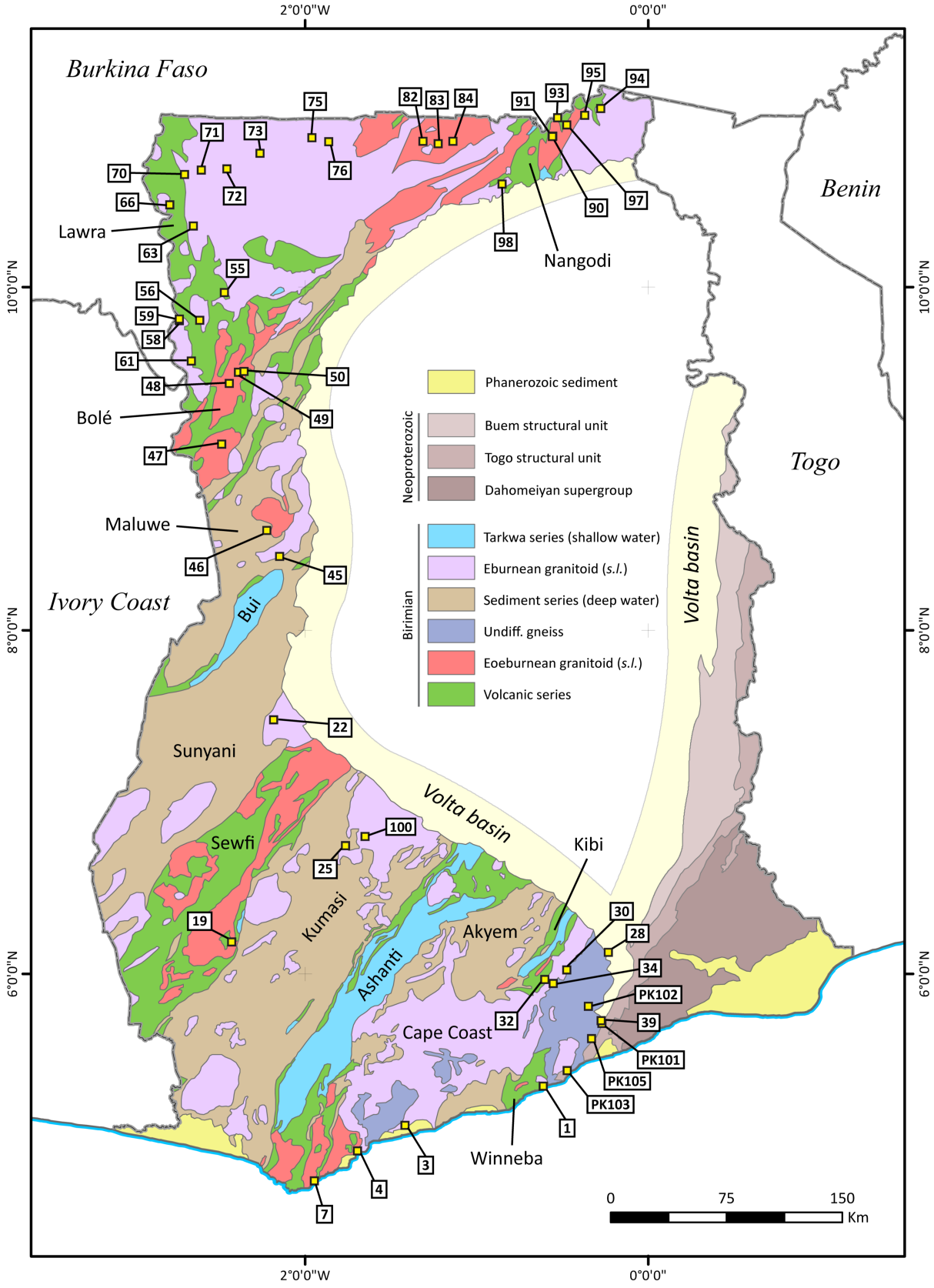

Sample	Latitude	Longitude	Petrography	Fe-index	MALI	ASI-index	ASI	Mg#	K_2O/Na_2O	Eu/Eu*	∑REE
ASGH 001A	5,34599	-0,61380	Bt granite	magnesian	alkali-calcic	peraluminous	1,09	0,36	1,10	0,63	321,35
ASGH 003A	5,11717	-1,41801	Bt granodiorite	magnesian	calcic	peraluminous	1,04	0,35	0,22	2,16	42,01
ASGH 003B	5,11717	-1,41801	Bt granodiorite	magnesian	alkali-calcic	peraluminous	1,06	0,37	0,62	0,95	122,16
ASGH 004B	4,96982	-1,69560	Bt-Amp tonalite	magnesian	calc-alkalic	metaluminous	0,93	0,51	0,64	0,95	106,80
ASGH 007A	4,79348	-1,94555	Amp-Bt granodiorite-tonalite (altered)	magnesian	calc-alkalic	metaluminous	0,98	0,45	0,43	1,16	57,68
ASGH 019A	6,18632	-2,42668	Bt-Amp granodiorite-tonalite (altered)	magnesian	calcic	metaluminous	0,86	0,40	0,23	0,99	73,93
ASGH 022A	7,48071	-2,18361	Ms-Bt granodiorite-tonalite	magnesian	calcic	peraluminous	1,32	0,35	0,69	0,83	130,09
ASGH 022D	7,48071	-2,18361	Ms-Bt granodiorite-tonalite	magnesian	alkali-calcic	peraluminous	1,21	0,43	0,38	1,11	49,57
ASGH 022E	7,48071	-2,18361	Bt-Ms granodiorite	magnesian	calc-alkalic	peraluminous	1,10	0,51	0,39	1,40	32,44
ASGH 025A	6,74787	-1,76559	Bt-Amp (act) tonalite	magnesian	calcic	peraluminous	1,01	0,42	0,24	1,10	44,85
ASGH 028A	6,12481	-0,23249	Bt granite	ferroan	calc-alkalic	metaluminous	0,98	0,28	0,74	0,81	116,15
ASGH 028B	6,12481	-0,23249	Bt-Amp granodiorite	magnesian	alkali-calcic	metaluminous	0,93	0,32	0,72	0,62	131,60
ASGH 030A	6,02396	-0,47537	Bt-Amp granite	magnesian	calc-alkalic	metaluminous	0,99	0,39	0,53	1,11	111,37
ASGH 032A	5,96705	-0,60235	Bt-Amp tonalite	magnesian	calc-alkalic	metaluminous	0,99	0,46	0,54	1,05	89,76
ASGH 032B	5,96705	-0,60235	Bt granodiorite (rounded mafic enclave)	magnesian	alkali-calcic	metaluminous	0,88	0,47	0,63	0,87	132,65
ASGH 034A	5,94408	-0,55392	Bt-Amp granite	magnesian	calc-alkalic	metaluminous	0,99	0,42	0,40	1,11	84,52
ASGH 039A	5,72725	-0,27535	Bt granite	magnesian	calc-alkalic	peraluminous	1,04	0,40	0,47	0,87	173,35
ASGH 045A	8,43159	-2,14766	Bt-Hbl granodiorite	magnesian	calc-alkalic	metaluminous	0,94	0,54	0,52	0,95	106,09
ASGH 046A	8,58226	-2,22371	Bt-Ms granodiorite (altered)	ferroan	calc-alkalic	peraluminous	1,17	0,26	0,47	0,61	184,00
ASGH 046C	8,58226	-2,22371	sedimentary xenolith				1,44	0,32	0,78	1,22	72,73
ASGH 047A	9,08432	-2,48615	Bt granodiorite	magnesian	calcic	peraluminous	1,01	0,34	0,67	0,74	124,40
ASGH 047B	9,08432	-2,48615	fine grained mafic enclave				0,62	0,48	0,38	0,96	79,00
ASGH 048A	9,43918	-2,44193	Bt granodiorite-tonalite	magnesian	calc-alkalic	peraluminous	1,09	0,46	0,42	1,06	211,61
ASGH 049A	9,50423	-2,38710	Bt granodiorite-tonalite	magnesian	calc-alkalic	peraluminous	1,09	0,37	0,41	0,89	235,62
ASGH 050A	9,50905	-2,35492	Bt schist				1,17	0,39	0,56	0,89	125,24
ASGH 055A	9,96387	-2,46157	Bt-Amp granodiorite	magnesian	calc-alkalic	metaluminous	0,97	0,46	0,60	1,05	151,41
ASGH 056A	9,80707	-2,61305	Amp-Bt granodiorite-tonalite	magnesian	calc-alkalic	metaluminous	0,88	0,62	0,49	0,96	180,99

Table 1. Brief petrological descriptino and geochemical paramters for samples collected by A. Scherstén (ASGH) and P. Kalvig (PK). Coordinates given iwith th WGS 1984 datum

Sample	Latitude	Longitude	Petrography	Fe-index	MALI	ASI-index	ASI	Mg#	K_2O/Na_2O	Eu/Eu*	∑REE
ASGH 058A	9,80433	-2,73340	Bt-Ms leucogranite	magnesian	calc-alkalic	peraluminous	1,06	0,35	0,42	1,02	84,22
ASGH 059B	9,81378	-2,73351	Ms leucogranite	magnesian	alkali-calcic	peraluminous	1,13	0,26	0,74	0,30	28,78
ASGH 061B	9,56953	-2,66284	Bt granodiorite-tonalite	magnesian	calcic	peraluminous	1,05	0,41	0,08	1,34	103,01
ASGH 061C	9,56953	-2,66284	Bt andesite-dacite	magnesian	calc-alkalic	peraluminous	1,07	0,40	0,35	1,15	153,39
ASGH 061D	9,56953	-2,66284	metasediment, country rock				1,19	0,44	0,85	1,51	48,37
ASGH 062A	9,63475	-2,69174	Bt andesite-dacite	magnesian	calc-alkalic	peraluminous	1,03	0,40	0,59	1,07	114,43
ASGH 063A	10,35689	-2,65052	Bt-Amp tonalite	magnesian	calcic	metaluminous	0,99	0,42	0,25	0,94	47,95
ASGH 063B	10,35689	-2,65052	Bt leucocratic granitoid	magnesian	calc-alkalic	peraluminous	1,12	0,31	0,28	0,56	70,86
ASGH 066A	10,47880	-2,78837	Amp-Bt tonalite (altered)	magnesian	calc-alkalic	metaluminous	0,85	0,58	0,64	0,93	119,84
ASGH 070A	10,65636	-2,70157	Bt granite	magnesian	calc-alkalic	peraluminous	1,04	0,39	0,67	1,01	121,17
ASGH 071A	10,68170	-2,60563	Bt-Amp granodiorite-tonalite	magnesian	calcic	metaluminous	1,00	0,38	0,31	1,44	61,87
ASGH 072A	10,68797	-2,45668	Amp-Bt tonalite	magnesian	calc-alkalic	metaluminous	0,91	0,44	0,24	1,02	117,35
ASGH 073B	10,77895	-2,26145	Bt leucogranite	ferroan	calc-alkalic	peraluminous	1,06	0,16	1,12	0,68	39,35
ASGH 075A	10,86961	-1,95943	Bt granite	magnesian	alkali-calcic	peraluminous	1,06	0,31	1,09	0,66	275,58
ASGH 075B	10,86961	-1,95943	Bt-Amp tonalite	magnesian	calcic	metaluminous	0,90	0,40	0,28	1,17	104,03
ASGH 076A	10,84592	-1,86204	Bt granite	magnesian	alkali-calcic	peraluminous	1,06	0,29	1,23	0,64	211,36
ASGH 082A	10,84909	-1,31225	Bt-Amp granodiorite	ferroan	calcic	peraluminous	1,04	0,23	0,74	0,53	151,47
ASGH 083A	10,83419	-1,22398	Bt-Amp granodiorite-granite	magnesian	calc-alkalic	metaluminous	0,94	0,48	0,48	1,11	86,93
ASGH 084A	10,85027	-1,13940	Bt granite	magnesian	calcic	peraluminous	1,04	0,34	1,07	0,55	95,29
ASGH 090A	10,87902	-0,55763	Bt granite	magnesian	calc-alkalic	peraluminous	1,04	0,29	0,42	1,33	37,92
ASGH 091A	10,87655	-0,55897	Bt granite	magnesian	calc-alkalic	peraluminous	1,03	0,37	0,47	1,01	60,36
ASGH 091B	10,87655	-0,55897	Bt granite-granodiorite	magnesian	calcic	peraluminous	1,06	0,34	0,33	1,24	38,49
ASGH 093A	10,98672	-0,53001	Amp-Bt tonalite (altered)	magnesian	calcic	metaluminous	0,92	0,40	0,44	0,93	101,20
ASGH 094A	11,04032	-0,27865	Bt-Amp granodiorite	magnesian	calc-alkalic	peraluminous	1,01	0,34	0,47	0,88	150,57
ASGH 095A	11,00155	-0,37147	Bt-Amp granodiorite	magnesian	calc-alkalic	metaluminous	0,98	0,41	0,34	1,07	91,59
ASGH 097A	10,94423	-0,47421	Bt leucotonalite (altered)	magnesian	calc-alkalic	peraluminous	1,04	0,32	0,41	1,19	49,97
ASGH 098A	10,60046	-0,85214	Ms-Bt leucogranite	ferroan	alkali-calcic	peraluminous	1,12	0,24	0,89	0,61	74,48
ASGH 100A	6,79974	-1,65042	Bt granite	magnesian	calc-alkalic	peraluminous	1,09	0,44	0,29	1,50	46,57
ASGH 100B	6,79974	-1,65042	Ms-Bt granodiorite	magnesian	alkali-calcic	peraluminous	1,06	0,29	0,96	0,61	40,84
PK101	5,71217	-0,27117	Bt±Amp tonalite-granodiorite	magnesian	calc-alkalic	peraluminous	1,03	0,41	0,40	0,93	186,91
PK102	5,81100	-0,34975	Bt-Amp granodiorite	magnesian	calcic	metaluminous	0,94	0,40	0,55	0,97	78,79
PK103	5,43639	-0,47286	Bt-Amp granodiorite	magnesian	calc-alkalic	metaluminous	0,94	0,44	0,92	0,88	182,41
PK105	5,62200	-0,33006	Bt-Amp granodiorite	magnesian	calcic	metaluminous	0,97	0,34	0,33	0,83	165,49

Table 1. Cont.

Sample	Age (Ma)	Method	Source	Reference
ASGH 001A	2113±1	TIMS on zircon	Inferred	Agyei Duodu et al. 2009
ASGH 003A	2124±3	SIMS on zircon	Measured	Anders Schersten (unpublished)
ASGH 003B	2124±3	SIMS on zircon	Inferred	Anders Schersten (unpublished)
ASGH 004B	2174±2	TIMS on zircon	Inferred	Oberthur et al. 1998
ASGH 007A	2172±12	SIMS on zircon	Measured	Anders Schersten (unpublished)
ASGH 019A	2169±13	SIMS on zircon	Measured	Anders Schersten (unpublished)
ASGH 022A	2094±4	SIMS on zircon	Measured	Anders Schersten (unpublished)
ASGH 022D	2094±4	SIMS on zircon	Inferred	Anders Schersten (unpublished)
ASGH 022E	2094±4	SIMS on zircon	Inferred	Anders Schersten (unpublished)
ASGH 039A	2130±10	SIMS on zircon	Inferred	Anders Schersten (unpublished)
ASGH 045A	2121±4	SHRIMP on zircon	Inferred	de Kock et al. 2009
ASGH 047A	2195±4	SHRIMP on zircon	Inferred	Siegfried et al. 2009
ASGH 048A	2128±20	SHRIMP on zircon	Inferred	Siegfried et al. 2009
ASGH 070A	2124±2	TIMS on zircon	Inferred	Agyei Duodu et al. 2009
ASGH 075A	2112±1	TIMS on zircon	Inferred	Agyei Duodu et al. 2009
ASGH 082A	2156±1	TIMS on zircon	Inferred	Agyei Duodu et al. 2009
ASGH 084A	2156±1	TIMS on zircon	Inferred	Agyei Duodu et al. 2009
ASGH 095A	2134±1	TIMS on zircon	Inferred	Agyei Duodu et al. 2009
ASGH 097A	2150-2168	TIMS on zircon	Inferred	Agyei Duodu et al. 2009
PK101	2130±10	SIMS on zircon	Measured	Anders Schersten (unpublished)
PK102	2180±4	SIMS on zircon	Measured	Anders Schersten (unpublished)
PK103	2134±10	SIMS on zircon	Measured	Anders Schersten (unpublished)
PK105	2232±5	SIMS on zircon	Measured	Anders Schersten (unpublished)

Table 2a. Measured or inferred radiometric ages for samples presented in table 1. Inferred ages include those obtained from the same outcrop or other localities interpreted as being coeval with the given sample.

Sample	eNdt	eNdt source	eNdt reference
ASGH 001A	-5,4	Inferred	Leube et al. 1990
ASGH 003A	1,5	Measured	Anders Schersten (unpublished)
ASGH 007A	1,4	Measured	Anders Schersten (unpublished)
ASGH 019A	1,7	Measured	Anders Schersten (unpublished)
ASGH 022A	1,1	Measured	Anders Schersten (unpublished)
PK102	1,7	Measured	Anders Schersten (unpublished)
PK105	1,7	Measured	Anders Schersten (unpublished)

Table 2b. eNdt values for samples presented in table 1. Inferred isotpic data for sample ASGH 001A from the same pluton (Winneba)

Sample	001A	003A	003B	004B	007A	019A	022A	022D	022E	025A	028A	028B	030A	032A	032B
Major elements (wt. %) - ICP-ES															
SiO_2	66,81	72,27	67,9	61,21	66,54	56,45	72,56	68,8	72,65	70,93	67,42	63,93	69,35	67,93	60,22
Al_2O_3	15,88	15,95	16,79	15,62	15,75	17,03	15,12	17,95	15,47	14,47	15,52	15,43	15,78	15,46	16,58
FeO_{tot}	3,45	1,02	2,36	6,37	3,45	8,04	1,75	1,45	0,84	2,99	3,94	5,82	2,05	2,89	4,99
MgO	1,08	0,31	0,78	3,78	1,58	2,96	0,53	0,61	0,49	1,23	0,88	1,57	0,75	1,39	2,48
CaO	2,58	2,88	2,6	4,86	3,73	7,2	1,59	1,87	1,71	2,8	2,9	3,51	2,47	2,89	4,28
Na_2O	3,58	5,38	4,88	3,49	4,48	3,61	3,65	5,62	5,35	4,94	4,39	4,3	5,24	4,72	4,93
K_2O	3,93	1,18	3,01	2,22	1,94	0,83	2,51	2,13	2,07	1,18	3,27	3,11	2,78	2,56	3,1
TiO_2	0,57	0,13	0,33	0,65	0,32	0,86	0,42	0,21	0,16	0,35	0,43	0,71	0,24	0,37	0,58
P_2O_5	0,17	0,02	0,12	0,22	0,1	0,19	0,12	0,09	0,06	0,11	0,1	0,17	0,1	0,13	0,36
MnO	0,03	0,02	0,02	0,13	0,07	0,11	0,02	0,01		0,03	0,05	0,08	0,03	0,05	0,08
LOI	1,5	0,7	1	1,2	1,8	2,5	1,5	1,1	1	0,7	0,8	1,1	0,8	1,3	2,1
Sum	99,62	99,84	99,77	99,77	99,76	99,79	99,77	99,85	99,75	99,74	99,73	99,74	99,6	99,71	99,68
Trace elements (ppm) - ICP-MS															
Cr			13,68	136,84	27,37					20,53		27,37	13,68	41,05	41,05
Ni	6	3,9	5,5	39,3	11,5	12,1	1,8	3,4	3,3	15	4,9	11,6	8,6	16,9	18,3
Sc	5	3	4	16	8	22	2	2	2	5	7	10	4	6	11
Ba	1270	126	746	378	739	276	735	341	539	514	1190	878	1340	893	1074
Co	102,1	94,9	57,9	52,2	49,6	61,4	65,5	54,2	113,5	100,7	69,1	76,5	101,3	104,7	58,1
Cs	5,1	1,7	2,1	11,8	1	0,3	1,6	2,9	1,4	8,5	1,7	3,2	3,3	2,5	5,6
Ga	19,5	16,8	20,5	16,8	17,8	17,1	20,5	26,4	20,8	21,1	17,6	18,8	16,4	20,3	22,7
Hf	7,1	2,4	4,5	3,3	2,9	2,7	5,6	2,4	2	2,7	5,6	5,1	3,1	3,6	4
Nb	13	3,4	5,6	5,7	2,4	4,2	3,2	1,6	1,1	1,7	6,2	10,6	6,9	3,8	10,4
Rb	163,7	41	96,5	135,9	47,4	21,3	88,4	82,8	61,7	34,6	81	101,8	74,8	75,5	94,9
Sr	446,8	512,4	462,8	463,2	660,6	350,4	450,3	467,9	634,6	647,6	367,7	370,4	1133,8	536,3	559,4
Ta	1,3	0,4	0,3	0,3	0,1	0,2	0,3		0,2	0,2	0,4	0,5	0,6	0,3	0,8
Th	41,2	4,3	12,8	2	2,3	1,8	10,9	2,3	1,9	0,8	5,6	5	5,7	4,1	4,3
U	2,5	4,7	1,5	1,1	1,6	0,5	1	5,1	1,7	0,6	0,5	0,5	2,3	1,6	3,8
V	54		41	126	61	146	27	25	19	52	25	47	28	46	91
Zr	248,2	67,4	159,6	137,3	89,4	77,9	195	82	62,3	106,1	184,6	177,2	104,6	111,1	139,9
Y	14,2	3,8	5,2	18,3	8,4	17,2	4	1,7	0,8	4,8	15,8	26	5,2	7,1	15,5
Mo	0,3	0,5	1,3		0,1	0,3	0,1		0,1	0,1	1	3	0,1	0,2	
Cu	17,8	0,4	1,5	31,2	19,5	40,8	54,7	0,5	0,4	11,3	12,8	4	2,4	7,7	78,5
Pb	11,1	2,8	5	1,1	3,7	1,9	2,3	1,8	2,8	1,3	3,2	2,8	5,2	6,5	7,8
Zn	67	23	52	65	42	53	54	50	40	67	56	74	35	55	88
La	79,1	9,8	29,4	19,2	11,8	13,2	28,8	9,9	6,6	8	26,5	26,3	26	19	22,8
Ce	153	19,2	57,8	44,1	24,3	28	61,6	20,9	14,2	18,4	51,7	55,6	51	40,1	54,3
Pr	15,73	2,14	5,98	5,28	2,8	3,45	6,73	2,58	1,69	2,23	5,2	6,12	5,55	4,62	6,97
Nd	52	6,5	20,3	20,4	11	14,5	24	11	6,7	9,8	18	22,5	20,9	16,8	29,5
Sm	7,85	1,08	3,07	4,03	1,87	2,92	3,68	2,19	1,33	1,9	3,29	4,45	2,72	2,95	5,94
Eu	1,37	0,68	0,79	1,24	0,68	0,97	0,81	0,63	0,51	0,63	0,86	0,9	0,84	0,89	1,49
Gd	5,69	0,86	2,11	3,93	1,73	3,1	2,4	1,38	0,93	1,61	3,2	4,38	1,96	2,28	4,66
Tb	0,68	0,12	0,27	0,57	0,25	0,5	0,25	0,15	0,09	0,21	0,5	0,72	0,23	0,28	0,61
Dy	3	0,63	1,07	3,18	1,37	3	0,99	0,42	0,27	0,9	2,86	4,13	1,05	1,29	2,93
Ho	0,49	0,12	0,19	0,63	0,26	0,59	0,15	0,08	0,03	0,18	0,56	0,9	0,17	0,23	0,49
Er	1,22	0,4	0,51	1,85	0,7	1,67	0,33	0,16	0,05	0,44	1,58	2,51	0,43	0,61	1,39
Tm	0,16	0,05	0,09	0,27	0,1	0,24	0,06	0,04	0,02	0,07	0,21	0,34	0,06	0,07	0,17
Yb	0,9	0,37	0,48	1,81	0,71	1,55	0,24	0,11		0,41	1,48	2,39	0,39	0,56	1,22
Lu	0,16	0,06	0,1	0,31	0,11	0,24	0,05	0,03	0,02	0,07	0,21	0,36	0,07	0,08	0,18

Table 3. Major and trace elements for analyzed samples. Analyzed at ACME laboratories (acmelab.com, last accessed 2013-12-03)

Sample	034A	039A	045A	046A	046C	047A	047B	048A	049A	050A	055A	056A	058A	059B	061B
Major elements (wt. %) - ICP-ES															
SiO_2	69,43	67,08	66,34	69,08	52,3	71,71	47,67	66,45	65,28	64,95	63,3	61,36	70,63	74,52	72,75
Al_2O_3	15,61	16,03	14,71	15,6	18,92	13,83	14,3	16,36	16,76	15,72	16,59	14,98	15,82	14,96	15,8
FeO_{tot}	2,38	3,53	3,92	2,19	11,08	2,71	13,86	3,37	4,01	5,93	4,49	5,21	1,66	0,26	1
MgO	0,95	1,34	2,53	0,43	2,94	0,8	7,15	1,6	1,32	2,11	2,16	4,75	0,51	0,05	0,39
CaO	2,89	3,33	3,67	1,96	1,77	2,49	10,45	3,03	3,12	2,11	4,16	4,67	2	0,71	2,93
Na_2O	5,11	4,46	4,1	4,66	3,98	3,91	2,11	4,66	4,82	4,36	4,26	4,04	5,42	4,89	5,67
K_2O	2,02	2,08	2,14	2,17	3,1	2,63	0,81	1,96	1,97	2,42	2,54	1,99	2,29	3,63	0,44
TiO_2	0,26	0,4	0,4	0,37	1,22	0,34	1,59	0,4	0,69	0,66	0,55	0,58	0,31	0,01	0,17
P_2O_5	0,11	0,16	0,13	0,19	0,02	0,08	0,27	0,23	0,31	0,13	0,25	0,3	0,12	0,05	0,05
MnO	0,04	0,04	0,05	0,03	0,09	0,05	0,2	0,06	0,04	0,07	0,06	0,07	0,02		0,01
LOI	0,9	1,2	1,6	3,1	4,2	1,2	1,3	1,4	1,3	1,3	1,3	1,6	0,9	0,7	0,5
Sum	99,68	99,7	99,66	99,75	99,64	99,72	99,76	99,57	99,61	99,74	99,65	99,57	99,67	99,75	99,7
Trace elements (ppm) - ICP-MS															
Cr	20,53		95,79		143,68		266,84	27,37		102,63	41,05	218,94			
Ni	6,8	8,4	33,7	3,8	84,1	5,8	59,1	23,9	2,9	33,2	14,2	81,5	1,2	0,7	1,4
Sc	4	4	9	4	16	7	35	6	4	14	7	12	2	1	2
Ba	1163	879	639	728	893	877	52	983	1047	606	942	1093	1096	1081	747
Co	78,7	53,6	103,2	69,3	81,5	109,7	73,1	72,9	67,4	70,7	70,7	72,4	72,8	103	64,8
Cs	2,9	0,5	3,1	1,9	3,6	0,8		2,4	1,3	3,7	2,9	1,2	1,2	1	0,7
Ga	17,9	17,9	20,6	23	36,4	15,8	17,8	21,2	21,5	19,1	20,3	19,2	20,6	18,3	19,7
Hf	3,3	3,7	3,4	4,6	6,9	5,1	2,5	4,8	6,1	3,8	4,7	4,1	3,5	1,1	2,8
Nb	4,1	4,2	5,9	4,9	12,8	7,3	9	5,3	9,5	5,7	5,5	4,4	2,2	2,4	1,5
Rb	59,1	67,3	72,3	87	156,5	85,2	10,6	86,7	61	87,7	74,7	55,8	57,5	92,3	12,8
Sr	783	851,3	683,8	465,5	433,7	240,9	169,3	1397,7	963,2	401,1	926,5	1066,2	1071,9	271,4	1243,9
Ta	0,2	0,3	0,5	0,3	0,7	0,7	0,5	0,3	0,5	0,4	0,4	0,3	0,2	0,3	0,1
Th	4,8	13,4	4,7	5,9	3,1	7,2	0,6	7,7	10,1	4,7	4,9	3,4	3	0,8	1,8
U	0,6	0,5	1,3	2,2	1	2,3	0,1	2,1	0,6	1,5	2	0,9	1,3	1,3	0,7
V	33	39	85	60	230	43	290	45	65	129	75	102	10		
Zr	120,4	145,3	123,9	168,2	259,1	188,8	97,2	204,7	273,4	153,9	166,9	170,2	126,4	22,4	111,1
Y	5,8	5,6	9,6	9,5	3,1	21	27,4	9	11,9	15	9,2	14,1	3,9	3,3	4,9
Mo	0,1	0,2	0,3	1	29,4	0,2	0,3	0,2	0,2	0,4	0,1	0,6	0,1	0,9	0,2
Cu	22,2	38,3	14,7	13,5	176	4,4	56,5	26,3	12,3	42,1	10,9	23,5	4,2	4,3	7,6
Pb	2,3	3,1	2,3	9,5	6,4	2,9	0,6	4,6	3,2	2,4	4,1	2,6	7,8	8,9	2,1
Zn	43	60	50	53	199	39	47	79	83	66	67	56	58	11	28
La	20,8	44,4	23,3	39,8	15,8	27	10	49,3	52	26,4	32,7	35,1	18,1	5,3	25
Ce	38	83,3	44,4	80,3	31,7	51,2	25,4	98,2	104,3	51,5	65,6	77,7	37,8	11,9	44,8
Pr	3,99	8,37	5,34	10,19	3,89	5,93	3,73	11,32	12,61	6,24	7,93	9,55	4,38	1,49	5,59
Nd	14,6	27,1	20,9	37,8	14,7	22,5	15,8	37,9	46,9	24,3	30,8	38,5	17	6	21,2
Sm	2,27	3,78	3,83	6,36	2,32	3,96	4,21	5,91	7,65	4,24	4,94	7,09	2,75	1,37	2,49
Eu	0,68	0,91	1,04	1,02	0,74	0,91	1,44	1,56	1,81	1,14	1,42	1,82	0,74	0,12	0,85
Gd	1,55	2,73	2,91	4,07	1,48	3,6	4,95	3,45	5,02	3,6	3,46	4,77	1,78	1,11	1,52
Tb	0,21	0,29	0,37	0,47	0,15	0,56	0,8	0,39	0,54	0,49	0,4	0,59	0,22	0,15	0,15
Dy	0,99	1,34	1,78	2,27	0,75	3,18	5,22	1,58	2,62	3,2	1,96	2,7	0,8	0,69	0,73
Ho	0,2	0,2	0,33	0,29	0,1	0,66	0,96	0,29	0,41	0,58	0,3	0,45	0,11	0,1	0,09
Er	0,54	0,46	0,84	0,69	0,31	2,11	2,88	0,78	0,89	1,62	0,85	1,36	0,28	0,29	0,24
Tm	0,08	0,05	0,12	0,07	0,06	0,29	0,41	0,11	0,11	0,22	0,1	0,16	0,03	0,03	0,03
Yb	0,54	0,37	0,81	0,58	0,6	2,19	2,82	0,71	0,67	1,49	0,83	1,05	0,21	0,2	0,29
Lu	0,07	0,05	0,12	0,09	0,13	0,31	0,38	0,11	0,09	0,22	0,12	0,15	0,02	0,03	0,03

Table 3 continued

Sample	061C	061D	062A	063A	063B	066A	070A	071A	072A	073B	075A	075B	076A	082A	083A
Major elements (wt. %) - ICP-ES															
SiO_2	66,54	62,13	68,75	68,73	73,02	64,25	70,55	66,55	60,68	75,47	69,68	63,59	71,13	74,04	67,29
Al_2O_3	16,53	15,95	15,37	15,91	15,76	14,56	15,35	15,98	16,96	13,65	15,1	16,33	14,63	13,23	15,33
FeO_{tot}	3,43	7,01	2,24	2,88	0,87	4,15	1,89	3,91	6,07	0,64	2,46	5,04	2,26	2,4	3,44
MgO	1,28	3,12	0,85	1,19	0,22	3,27	0,67	1,32	2,63	0,07	0,61	1,85	0,53	0,4	1,75
CaO	3,21	2,75	2,4	4,01	1,79	4,33	2,11	3,87	5,6	0,83	1,88	5,34	1,55	1,62	3,63
Na_2O	4,93	3,33	4,7	4,64	5,6	4,08	4,66	4,64	4,59	3,98	3,88	4,5	3,74	4,01	4,54
K_2O	1,72	2,83	2,77	1,17	1,55	2,6	3,13	1,46	1,1	4,47	4,23	1,26	4,61	2,97	2,18
TiO_2	0,66	0,66	0,42	0,33	0,08	0,44	0,31	0,4	0,73	0,05	0,42	0,59	0,22	0,31	0,41
P_2O_5	0,28	0,14	0,15	0,09	0,02	0,18	0,11	0,17	0,28	0,02	0,14	0,25	0,11	0,06	0,14
MnO	0,03	0,09	0,03	0,04	0,02	0,08	0,02	0,07	0,09	0,02	0,04	0,07	0,03	0,04	0,05
LOI	1,1	1,6	2	0,8	0,8	1,6	0,9	1,3	0,9	0,6	1,1	0,9	0,9	0,6	1
Sum	99,66	99,64	99,68	99,76	99,73	99,61	99,7	99,69	99,67	99,77	99,59	99,78	99,71	99,74	99,75
Trace elements (ppm) - ICP-MS															
Cr	13,68	116,31				157,37	13,68	13,68				13,68			27,37
Ni	5,5	34,9	4,5	11,6	1,8	43,1	2,8	8,1	20,9	1,1	2,8	15,8	4,9	4,4	18,8
Sc	3	17	3	5	5	10	3	6	11	1	3	9	1	6	7
Ba	1078	1262	1191	387	440	1102	1208	674	588	677	1965	239	1135	858	695
Co	46,5	46,3	65,8	75,6	99,1	44,2	63,2	92	60,7	140,1	56,8	54,5	80,6	89,7	57,9
Cs	1,8	4,6	1,4	0,6	0,6	1,7	2,4	0,7	0,4	1,5	1,1	2,9	1,9	1,2	2
Ga	21,1	18,4	19,7	21,8	19,6	18,2	20,3	17,5	20,7	18,8	18,6	19,4	18,1	13,6	17,9
Hf	4,9	3,4	4,2	2,8	2,1	3,8	4,6	2,2	2,4	2,4	8,2	4,9	6,4	6,5	2,9
Nb	5,1	7,1	3,4	1,9	2,3	4,9	4,5	1,8	3,9	3,8	7,3	5,8	3,2	7,8	2,8
Rb	59,8	98,3	69	24,4	34,7	69,7	99,7	29,8	22,9	150,5	158,7	44,8	120,3	88,7	52,5
Sr	989,5	730	802,8	764,2	987,6	1150,1	682,6	1008,5	1136,3	170,6	500,8	574,6	352,8	150,4	640,1
Ta	0,3	0,4	0,3	0,2	0,2	0,3	0,4	0,1	0,3	0,4	0,8	0,5	0,2	0,8	0,3
Th	6,1	2,9	3,2	1,1	2,6	4,1	6,1	1,2	1	6,2	6,6	0,7	12,1	7,5	3,6
U	1,5	0,8	1,1	0,3	0,8	1,7	1,2	0,2	0,4	2	1,7	0,4	3,1	3,1	1,1
V	46	130	27	47		80	22	56	109		22	62	14		48
Zr	198,3	132,6	155,2	91,6	66	138,8	152,2	87,9	106,4	53,7	284,1	208,9	193,8	224,4	106
Y	8,1	11,1	3,8	5	3,5	10,9	3,7	4,3	12,9	4,6	11,2	8,4	8,5	30	6,4
Mo	0,1	0,3	0,3		0,1	0,2	0,1	0,2	0,4	0,2	0,2	0,2	0,4	0,3	0,2
Cu	9,3	30	18	7,4	3,3	34,3	5,7	11,4	51,8	15,9	7,8	18,6	3,7	4,8	13,6
Pb	3	1,9	9,4	1,9	4,4	10,1	6,4	1,4	1,1	9,4	6,5	0,8	6,3	4,3	2,3
Zn	78	99	57	55	32	34	54	62	59	22	62	61	52	52	41
La	32,7	11	27,2	9,7	15,6	25,6	31,5	13,8	21,7	8,5	65,4	23,3	49,5	29,5	20,2
Ce	71,6	17,9	53,1	19,1	30,4	50	56,8	25,5	48,3	15,7	129,3	44,8	100,1	62,5	38,7
Pr	7,74	1,98	5,97	2,66	3,69	6,16	6,21	3,21	6,46	1,88	14,26	5,39	10,97	7,37	4,46
Nd	28,8	9	20,5	9,6	14,9	23,9	19,9	13	25,3	7,7	48,6	19,4	36,8	28,3	15,3
Sm	4,88	1,44	3,23	2,23	2,47	4,49	2,74	1,96	4,89	1,8	6,72	3,32	5,47	4,76	2,46
Eu	1,48	0,64	0,84	0,62	0,37	1,17	0,67	0,8	1,38	0,35	1,12	1,09	0,91	0,8	0,76
Gd	3,18	1,16	1,8	1,84	1,65	3,29	1,5	1,47	3,48	1,37	4,06	2,45	3,48	4,56	1,79
Tb	0,35	0,19	0,19	0,21	0,16	0,42	0,15	0,17	0,46	0,18	0,48	0,32	0,37	0,77	0,23
Dy	1,57	1,18	0,79	0,94	0,79	2,22	0,77	0,81	2,26	0,81	2,61	1,78	1,66	4,84	1,26
Ho	0,25	0,37	0,12	0,15	0,09	0,36	0,1	0,15	0,42	0,14	0,36	0,32	0,28	1,15	0,23
Er	0,49	1,39	0,36	0,4	0,34	1,07	0,38	0,48	1,17	0,4	1,24	0,82	0,77	3,07	0,67
Tm	0,05	0,22	0,04	0,06	0,04	0,14	0,04	0,06	0,15	0,04	0,16	0,11	0,1	0,49	0,08
Yb	0,26	1,66	0,26	0,39	0,32	0,89	0,35	0,41	1,22	0,44	1,11	0,82	0,83	2,92	0,7
Lu	0,04	0,24	0,03	0,05	0,04	0,13	0,06	0,05	0,16	0,04	0,16	0,11	0,12	0,44	0,09

Table 3 continued

Sample	084A	090A	091A	091B	093A	094A	095A	097A	098A	100A	100B	PK101	PK102	PK103	PK105
Major elements (wt. %) - ICP-ES															
SiO_2	74,97	72,47	71,38	72,19	66,13	68,15	68,94	72,77	73,58	68,37	74,17	63,95	67,55	66,07	70,34
Al_2O_3	12,73	15,22	15,17	15,22	15,17	15,64	15,59	15,05	15,02	16,22	14,72	17,06	15,04	15,01	14,53
FeO_{tot}	1,89	1,11	1,71	1,53	4,01	3,36	2,57	1,23	0,88	2,95	0,26	4,44	3,76	4,26	3,22
MgO	0,54	0,25	0,57	0,45	1,48	0,97	1,01	0,32	0,16	1,29	0,06	1,76	1,41	1,88	0,93
CaO	1,35	2,07	2,32	2,46	4,3	3,19	3,19	1,89	1,02	2,75	0,99	3,74	3,89	3,41	3,81
Na_2O	3,49	5,21	4,95	4,99	4,17	4,58	5,06	5,29	4,42	5,1	4,57	4,84	4,06	3,74	4,06
K_2O	3,75	2,18	2,31	1,64	1,85	2,13	1,74	2,16	3,94	1,46	4,39	1,94	2,23	3,45	1,35
TiO_2	0,21	0,12	0,23	0,2	0,43	0,36	0,33	0,14	0,06	0,37	0,02	0,58	0,41	0,42	0,3
P_2O_5	0,05	0,04	0,08	0,07	0,15	0,13	0,12	0,05	0,03	0,1	0,1	0,23	0,09	0,16	0,09
MnO	0,03	0,02	0,02	0,02	0,07	0,05	0,05	0,02	0,04	0,03		0,04	0,06	0,07	0,04
LOI	0,8	1	1	1	2	1,1	1,1	0,8	0,6	1,1	0,5	1,2	1,2	1,1	1,2
Sum	99,76	99,73	99,74	99,74	99,78	99,68	99,68	99,76	99,75	99,69	99,78	99,75	99,71	99,59	99,82
Trace elements (ppm) - ICP-MS															
Cr										34,21		27,37	54,74	27,37	
Ni	6,6	0,8	3,4	4,2	18,5	5,6	8,1	1,6	0,4	17,1	0,9	13,9	12,3	9,7	6,8
Sc	3	2	3	2	8	5	5	2	2	6	1	3	9	10	6
Ba	905	890	1007	751	582	913	751	774	920	498	550	495	1021	1642	381
Co	92,7	94,9	71	90,5	63,1	85,1	95,6	64,2	74,1	69,8	101,2	49,4	99,9	78,4	66,4
Cs	1,7	0,5	0,8	0,6	0,7	1,2	1,2	0,5	2,5	5,7	4,5	0,6	1,5	0,6	0,2
Ga	13,9	15,4	16,8	16,6	16,5	18,7	16,4	16,9	17,9	20,3	14,8	18,5	14,6	15,4	14,8
Hf	3,6	2,7	2,2	2,5	2,8	4,2	3	3	2,1	2,5	1,3	6	4,1	3,8	5,4
Nb	4	1	2,3	1,7	3,5	4,8	3	0,9	5,9	2,4	1,3	5,3	6,1	3,9	2,8
Rb	87,7	54,3	49,6	39,2	42,1	50,5	41,7	36,2	114,6	92,2	167,7	69,9	59,4	70,6	30,5
Sr	133,4	584,7	588,7	556,5	517,6	573,5	809,8	661,6	246,9	663	168,4	702,1	352,6	748,3	242,2
Ta	0,6	0,2	0,2	0,2	0,3	0,6	0,4	0,1	0,6		0,2	0,2	0,6	0,2	0,2
Th	8,7	1,5	1,8	1,4	3,7	5,2	2,6	1,8	4,4	1,4	5,9	11,9	3,7	19,6	21,8
U	3,8	0,4	0,9	0,7	0,8	0,8	0,8	0,6	1,4	7,8	4,2	0,4	1,1	0,3	0,4
V	11		21	20	63	35	31			52		55	52	67	43
Zr	111,3	92,2	88,1	95,6	119,4	157,5	107,4	85,2	50,5	101,7	43,4	218,5	128,3	145,9	207,2
Y	11,3	2,8	4,3	3,4	10,1	16,2	6,3	2,1	10,3	3,5	2,4	4,7	13,4	9,6	8,1
Mo	0,2	0,1	0,2	0,2	0,3	0,3	0,2	0,1	0,1	0,3	0,2	0,1	0,3	0,2	0,2
Cu	21,1	4	10,7	15,6	25	9	13,6	6	2,2	18,8	1,4	0,5	16,9	19,8	10,6
Pb	4,9	3,6	3,3	2,8	2,7	2,9	2,3	6,4	3	1,7	3,4	2,1	2,9	5,7	5,1
Zn	33	30	39	34	51	61	47	40	41	58	22	69	38	54	34
La	24	8	13	8,5	21,5	43,3	19,3	11,1	16,6	9,8	9,7	51,2	15,7	44,9	43,1
Ce	42,8	19	26,3	16,4	43,7	54	40,1	22,7	32,9	19,6	18,7	92,9	32,8	87,7	81,9
Pr	4,45	1,78	3,13	1,88	5,45	8,37	5	2,61	3,63	2,42	1,98	8,55	3,75	8,61	7,43
Nd	14,7	5,8	11,8	7,3	18,6	28,6	18,7	9,3	12,6	9,4	6,6	26	13,9	28,9	23,3
Sm	2,23	1,02	2,04	1,33	3,51	4,74	3,1	1,67	2,3	1,72	1,35	3	2,8	3,91	2,9
Eu	0,36	0,35	0,57	0,48	0,93	1,27	0,83	0,47	0,43	0,72	0,24	0,79	0,87	0,98	0,72
Gd	1,79	0,63	1,47	1,05	2,69	4,12	1,81	0,88	2,03	1,26	1,07	2,23	2,7	2,94	2,42
Tb	0,3	0,09	0,17	0,13	0,35	0,5	0,24	0,11	0,28	0,15	0,12	0,21	0,43	0,38	0,28
Dy	1,62	0,5	0,82	0,7	1,95	2,64	1	0,51	1,52	0,75	0,54	0,94	2,43	1,79	1,43
Ho	0,36	0,07	0,14	0,09	0,35	0,48	0,21	0,08	0,31	0,12	0,06	0,16	0,46	0,33	0,27
Er	1,09	0,25	0,43	0,31	0,97	1,22	0,55	0,25	0,82	0,24	0,22	0,41	1,32	0,91	0,77
Tm	0,18	0,04	0,06	0,03	0,13	0,17	0,09	0,02	0,12	0,05	0,03	0,05	0,17	0,11	0,09
Yb	1,22	0,35	0,38	0,25	0,95	1,02	0,57	0,24	0,83	0,29	0,21	0,42	1,27	0,83	0,76
Lu	0,19	0,04	0,05	0,04	0,12	0,14	0,09	0,03	0,11	0,05	0,02	0,05	0,19	0,12	0,12

Table 3 continued

Tidigare skrifter i serien ”Examensarbeten i Geologi vid Lunds universitet”:

325. Härling, Jesper, 2012: The fossil wonders of the Silurian Eramosa Lagerstätte of Canada: the jawed polychaete faunas. (15 hp)
326. Qvarnström, Martin, 2012: An interpretation of oncoid mass-occurrence during the Late Silurian Lau Event, Gotland, Sweden. (15 hp)
327. Ulmius, Jan, 2013: P-T evolution of paragneisses and amphibolites from Romeleåsen, Scania, southernmost Sweden. (45 hp)
328. Hultin Eriksson, Elin, 2013: Resistivitets-mätningar för avgränsning av lak-vattenplym från Kejsarkullens deponis infiltrationsområde. (15 hp)
329. Mozafari Amiri, Nasim, 2013: Field relations, petrography and 40Ar/39Ar cooling ages of hornblende in a part of the eclogite-bearing domain, Sveconorwegian Orogen. (45 hp)
330. Saeed, Muhammad, 2013: Sedimentology and palynofacies analysis of Jurassic rocks Eriksdal, Skåne, Sweden. (45 hp)
331. Khan, Mansoor, 2013: Relation between sediment flux variation and land use patterns along the Swedish Baltic Sea coast. (45 hp)
332. Bernhardson, Martin, 2013: Ice advance-retreat sediment successions along the Logata River, Taymyr Peninsula, Arctic Siberia. (45 hp)
333. Shrestha, Rajendra, 2013: Optically Stimulated Luminescence (OSL) dating of aeolian sediments of Skåne, south Sweden. (45 hp)
334. Fullerton, Wayne, 2013: The Kalgoorlie Gold: A review of factors of formation for a giant gold deposit. (15 hp)
335. Hansson, Anton, 2013: A dendroclimatic study at Store Mosse, South Sweden – climatic and hydrologic impacts on recent Scots Pine (*Pinus sylvestris*) growth dynamics. (45 hp)
336. Nilsson, Lawrence, 2013: The alteration mineralogy of Svartliden, Sweden. (30 hp)
337. Bou-Rabee, Donna, 2013: Investigations of a stalactite from Al Hota cave in Oman and its implications for palaeoclimatic reconstructions. (45 hp)
338. Florén, Sara, 2013: Geologisk guide till Söderåsen – 17 geologiskt intressanta platser att besöka. (15 hp)
339. Kullberg, Sara, 2013: Asbestkontamination av dricksvatten och associerade risker. (15 hp)
340. Kihlén, Robin, 2013: Geofysiska resistivitetsmätingar i Sjöcrona Park, Helsingborg, undersökning av områdets geologiska egenskaper samt 3D modellering i GeoScene3D. (15 hp)
341. Linders, Wictor, 2013: Geofysiska IP-undersökningar och 3D-modellering av geofysiska samt geotekniska resultat i GeoScene3D, Sjöcrona Park, Helsingborg, Sverige. (15 hp)
342. Sidenmark, Jessica, 2013: A reconnaissance study of Rävliden VHMS-deposit, northern Sweden. (15 hp)
343. Adamsson, Linda, 2013: Peat stratigraphical study of hydrological conditions at Stass Mosse, southern Sweden, and the relation to Holocene bog-pine growth. (45 hp)
344. Gunterberg, Linnéa, 2013: Oil occurrences in crystalline basement rocks, southern Norway – comparison with deeply weathered basement rocks in southern Sweden. (15 hp)
345. Peterffy, Olof, 2013: Evidence of epibenthic microbial mats in Early Jurassic (Sinemurian) tidal deposits, Kulla Gunnarstorp, southern Sweden. (15 hp)
346. Sigeman, Hanna, 2013: Early life and its implications for astrobiology – a case study from Bitter Springs Chert, Australia. (15 hp)
347. Glommé, Alexandra, 2013: Texturella studier och analyser av baddeleyitomvandlingar i zirkon, exempel från sydöstra Ghana. (15 hp)
348. Brådenmark, Niklas, 2013: Alunskiffer på Öland – stratigrafi, utbredning, mäktigheter samt kemiska och fysikaliska egenskaper. (15 hp)
349. Jalnefur Andersson, Evelina, 2013: En MIFO fas 1-inventering av fyra potentiellt förorenade områden i Jönköpings län. (15 hp)
350. Eklöv Pettersson, Anna, 2013: Monazit i Obbhult-komplexet: en pilotstudie. (15 hp)
351. Acevedo Suez, Fernando, 2013: The reliability of the first generation infrared refractometers. (15 hp)

352. Murase, Takemi, 2013: Närkes alunskiffer – utbredning, beskaffenhet och oljeinnehåll. (15 hp)
353. Sjöstedt, Tony, 2013: Geoenergi – utvärdering baserad på ekonomiska och drifttekniska resultat av ett passivt geoenergisystem med värmeuttag ur berg i bostadsrättsföreningen Mandolinen i Lund. (15 hp)
354. Sigfúsdóttir, Thorbjörg, 2013: A sedimentological and stratigraphical study of Veiki moraine in northernmost Sweden. (45 hp)
355. Månsson, Anna, 2013: Hydrogeologisk kartering av Hultan, Sjöbo kommun. (15 hp)
356. Larsson, Emilie, 2013: Identifying the Cretaceous–Paleogene boundary in North Dakota, USA, using portable XRF. (15 hp)
357. Anagnostakis, Stavros, 2013: Upper Cretaceous coprolites from the Münster Basin (northwestern Germany) – a glimpse into the diet of extinct animals. (45 hp)
358. Olsson, Andreas, 2013: Monazite in metasediments from Stensjöstrand: A pilot study. (15 hp)
359. Westman, Malin, 2013: Betydelsen av raka borrhål för större geoenergisystem. (15 hp)
360. Åkesson, Christine, 2013: Pollen analytical and landscape reconstruction study at Lake Storsjön, southern Sweden, over the last 2000 years. (45 hp)
361. Andolfsson, Thomas, 2013: Analyses of thermal conductivity from mineral composition and analyses by use of Thermal Conductivity Scanner: A study of thermal properties in Scanian rock types. (45 hp)
362. Engström, Simon, 2013: Vad kan inneslutningar i zirkon berätta om Varbergscharnockiten, SV Sverige. (15 hp)
363. Jönsson, Ellen, 2013: Bevarat maginnehåll hos mosasaurier. (15 hp)
364. Cederberg, Julia, 2013: U-Pb baddeleyite dating of the Pará de Minas dyke swarm in the São Francisco craton (Brazil) – three generations in a single swarm. (45 hp)
365. Björk, Andreas, 2013: Mineralogisk och malmpetrografisk studie av disseminerade sulfider i rika och fattiga prover från Kleva. (15 hp)
366. Karlsson, Michelle, 2013: En MIFO fas 1-inventering av förorenade områden: Kvarnar med kvicksilverbetning Jönköpings län. (15 hp)
367. Michalchuk, Stephen P., 2013: The Säm fold structure: characterization of folding and metamorphism in a part of the eclogite-granulite region, Sveconorwegian orogen. (45 hp)
368. Praszkier, Aron, 2013: First evidence of Late Cretaceous decapod crustaceans from Åsen, southern Sweden. (15 hp)
369. Alexson, Johanna, 2013: Artificial groundwater recharge – is it possible in Mozambique? (15 hp)
370. Ehlorsson, Ludvig, 2013: Hydrogeologisk kartering av grundvattenmagasinet Åsumsfältet, Sjöbo. (15 hp)
371. Santsalo, Liina, 2013: The Jurassic extinction events and its relation to CO2 levels in the atmosphere: a case study on Early Jurassic fossil leaves. (15 hp)
372. Svantesson, Fredrik, 2013: Alunskiffern i Östergötland – utbredning, mäktigheter, stratigrafi och egenskaper. (15 hp)
373. Iqbal, Faisal Javed, 2013: Paleoecology and sedimentology of the Upper Cretaceous (Campanian), marine strata at Åsen, Kristianstad Basin, Southern Sweden, Scania. (45 hp)
374. Kristinsdóttir, Bára Dröfn, 2013: U-Pb, O and Lu-Hf isotope ratios of detrital zircon from Ghana, West-African Craton – Formation of juvenile, Palaeoproterozoic crust. (45 hp)
375. Grenholm, Mikael, 2014: The Birimian event in the Baoulé Mossi domain (West African Craton) — regional and global context. (45 hp)

LUNDS UNIVERSITET

Geologiska institutionen
Lunds universitet
Sölvegatan 12, 223 62 Lund